To My Parents

# THE EFFECT OF AXIAL ROTATION ON FORCED CONVECTIVE HEAT AND MASS TRANSFER FROM BODIES OF REVOLUTION

A thesis submitted for the Degree of
DOCTOR OF PHILOSOPHY
in the Faculty of Engineering of the university
of London
by

Trevor Graham Sanders, B.Sc.(Eng. )

Department of Chemical Engineering
and Chemical Technology,
Imperial College of Science and Technology,
London S.W.7
November 1969

## ABSTRACT

The boundary layer equations have been derived in terms of a general orthogonal curvilinear co-ordinate system in order to predict local rates of mass or heat transfer from any axisymmetric body rotating in axial flow.

Substitution of suitable power series forms for velocity components, concentration (or temperature) distribution and scale factors reduced these equations to three infinite sets of ordinary differential equations. The two coupled infinite sets of hydrodynamic equations were dependent on shape and on spin parameter (a measure of the rotational velocity of the body compared with the main stream velocity). The mass (or heat) transfer sets were dependent on shape and Schmidt (or Prandtl) number.

The first pair of hydrodynamic equations were non-linear and their solution was obtained for spin parameters below ten using a finite difference technique. For higher spin parameters it was found necessary to use the technique of quasilinearisation.

The remaining sets of hydrodynamic equations and the transfer equations were linear and were solved using the principle of superposition. A computer programme was produced to generate and solve the general equations of these sets.

The analysis was used to study the effect of rotation on local rates of mass transfer from spheres, disks and spheroids with width to height ratios of 10/16 and 7/16. Solutions were obtained for the first five sets of the ordinary differential equations at spin

parameters from zero to twenty and at Schmidt numbers from 0.7 to 10.0, the effect of rotation at infinite Schmidt number was also studied. The results obtained showed that local rates of mass transfer increased substantially with increasing spin parameter.

The analysis was extended to predict local transfer rates from any axisymmetric body rotating in a quiescent fluid. In this case local and overall mass transfer numbers have been obtained for the sphere, 13/16 and 10/16 spheroids at Schmidt numbers of 0.7 to 100.0.

## ACKNOWLEDGEMENTS

I would like to express my sincere gratitude to Dr. A.R.H. Cornish, who gave me constant help and advice during all stages of the preparation of this thesis.

I would also like to thank Dr. M.B. Green who gave me much assistance in the initial stages of this work.

To the Science Research Council I extend my gratidude for the reasearch studentship that they gave me.

Finally, I would like to thank my parents for the many sacrifices that they made during my studies.

# LIST OF CONTENTS


| | | PAGE NO. |
|---|---|---|
| ABSTRACT | | 3 |
| ACKNOWLEDGEMENTS | | 5 |
| LIST OF CONTENTS | | 6 |
| CHAPTER I | INTRODUCTION | 9 |
| CHAPTER II | LITERATURE SURVEY | 12 |
| 2.1 | INTRODUCTION | 12 |
| 2.2 | AXISYMMETRIC BODY ROTATING IN AXIAL FLOW | 13 |
| | 2.2.1 Theoretical Studies | 13 |
| | 2.2.2 Experimental Results | 16 |
| 2.3 | STATIONARY BODY IN AXIAL FLOW | 17 |
| | 2.3.1 Theoretical Studies | 17 |
| | 2.3.2 Experimental Work on Stationary Bodies | 18 |
| 2.4 | AXISYMMETRIC BODY ROTATING IN A QUIESCENT FLUID | 21 |
| | 2.4.1 Theoretical Solutions | 21 |
| | 2.4.2 Experimental Results | 28 |
| CHAPTER III | THEORETICAL ANALYSIS | 33 |
| 3.1 | INTRODUCTION | 33 |
| 3.2 | DERIVATION OF THE BOUNDARY LAYER EQUATIONS FOR AN AXISYMMETRIC BODY IN ORTHOGONAL CURVILINEAR CO-ORDINATES | 34 |
| | 3.2.1 Navier-Stokes Equations for an Axisymmetric Body | 34 |
| | 3.2.2 Derivation of Boundary Layer Equations for a Body of Revolution Rotating in Axial Flow | 38 |
| | 3.2.3 Derivation of Boundary Layer Equations for a Body of Revolution Rotating in a Quiescent Fluid | 48 |
| 3.3 | SOLUTION OF THE LAMINAR BOUNDARY LAYER EQUATIONS FOR AN AXISYMMETRIC BODY ROTATING ABOUT ITS AXIS OF SYMMETRY IN AXIAL FLOW | 50 |
| | 3.3.1 Velocity Boundary Layer Equations | 51 |
| | 3.3.2 Definition of Characteristic Dimension and Co-ordinates | 59 |
| | 3.3.3 Mass (or Heat) Transport Boundary Layer Equation for Finite Non-Zero Schmidt or Prandtl Numbers | 64 |

PAGE NO.


3.3.4 Final Form of Differential Equations for Determination of Local Mass or Heat Transfer Coefficients (For Finite and Non-zero Schmidt and Prandtl numbers) 67

3.4 SERIES SOLUTION OF THE LAMINAR BOUNDARY LAYER EQUATIONS FOR AN AXISYMMETRIC BODY ROTATING ABOUT ITS AXIS OF SYMMETRY IN A QUIESCENT FLUID 70
3.4.1 Velocity Boundary Layer Equations 70
3.4.2 Mass or Heat Transfer Boundary Layer Equation 74

3.5 POINT MASS TRANSFER FUNCTIONS 75
3.5.1 Body with Constant Surface Concentration or Constant Surface Temperature 75
3.5.2 Body with Non-uniform Surface Temperature or Concentration 78

3.6 POINT MASS TRANSFER NUMBER FOR LIMIT AS $\overline{Pr} \to \infty$ AND $\overline{Pr} \to 0$ 79
3.6.1 Axisymmetric Body Rotating in Axial Flow as $\overline{Pr} \longrightarrow \infty$ 79
3.6.2 Axisymmetric Body Rotating in a Quiescent Fluid as $\overline{Pr} \longrightarrow \infty$ 82
3.6.3 Axisymmetric Body Rotating in Axial Flow as $\overline{Pr} \to 0$ 82
3.6.4 Axisymmetric Body Rotating in a Quiescent Fluid as $\overline{Pr} \to 0$ 83

3.7 APPLICATION OF METHOD TO THE OBLATE SPHEROID 84

CHAPTER IV NUMERICAL TECHNIQUES 87

4.1 INTRODUCTION 87

4.2 SOLUTION OF NON-LINEAR HYDRODYNAMIC STAGNATION POINT EQUATIONS FOR A BODY ROTATING IN AXIAL FLOW 88
4.2.1 Theoretical 88
4.2.2 Numerical Technique 95

4.3 SOLUTION OF THE LINEAR HYDRODYNAMIC EQUATIONS 101

4.4 SOLUTION OF MASS TRANSFER EQUATIONS 106

4.5 GENERAL METHOD OF SOLUTION OF EQUATIONS 107
4.5.1 Body Rotating in Axial Flow 107
4.5.2 Body Rotating in a Quiescent Fluid 111
4.5.3 Flow Diagram for Solution of all Linear Equations 113

4.6 NUMERICAL DETERMINATION OF COEFFICIENTS IN THE POWER SERIES EXPANSION FOR POTENTIAL FLOW AND SCALE FACTORS FOR OBLATE SPHEROIDS 119
4.6.1 Expansion of $h_{\theta,0}$ 119
4.6.2 Potential Flow Expansion 121

CHAPTER V RESULTS 123

5.1 INTRODUCTION 123

PAGE NO.


5.2 STAGNATION POINT SOLUTIONS FOR AN AXISYMMETRIC BOOM ROTATING IN AXIAL FLOW 124
5.2.1 The Hydrodynamic Stagnation Point Solutions 124
5.2.2 Mass Transfer Stagnation Point Solutions 130
5.2.3 Boundary Values for Oblate Spheroids Rotating in Axial Flow 132
5.2.4 Local Mass Transfer Numbers for Oblate Spheroids Rotating in Axial Flow 134

5.3 STAGNATION POINT SOLUTIONS FOR AN AXIALLY SYMMETRIC BODY ROTATING IN A QUIESCENT FLUID 138
5.3.1 Hydrodynamic Stagnation Point Solution 138
5.3.2 Mass Transfer Stagnation Point Solutions 138
5.3.3 Boundary Values for an Oblate Spheroid Rotating in a Quiescent Fluid 139
5.3.4 Local and Overall Mass Transfer Number Oblate Spheroids Rotating in Quiescent Fluid 140

CHAPTER VI CONCLUSIONS 167

APPENDIX A NAVIER-STOKES EQUATIONS 171

APPENDIX B FINITE DIFFERENCE PROCEDURE 174

APPENDIX C DEFINITION OF CO-ORDINATE SYSTEM 177

APPENDIX D COMPUTER PROGRAMMES 178

APPENDIX E TABLES 209

LIST OF FIGURES 224

LIST OF SYMBOLS 226

BIBLIOGRAPHY 232

# CHAPTER I

## INTRODUCTION

In the chemical industry, processes involving the dispersion of one phase in a second continuous phase are frequently encountered, the first phase takes the form of bubbles of gas (or vapour), drops of liquid or particles of solid. The mode of operation of such plant is to facilitate a high rate of heat or mass transfer between the two phases, it is hence necessary to understand the mechanisms of heat or mass transfer between the phases in order to design efficient plant.

Most analyses of heat or mass transfer from droplets, bubbles or particles previously presented have assumed that these bodies move through the continuous phase in 'pure' axial flow with no secondary motion taking place. In practice it is found that this is a highly idealised model more complex motions being the norm rather than the exception.

Solid particles have no internal mobility in consequence they tend to exhibit less complex motions than droplets or bubbles, their motions however are far from simple. Marchildon et al (1964) found that the translational motion of a solid particle through a stationary fluid is often accompanied by some form of induced secondary motion, they found that disks and cylinders rotate, oscillate and have a spiral motion about their mean path. These secondary motions first appear in the Reynolds number range of one

hundred to one thousand and become fully developed when the Reynolds number exceeds one thousand. Jefferey (1922-23) furnished theoretical evidence for secondary motions of ellipsoids of revolution, by assuming that particles adopt that motion which corresponds to the least dissipation of energy he found that: a) prolate spheroidal particles immersed in fluids in laminar motion will tend to orientate themselves with their axis of symmetry perpendicular to the plane of undisturbed motion of the fluid and will rotate about this axis with constant angular velocity, b) oblate spheroidal particles immersed in a fluid in laminar motion will tend to orientate themselves with an equatorial diameter perpendicular to the plane of undisturbed motion of the fluid and will rotate about this diameter with variable angular velocity.

For clusters of particles the motion of the individual particle becomes more complex because of the interaction of boundary layers, Jayaneera et al (1964) studied the behaviour of clusters of solid spheres and found that for Reynolds number range $10^{-4} < Re < 10$ (Reynolds number based on sphere diameter) pairs of spheres rotate towards one another when falling through a viscous fluid.

Droplets and bubbles, because of their ability to deform in shape and their internal mobility, are able to exhibit a far wider range of motions than solid particles. The ability of droplets to oscillate in an oblate-prolate motion has been widely reported in the literature, many other workers, e.g. Tibor and Harmathy (1960); Warshay et al (1959); Gibbons et al (1962); Hu and Kitner (1955), have all reported that droplets fall or rise in zig-zag or helical paths. Valentine et al (1965) state that droplets can exhibit rotational displacement, Krishna et al (1959) have observed this

experimentally. In general it would be expected that bodies falling through a continuous phase and subjected to a couple (e.g. in a mixing process or near to a boundary) would rotate.

The present work was started in order to determine theoretically the effects of secondary motions on heat and mass transfer through laminar boundary layers. Because of the complexity of the secondary motions exhibited by bubbles, droplets and solid particles it was decided that one secondary motion of particular importance should be studied in detail. The particular secondary motion chosen for study was that of steady axial rotation in laminar axial flow, this type of motion is also important in other fields of research (e.g. mechanics, ballistics etc.) in consequence the analysis of the pertinent laminar boundary layer equations was made as general as possible in order to be able to predict the local rates of heat or mass transfer from any axisymmetric body.

It has been reported by many workers that droplets are only spherical in shape when the Reynolds number is low, a more realistic model for the drop being the oblate spheroid. In order to determine the effect of rotation on local transfer rates of droplets the general theory that was developed in this thesis was used to study mass or heat transfer from solid oblate spheroid shapes.

The limiting case of axisymmetric bodies rotating in a quiescent fluid is also of interest, here once again the pertinent boundary layer equations are analysed in as general a form as possible in order that local heat or mass transfer rates may be determined for any solid axisymmetric body. Because of its relevance to the prediction of local heat or mass transfer rates from drops rotating in a quiescent fluid the oblate spheroid body once again is studied in particular.

# CHAPTER II

# LITERATURE SURVEY

## 2.1 INTRODUCTION

Heat or mass transfer and the hydrodynamics of axisymmetric bodies rotating in axial flow has so far received limited attention both theoretically and experimentally. Some attention has been given to disks, cones and spheres, however their theoretical treatment has been of such a form as to preclude any extension to more complex axisymmetric shapes.

Research into the effect of rotation on boundary layers associated with axially symmetric bodies primarily arose in connection with turbine construction. Research into flow around rotating disks arose from components in the turbine such as flat plates rotating in forced flow, rotating bodies of revolution became of further practical significance with the design of cooling elements in electrical motors and moving parts in hydro-machinery. The field of study has been further extended by ballistics and rocket technology into the study of flow around rotating cones.

Interest has also been shown in the case of flow induced by bodies rotating in an otherwise stagnant media, whilst this does not as yet have the same practical significance as its analogy in forced flow it is of fundamental theoretical interest in the extension of our understanding of the effects of secondary motions on boundary layers.

## 2.2 AXISYMMETRIC BODY ROTATING IN AXIAL FLOW

### 2.2.1 Theoretical Studies

As previously stated, for the case of axially symmetric bodies rotating in axial flow very few solutions exist of the hydrodynamic and transfer boundary layer equations. One of the first attempts to present an analysis was made by Tifford and Chu (1953) who stated that when:

a) Reynolds number is large compared to unity;

b) Prandtl number is of order unity;

c) Boundary layer is thin compared with the body's radius of curvature;

d) Body not extremely thick (cones however may be of arbitrary thickness);

e) Order of magnitude of peripheral speed is not greater than that of the free stream velocity;

f) Surface variation of temperature difference ($T_W - T_A$) and moment of angular momentum are linearly related; then for laminar conditions the rate of heat transfer from the body is proportional to the spinning torque.

The two major papers on the solution of the laminar hydrodynamic equations associated with a rotating axisymmetric body in axial flow are those of Hoskin (1955) and Schlichting (1956). Both workers have found that their solutions were not dependent on the axial velocity or rotational velocity of the body in isolation but a measure of the ratio of these two (the so-called Spin parameter).

Hoskin presented a solution of the pertinent laminar boundary layer equations using power series forms for the velocity components, shape factors and potential flow. The series forms were expressed in powers

of the meridional co-ordinate (which is the distance along a meridian curve from the front stagnation point), the substitutions reduced the two simultaneous partial differential boundary layer equations to two infinite sets of ordinary differential equations, the first four of which Hoskin solved for the spin parameter ($\lambda$) range $0 \leq \lambda \leq 10$ and used his results to show that the angle of separation for the rotating sphere moves toward the forward stagnation point for increasing spin parameter.

The analysis of the hydrodynamic boundary layer equations presented by Hoskin has, however, the following restrictions:

a) The form of the boundary layer equations that he presents requires that both the potential flow and the radius of transverse cross-section are able to be presented in terms of a power series of the meridional co-ordinate, this is not possible for some complex axisymmetric shapes such as the oblate spheroid.

b) Hoskin's procedure for determination of the stagnation point solutions from the non-linear simultaneous stagnation point equations is by means of a finite difference procedure which requires very accurate guesses for convergence. This represents a limitation on the range of spin parameter studied.

c) The four sets of ordinary differential equations presented by Hoskin are valid for the sphere only.

d) The number of sets of ordinary differential equations presented is limited to four.

Sickmann (1962) used the results of Hoskin to predict the local Nusselt numbers from rotating spheres by the introduction of the heat transfer boundary layer equation. He showed that spin increased the value of the local Nusselt number and gave results for Prandtl numbers

0.7 and 1.0 for the three spin parameters $\lambda$ = 0, 2 and 4.

Schlichting presented an approximate solution of the hydrodynamic boundary layer equations for the case of an arbitrary axisymmetric body rotating about its axis of symmetry in axial flow. Using Pohlhausen type velocity profiles for both azimuthal and meridional directions he was able to determine the effect of spin on the torque and separation point of a sphere from the momentum form of the boundary layer equations. From his equations he found that results were dependent on a spin parameter ($\Omega$ / $\bar{a}$), where $\Omega$ is the angular velocity, $\bar{a}$ is the value of dU/dx at x=0 and U is the potential flow at x, x being the co-ordinate distance in the meridional direction. He found that as the spin parameter increased the separation point moved from the rear half of the sphere toward the equator. He also found that for increasing spin parameter there was a small decrease in the torque coefficient. The disadvantage of the approximate method of Schlichting is the fact that the method fails for spin parameters greater than 0.815 (i.e. $\Omega/\bar{a} \gg 0.815$), failure being probably due to the inability of the Pohlhausen velocity profiles to describe the true velocity distribution when $\Omega/\bar{a}$ becomes greater than 0.815.

Yamaga (1956) extended Schlichting's theory to cover the effect of rotation on local heat transfer rates. He found that the local heat transfer coefficients increased with an increase in spin parameter, however, he also was limited to the maximum value of spin parameter of 0.815.

More recently Rittman (1969) studied the sphere and disk rotating in axial flow. Using a similarity type transformation and the azimuthal, meridional and perpendicular distances for his co-ordinate system he was able to study the hydrodynamic boundary layer equations

for the two bodies for spin parameter ($\Omega / \bar{a}$) of up to 2 by means of a finite difference technique.

Illingworth (1953) presented a method of series solution for the hydrodynamic boundary layer equations for the cone rotating in axial flow. Using series representations in powers of a spin parameter he presented a method of solution of the boundary layer equations valid when the potential flow along a body remains constant.

Analysis of forced flow against an axially rotating disk was first attempted by Hannah (1952) who gave an exact solution of the boundary layer equations, Tifford and Chu (1952) obtained the same solution independently. Schlichting and Truckenbrodt (1952) were the first to give an approximate solution for this case.

The search for similarity solutions for axisymmetric bodies rotating in axial flow has been carried out by Ishizawa (1963) who found that similarity solutions exist for the flat plate and the front stagnation point of the cone and bodies of revolution.

From the literature survey it can be seen that only a limited amount of theoretical work on the effects of spin on mass or heat transfer phenomena has been attempted. It can be seen that a general method of solution of the pertinent boundary layer equations is required in order to determine the local rates of heat or mass transfer from any axisymmetric body at any spin parameter and Schmidt (or Prandtl) number.

### 2.2.2 Experimental Results

For the axisymmetric body rotating about an axis of symmetry in axial flow there are very few experimental results in the literature.

Schlichting (1956) has described the work of Wielselberger (1927) who found that the drag of slender bodies of revolution showed a

considerable increase when there was an increase in the circumferential velocity relative to the main stream velocity.

Luthander and Rydberg (1935) found that there was a similar effect for spheres.

Noordsij and Rotte (1968) have given relationships for the overall Sherwood number for a sphere rotating with translational motion, however the spheres axis of rotation was perpendicular to the translational vector.

## 2.3 STATIONARY BODY IN AXIAL FLOW

### 2.3.1 Theoretical Studies

The case of a stationary body in axial flow is a limiting case of the present work (spin being zero) and as such deserves some attention.

The first attempt to obtain an approximate solution of the boundary layer equations for the case of an axisymmetric body in axial flow was put forward by Tomotika (1936) who used Millikan's (1932) momentum integral for axisymmetric flow and Pohlhausen's (1921) quartic velocity profile within the boundary layer. Aksel'rud(1953) and Grafton (1963) developed approximate solutions for transfer from a sphere, Beg (1966) extended this to the case of the oblate spheroid. Rojey (1967) used a Pohlhausen type polynomial to express the concentration distribution within the boundary layer and then solved the transfer equation to obtain point mass transfer coefficients within the boundary layer region of oblate spheroids.

Exact solutions of the boundary layer equations for axial flow around axisymmetric bodies of revolution are few, the most important being those of Frossling (1958) and Green (1968). Frossling used a curvilinear co-ordinate system based on perpendicular, azimuthal and meridional distances on the body surface, he then substituted the

Blasius (1950) power series for the stream function together with power series forms for the potential flow, contour function and concentration distribution into the transfer and hydrodynamic boundary layer equations. Comparison of like powers of the meridional co-ordinate yielded two infinite sets of ordinary differential equations; the first pair being the stagnation point equations which are independent of shape. By the introduction of suitable universal functions Frossling was able to remove the shape dependence of the remaining equations, however, in so doing he increased the number of equations to be solved substantially. The first three sets of these universal functions were solved by Frossling, Scholkemeier (1949) extended the theory to the fourth set.

The co-ordinate system used by Frossling did not permit direct application to more complex shapes such as the oblate spheroid (Green (1968)). Green removed this disadvantage by solving the boundary layer equations by an exact method using a more general co-ordinate system, however the solutions that he presented were shape dependent.

### 2.3.2 Experimental Work on Stationary Bodies

A large number of experimental studies have been published on overall heat or mass transfer coefficients from solid spheres, most correlations are of the form

$$Nu_o (\text{or } Sh_o) = A + B\, Re^n\, Pr^m (\text{or } Sc^m) \qquad (2\text{-}1)$$

Frossling (1938) on theoretical grounds substituted $n = \frac{1}{2}$; $A = 2$ and $m = \frac{1}{3}$ into (2-1) and obtained

$$Sh_o = 2 + 0.552\, Sc^{\frac{1}{3}}\, Re^{\frac{1}{2}} \qquad (2\text{-}2)$$

after correlating experimental data obtained from the evaporation of nitrobenzine, analine and water drops in air and the sublimation of

solid naphthalene spheres in air.

Linton and Sherwood (1950) studied benzoic acid spheres in a water tunnel and correlated their experimental data obtained in the form

$$Sh_D = 0.33\ Re^{\frac{1}{2}}\ Sc^{\frac{1}{3}} \qquad (2\text{-}3)$$

Linton and Sutherland (1960) conducted an extensive study into the dissolution of benzoic acid spheres in water for the Reynolds number range $490 < Re < 7580$ and correlated their obtained data in the form

$$Sh_D = 0.582\ Re^{\frac{1}{2}}\ Sc^{\frac{1}{3}} \qquad (2\text{-}4)$$

They also studied local rates of mass transfer and found good agreement with the theoretical results of Frossling and Akselrud.

Garner and Suckling (1958) studied mass transfer from both benzoic and adipic acid spheres in a water tunnel, from their data they obtained the correlation

$$Sh_D = 2 + 0.95\ Re^{0.5}\ Sc^{0.33} \qquad (2\text{-}5)$$

for the Reynolds number range $100 < Re < 700$.

Akselrud (1953) carried out experimental work on mass transfer from benzoic acid, sodium chloride and potassium nitrate spheres in water and found for the Reynolds number range $200 < Re < 4000$

$$Sh_D = 0.82\ Re^{\frac{1}{2}}\ Sc^{\frac{1}{3}} \qquad (2\text{-}6)$$

Kramers (1946) studied heat transfer from different sizes of steel spheres to water, air and oil and was able to correlate his data

$$Nu_D = 2.0 + 1.3\ Pr^{0.15} + 0.66\ Pr^{0.31} Re^{0.5} \qquad (2\text{-}7)$$

The correlation was found to be within $\pm$ 10% of his experimental data for the Reynolds number range $0 < Re < 1460$ and Prandtl number range $0.7 < Pr < 400$.

A most comprehensive literature survey into heat and mass transfer from spheres has been carried out by Rowe, Claxton and Lewis (1965).

They found that the majority of heat transfer data previously reported had been made in an air system and the majority of mass transfer measurements had been made in a water system. They decided that it was necessary to carry out new experimental studies of mass and heat transfer in both air and water. Using internally heated copper spheres for heat transfer measurements in both air and water, benzoic acid spheres for mass transfer measurements of dissolution in water and naphthalene spheres for measurement of mass transfer by sublimation in air they found that their experimental data was best represented by the following correlations.

for air system $$Nu_o(\text{or } Sh_o) = 2 + 0.69\, Re^{\frac{1}{2}}\, Pr^{\frac{1}{3}}(\text{or } Sc^{\frac{1}{3}}) \qquad (2\text{-}8)$$

for water system $$Nu_o(\text{or } Sh_o) = 2 + 0.79\, Re^{\frac{1}{2}}\, Pr^{\frac{1}{3}}(\text{or } Sc^{\frac{1}{3}}) \qquad (2\text{-}9)$$

the deviation of the correlation of $Nu_o$(or $Sh_o$) from experimental data being $\pm$ 0.3 $Pr^{\frac{1}{3}}$(or $Sc^{\frac{1}{3}}$).

They also presented a combined correlation for all their work

$$Nu_o(\text{or } Sh_o) = 2 + 0.72\, Re^{\frac{1}{2}}\, Pr^{\frac{1}{3}}(\text{or } Sc^{\frac{1}{3}}) \qquad (2\text{-}10)$$

which has a deviation from the experimental data of $\pm$ 10%. The range of all their correlations being $30 < Re < 2000$.

The effect of shape on forced convective transfer from oblate spheroids was studied by Skelland and Cornish (1963). Using Pasternak and Gauvin's (1960) characteristic dimension (total surface area of body divided by maximum perimeter normal to flow) they were able to correlate their experimental data by the single expression

$$Sh_o = 0.74\, Re^{\frac{1}{2}}\, Sc^{\frac{1}{3}} \qquad (2\text{-}11)$$

The experiments were made by studying the mass transfer by sublimation of naphthalene oblate spheroids with width to height ratios between 1:1 and 1:3 in air at 50°C within a Reynolds number range $100 < Re < 6000$. They found their correlation to have an

estimated standard deviation of 2.1%.

Beg (1966) extended the work of Skelland and Cornish by working on spheres, oblate spheroids, spheroids for which the front half was flatter than the back and disks. For spheroids his final correlations were

$$Sh_c = 0.62\ Re^{0.5}\ Sc^{\frac{1}{3}} \qquad 200 < Re < 2000 \qquad (2\text{-}12)$$

$$Sh_c = 0.26\ Re^{0.61} Sc^{\frac{1}{3}} \qquad 2000 < Re < 32{,}000 \qquad (2\text{-}13)$$

with a standard deviation of 3.75% and 3.50% respectively. For disks his final correlation was

$$Sh_c = 0.27\ Re^{0.6}\ Sc^{\frac{1}{3}} \qquad 270 < Re < 34{,}900 \qquad (2\text{-}14)$$

the standard deviation being 2%. Again Pasternak and Gauvin's characteristic dimension was used.

Beg extended this work to determine local rates of mass transfer and found that his experimental results were in good agreement with his theoretical predictions up to a parametric angle $60^{\circ}$ around the body.

## 2.4 AXISYMMETRIC BODY ROTATING IN A QUIESCENT FLUID

### 2.4.1 Theoretical Solutions

The flow induced by an axisymmetric body rotating in an otherwise undisturbed fluid for incompressible flow has received much attention over the last century.

The first analysis of such a flow was presented by Von Karman (1921) who assumed that the flow induced by a disc could be treated as a similarity flow. His equations were later solved using an asymptotic expansion method by Cochran (1934) whose solutions were an exact solution of the Navier-Stokes equations.

The body that has received most attention however has been the sphere. The first attempt to present a theoretical analysis of the

flow induced by a sphere rotating in an incompressible quiescent fluid was made by Howarth (1951) who extended Von Karmans' previous work on the disc. Being more interested in the equatorial region of the sphere he attempted an approximate solution of the relevent boundary layer equations utilising Pohlhausen type velocity profiles. He believed this type of solution would be of more use than an exact solution by series method as the series solution would probably not have the desired convergence in the viscinity of the equator.

Howarth assumed that because of symmetry the boundary layer region could be considered as being composed of two hemispherical boundary layers, the circumferential velocity of the body inducing a secondary flow in a direction pole to equator, the occurrence of this in both hemispheres would lead to an eruption of both flows at the equator. His theoretical results suggested that there would be an inflow over the whole boundary layer - an obviously incorrect result, continuity not being satisfied. Howarth came to the conclusion that in order to satisfy continuity an outflow had to occur in the equatorial region, he was of the opinion that boundary layer theory broke down in this region, the parabolic form of the boundary layer equations failing to describe accurately the flow.

Bowden and Lord (1963) used the theory of Howarth to obtain an expression

$$T = -2.93\, a^3 \mu R_s^{\frac{1}{2}} \Omega \qquad (2\text{-}15)$$

for the torque associated with a rotating sphere.

Nigam (1954) disagreed with Howarth's assessment of the failure of the boundary layer equations in the viscinity of the equator. Introducing a slightly different form of series expansion for the velocity components from Howarth his results suggested that up to a

critical parametric angle of $54.7^{\circ}$ there was inflow into the boundary layer, this then being balanced by outflow over the rest of the hemisphere. His results suggest that at the equator the boundary layers have lost all their fluid and hence no erruption occurs.

Benton (1965) has shown that Nigam's expansions predict that the boundary layer has a constant thickness, an obviously wrong result as shown by the experimental evidence of Kreith et al (1963) and Kobashi (1957).

Stewartson (1957) has also shown in a qualitative manner that Nigam's results are wrong and that collision of the boundary layers at the equator is unavoidable. Stewartson came to the conclusion that a radial jet would be formed and that the region of boundary layer breakdown would be within a distance $O(\nu^{\frac{1}{2}})$ from the equator.

Banks (1965) presented a more recent analysis of the same problem in which he utilised the series solution method proposed in Howarth's (1951) paper; namely if r, $\theta$, $\phi$ are the normal spherical polar co-ordinates and w, u, v are the respective velocity components then

$$\begin{aligned} u &= a\Omega(\theta F_1 + \theta^3 F_3 + \ldots\ldots) \\ v &= a\Omega(\theta G_1 + \theta^3 G_3 + \ldots\ldots) \\ w &= (\nu\Omega)^{\frac{1}{2}}(\bar{H}_1 + \theta^2 \bar{H}_3 + \ldots\ldots) \end{aligned} \qquad (2\text{-}16)$$

are the expansions. Here a is the sphere radius, $\Omega$ is its angular velocity and the F's, G's and $\bar{H}$'s are functions of the dimensionless perpendicular distance Z from the body surface defined as follows:

$$Z = (\Omega/\nu)^{\frac{1}{2}}(r-a) \qquad (2\text{-}17)$$

The boundary values proposed being

$$\begin{aligned} F_n(o) &= H_n(o) = G_n(o) - \frac{(-1)^{\frac{(n-1)}{2}}}{n!} = 0 \\ F_n(\infty) &= G_n(\infty) = 0 \end{aligned} \qquad (2\text{-}18)$$

However this theory still has the disadvantage that the value of $H(\infty)$ is finite and negative, thus predicting radial inflow over the entire boundary layer right up to the equator, the same result as Howarth. However, it is interesting to note that Banks'(1965) expression for torque

$$T = -3.27\, a^3 \mu R_s^{\frac{1}{2}} \Omega \qquad (2\text{-}19)$$

which was calculated on the basis of the first four terms of the v expansion is within 6% of Bowden and Lord's (1963) experimental result. Banks(1965)[2] criticised Hoskin's (1955) theoretical results for separation angle because they fail to take into account that a rotating sphere in axial flow can still induce a hemispherical boundary layer in the wake region. He suggests that Hoskin's method for calculation of separation angle is only valid when the spin parameter is small when compared to unity.

A finite difference method of solving the boundary layer equations has been demonstrated by Manohar (1967) whose results agree to three significant figures with those of Howarth and to six significant figures with those of Banks (1965). Manohar presented the expression

$$T = -3.265\, a^3 \mu R_s^{\frac{1}{2}} \Omega \qquad (2\text{-}20)$$

for torque.

The same problem has also been studied by Dorfman et al (1965) whose solutions of the boundary layer equations were obtained by dividing the surface of an arbitrary body into small sections each being treated as a 'similarity' shape, his results are in good agreement with previously mentioned workers.

A critical analysis of both approximate and exact solutions of the pertinent boundary layer equations for axisymmetric bodies

rotating in a quiescent fluid has been presented by Benton (1965). Benton gave the following reasons for the inaccuracy of boundary layer solutions.

a) When the boundary layer approximations are applied to the Navier-Stokes equations there is a change in mathematical classification of the partial differential equations from elliptic to parabolic.

b) Karman-Pohlhausen type approximate solutions use only a polynominal approximation of the velocity distributions.

c) The neglection of the radial pressure gradient lowers the order of the mathematical system by unity, hence one boundary condition cannot be satisfied. This final objection leads to qualitatively incorrect results such as the prediction of radial inflow over the whole boundary layer surface.

Benton suggested a more realistic model would be obtained from a solution of the Navier-Stokes equations using the criteria of all velocity components vanishing toward infinity for the boundary conditions.

Solutions of the boundary layer heat or mass transfer equations have been put forward by researchers who have utilised the hydrodynamic theory previously described. Singh (1960) used Nigam's (1954) method and found that the constant boundary layer thickness overestimated the effect of rotation on heat transfer at the polar region and underestimated it in the equatorial region.

Banks (1965)[1] extended his own work (1965)[2] to study local heat transfer rates, he obtained four terms in his series expansion

$$\frac{Nu}{R_s^{\frac{1}{2}}} = -\sum_{n=0}^{\infty} \Theta'_{2n+1}(o)\,\theta^{2n} \qquad (2\text{-}21)$$

for Prandtl numbers of 0.7 and 1.0, his results gave

$$\frac{Nu_o}{R^{\frac{1}{2}}} = 0.25 \qquad Pr = 0.7$$

$$\frac{Nu_o}{R^{\frac{1}{2}}} = 0.30 \qquad Pr = 1.0 \qquad (2\text{-}22)$$

Other bodies have been studied, Fadnis (1954) has extended Nigam's approximate solution to cover oblate and prolate spheroids, most other work however seems to have been done on discs and cones, both bodies being treated as similarity shapes extending either Von Karman's exact solution of the Navier-Stokes equations or other workers approximate solutions.

The first approximate solution for heat transfer from a rotating disc under laminar flow conditions was presented by Wagner (1948), Millsaps and Pohlhausen (1952) extended Von Karman's method to cover the case of heat transfer. Ostrach and Thornton (1958) neglected viscous dissipation and solved the heat transfer boundary layer equation for the case of an isothermal disk at Prandtl number 0.72, Sparrow and Gregg (1959) extended these results to a wider range of Prandtl number.

For the cone an analytical solution was first presented by Wu (1959) who showed that for the boundary layer equations his results for the velocity distribution could be obtained from solutions pertaining to the flow induced by a rotating disk. Tien (1960) extended this work to show that the heat transfer from rotating cones in a quiescent fluid could be predicted from analogous results for the rotating disc.

A most comprehensive literature survey on the effect of rotation of cones and discs has been presented by Subramaniyan et al (1956).

Theoretical results for heat transfer from rotating cones and disks have been published in the form

$$Nu_o \equiv (h_c x_o/K) = C(\Omega X_o^2 \sin\alpha/\nu)^{0.5} = C\, Re_o^{0.5} \qquad (2\text{-}23)$$

For Prandtl number 0.72

Ostrach and Thornton (1958) gave $C = 0.329$

Wagner (1948) $= 0.335$

Millsaps and Pohlhausen (1952) $= 0.28$ (2-24)

For Prandtl number 2.42

Sparrow and Gregg (1959 gave $C = 0.625$

Work has been carried out on similarity solutions for other axisymmetric bodies rotating in a quiescent fluid. Geis (1956) has shown that the disc and the cone are but two examples of a broader class of geometrical shapes for which similarity solutions of the boundary layer equations exist. He has shown that when the body shape can be expressed in the form

$$r(X) = L_c.(\frac{X}{L_c})^{(2m-1)/3}, \quad m \geqslant 2 \qquad (2\text{-}25)$$

where r(X) - radius of revolution of the body

X - distance from front stagnation point measured along meridian curve

$L_c$ - characteristic length of body

m - a parameter

then a similarity solution exists for that body. Hayday (1964/65) extended the theory to cover the case of heat transfer and showed that when the surface temperature distribution is given by

$$T_W - T_A = \text{constant } (X/L_c)^n \qquad (2\text{-}26)$$

where n is another parameter, then similarity solutions exist for the heat transfer boundary layer equations.

It can be seen from the literature survey that whilst much work has been done on the sphere, cone and the disk there is as yet no

general theoretical approach that is suitable for all shapes. In particular whilst overall heat transfer coefficients have been published for the sphere at a few Prandtl numbers no results have been published for oblate spheroids.

It was hence decided that for the case of an axisymmetric body rotating in a quiescent fluid a general solution of the hydrodynamic and energy (or mass) transfer boundary layer equations should be presented, also the overall heat (or mass) transfer coefficients for some oblate spheroids should be presented, these results being a limiting case of the main work. It was decided that the method of approach should follow that as outlined by Howarth, experimental evidence suggesting that this method is superior to that of Nigam.

### 2.4.2 Experimental Results

An insight into the limitations of different theoretical analyses has come from visual observation of the induced flow itself.

The first comment on this type of induced flow was that of Sir G.G. Stokes (1845) who described the flow around a rotating sphere,

> "The sphere acts like a centrifugal fan, the motion at a distance from the sphere consisting of flow outwards from the equator and inwards towards the poles, superimposed on a motion of rotation."

Kreith et al (1963) used smoke to visualise flow in the boundary layer of a rotating sphere. They found that the smoke entered at the poles where it was transported through the boundary layer to the equator where the two streams collided.

Similar investigations were carried out by Bowden and Lord (1963) who, using a Schlieren technique obtained the same qualitative results as Kreith et al.

The results of Kobashi (1957) however are in direct contradiction

to those of Kreith et al and Bowden and Lord. Kobashi found inflow occupied up to $54.5^{\circ}$ parametric angle around the sphere and then outflow which seems to confirm Nigam's (1954) theory, however Kreith is highly critical of Kobashi's experimental technique which determined the resultant velocity vector using a hot wire anemometer.

Bowden and Lord (1963) have measured the torque coefficient of the rotating sphere experimentally and found it to be -3.5, this is slightly different from the value -3.27 predicted by Banks (1965) who derived his result on the basis of boundary layer theory, this represents a difference of about $6\frac{1}{2}\%$.

Kreith et al (1963) performed heat transfer experiments on a rotating sphere in different fluids they obtained the following correlations

$$Nu_o = 0.43\, R_s^{0.5}\, Pr^{0.4} \qquad \left.\begin{array}{l} Gr < 0.1\, R_s^2 \\ R_s < 5\times10^5 \\ 0.7 < Pr < 217 \end{array}\right\} \qquad (2\text{-}27)$$

$$Nu_o = 0.066\, R_s^{0.67}\, Pr^{0.4} \qquad \left.\begin{array}{l} Gr < 0.1\, R_s^2 \\ 5\times10^5 < R_s < 7\times10^6 \\ 0.7 < Pr < 7 \end{array}\right\} \qquad (2\text{-}28)$$

Both correlations (2-27) and (2-28) were found to be within 15% of experimental results. Kreith found that for $R_s < 5\times10^5$ the laminar regime existed except in the viscinity of the poles. He found also that below $R_s$ of $5\times10^4$ no appreciable outflow occurred from the boundary layer over the sphere except in the narrow equatorial zone.

Subraminiyan (1956) et al used a diffusion controlled electrode reaction system to show that for cones with apex angle $> 40^{\circ}$

$$Sh_o = 0.345\, (l^2\Omega \sin\alpha/\nu)^{0.5}\, Sc^{0.4} \qquad (2\text{-}29)$$

for disks

$$Sh_o = 0.345\ (\Omega d^2/\nu)^{0.5}\ Sc^{0.4} \qquad (2\text{-}30)$$

and for the sphere

$$Sh_o = 0.25\ (\Omega d^2/\nu)^{0.5}\ Sc^{0.4} \qquad (2\text{-}31)$$

These correlations have an average deviation of ±10% from the experimental results.

Tien and Campbell (1963) found that for the naphthalene air system cones with a vertex angle greater than $90^o$ gave experimental results for mass transfer that are in excellent agreement with the predicted value of Sparrow and Gregg (1959). They also found that the spin Reynolds number of transition from laminar to turbulent flow is in the range

$$2x10^5 < (R_s)_{critical} < 2.5x10^5$$

Gregory and Walker (1960) found that for a polished disk the critical Reynolds number was $1.35x10^5$.

Nordlie and Kreith (1961-62) obtained heat transfer data from a rotating heated aluminium sphere in still air, they presented the following correlations:

$$Nu_o = 2 + 0.34\ (Gr)^{0.27} \qquad 0 < Gr < 2x10^7 \qquad (2\text{-}32)$$

which has an average deviation from experimental data of ±20%

$$Nu_o = 2(R^2 + Gr)^{0.164} \qquad \begin{matrix} Gr/R^2 > 0.1 \\ 1x10^3 < R < 1.8x10^4 \end{matrix} \qquad (2\text{-}33)$$

$$Nu_o = 0.29\ R^{0.527} \qquad \begin{matrix} Gr/R^2 < 0.1 \\ 1.8x10^4 < R < 1.3x10^5 \end{matrix} \qquad (2\text{-}34)$$

with an average deviation from experimental data of ±12% here $R_s$

the spin Reynolds number being given by $R_s = \Omega D^2/\nu$. Using both shadow photography and smoke patterns they also studied the flow field around the rotating sphere, these qualitative studies agreed with the results obtained by both Bowden and Lord and Kreith et al.

Noordzij and Rotte (1967) have also obtained experimental data for rotating spheres by means of an electro-chemical method, their results were correlated as follows,

$$\left.\begin{aligned} \frac{h_c d}{\alpha_v} &= 10 + 0.43\left(\frac{\Omega d^2}{\nu}\right)^{\frac{1}{2}} \left(\frac{\nu}{\alpha_v}\right)^{\frac{1}{3}} \\ \text{for range } \quad 0.8\times10^3 &< \left(\frac{\Omega d^2}{\nu}\right) < 27\times10^3 \\ 0.5\times10^3 &< \left(\frac{\nu}{D_v}\right) < 2\times10^3 \end{aligned}\right\} \qquad (2\text{-}35)$$

Their correlation had an average deviation from their experimental data of $\pm 5\%$.

The experimental evidence presented by all workers (except Kobashi) agrees with the model presented by Howarth, namely the rotation of the body induces a flow from pole to equator. This forms two hemispherical boundary layers which collide in the equatorial region. Hence inflow occurs at the two poles and erruption occurs at the equator no flow occurring across the boundary layer at any other point.

Although Benton (1965) has made criticisms of the boundary layer technique in solving our particular problem, the boundary layer theory is still capable of giving an accurate quantitative value for the torque coefficient of a rotating sphere. There is only a $6\frac{1}{2}\%$ difference between the experimentally measured value of Bowden and Lord and Banks' theoretical values this probably being due to the boundary layer theory having more validity at the body-fluid interface

although giving a qualitatively incorrect picture at the edge of the boundary layer.

Hence from experimental results of other workers it would seem that

1) The flow field for the rotating sphere as described by Howarth is correct, also oblate spheroids and other enclosed bodies of revolution when rotating about their axis of symmetry would have similar flow patterns, i.e. inflow at poles and erruption at the equator.

2) The boundary layer theory would probably yield good theoretical results for local mass or heat transfer coefficients as these are dependent on concentration or temperature gradients at the body-fluid interface (where the boundary layer theory is most valid).

3) For the sphere or oblate spheroid rotating in a quiescent fluid, boundary layer theory can be used to predict mass or heat transfer effects in all but a very thin eruption area around the equator. Hence it is possible to calculate overall mass or heat transfer coefficients from boundary layer theory alone.

# CHAPTER III

# THEORETICAL ANALYSIS

## 3.1 INTRODUCTION

We have shown in the literature survey that very few solutions of the laminar boundary layer equations exist for the cases of a) an axisymmetric body rotating about its axis of symmetry in axial flow; b) an axisymmetric body rotating about its axis of symmetry in a quiescent fluid. Those analyses that do exist are of such a form as to restrict their extension to more complex axisymmetric shapes, this being primarily due to the non-general co-ordinate systems employed.

In the present analysis we are concerned with both cases a) and b) above, the analysis is in a general form utilising non-rotating orthogonal curvilinear co-ordinates. The velocity components and scale factors are represented by power series which when substituted into the boundary layer equations transform them from partial differential equations to sets of ordinary differential equations in the form of boundary value problems.

The analyses of the two types of situation are given in such a form as to make the solution of the pertinent equations straightforward by means of a computer routine. It was found that this routine was sufficiently general to require just one subroutine (supplying power series forms of the potential flow and scale factors) for each axisymmetric shape analysed.

As an example of the use of this programme an analysis of the

heat or mass transfer process for rotating spheres and oblate spheroids is given.

The present analysis is limited to solid isothermal bodies rotating about their axis of symmetry in incompressible flow with laminar boundary layers. In the analysis it is also assumed that heat generated by viscous dissipation is negligible.

## 3.2 DERIVATION OF THE BOUNDARY LAYER EQUATIONS FOR AN AXISYMMETRIC BODY IN ORTHOGONAL CURVILINEAR CO-ORDINATES

### 3.2.1 Navier-Stokes Equations for an Axisymmetric Body

The equations governing the momentum and mass (or heat) transfer at a point in an incompressible fluid for which heat generation by viscous dissipation is negligable are:

$$\frac{D\underline{v}}{Dt} = -\frac{1}{\rho}\nabla P + \nu\nabla^2\underline{v} \qquad \text{Navier-Stokes equation} \qquad (3\text{-}1)$$

$$\nabla\cdot\underline{v} = 0 \qquad \text{Continuity equation} \qquad (3\text{-}2)$$

$$\frac{DX}{Dt} = \alpha_v\nabla^2 X \qquad \text{Heat or mass transfer equation} \qquad (3\text{-}3)$$

Here $\underline{v}$ is the velocity vector, $\rho$ the density of the fluid, the kinematic viscosity, $\alpha_v$ the diffusivity, P the pressure and X is the temperature or solute concentration all measured at the point itself. The term $\frac{D}{Dt}$ is the substantial derivative and is defined as

$$\frac{D}{Dt} = \frac{\partial}{\partial t} + (\underline{v}\cdot\nabla)$$

To define fully our system we have to introduce our boundary conditions on the velocity vector $\underline{v}$ and the transfer function X, to obtain these we assume the following,

a) at the solid-fluid interface there is no slip between the solid and the fluid,

b) for mass transfer the flux at the interface is small enough to be negligible,

c) for heat transfer, temperature differences are small enough to assume that changes in the physical properties of the fluid are negligible,

d) the velocity and concentration (or temperature) distributions become asymptotic to their values in the undisturbed fluid as the distance from the body increases.

We hence obtain the following boundary conditions:

$$\begin{aligned} \underline{n} &= 0 \qquad \underline{v} = (\underline{v})_s \qquad X = X_s \\ \underline{n} &\longrightarrow \infty \qquad \underline{v} \longrightarrow (\underline{v})_\infty \qquad X \longrightarrow X_m \end{aligned} \tag{3-4}$$

where $\underline{n}$ is the vector normal to the body surface,

$X_s$ is the temperature or concentration at the surface,

$X_m$ is the temperature or concentration in the main stream,

$(\underline{v})_s$ is the velocity vector at body surface (not zero for a rotating body),

$(\underline{v})_\infty$ is the velocity vector in the main stream.

If we assume that our flow is time independent then $\frac{\partial}{\partial t} = 0$ and our equations (3-1) to (3-3) reduce to

$$(\underline{v}.\nabla \underline{v}) = -\frac{1}{\rho}\nabla P + \nu \nabla^2 \underline{v} \tag{3-5}$$

$$\nabla . \underline{v} = 0 \tag{3-6}$$

$$(\underline{v}.\nabla)X = \alpha_v \nabla^2 X \tag{3-7}$$

We now wish to express our vector equations in terms of the orthogonal co-ordinate system $(x_1, x_2, x_3)$, $x_1$ will be measured as positive in the direction of fluid flow and is termed the meridional co-ordinate, $x_2$ is taken as positive in the direction of rotation of

the solid about its axis and is termed the azimuthal direction, $x_3$ is the third of the triply orthogonal set and is perpendicular to the other two co-ordinates, all three surfaces $x_1$ = constant, $x_2$ = constant and $x_3$ = constant being mutually perpendicular.

The transformation of the equations (3-5) to (3-7) into the orthogonal co-ordinate system is presented in appendix A for the general case of a three dimensional body in incompressible flow. If the body has an axis of symmetry and is in an axisymmetric flow field then functions will be independent of the azimuthal direction and hence

$$\frac{\partial}{\partial x_2} = 0 \tag{3-8}$$

We can thus simplify the general three dimensional equations for mass (or heat), momentum and continuity for an axisymmetric body in an axisymmetric flow field to:

<u>momentum meridional direction</u>:

$$\frac{V_1(V_1)_{x_1}}{h_1} - \frac{V_2^2(h_2)_{x_1}}{h_1h_2} + \frac{V_3(V_1h_1)_{x_3}}{h_3h_1} - \frac{V_3^2(h_3)_{x_1}}{h_3h_1} =$$

$$-\frac{1}{\rho h_1}(P)_{x_1} + \frac{\nu}{h_2h_3}\left(\frac{h_2}{h_3h_1}\left\{(V_1h_1)_{x_3} - (V_3h_3)_{x_1}\right\}\right)_{x_3} \tag{3-9}$$

<u>momentum azimuthal direction</u>:

$$\frac{V_3}{h_2h_3}(V_2h_2)_{x_3} + \frac{V_1}{h_1h_2}(V_2h_2)_{x_1} =$$

$$\frac{\nu}{h_1h_3}\left[\left\{\frac{h_1}{h_2h_3}(V_2h_2)_{x_3}\right\}_{x_3} - \left\{\frac{h_3}{h_1h_2}(V_2h_2)_{x_1}\right\}_{x_1}\right] \tag{3-10}$$

momentum normal direction:

$$\frac{V_1}{h_3}(V_1)_{x_3} + \frac{V_2}{h_3}(V_2)_{x_3} + \frac{V_3}{h_3}(V_3)_{x_3} - \frac{V_1}{h_3 h_1}\left\{(V_1 h_1)_{x_3} - (V_3 h_3)_{x_1}\right\}$$

$$- \frac{V_2}{h_2 h_3}(V_2 h_2)_{x_3} = -\frac{1}{\rho h_3}(P)_{x_3} - \frac{\nu}{h_1 h_2}\left(\frac{h_2}{h_3 h_1}\left\{(V_1 h_1)_{x_3} - (V_3 h_3)_{x_1}\right\}\right)_{x_1} \tag{3-11}$$

continuity:

$$\frac{1}{h_1 h_2 h_3}\left[(h_2 h_3 V_1)_{x_1} + (h_1 h_2 V_3)_{x_3}\right] = 0 \tag{3-12}$$

mass (or heat) transport:

$$\frac{V_1}{h_1}(X)_{x_1} + \frac{V_3}{h_3}(X)_{x_3} = \frac{\alpha_v}{h_1 h_2 h_3}\left[\left(\frac{h_2 h_3}{h_1}(X)_{x_1}\right)_{x_1} + \left(\frac{h_1 h_2}{h_3}(X)_{x_3}\right)_{x_3}\right] \tag{3-13}$$

where $h_1$, $h_2$, $h_3$ are the scale factors for co-ordinate $x_1$, $x_2$, $x_3$ respectively. Our boundary conditions in terms of the new co-ordinate system are:

$$\begin{aligned} &\text{at } x_3 = (x_3)_s \quad V_1 = V_3 = 0; \quad V_2 = (V_2)_s; \quad X = X_s \\ &\text{as } x_3 \to \infty \quad V_1 \to (V_1)_\infty \; ; \; V_3 \to (V_3)_\infty \; ; \; V_2 \to 0; \; X \to X_m \end{aligned} \tag{3-14}$$

where $(x_3)_s$ is the value of co-ordinate $x_3$ at the body surface, $(V_2)_s$ is the value of the velocity component $V_2$ at the body surface and $(V_1)$ and $(V_3)$ are the components of $V_1$ and $V_3$ in the bulk flow. It should be noted that we have used the following nomenclature for partial differentiation:

$$\frac{\partial A}{\partial x_i} \equiv (A)_{x_i} \text{ and } \frac{\partial^2 A}{\partial x_i^2} \equiv (A)_{x_i, x_i}$$

### 3.2.2 Derivation of the Boundary Layer Equations for a Body of Revolution Rotating in Axial Flow

It can be seen from the complexity of the Navier-Stokes equations (as derived in section 3.2.1) that their solution presents us with a formidable task, first, the partial differential equations are non-linear, second, the scale factors are variables which brings added difficulty.

Prandtl (1904) presented a method of simplification of the Navier-Stokes equations by introducing the concept of the boundary layer. He showed that the flow of a fluid over a body wall could be divided into two regions, the first in the immediate neighbourhood of the body wall, here the velocity gradient normal to the wall $(\frac{1}{h_3}\frac{\partial V_1}{\partial x_3})$ is very large, hence the shearing stress $\tau = \mu(\frac{1}{h_3}\frac{\partial V_1}{\partial x_3})$ can also be high despite a low viscosity $\mu$. In this region then the viscosity of the fluid exerts a decisive influence on the fluid flow. The remaining region is characterised by a low normal velocity gradient, here the effect of viscosity is negligible, the flow being treated as potential. The first region described was termed by Prandtl 'the boundary layer' and in general it diminishes in thickness as the Reynolds number increases.

Utilising the fact that the boundary layer thickness will tend to zero as the Reynolds number approaches infinity (assuming a turbulent boundary layer is not formed) Rosenhead (1965) presented a method for obtaining the boundary layer equations by taking the limiting form of the Navier-Stokes equations as the Reynolds number approaches infinity. These boundary layer equations although only strictly valid in the limit of infinite Reynolds number should give a good approximation of the flow for which Reynolds number is large but not infinite.

In order to reduce the Navier-Stokes equations to a more

manageable form it is necessary to determine the relative importance of each term in each equation. This present work is concerned with the forced convective region of mass and heat transfer, it being assumed that the Reynolds number is high enough for Prandtl's boundary layer assumptions to be valid.

First it is necessary to put the Navier-Stokes equations into a dimensionless form by defining a characteristic dimension $L_c$ and a characteristic velocity $U_c$ which could be for example the main stream velocity $U_\infty$ . It should be noted that the dimension of a scale factor is dependent on the dimension of its associated co-ordinate. In general the incremental distance ds between two points $(x_1, x_2, x_3)$ and $(x_1+dx_1, x_2+dx_2, x_3+dx_3)$ is given by the expression

$$(ds)^2 = h_1^2 dx_1^2 + h_2^2 dx_2^2 + h_3^2 dx_3^2 \qquad (3\text{-}15)$$

Now the incremental distance ds has the dimension of length hence the product $h_i dx_i$ must have the dimension length, i.e. if a co-ordinate has a dimension of length then its scale factor is dimensionless, the converse is also true. We can thus define the following dimensionless groups,

$$V_1^* = \frac{V_1}{U_c} \; ; \; V_2^* = \frac{V_2}{U_c} \; ; \; V_3^* = \frac{V_3}{U_c} \qquad (3\text{-}16)$$

and

$$h_i^* dx_i^* = h_i dx_i / L_c \qquad i = 1,2,3 \qquad (3\text{-}17)$$

The dimensionless form of pressure being defined

$$P^* = P/\rho U_c^2 \qquad (3\text{-}18)$$

and the dimensionless temperature or concentration

$$X^* = (X - X_m)/(X_s - X_m)$$

The substitution of these dimensionless forms leads to the following form of the Navier-Stokes equations.

momentum meridional direction:

$$\frac{V_1^*}{h_1^*}(V_1^*)_{x_1^*} - \frac{V_2^{*2}}{h_1^* h_2^*}(h_2^*)_{x_1^*} + \frac{V_3^*}{h_3^* h_1^*}(V_1^* h_1^*)_{x_3^*} - \frac{V_3^{*2}}{h_3^* h_1^*}(h_3^*)_{x_1^*} =$$

$$- \frac{1}{h_1^*}(P^*)_{x_1^*} + \frac{1}{Re} \cdot \frac{1}{h_2^* h_3^*}\left(\frac{h_2^*}{h_3^* h_1^*}\left\{(V_1^* h_1^*)_{x_3^*} - (V_3^* h_3^*)_{x_1^*}\right\}\right)_{x_3^*} \qquad (3\text{-}19)$$

momentum azimuthal direction:

$$\frac{V_3^*}{h_2^* h_3^*}(V_2^* h_2^*)_{x_3^*} + \frac{V_1^*}{h_1^* h_2^*}(V_2^* h_2^*)_{x_1^*} = \frac{1}{Re} \cdot \frac{1}{h_1^* h_3^*}\left[\left\{\frac{h_1^*}{h_2^* h_3^*}(V_2^* h_2^*)_{x_3^*}\right\}_{x_3^*} - \left\{\frac{h_3^*}{h_1^* h_2^*}(V_2^* h_2^*)_{x_1^*}\right\}_{x_1^*}\right] \qquad (3\text{-}20)$$

momentum normal direction:

$$\frac{V_1^*}{h_3^*}(V_1^*)_{x_3^*} + \frac{V_2^*}{h_3^*}(V_2^*)_{x_3^*} + \frac{V_3^*}{h_3^*}(V_3^*)_{x_3^*} - \frac{V_1^*}{h_3^* h_1^*}\left\{(V_1^* h_1^*)_{x_3^*} - (V_3^* h_3^*)_{x_1^*}\right\}$$

$$- \frac{V_2^*}{h_2^* h_3^*}(V_2^* h_2^*)_{x_3^*} = - \frac{1}{h_3^*}(P^*)_{x_3^*} - \frac{1}{Re} \cdot \frac{1}{h_1^* h_2^*}\left[\frac{h_2^*}{h_3^* h_1^*}\left\{(V_1^* h_1^*)_{x_3^*} - (V_3^* h_3^*)_{x_1^*}\right\}\right]_{x_1^*} \qquad (3\text{-}21)$$

continuity equation:

$$\frac{1}{h_1^* h_2^* h_3^*}\left[(h_2^* h_3^* V_1^*)_{x_1^*} + (h_1^* h_2^* V_3^*)_{x_3^*}\right] = 0 \qquad (3\text{-}22)$$

mass (or heat) transport equation:

$$\frac{V_1^*}{h_1^*}(X^*)_{x_1^*} + \frac{V_3^*}{h_3^*}(X^*)_{x_3^*} = \frac{1}{\overline{Pr}} \cdot \frac{1}{Re} \cdot \frac{1}{h_1^* h_2^* h_3^*} \left[ \left( \frac{h_2^* h_3^*}{h_1^*}(X^*)_{x_1^*} \right)_{x_1^*} + \left( \frac{h_1^* h_2^*}{h_3^*}(X^*)_{x_3^*} \right)_{x_3^*} \right] \tag{3-23}$$

Our boundary conditions now become:

$$\text{At } x_3^* = (x_3^*)_s \quad V_1^* = V_3^* = 0; \quad V_2^* = (V_2^*)_s; \quad X^* = 1$$

$$\text{as } x_3^* \longrightarrow \infty \qquad V_1^* \longrightarrow (V_1^*)_\infty \quad ; \quad V_3^* \longrightarrow (V_3^*)_\infty \quad ; \quad V_2 \longrightarrow 0; \quad X^* \longrightarrow 0 \tag{3-24}$$

which are all dimensionless. In the above equations Re is the Reynolds number and is given by $Re = U_c L_c/\nu$ and $\overline{Pr}$ is the Schmidt number for mass transfer (or Prandtl number for heat transfer) and is given by $\overline{Pr} = \nu/\alpha$.

In order to make an order of magnitude analysis of our equations we have to make certain assumptions. First because our axisymmetric body is smoothly curved we assume that the scale factors and their derivatives with respect to the co-ordinates are of order unity. The dimensionless co-ordinates must be of the same order of magnitude as the dimensionless distances over which they are measured. If we define a dimensionless hydrodynamic boundary layer thickness as $\delta^*$ then

$$\begin{aligned} h_1^* x_1^* &= O(1) \\ h_2^* x_2^* &= O(1) \\ h_3^* x_3^* &= O(\delta^*) \end{aligned} \tag{3-25}$$

Now the velocity $V_1$ increases from zero at the body surface to the potential velocity at the edge of the boundary layer hence

$$\begin{aligned} V_1^* &= O(1) \\ \frac{1}{h_1^*}(V_1^*)_{x_1^*} &= O(1) \\ \frac{1}{h_3^*}(V_1^*)_{x_3^*} &= O(1/\delta^*) \end{aligned} \tag{3-26}$$

From the continuity equation it can be seen that as the order of magnitude of $(h_2^* h_3^* V_1^*)_{x_1^*}$ must be the same as that of $-(h_1^* h_2^* V_3^*)_{x_3^*}$, then we have $(V_3^*)_{x_3^*} = O(1)$ as the order of magnitude of the scale factors is unity, hence $V_3^* = O(\delta^*)$. Rosenhead (1965) has shown that over the region for which Prandtl's boundary layer simplifications hold true the dimensionless hydrodynamic boundary layer thickness has an order of magnitude given by

$$\delta^* = O(1/Re^{\frac{1}{2}}) \tag{3-27}$$

Rosenhead hence suggested the substitution

$$\begin{aligned} V_3^{**} &= V_3^* Re^{\frac{1}{2}} \\ X_3^{**} &= X_3^* Re^{\frac{1}{2}} \end{aligned} \tag{3-28}$$

into the dimensionless Navier-Stokes equations in order that an analysis may be made of the relevant importance of each term in the limiting case as the Reynolds number $Re \rightarrow \infty$.

On substitution of (3-28) into the dimensionless Navier-Stokes equation we obtain

momentum (meridional) equation:

$$\frac{V_1^*}{h_1^*}(V_1^*)_{x_1^*} - \frac{V_2^{*2}}{h_1^* h_2^*}(h_2^*)_{x_1^*} + \frac{V_3^{**}}{h_3^* h_1^*}(V_1^* h_1^*)_{x_3^{**}} - \frac{V_3^{**2}}{Re.h_3^* h_1^*}(h_3^*)_{x_1^*} =$$

$$- \frac{1}{h_1^*}(P^*)_{x_1^*} + \frac{1}{h_2^* h_3^*}\left(\frac{h_2^*}{h_3^* h_1^*}(V_1^* h_1^*)_{x_3^{**}}\right)_{x_3^{**}} - \frac{1}{Re}\cdot\frac{1}{h_2^* h_3^*}\left(\frac{h_2^*}{h_3^* h_1^*}(V_3^{**} h_3^*)_{x_1^*}\right)_{x_3^{**}} \tag{3-29}$$

momentum (azimuthal) equation:

$$\frac{V_3^{**}}{h_2^* h_3^*}(V_2^* h_2^*)_{x_3^{**}} + \frac{V_1^*}{h_1^* h_2^*}(V_2^* h_2^*)_{x_1^*} = \frac{1}{h_1^* h_3^*}\left(\frac{h_1^*}{h_2^* h_3^*}(V_2^* h_2^*)_{x_3^{**}}\right)_{x_3^{**}}$$

$$- \frac{1}{Re}\cdot\frac{1}{h_1^* h_3^*}\left(\frac{h_3^*}{h_1^* h_2^*}(V_2^* h_2^*)_{x_1^*}\right)_{x_1^*} \tag{3-30}$$

momentum (normal) equation:

$$\frac{V_1^*}{h_3^*}(V_1^*)_{x_3^{**}} + \frac{V_2^*}{h_3^*}(V_2^*)_{x_3^{**}} + \frac{1}{Re}\frac{V_3^{**}}{h_3^*}(V_3^{**})_{x_3^{**}} - \frac{V_1^*}{h_3^* h_1^*}(V_1^* h_1^*)_{x_3^{**}}$$

$$+ \frac{1}{Re}\frac{V_1^*}{h_3^* h_1^*}(V_3^{**} h_3^*)_{x_1^*} - \frac{V_2^*}{h_2^* h_3^*}(V_2^* h_2^*)_{x_3^{**}} = - \frac{1}{h_3^*}(P^*)_{x_3^{**}}$$

$$- \frac{1}{Re}\frac{1}{h_1^* h_2^*}\left(\frac{h_2^*}{h_3^* h_1^*}(V_1^* h_1^*)_{x_3^{**}}\right)_{x_1^*} + \frac{1}{Re^2}\frac{1}{h_1^* h_2^*}\left(\frac{h_2^*}{h_3^* h_1^*}(V_3^{**} h_3^*)_{x_1^*}\right)_{x_1^*} \tag{3-31}$$

continuity equation:

$$\frac{1}{h_1^* h_2^* h_3^*}\left[(h_2^* h_3^* V_1^*)_{x_1^*} + (h_1^* h_2^* V_3^{**})_{x_3^{**}}\right] = 0 \tag{3-32}$$

heat or mass transport equation:

$$\frac{V_1^*}{h_1^*}(X^*)_{x_1^*} + \frac{V_3^{**}}{h_3^*}(X^*)_{x_3^{**}} = \frac{1}{\overline{Pr}.Re} \cdot \frac{1}{h_1^* h_2^* h_3^*}\left(\frac{h_2^* h_3^*}{h_1^*}(X^*)_{x_1^*}\right)_{x_1^*}$$

$$+ \frac{1}{\overline{Pr}} \cdot \frac{1}{h_1^* h_2^* h_3^*}\left(\frac{h_1^* h_2^*}{h_3^*}(X^*)_{x_3^{**}}\right)_{x_3^{**}} \qquad (3\text{-}33)$$

Now for large Reynolds number $x_3^*$ and $V_3^*$ are both $O(Re^{-\frac{1}{2}})$, hence both $x_3^{**}$ and $V_3^{**}$ remain finite for large Reynolds number. As the Reynolds number becomes large the dimensionless boundary layer becomes very thin and over its width (i.e. the $x_3$ direction) the scale factors will vary little and can hence be treated as independent of $x_3^{**}$.

We can thus see that the equations reduce to the following form as $Re \longrightarrow \infty$. These are the boundary layer equations in terms of dimensional variables.

momentum (meridional) equation:

$$\frac{V_1}{h_1}(V_1)_{x_1} - \frac{V_2^2}{h_1 h_2}(h_2)_{x_1} + \frac{V_3}{h_3}(V_1)_{x_3} = -\frac{1}{\rho h_1}(P)_{x_1} + \frac{\nu}{h_3^2}(V_1)_{x_3,x_3} \qquad (3\text{-}34)$$

momentum (azimuthal) equation:

$$\frac{V_1}{h_1}(V_2)_{x_1} + \frac{V_1 V_2}{h_1 h_2}(h_2)_{x_1} + \frac{V_3}{h_3}(V_2)_{x_3} = \frac{\nu}{h_3^2}(V_2)_{x_3,x_3} \qquad (3\text{-}35)$$

momentum (normal) equation:

$$\frac{1}{h_3}(P)_{x_3} = 0 \qquad (3\text{-}36)$$

continuity equation:

$$(h_2 h_3 V_1)_{x_1} + h_1 h_2 (V_3)_{x_3} = 0 \qquad (3\text{-}37)$$

heat (or mass) transport equation:

$$\frac{V_1}{h_1}(X)_{x_1} + \frac{V_3}{h_3}(X)_{x_3} = \frac{\alpha_x}{h_3^2}(X)_{x_3,x_3} \qquad (3\text{-}38)$$

It is interesting to note that equation (3-36) shows that the pressure drop across the boundary layer is very small and hence the pressure can be assumed to be that pressure impressed by the main stream. Now in the main stream we can assume that potential flow exists and hence for pure axial flow

$$V_1 \rightarrow U(x_1) \quad V_2 \rightarrow 0$$

where $U(x_1)$ is the potential velocity at $x_1$. Substitution in (3-34) yields:

$$U(U)_{x_1} = -\frac{1}{\rho}(P)_{x_1} \qquad (3\text{-}39)$$

substitution of (3-39) into (3-34) gives us the momentum meridional boundary layer in terms of the potential flow

$$\frac{V_1}{h_1}(V_1)_{x_1} - \frac{V_2^2}{h_1 h_2}(h_2)_{x_1} + \frac{V_3}{h_3}(V_1)_{x_3} = \frac{U}{h_1}(U)_{x_1} + \frac{\vartheta}{h_3^2}(V_1)_{x_3,x_3} \qquad (3\text{-}40)$$

In the above order of magnitude analysis it was stipulated that because we treat the boundary layer as being extremely thin then over the boundary layer region the scale factors could be treated as being independent of $x_3$, we hence take the scale factors as being those at the surface of the body(which is valid in the limit $Re \rightarrow \infty$). These scale factors will hence be functions of $x_1$ the meridional co-ordinate

only and in future will be denoted by

$$h_{1,0}(x_1) \; ; \; h_{2,0}(x_1) \tag{3-41}$$

A further simplification can be made with regard to the normal co-ordinate which is orthogonal to the other two co-ordinates, again because our analysis is dealing with the limiting case as $Re \to \infty$ when the boundary layer is extremely thin then we can substitute the distance normal to the body surface instead of the normal orthogonal and introduce little error. If we represent this new normal co-ordinate by N then $\partial N$ replaces $h_3 \partial x_3$ in our equations, in their new form the boundary layer equations are:

momentum (meridional) equation:

$$\frac{V_1}{h_{1,0}}(V_1)_{x_1} - \frac{V_2^2}{h_{1,0}h_{2,0}}(h_{2,0})_{x_1} + V_N(V_1)_N = \frac{U}{h_{1,0}}(U)_{x_1} + \nu(V_1)_{N,N} \tag{3-42}$$

momentum (azimuthal) equation:

$$\frac{V_1}{h_{1,0}}(V_2)_{x_1} + \frac{V_1V_2}{h_{1,0}h_{2,0}}(h_{2,0})_{x_1} + V_N(V_2)_N = \nu(V_2)_{N,N} \tag{3-43}$$

continuity:

$$(h_{2,0}\, V_1)_{x_1} + h_{1,0}\, h_{2,0}(V_N)_N = 0 \tag{3-44}$$

heat (or mass) transport:

$$\frac{V_1}{h_{1,0}}(X)_{x_1} + V_N(X)_N = \alpha_v(X)_{N,N} \tag{3-45}$$

the pertinent boundary conditions

$$\begin{aligned} &\text{at } N = 0 \quad V_1 = V_N = 0 \quad V_2 = (V_2)_s \quad X = X_s \\ &\text{as } N \to \infty \quad V_1 \longrightarrow U(x_1) \quad V_2 \longrightarrow 0 \quad X \longrightarrow X_m \end{aligned} \tag{3-46}$$

where $V_N$ is the velocity component in the direction normal to the body surface.

It should be noted that a change of mathematical form has taken place in using the boundary layer simplifications. The original Navier-Stokes equations were elliptic in mathematical form but the boundary layer equations are parabolic. This change will undoubtably have an adverse effect on the accuracy of our solutions, this, however, is the penalty one must pay when simplifying the Navier-Stokes equations to a more manageable form.

The simplifications are based on the assumption that a thin boundary layer exists, it thus restricts our analysis to the boundary layer region of the axisymmetric body, the wake region being outside the bounds of the theory.

The boundary layer simplifications were used in the momentum equation for the normal direction to show that the pressure drop across the boundary layer (in the normal direction) tends to zero as the Reynolds number tends to infinity. However the boundary layer simplifications effectively 'remove' the momentum normal equation from our mathematical system and hence reduce the order of the system by unity. Whereas previously we had two first order and two second order partial differential equations (with respect to $x_3$) we now have two second order and only one first order partial differential equations. This means that all of the six hydrodynamic boundary conditions as defined in (3-14) cannot be satisfied as this would mean an over defined system, it hence becomes necessary to leave the velocity component $V_3$ unspecified at infinity. $V_3$ should in fact be the potential flow value of the normal component in the main stream, however as it is not specified as this value it can be seen that the boundary layer equations are capable of giving qualitatively different

results from that observed in practice, this phenomena has been previously explained by Benton (1965).

These limitations on the boundary layer equations must be balanced against the tremendous simplification that has been achieved, whilst at infinity we cannot satisfy the boundary condition for $V_3$ it is expected that on the body surface all boundary values will be determined accurately, hence point heat or mass transfer coefficients (which are dependent on $\partial X/\partial x_3$ at the surface) should also be determined accurately.

### 3.2.3 Derivation of the Boundary Layer Equations for an Axisymmetric Body Rotating in a Quiescent Fluid

We must now make an order of magnitude analysis of the Navier-Stokes equations ((3-19) to (3-23)) for the case of a body rotating in a quiescent fluid. Because there is no main stream flow a different characteristic velocity must be defined, this velocity which we shall call $V_s$ will be the peripheral or rotational velocity at a defined point on the surface of the body. Again the characteristic length shall be defined as $L_c$, hence all the dimensionless variables will remain the same except the velocities now defined:

$$V_1^* = V_1/V_s \qquad V_2^* = V_2/V_s \qquad V_3^* = V_3/V_s \tag{3-47}$$

the boundary conditions being

$$\begin{aligned} &\text{at } x_3^* = (x_3^*)_s \quad V_1^* = V_3^* = 0 \quad V_2^* = (V_2^*)_s \quad X^* = 1 \\ &\text{as } x_3^* \longrightarrow \infty \quad V_1^* \longrightarrow 0 \quad V_2^* \longrightarrow 0 \quad V_3^* \longrightarrow 0 \quad X^* \longrightarrow 0 \end{aligned} \tag{3-48}$$

Once again using equations (3-25) and (3-26) the largest order of magnitude of the inertial terms on the left hand side of equations (3-19) are $O(1)$, whilst the highest on the right hand side, the viscous, terms, are $O(R_s^{-1}/\delta^{*2})$ where $\delta^*$ is a dimensionless boundary

layer thickness. Thus the order of magnitude of $\delta^*$ is given by

$$\delta^* = O(R_s^{-\frac{1}{2}}) \tag{3-49}$$

This is the same form of result as obtained in the case of a body rotating in axial flow, Re the axial Reynolds number being replaced by $R_s$ the spin Reynolds number, $R_s$ based on the peripheral velocity $V_s$.

We are now able to proceed with the same analysis as in section (3.2.2) to obtain the same boundary layer equations as in (3-42) to (3-45) with the exception of the potential flow term, if U = 0 is substituted into equation (3-39) we obtain

$$\frac{\partial P}{\partial x_1} = 0 \tag{3-50}$$

The boundary layer equations for the case of a body rotating in a quiescent fluid are thus:

momentum meridional direction:

$$\frac{V_1}{h_{1,0}}(V_1)_{x_1} - \frac{V_2^2}{h_{1,0}h_{2,0}}(h_{2,0})_{x_1} + V_N(V_1)_N = \nu (V_1)_{N,N} \tag{3-51}$$

momentum azimuthal direction:

$$\frac{V_1}{h_{1,0}}(V_2)_{x_1} + \frac{V_1V_2}{h_{1,0}h_{2,0}}(h_{2,0})_{x_1} + V_N(V_2)_N = \nu (V_2)_{N,N} \tag{3-52}$$

continuity:

$$(h_{2,0}V_1)_{x_1} + h_{1,0}\, h_{2,0}(V_N)_N = 0 \tag{3-53}$$

heat or mass transport:

$$\frac{V_1}{h_{1,0}}(X)_{x_1} + V_N(X)_N = \alpha_v (X)_{N,N} \tag{3-54}$$

with the pertinent boundary conditions

$$\begin{array}{llll} \text{at } N = 0 & V_1 = V_N = 0 & V_2 = (V_2)_s & X = X_s \\ \text{as } N \longrightarrow \infty & V_1 \longrightarrow 0 & V_2 \longrightarrow 0 & X \longrightarrow X_m \end{array} \qquad (3\text{-}55)$$

Again as in the case of a body rotating in axial flow it is necessary to remove the boundary condition $V_N \longrightarrow 0$ as $N \longrightarrow \infty$ in order that our mathematical system is not overdefined. The system again gives a qualitatively incorrect picture of the hydrodynamic process at infinity and as a consequence $V_N$ becomes finite at infinity. This is in direct contradiction to the findings of Kreith et al (1963) and Bowden and Lord (1963) who found that flow into the boundary layer takes place at the poles only and outflow occurs by eruption at the equator.

## 3.3 SOLUTION OF THE LAMINAR BOUNDARY LAYER EQUATIONS FOR AN AXISYMMETRIC BODY ROTATING ABOUT ITS AXIS OF SYMMETRY IN AXIAL FLOW

The severe limitations imposed on the domain of validity of Schlichting's (1956) approximate method of solution of the boundary layer equations suggests that the simplifications made in obtaining such solutions may not be valid for bodies rotating in axial flow, it was hence decided not to use an approximate method of solution of the boundary layer equations.

The solution of the parabolic boundary layer equations by finite difference (or 'marching') procedures requires that an initial set of conditions is known at a suitable boundary, for our physical system the suitable boundary would be at the front stagnation point. In order to obtain conditions at the front stagnation point the stagnation point equations have to be obtained.

It was hence decided that the boundary layer equations would be

solved by means of suitable power series substitutions as a method such as this would be required to determine the stagnation point equations for the 'marching' procedure anyway. It was decided that the method would be of such a form that no mathematical limitations would be placed on the number of coefficients that could be determined in the resulting power series expressions for the local Sherwood (or Nusselt) number.

### 3.3.1 Velocity Boundary Layer Equations

In order to maintain the consistency of our general analysis we shall work with the dimensionless form of the boundary layer equations. The only assumption made initially about the co-ordinate system used is that the normal distance from the body surface N.

The pertinent boundary layer equations are:

momentum meridional direction:

$$\frac{V_1^*}{h_{1,0}^*}(V_1^*)_{x_1^*} - \frac{V_2^{*2}}{h_{1,0}^* h_{2,0}^*}(h_{2,0}^*)_{x_1^*} + V_N^*(V_1^*)_{N^*} = \frac{U^*}{h_{1,0}^*}(U^*)_{x_1^*} + \frac{1}{Re}(V_1^*)_{N^*,N^*} \tag{3-56}$$

momentum azimuthal direction:

$$\frac{V_1^*}{h_{1,0}^*}(V_2^*)_{x_1^*} + \frac{V_1^* V_2^*}{h_{1,0}^* h_{2,0}^*}(h_{2,0}^*)_{x_1^*} + V_N^*(V_2^*)_{N^*} = \frac{1}{Re}(V_2^*)_{N^*,N^*} \tag{3-57}$$

continuity equation:

$$(h_{2,0}^* V_1^*)_{x_1^*} + (V_N^*)_{N^*} h_{1,0}^* h_{2,0}^* = 0 \tag{3-58}$$

the boundary conditions being:

at $N^* = 0$ $\quad V_1^* = V_N^* = 0 \; ; \; V_2^* = (V_2^*)_s$

as $N^* \longrightarrow \infty$ $\quad V_1^* \longrightarrow U_1^* \; ; \; V_2^* \longrightarrow 0$

here the characteristic velocity is $U_c$ which we will not yet define, similarly $L_c$ the characteristic length shall not yet be defined, Re the Reynolds number is given by $Re = U_c L_c/\nu$ and $N^* = N/L_c$.

In order to reduce the number of simultaneous partial differential equations from three to two we can introduce the dimensionless stream function $\psi^*$ and thus eliminate the continuity equation

$$V_1^* = (\psi^*)_{N^*} \tag{3-59}$$

now as $h_{2,0}^*$ is not a function of $N^*$ in the boundary layer region we may write

$$V_1^* = h_{2,0}^{*-1} (\psi^* h_{2,0}^*)_{N^*} \tag{3-60}$$

If we substitute this stream function into (3-58) we obtain the relationship

$$V_N^* = -\frac{1}{h_{1,0}^* h_{2,0}^*}(\psi^* h_{2,0}^*)_{x_1^*} \tag{3-61}$$

This form of the stream function is also the dimensionless form of the stream function used by Frossling (1958) for analysis of mass transfer from a stationary sphere.

Substitution of the above defined stream function into equations (3-56) and (3-57) yields:

$$(\psi^*)_{N^*}(\psi^*)_{x_1^*,N^*} - (\psi^*)_{x_1^*}(\psi^*)_{N^*,N^*} - \frac{\psi^*}{h_{2,0}^*}(h_{2,0}^*)_{x_1^*}(\psi^*)_{N^*,N^*}$$

$$- \frac{V_2^{*2}}{h_{2,0}^*}(h_{2,0}^*)_{x_1^*} = U^*(U^*)_{x_1^*} + \frac{h_{1,0}^*}{Re}(\psi^*)_{N^*,N^*,N^*} \tag{3-62}$$

$$(\psi^*)_{N^*}(V_2^*)_{x_1^*} - \frac{(h_{2,0}^*)_{x_1^*}}{h_{2,0}^*}\psi^*(V_2^*)_{N^*} - (\psi^*)_{x_1^*}(V_2^*)_{N^*}$$

$$+ \frac{(h^*_{2,0})_{x^*_1}}{h^*_{2,0}} V^*_2 (\psi^*)_{N^*} = \frac{h^*_{1,0}}{Re} (V^*_2)_{N^*,N^*} \qquad (3\text{-}63)$$

It is useful to note that equation (3-62) without the spin term $\frac{V^{*2}_2}{h^*_{2,0}}(h^*_{2,0})_{x^*_1}$ has been previously obtained by Green (1968) for the case of a non-rotating body.

Our boundary conditions now become:

$$\begin{aligned} &\text{at } N^* = 0 \quad (\psi^*)_{N^*} = \frac{1}{h^*_{1,0} h^*_{2,0}} (\psi^* h^*_{2,0})_{x^*_1} = 0 \; ; \; V^*_2 = (V^*_2)_s \\ &\text{as } N^* \to \infty \quad (\psi^*)_{N^*} \to U^* \qquad V^*_2 \to 0 \end{aligned} \qquad (3\text{-}64)$$

The solution of equations (3-62) and (3-63) with the pertinent boundary conditions (3-64) shall be obtained on the assumption that $\psi^*$, $U^*$, $h^*_{1,0}$, $h^*_{2,0}$ and $V^*_2$ can all be represented by power series in the dimensionless curvilinear co-ordinate $x^*_1$.

Let us consider the origin of our co-ordinate system as being the front stagnation point of our axisymmetric body. From fig.1 (in appendix C) which defines our general co-ordinate system we assume for any axisymmetric shape

$$\left.\begin{aligned} U^*(x^*_1) &= - U^*(-x^*_1) \\ r^*(x^*_1) &= - r^*(-x^*_1) \\ h^*_{1,0}(x^*_1) &= h^*_{1,0}(-x^*_1) \\ h^*_{2,0}(x^*_1) &= - h^*_{2,0}(-x^*_1) \end{aligned}\right\} \qquad (3\text{-}65)$$

Now $U^*$, $r^*$, $h^*_{2,0}$ must be odd functions of $x^*_1$ and hence power series expansions of these functions contain only odd powers of $x^*_1$, $h^*_{1,0}$, however, is an even function of $x^*_1$ and so will contain only even powers of $x^*_1$.

Hence

$$\left.\begin{aligned} U^* &= U_1 x_1^* + U_3 x_1^{*3} + \cdots\cdots \\ r^* &= r_1 x_1^* + r_3 x_1^{*3} + \cdots\cdots \\ h^*_{1,0} &= l_0 + l_2 x_1^{*2} + \cdots\cdots \\ h^*_{2,0} &= K_1 x_1^* + K_3 x_1^{*3} + \cdots\cdots \end{aligned}\right\} \qquad (3\text{-}66)$$

where all the coefficients are dimensionless, in short form we have:

$$\left.\begin{aligned} U^* &= \sum_{n=1}^{\infty} U_{2n-1}\, x_1^{*2n-1} \\ r^* &= \sum_{n=1}^{\infty} r_{2n-1}\, x_1^{*2n-1} \\ h^*_{1,0} &= \sum_{n=1}^{\infty} l_{2(n-1)}\, x_1^{*2(n-1)} \\ h^*_{2,0} &= \sum_{n=1}^{\infty} K_{2n-1}\, x_1^{*2n-1} \end{aligned}\right\} \qquad (3\text{-}67)$$

We may define a dimensionless perpendicular distance $\eta$ as follows:

$$\eta = N\sqrt{U_c/\nu L_c}$$

this may be re-written

$$\eta = \frac{N}{L_c}\sqrt{\frac{U_c L_c}{\nu}}$$

or

$$\eta = N^* \, Re^{\frac{1}{2}} \qquad (3\text{-}68)$$

this $\eta$ is the same as that used by Hoskin. We shall also define a Blasius form of the stream function analogous to that used by Hoskin only in dimensionless form - this will enable us to make comparisons with Hoskin's results for the rotating sphere later in the thesis.

$$\psi^*(x_1^*,N^*) = Re^{-\frac{1}{2}} \sum_{n=1}^{\infty} U_{2n-1}\, f_{2n-1}(\eta) x_1^{*2n-1} \qquad (3\text{-}69)$$

Here the dimensionless coefficients $f_{2i-1}$ are functions of our dimensionless co-ordinate $\eta$ . The Blasius form of the stream function being chosen in order to free the boundary values of the functions $f_{2i-1}$ from dependence on the Reynolds number. It follows that the pertinent boundary values will be

$$\begin{aligned} &\text{at } \eta = 0 \quad f_{2i-1} = f'_{2i-1} = 0 \\ &\text{as } \eta \longrightarrow \infty \quad f'_{2i-1} \longrightarrow 1 \end{aligned} \qquad (3\text{-}70)$$

$$\text{for all } i \geqslant 1$$

here the dash (') denotes differentiation with respect to $\eta$ . We must now choose a power series form for $V_2$. This power series must be of such a form that at the body surface ($\eta$ =0) $V_2$ is the peripheral or circumferential velocity $(V_2)_s$. Now as the body rotates about its axis of symmetry with an angular velocity Ω (radians/time) the peripheral velocity at a point $P(x_1)$ on the body surface will be given by

$$(V_2)_s = \Omega\, r(x_1) \qquad (3\text{-}71)$$

see fig.1 appendix C

Equation (3-71) may be rearranged to yield at $\eta$ = 0

$$(V_2^*)_s = \frac{(\Omega L_c)}{U_c}\, r^*(x_1^*) \qquad (3\text{-}72)$$

We can consequently choose the power series expansion for $V_2^*$ as

$$V_2^* = \frac{(\Omega L_c)}{U_c} \sum_{n=1}^{\infty} r_{2n-1}\, g_{2n-1}(\eta) x_1^{*2n-1} \qquad (3\text{-}73)$$

The boundary conditions for the coefficients $g_{2i-1}$ are

$$\begin{aligned} &\text{at } \eta = 0 \qquad g_{2i-1} = 1 \\ &\text{as } \eta \to \infty \qquad g_{2i-1} \longrightarrow 0 \end{aligned} \tag{3-74}$$

Assuming that these series expressions are absolutely convergent and also that the series which represent their derivatives are absolutely convergent we substitute them into equations (3-62) and (3-63) respectively and obtain, after simplification:

$$\begin{aligned} &\sum K_{2n-1}X_1^{*2n-1} \cdot \sum U_{2n-1}f'_{2n-1}X_1^{*2n-1} \cdot \sum (2n-1)U_{2n-1}f'_{2n-1}X_1^{*2(n-1)} \\ &- \sum K_{2n-1}X_1^{*2n-1} \cdot \sum (2n-1)U_{2n-1}f_{2n-1}X_1^{*2n-1} \cdot \sum U_{2n-1}f''_{2n-1}X_1^{*2n-1} \\ &- \sum U_{2n-1}f_{2n-1}X_1^{*2n-1} \cdot \sum (2n-1)\,K_{2n-1}X_1^{*2(n-1)} \cdot \sum U_{2n-1}f''_{2n-1}X_1^{*2n-1} \\ &- \lambda \sum (2n-1)\,K_{2n-1}X_1^{*2(n-1)} \cdot \sum r_{2n-1}g_{2n-1}X_1^{*2n-1} \cdot \sum r_{2n-1}g_{2n-1}X_1^{*2n-1} \\ &= \sum K_{2n-1}X_1^{*2n-1} \cdot \sum U_{2n-1}X_1^{*2n-1} \cdot \sum (2n-1)U_{2n-1}X_1^{2(n-1)} \\ &+ \sum K_{2n-1}X_1^{*2n-1} \cdot \sum l_{2(n-1)}X_1^{*2(n-1)} \cdot \sum U_{2n-1}f'''_{2n-1}X_1^{*2n-1} \end{aligned} \tag{3-75}$$

which is the power series form of the momentum meridional boundary layer equation, and

$$\begin{aligned} &\sum K_{2n-1}X_1^{*2n-1} \cdot \sum U_{2n-1}f'_{2n-1}X_1^{*2n-1} \cdot \sum (2n-1)r_{2n-1}g_{2n-1}X_1^{*2(n-1)} \\ &- \sum U_{2n-1}f_{2n-1}X_1^{*2n-1} \cdot \sum (2n-1)\,K_{2n-1}X_1^{*2(n-1)} \cdot \sum r_{2n-1}g'_{2n-1}X_1^{*2n-1} \\ &- \sum K_{2n-1}X_1^{*2n-1} \cdot \sum (2n-1)U_{2n-1}f_{2n-1}X_1^{*2(n-1)} \cdot \sum r_{2n-1}g'_{n-1}\,X_1^{*2n-1} \\ &+ \sum r_{2n-1}g_{2n-1}X_1^{*2n-1} \cdot \sum U_{2n-1}f'_{2n-1}X_1^{*2n-1} \cdot \sum (2n-1)\,K_{2n-1}X_1^{*2(n-1)} \\ &= \sum l_{2(n-1)}X_1^{*2(n-1)} \cdot \sum K_{2n-1}X_1^{*2n-1} \cdot \sum r_{2n-1}g''_{2n-1}X_1^{*2n-1} \end{aligned} \tag{3-76}$$

which is the power series form of the momentum azimuthal boundary layer equation. The following notation has been used

$$\sum \equiv \sum_{n=1}^{\infty}$$

and $\lambda$, the so-called 'spin-parameter', is defined

$$\lambda = \left(\frac{\Omega L_c}{U_c}\right)^2 \qquad (3\text{-}77)$$

We shall now use two theorems for series in order to obtain differential equations defining our variable coefficients $f_{2i-1}(\eta)$ and $g_{2i-1}(\eta)$.

Knopp (1956) has defined an absolutely convergent series as follows, 'a series $\sum a_\nu$ is said to be absolutely convergent, if the series $\sum |a|$ which is a series of positive terms, converges'.

The Cauchy theorem states that 'If $\sum a_x$ and $\sum b_\lambda$ are two absolutely convergent series then their Cauchy product $\sum_{m=0}^{\infty} C_m$ with $C_m = a_o b_m + a_1 b_{m-1} + \ldots + a_m b_o$ is also absolutely convergent'.

A further useful theorem is the identity theorem for power series which states that 'If each of the two series $\sum a Z^\nu$ and $\sum b_\nu Z^\nu$ has a radius of convergence greater than zero and if they have the same values in the neighbourhood (no matter how small) of the origin, then they are completely identical, i.e. $a_\nu = b_\nu$ for all $\nu = 0, 1, 2, \ldots$'

Now because our series $\sum$ are assumed to be absolutely convergent then the products $\sum \cdot \sum \cdot \sum$ are also assumed to be absolutely convergent they thus have a finite non-zero radius of convergence and satisfy the first condition of the identity theorem. The second condition is also satisfied because the equations obtained by neglect of all but the first terms in the power series representations are identical with the Navier-Stokes stagnation point equations (3-89), (3-90). Thus we can expand both equations (3-75) and (3-76) and compare the coefficients of like

powers of $X_1^*$ on both sides of both equations in turn and obtain two infinite sets of ordinary differential equations in the functions $f_{2i-1}(\eta)$ and $g_{2i-1}(\eta)$.

We obtain, on equating the coefficients of $X_1^{*2n}$, the following equation from the momentum meridional equation.

$$f'''_{2n-1} = \frac{1}{l_o K_1 U_{2n-1}} \left[ \sum_{s=1}^{n} \left[ (2(n-s)+1)\, U_{2(n-s)+1} f'_{2(n-s)+1} \sum_{q=1}^{s} K_{2(s-q)+1} U_{2q-1} f'_{2q-1} \right] \right.$$

$$- \sum_{s=1}^{n} \left[ U_{2(n-s)+1} f''_{2(n-s)+1} \sum_{q=1}^{s} (2q-1) U_{2q-1} f_{2q-1} K_{2(s-q)+1} \right]$$

$$- \sum_{s=1}^{n} \left[ U_{2(n-s)+1} f''_{2(n-s)+1} \sum_{q=1}^{s} (2q-1) K_{2q-1} U_{2(s-q)+1} f_{2(s-q)+1} \right]$$

$$- \lambda \sum_{s=1}^{n} \left[ r_{2(n-s)+1} g_{2(n-s)+1} \sum_{q=1}^{s} (2q-1) K_{2q-1} r_{2(s-q)+1} g_{2(s-q)+1} \right]$$

$$- \sum_{s=1}^{n} \left[ (2(n-s)+1)\, U_{2(n-s)+1} \sum_{q=1}^{s} U_{2(s-q)+1} K_{2q-1} \right]$$

$$- l_o \sum_{q=1}^{n-1} \left[ U_{2q-1} f'''_{2q-1} K_{2(n-q)+1} \right] - \sum_{s=2}^{n} \left[ U_{2(n-s)+1} f'''_{2(n-s)+1} \sum_{q=2}^{s} l_{2(q-1)} \right.$$

$$\left. \left. K_{2(s-q)+1} \right] \right] \qquad (3\text{-}78)$$

From the momentum azimuthal equation:

$$g''_{2n-1} = \frac{1}{K_1 l_o K_{2n-1}} \left[ \sum_{s=1}^{n} \left[ (2(n-s)+1)\, r_{2(n-s)+1} g_{2(n-s)+1} \sum_{q=1}^{s} K_{2(s-q)+1} U_{2q-1} f'_{2q-1} \right] \right.$$

$$\left. - \sum_{s=1}^{n} \left[ r_{2(n-s)+1} g'_{2(n-s)+1} \sum_{q=1}^{s} (2q-1) K_{2q-1} U_{2(s-q)+1} f_{2(s-q)+1} \right] \right.$$

$$- \sum_{s=1}^{n}\left[r_{2(n-s)+1} g'_{2(n-s)+1} \sum_{q=1}^{s}(2q-1)\, K_{2(s-q)+1} U_{2q-1} f_{2q-1}\right]$$

$$+ \sum_{s=1}^{n}\left[r_{2(n-s)+1} g_{2(n-s)+1} \sum_{q=1}^{s}(2q-1)\, K_{2q-1} U_{2(s-q)+1} f'_{2(s-q)+1}\right]$$

$$- 1_o \sum_{q=1}^{n-1} r_{2q-1} g''_{2q-1}\, K_{2(n-q)+1} - \sum_{s=2}^{n}\left[r_{2(n-s)+1} g''_{2(n-s)+1} \sum_{q=2}^{s} 1_{2(q-1)}\, K_{2(s-q)+1}\right] \qquad (3\text{-}79)$$

where $n \geqslant 1$ and $\sum_{s=2}^{1} = 0$ by definition.

The boundary values are

$$\begin{aligned} &\text{at } \eta = 0 \quad f_{2i-1} = f'_{2i-1} = 0 \quad g_{2i-1} = 1 \\ &\text{as } \eta \to \infty \quad f'_{2i-1} \longrightarrow 1 \qquad\qquad g_{2i-1} \longrightarrow 0 \\ &\qquad\qquad \text{for all } i \geqslant 1 \end{aligned} \qquad (3\text{-}80)$$

Using equations (3-78) and (3-79) with the pertinent boundary values (3-80) it is hence possible to solve the hydrodynamic boundary layer equations for all axisymmetric bodies at any spin parameter. The advantage of the use of this general form is that we can determine any functional coefficient $f'''_{2i-1}$ or $g''_{2n-1}$ from two expressions, i.e. (3-78) and (3-79). This has a distinct advantage over the method of Hoskin in which each of the functions $f'''_1$, $f'''_3$ ....; $g'''_1$, $g'''_3$ ...., has to be individually prescribed in a separate equation.

### 3.3.2 Definition of Characteristic Dimension and Co-ordinates

The only assumption that has so far been made in our analysis is that the co-ordinate $x_3$ is taken as being in the direction of the normals to the body surface, on the body surface itself the co-ordinates are triply orthogonal.

In our analysis of the boundary layer equations we have shown that it is necessary to define certain characteristic dimensions in order that the solutions presented are as general as possible, we must hence decide the form that these characteristic dimensions should take.

If we denote the perpendicular distance between the axis of symmetry and the point $P(x_1)$ on the body surface as $r(x_1)$ then a co-ordinate that would be common to all bodies of revolution is the angle $\phi$ subtended by $r(x_1)$ on to a fixed plane through the axis of symmetry (see fig.2 appendix C). If we take this angle as the $x_2$ co-ordinate we have

$$h_{2,0}(x_1) = r(x_1)$$

and thus $$K_{2i-1} = r_{2i-1} \qquad \text{all } i \geqslant 1 \tag{3-81}$$

$h_{2,0}(x_1)$ having the dimension $[L]$.

The power series expansion of the scale factor $h_{2,0}(x_1)$ will be of the form

$$h_{2,0} = \sum_{n=1}^{\infty} \hat{K}_{2n-1} x_1^{2n-1} \tag{3-82}$$

by choosing an appropriate characteristic dimension we may put $h_{2,0}$ into its dimensionless form, i.e.

$$h^*_{2,0} = \sum_{n=1}^{\infty} K_{2n-1} x_1^{*2n-1} \tag{3-83}$$

If we assume that the co-ordinate $x_1$ has the dimension $[L]^m$ where m is any real number it follows that $\hat{K}_{2n-1}$ has the dimension $[L]^{1-m(2n-1)}$. Dividing both sides of (3-82) by the characteristic dimension $L_c$ we obtain:

$$\frac{h_{2,0}}{L_c} = h^*_{2,0} = \sum_{n=1}^{\infty} \frac{\hat{K}_{2n-1}}{L_c} (L_c)^{m(2n-1)} x_1^{*2n-1} \tag{3-84}$$

where $x_1^* = x_1/L_c^m$.

If we put $K_1 = 1$ in (3-83) we find that it follows from equation (3-84) that

$$L_c = \hat{K}_1^{1/1-m} \quad m \neq 1 \tag{3-85}$$

Thus if the dimension of co-ordinate $x_1$ is $[L]^m$ $m \neq 0$ and $h_{2,0}$ is given by $h_{2,0} = \sum_{n=1}^{\infty} \hat{K}_{2n-1} x_1^{2n-1}$ then by choosing our characteristic dimension $L_c$ as $(\hat{K}_1)^{1/1-m}$ then $K_1 = 1$ in the expansion of $h^*_{2,0} = \sum_{n=1}^{\infty} K_{2n-1} x_1^{*2n-1}$.

If $x_1$ has the dimension $[L]$ then we have to choose a characteristic dimension other than $K_1$ ( as $K_1$ is dimensionless) it should be noted that in this case $K_1 \neq 1$.

It should also be noted that for the particular case of a bluff body (a body with a finite radius of curvature at the front stagnation point) a relationship can be obtained between $K_1$ and $l_o$ in the expansion $h^*_{1,0} = \sum_{n=1}^{\infty} l_{2(n-1)} x_1^{2n-1}$.

Let us consider the elemental distance ds along the meridional curve $\Gamma$ (see fig.2 appendix C)

here $$ds = h_{1,0}\, dx_1$$

now $$h_{1,0} = \sum \hat{l}_{2(n-1)} x_1^{2(n-1)}$$

and consequently in the vicinity of the front stagnation point ($x_1 = 0$) we have

$$ds = \hat{l}_o dx_1$$

However at the front stagnation point, for a bluff body $r(x_1)$ becomes identical with ds, but $r(x_1) = h_{2,0}(x_1)$ and this region $h_{2,0} = \hat{K}_1 x_1$

thus

$$\hat{l}_o x_1 = \hat{K}_1 x_1$$

$$\text{i.e.} \hat{l}_o = \hat{K}_1 \tag{3-86}$$

Thus in the case of a bluff body the characteristic length dimension is $\hat{K}^{1/1-m}$ (providing $m \neq 1$) and

$$l_o = K_1 = 1 \tag{3-86A}$$

It should be noted however that $\hat{l}_o = \hat{K}_1$ irrespective of the dimension of $x_1$. If $x_1$ has dimension $[L]$ then

$$l_o = \hat{l}_o = \hat{K}_1 = K_1 \tag{3-86B}$$

If we now define an alternative expression for the potential flow U

$$\text{i.e.} \quad U = \sum_{n=1}^{\infty} \bar{U}_{2n-1} x_1^{*2n-1} \tag{3-87}$$

where it will be noted that coefficients $\bar{U}_{2i-1}$ are of dimension $[LT^{-1}]$. The dimensionless form of the potential flow $U^*$ has already been defined in (3-67)

$$\text{i.e.} \quad U^* = \sum_{n=1}^{\infty} U_{2n-1} x_1^{*2n-1}$$

If we now define the characteristic velocity $U_c$ as $\bar{U}_1$

$$\left.\begin{aligned} &\text{i.e.} \quad U_c \equiv \bar{U}_1 \\ &\text{then} \quad U_1 = 1 \; ; \; U_3 = \bar{U}_3/\bar{U}_1, \ldots U_{2n-1} = \bar{U}_{2n-1}/\bar{U}_1 \end{aligned}\right\} \tag{3-88}$$

We can summarise the dependence of $K_1$ and $l_o$ in the expressions $h^*_{1,0} = \sum K_{2(n-1)} x_1^{*2\,n-1}$ and $h^*_{2,0} = \sum l_{2(n-1)} x_1^{*2(n-1)}$ on the body shape and the co-ordinates used as follows,

i) In general $K_1$ and $l_o$ are not equal and are not necessarily unity.

ii) For bluff bodies (and the disc) it can be shown that if we choose the characteristic length as $\hat{K}^{1/1-m}$ where $x_1$ has the dimension $[L]^m$, $m \neq 0$ and $h_{2,0} = \sum \hat{K}_{2n-1} x_1^{2n-1}$

then

$$K_1 = l_o = 1$$

iii) If $x_1$ has dimension $[L]$ (the body being bluff) then an alternative characteristic length has to be found because $\hat{K}_1$ and $\hat{l}_o$ are dimensionless, here

$$\hat{l}_o = l_o = \hat{K}_1 = K_1$$

iv) If $x_1$ is the meridional distance along the surface of a bluff body then $h_{1,o} = 1$ and consequently

$$\hat{l}_o = l_o = \hat{K}_1 = K_1 = 1$$

If we use the relationship $l_o = K_1 = 1$ and substitute into equations (3-78) and (3-79), n = 1 and n = 2 respectively we obtain the following differential equations:

$$f_1''' = -2f_1f_1''' + f_1'^2 - \lambda g_1^2 - 1 \qquad (3\text{-}89)$$

$$g_1'' = 2g_1f_1' - 2g_1'f_1 \qquad (3\text{-}90)$$

which are the stagnation point equations, and

$$f_3''' = -2f_1f_3''' + 4f_1'f_3' - 4f_1''f_3 - 4 - 2ff_1''\left(\frac{K_3}{U_3}\right) - 2\lambda\,(g_1^2 + g_1g_3)\left(K_{3/U_3}\right) \qquad (3\text{-}91)$$

$$g_3'' = 2f_1'g_1 + 4f_1'g_3 - 2f_1g_3' - 2g_1'f_1 + 2g_1f_3'(U_{3/K_3}) - 4g_1'f_3(U_{3/K_3}) - g_1''(l_{2/K_3}) \qquad (3\text{-}92)$$

It should be noted that the first set (n=1) of ordinary differential equations (3-89) and (3-90) are a non-linear set, whilst the second set (n=2) of ordinary differential equations (3-91) and (3-92) and all subsequent sets (n=3,4...etc.) are linear sets.

It is useful to compare the above sets of differential equations

with the first two sets of equations presented by Hoskin (1955) for the rotating sphere.

Hoskin used for his $x_1$ co-ordinate the distance from the front stagnation point of the sphere along a meridian curve, he thus obtained the relationship $l_o = K_1 = 1$ (see section (iv) of the summary in (3.3.2)), thus the stagnation point equations (3-89) and (3-90) are identical with those presented by Hoskin.

The term $r(x_1)$ for the sphere of radius a is given by Hoskin as:

$$r(x_1) = a \sin (x_1/a)$$

The potential flow is given by the expression

$$U(x_1) = \frac{3}{2} U_\infty \sin (x_1/a).$$

Defining the characteristic dimension as the sphere radius a and the characteristic velocity as $\frac{3}{2} U_\infty$ we find

$$r^*(x_1^*) = U^*(x_1^*) = \sin (x_1^*)$$

and consequently,

$$U_{2i-1} = \kappa_{2i-1}$$

Introducing this relationship into equations (3-91) and (3-92) we find that our second set of equations become identical with those presented by Hoskin for the special case of the sphere.

### 3.3.3 Mass (or heat) Transport Boundary Layer Equation for Finite Non-zero Schmidt or Prandtl Numbers

We have defined the transfer function X which could either be the temperature or concentration at a point. The boundary layer equation is in dimensionless form

$$\frac{V_1^*}{h_{1,0}^*}(X^*)_{x_1^*} + V_N^*(X^*)_{N^*} = \frac{1}{\overline{Pr}.Re}(X^*)_{N,N^*} \qquad (3\text{-}93)$$

On substitution of the dimensionless stream function $X^*$ we obtain

$$h^*_{2,0}(\psi^*)_{N^*}(X^*)_{x_1^*} - \psi^*(h^*_{2,0})_{x_1^*}(X^*)_{N^*} - h^*_{2,0}(\psi^*)_{x_1^*}(X^*)_{N^*}$$

$$= \frac{h^*_{1,0}h^*_{2,0}}{\overline{Pr}.\ \overline{Re}}\,(X^*)_{N^*,N^*} \qquad (3\text{-}94)$$

Again the transfer function $X^*$ is assumed to be representable in a power series of the meridional co-ordinate $x_1^*$ with coefficients that are functions of the dimensionless perpendicular distance $N^*$. As we would expect a symmetrical distribution of concentration around the front stagnation point the power series must be an even function of $x_1^*$

$$\text{i.e.} \quad X(x_1^*, N^*) = X^*(-x_1^*, N^*) \qquad (3\text{-}95)$$

and consequently only even powers of $x_1^*$ will be found in the power series expansion,

$$\text{i.e.} \quad X^* = \mathcal{H}_0(N^*) + \mathcal{H}_2(N^*)\,x_1^{*2} + \ldots + \mathcal{H}_{2n-1}(N^*)x_1^{*2(n-1)} + \ldots \qquad (3\text{-}96)$$

$$\text{or} \quad X^* = \sum_{n=1}^{\infty} \mathcal{H}_{2(n-1)}(N^*)\,x_1^{*2(n-1)} \qquad (3\text{-}97)$$

On substitution of power series forms into equation (3-94) we obtain:

$$\sum K_{2n-1}x_1^{*2n-1} \cdot \sum U_{2n-1}f'_{2n-1}x_1^{*2n-1} \cdot \sum 2(n-1)\mathcal{H}_{2(n-1)}x_1^{*2n-3}$$

$$- \sum (2n-1)\,K_{2n-1}x_1^{*2(n-1)} \cdot \sum U_{2n-1}f_{2n-1}x_1^{*2n-1} \sum \mathcal{H}'_{2(n-1)}x_1^{*2(n-1)}$$

$$- \sum K_{2n-1}x_1^{*2n-1} \sum (2n-1)U_{2n-1}f_{2n-1}x_1^{*2(n-1)} \sum \mathcal{H}'_{2(n-1)}x_1^{*2(n-1)}$$

$$= \frac{1}{Pr} \sum K_{2n-1}x_1^{*2n-1} \sum 1_{2(n-1)}x_1^{*2(n-1)} \sum \mathcal{H}''_{2(n-1)}x_1^{*2(n-1)}$$

(3-98)

Here again $\sum \equiv \sum_{n=1}^{\infty}$ and $\overline{Pr}$ denotes the Schmidt or Prandtl number. The dash (') denotes differentiation with respect to $\eta$. Our choice of power series substitutions has removed the Reynolds number from the equation.

Again using the Cauchy product theorem and the Identity theorem we obtain, on equating coefficients of $x_1^{*2n-1}$, the general differential equation

$$\mathcal{H}''_{2(n-1)} = \frac{\overline{Pr}}{K_1 l_o}\left\{ \sum_{s=2}^{n}\left[2(n-s+1)\,\mathcal{H}_{2(n-s+1)} \sum_{q=2}^{s} K_{2(s-q)+1} f'_{2q-3} U_{2q-3}\right]\right.$$

$$- \sum_{s=1}^{n}\left[\mathcal{H}'_{2(n-s)} \sum_{q=1}^{s}(2q-1)\,K_{2q-1} f_{2(s-q)+1} U_{2(s-q)+1}\right]$$

$$\left. - \sum_{s=1}^{n}\left[\mathcal{H}'_{2(n-s)} \sum_{q=1}^{s}(2q-1)\,K_{2(s-q)+1} f_{2q-1} U_{2q-1}\right]\right\}$$

$$- \frac{1}{K_1}\sum_{q=1}^{n-1} \mathcal{H}''_{2(n-q-1)} K_{2q+1} - \frac{1}{K_1 l_o}\sum_{s=1}^{n-1}\left[\mathcal{H}''_{2(n-s-1)} \sum_{q=1}^{s} K_{2q-1} l_{2(n-q)}\right] \qquad (3\text{-}99)$$

where again we define $\sum_{2}^{1} = 0$.

Using the fact that $U_1 = 1$ irrespective of co-ordinate system being used we obtain on substituting n=1 in (3-99)

$$\mathcal{H}''_0 = -\frac{2\overline{Pr}}{l_o} f_1 \mathcal{H}'_0 \qquad (3\text{-}100)$$

substitution of n=2 yields:

$$\mathcal{H}''_2 = \frac{\overline{Pr}}{l_o}\left\{2\mathcal{H}_2 f'_1 - 2\mathcal{H}'_2 f_1 - 2\mathcal{H}'_0(2f_3 U_3 + f_1(\frac{K_3}{K_1}))\right\} - \mathcal{H}'''_0(\frac{l_2}{l_o} + \frac{K_3}{K_1}) \qquad (3\text{-}101)$$

It can be seen that all the equations for the heat or mass transfer functional coefficients $\mathcal{H}''_{2(i-1)}$ are linear and can hence be solved by the superposition principle.

The pertinent boundary values for our functional coefficients are:

$$\left.\begin{aligned} &\text{at } \eta = 0 \quad \mathcal{H}_0 = 1 \; ; \quad \mathcal{H}_{2(i-1)} = 0 \quad \text{all } i \geq 2 \\ &\text{as } \eta \longrightarrow \infty \quad \mathcal{H}_{2(i-1)} \longrightarrow 0 \quad \text{all } i \end{aligned}\right\} \tag{3-102}$$

3.3.4 Final Form of Differential Equations for Determination of Local Mass or Heat Transfer Coefficients (for Finite and Non-zero Schmidt and Prandtl Numbers)

For certain bodies of revolution the potential flow coefficient $U_{2n-1}$ can become very small or even zero, if $U_{2n-1}$ does become zero it can be seen that a singularity occurs in equation (3-78) and as a consequence numerical integration of that equation is not possible. The occurrance of such singularities can be exemplified in the case of the oblate spheroid, it can be shown that the coefficient $U_3$ for the oblate spheroid is given by $U_3 = (\frac{2-3e^2}{2})$ where e is the ratio of minor to major axis of the body (see (3-188)), consequently for the oblate spheroid given by $e = {}^2/_3$ the coefficient $U_3$ is equal to zero and a singularity occurs in equation (3-91).

Difficulties also arise when $U_{2n-1}$ is very small but non-zero, here the right-hand side of equation (3-78) can become very large and subsequent numerical integration of $\bar{f}'''_{2n-1}$ can contain large inaccuracies. Similarly in equation (3-79) the right-hand side can become very large because coefficient $K_{2n-1}$ is very small for large n, again difficulty will be found in accurately integrating this equation numerically.

In order to overcome these difficulties we introduce two new variables defined as follows:

$$\bar{f}_{2n-1} = U_{2n-1} f_{2n-1} \tag{3-103}$$

$$\bar{g}_{2n-1} = K_{2n-1}\, g_{2n-1} \qquad (3\text{-}104)$$

Hence if $U_{2n-1}$ tends to zero then $\bar{f}_{2n-1}$ tends to zero and similarly as $K_{2n-1}$ tends to zero then $\bar{g}_{2n-1}$ tends to zero.

Using these substitutions equations (3-78) and (3-79) become respectively:

$$\bar{f}'''_{2n-1} = \frac{1}{l_o K_1}\left[\sum_{s=1}^{n}\left[\{2(n-s)+1\}\,\bar{f}'_{2(n-s)+1}\sum_{q=1}^{s}K_{2(s-q)+1}\,\bar{f}'_{2q-1}\right]\right.$$

$$-\sum_{s=1}^{n}\left[\bar{f}'_{2(n-s)+1}\sum_{q=1}^{s}(2q-1)\bar{f}_{2q-1}\,K_{2(s-q)+1}\right]-\sum_{s=1}^{n}\left[\bar{f}''_{2(n-s)+1}\sum_{q=1}^{s}(2q-1)\right.$$

$$\left.K_{2q-1}\bar{f}_{2(s-q)+1}\right]$$

$$-\lambda\sum_{s=1}^{n}\left[\bar{g}_{2(n-s)+1}\sum_{q=1}^{s}(2q-1)\,K_{2q-1}\bar{g}_{2(s-q)+1}\right]-\sum_{s=1}^{n}\left[\left\{2(n-s)+1\right\}\right.$$

$$\left.U_{2(n-s)+1}\sum_{q=1}^{s}U_{2(s-q)+1}\,K_{2q-1}\right]$$

$$\left.-l_o\sum_{q=1}^{n-1}\bar{f}'''_{2q-1}\,K_{2(n-q)+1}-\sum_{s=2}^{n}\left[\bar{f}'''_{2(n-s)+1}\sum_{q=2}^{n}l_{2(q-1)}\,K_{2(s-q)+1}\right]\right] \qquad (3\text{-}105)$$

$$\bar{g}''_{2n-1} = \frac{1}{K_1 l_o}\left[\sum_{s=1}^{n}\left[\left\{2(n-s)+1\right\}\bar{g}_{2(n-s)+1}\sum_{q=1}^{s}K_{2(s-q)+1}\bar{f}'_{2q-1}\right]\right.$$

$$-\sum_{s=1}^{n}\left[\bar{g}'_{2(n-s)+1}\sum_{q=1}^{s}(2q-1)\,K_{2q-1}\bar{f}_{2(s-q)+1}\right]-\sum_{s=1}^{n}\left[\bar{g}'_{2(n-s)+1}\sum_{q=1}^{s}(2q-1)\right.$$

$$\left.K_{2(s-q)+1}\bar{f}_{2q-1}\right]$$

$$+\sum_{s=1}^{n}\left[\bar{g}_{2(n-s)+1}\sum_{q=1}^{s}(2q-1)\,K_{2q-1}\bar{f}'_{2(s-q)+1}\right]-l_o\sum_{q=1}^{n-1}\bar{g}''_{2q-1}\,K_{2(n-q)+1}$$

$$\left.-\sum_{s=2}^{n}\left[\bar{g}''_{2(n-s)+1}\sum_{q=2}^{s}l_{2(q-1)}\,K_{2(s-q)+1}\right]\right] \qquad (3\text{-}106)$$

the new boundary values being

$$\left.\begin{aligned} &\text{at } \eta = 0 \quad \bar{f}_{2i-1} = \bar{f}'_{2i-1} = 0 \; ; \; \bar{g}_{2i-1} = K_{2i-1} \\ &\text{as } \eta \longrightarrow \infty \quad \bar{f}'_{2i-1} \longrightarrow U_{2i-1} \quad ; \; g_{2i-1} \longrightarrow 0 \end{aligned}\right\} \qquad (3\text{-}107)$$

$$\text{for all } i \geqslant 1$$

It should be noted that we have used the relationship $K_{2i-1} = r_{2i-1}$ (see (3-81)) to obtain these equations.

As can be seen the new substitutions make the boundary values shape dependent, this however adds little difficulty in the solution of the boundary value problems (3-105) and (3-106) (see chapter 4), the substitutions in fact save computer time because the multiplications $U_{2n-1} \times f_{2n-1}$ and $K_{2n-1} \times g_{2n-1}$ do not now take place.

Using these substitutions the mass (or heat) transfer equation (3-99) transforms to

$$\begin{aligned} \mathcal{H}''_{2(n-1)} = \frac{\overline{Pr}}{l_o K_1} \Bigg[ & \sum_{s=2}^{n} 2(n-s+1)\mathcal{H}_{2(n-s+1)} \sum_{q=2}^{s} K_{2(s-q)+1}\bar{f}'_{2q-3} \\ & - \sum_{s=1}^{n}\mathcal{H}_{2(n-s)} \sum_{q=1}^{s}(2q-1)\, K_{2q-1}\bar{f}_{2(s-q)+1}\Big] - \sum_{s=1}^{n}\Big[\mathcal{H}'_{2(n-s)} \sum_{q=1}^{s}(2q-1) \\ & K_{2(s-q)+1}\bar{f}_{2q-1}\Big]\Bigg] \\ & - \frac{1}{K_1}\sum_{q=1}^{n-1}\mathcal{H}''_{2(n-q-1)}\, K_{2q+1} - \frac{1}{K_1 l_o}\sum_{s=1}^{n-1}\Big[\mathcal{H}''_{2(n-s-1)} \sum_{q=1}^{s} K_{2q-1}\, l_{2(n-q)}\Big] \end{aligned} \qquad (3\text{-}108)$$

the boundary conditions in $\mathcal{H}_{2(i-1)}$ remaining as before, i.e.

$$\left.\begin{aligned} &\text{at } \eta = 0 \quad \mathcal{H}_o = 1 \; ; \; \mathcal{H}_{2(i-1)} = 0 \quad \text{all } i \geqslant 2 \\ &\text{as } \eta \longrightarrow \infty \quad \mathcal{H}_{2(i-1)} \longrightarrow 0 \quad \text{all } i \end{aligned}\right\} \qquad (3\text{-}109)$$

These equations are now in a form easily soluble by numerical

techniques on the computer, the methods of solution employed are explained in chapter 4.

## 3.4 SERIES SOLUTION OF THE LAMINAR BOUNDARY LAYER EQUATIONS FOR AN AXISYMMETRIC BODY ROTATING ABOUT ITS AXIS OF SYMMETRY IN A QUIESCENT FLUID

For this section we shall be using the same nomenclature as in section 3.3.

### 3.4.1 Velocity Boundary Layer Equations

The pertinent momentum boundary layer equations are from section 3.2.2;

momentum meridional direction

$$\frac{V_1^*}{h_{1,0}^*}(V_1^*)_{x_1^*} - \frac{V_2^{*2}}{h_{1,0}^* h_{2,0}^*}(h_{2,0}^*)_{x_1^*} + V_N^*(V_1^*)_{N^*} = \frac{1}{R_s}(V_1^*)_{N^*,N^*} \qquad (3\text{-}110)$$

momentum azimuthal direction

$$\frac{V_1^*}{h_{1,0}^*}(V_2^*)_{x_1^*} + \frac{V_1^* V_2^*}{h_{1,0}^* h_{2,0}^*}(h_{2,0}^*)_{x_1^*} + V_N^*(V_2^*)_{N^*} = \frac{1}{R_s}(V_2^*)_{N^*,N^*} \qquad (3\text{-}111)$$

continuity equation

$$(h_{2,0}^* V_1^*)_{x_1^*} + (V_N^*)_{N^*} h_{1,0}^* h_{2,0}^* = 0 \qquad (3\text{-}112)$$

and the boundary conditions

$$\begin{aligned} &\text{at } N^* = 0 \quad V_1^* = V_N^* = 0 \; ; \; V_2^* = (V_2^*)_s \\ &\text{as } N^* \longrightarrow \infty \quad V_1^* \longrightarrow 0 \quad ; \; V_2^* \longrightarrow 0 \end{aligned} \qquad (3\text{-}113)$$

where the Reynolds number $R_s$ is here defined

$$R_s = (V_s L_c / \nu) \qquad (3\text{-}114)$$

$V_s$ being the characteristic spinning velocity as defined in 3.2.3 and $L_c$ is a characteristic dimension yet to be defined.

Again, as in the case of an axisymmetric body in axial flow we shall use a series substitution method of solution of these equations, the method of Howarth (1951) being followed in order that comparisons of our solutions may be made with his for the case of the rotating sphere. We shall hence define a dimensionless perpendicular distance $\alpha$ given by:

$$\alpha = \left(\frac{\Omega}{\nu}\right)^{\frac{1}{2}} N \tag{3-115}$$

which may be re-written

$$\alpha = R_s^{\frac{1}{2}} N^* \tag{3-116}$$

$\Omega$ being the angular velocity of the body.

We now need to define power series forms for the velocity components. The positive direction for the normal velocity component $V_N$ is outward from the body surface it is hence independent of the sign of $x_1^*$. $V_1$ is measured as positive in the positive $x_1^*$ direction and $V_2$ is measured as positive in the direction of spin of the body, both $V_1$ and $V_2$ must hence be dependent on the sign of $x_1^*$,

i.e.

$$\begin{aligned} V_N^*(x_1^*,\alpha) &= V_N^*(-x_1^*,\alpha) \\ V_1^*(x_1^*,\alpha) &= -V_1^*(-x_1^*,\alpha) \\ V_2^*(x_1^*,\alpha) &= -V_2^*(-x_1^*,\alpha) \end{aligned} \tag{3-117}$$

Using $L_c$ the characteristic length we may now define a characteristic velocity for the case of a body rotating in a quiescent fluid, i.e.

$$V_s = L_c \Omega \tag{3-118}$$

$V_N^*$ is from (3-117) an even function of $x_1^*$ and $V_1^*$ and $V_2^*$ are both odd functions of $x_1^*$ we may hence represent them in the following power

series forms

$$V_1^* = x_1^* F_1(\alpha) + x_1^{*3} F_3(\alpha) + \cdots + x_1^{*2i-1} F_{2i-1}(\alpha) + \cdots = \sum_{n=1}^{\infty} x_1^{*2n-1} F_{2n-1}(\alpha) \tag{3-119}$$

$$V_2^* = x_1^* G_1(\alpha) + x_1^{*3} G_3(\alpha) + \cdots + x_1^{*2i-1} G_{2i-1}(\alpha) + \cdots = \sum_{n=1}^{\infty} x_1^{*2n-1} G_{2n-1}(\alpha) \tag{3-120}$$

$$V_N^* = R_s^{-\frac{1}{2}} (H_o(\alpha) + x_1^{*2} H_2(\alpha) + \cdots + x_1^{*2(i-1)} H_{2(i-1)}(\alpha) + \cdots = R_s^{-\frac{1}{2}} \sum_{n=1}^{\infty} x_1^{*2(n-1)} H_{2(n-1)}(\alpha) \tag{3-121}$$

the pertinent boundary values for these functional coefficients are:

$$\begin{aligned} &\text{at } \alpha = 0 \quad F_{2i-1} = G_{2i-1} - K_{2i-1} = H_{2(i-1)} = 0 \\ &\text{as } \alpha \to \infty \; ; \; F_{2i-1} \to 0 \; ; \; G_{2i-1} \to 0 \end{aligned} \tag{3-122}$$

where the relationship (3-81), i.e. $r_{2i-1} = K_{2i-1}$, has been used. Substitution of these power series representations into equations (3-110) to (3-112) yields, respectively

$$\begin{aligned} &\sum K_{2n-1} x_1^{*2n-1} \cdot \sum F_{2n-1} x_1^{*2n-1} \cdot \sum (2n-1) F_{2n-1} x_1^{*2(n-1)} \\ &- \sum G_{2n-1} x_1^{*2n-1} \cdot \sum G_{2n-1} x_1^{*2n-1} \cdot \sum (2n-1) K_{2n-1} x_1^{*2(n-1)} \\ &+ \sum H_{2(n-1)} x_1^{*2(n-1)} \cdot \sum F'_{2n-1} x_1^{*2n-1} \cdot \sum 1_{2(n-1)} x_1^{*2(n-1)} \cdot \sum K_{2n-1} x_1^{*2n-1} \\ &= \sum F''_{2n-1} x_1^{*2n-1} \cdot \sum 1_{2(n-1)} x_1^{*2(n-1)} \cdot \sum K_{2n-1} x_1^{*2n-1} \end{aligned} \tag{3-123}$$

$$\begin{aligned} &\sum K_{2n-1} x_1^{*2n-1} \cdot \sum F_{2n-1} x_1^{*2n-1} \cdot \sum (2n-1) G_{2n-1} x_1^{*2(n-1)} \\ &+ \sum F_{2n-1} x_1^{*2n-1} \cdot \sum G_{2n-1} x_1^{*2n-1} \cdot \sum (2n-1) K_{2n-1} x_1^{*2(n-1)} \end{aligned}$$

$$+ \sum l_{2(n-1)} x_1^{*2(n-1)} \cdot \sum K_{2n-1} x_1^{*2n-1} \cdot \sum H_{2(n-1)} x_1^{*2(n-1)} \cdot \sum G'_{2n-1} x_1^{*2n-1}$$

$$= \sum l_{2(n-1)} x_1^{*2(n-1)} \cdot \sum K_{2n-1} x_1^{*2n-1} \cdot \sum G''_{2n-1} x_1^{*2n-1} \tag{3-124}$$

$$\sum F_{2n-1} x_1^{*2n-1} \cdot \sum (2n-1) K_{2n-1} x_1^{*2(n-1)} + \sum (2n-1) F_{2n-1} x_1^{*2(n-1)} \cdot \sum K_{2n-1} x_1^{*2n-1}$$

$$+ \sum H'_{2(n-1)} x_1^{*2(n-1)} \cdot \sum l_{2(n-1)} x_1^{*2(n-1)} \cdot \sum K_{2n-1} x_1^{*2n-1} = 0 \tag{3-125}$$

As in section 3.3.1 we make use of the Cauchy product theorem and the Identity theorem to obtain the following ordinary differential equations after comparison of the coefficients of $x_1^{*2n}$ in equations (3-124) and (3-125).

$$F''_{2n-1} = \frac{1}{K_1 l_o} \left[ \sum_{s=1}^{n} \left[ K_{2(n-s)+1} \sum_{q=1}^{s} (2q-1) F_{2(s-q)+1} F_{2q-1} \right] + l_o \sum_{s=1}^{n} \left[ H_{2(n-s)} \sum_{q=1}^{s} F'_{2(s-q)+1} K_{2q-1} \right] \right.$$

$$+ \sum_{T=1}^{n-1} \left[ l_{2(n-T)} \sum_{s=1}^{T} \left[ H_{2(T-s)} \sum_{q=1}^{s} K_{2q-1} F'_{2(s-q)+1} \right] \right] - \sum_{s=1}^{n} \left[ G_{2(n-s)+1} \sum_{q=1}^{s} (2q-1) K_{2q-1} G_{2(s-q)+1} \right]$$

$$\left. - l_o \sum_{q=1}^{n-1} F''_{2q-1} K_{2(n-q)+1} - \sum_{2}^{n} \left[ F''_{2(n-s)+1} \sum_{q=2}^{s} l_{2(q-1)} K_{2(s-q)+1} \right] \right] \tag{3-126}$$

$$G''_{2n-1} = \frac{1}{K_1 l_o} \left[ \sum_{s=1}^{n} \left[ K_{2(n-s)+1} \sum_{q=1}^{s} (2q-1) F_{2(s-q)+1} G_{2q-1} \right] + l_o \sum_{s=1}^{n} \left[ H_{2(n-s)} \right. \right.$$

$$\sum_{q=1}^{s} K_{2q-1} G'_{2(s-q)+1} \Big]$$

$$+ \sum_{T=1}^{n-1} \Big[ l_{2(n-T)} \sum_{s=1}^{T} \Big[ H_{2(T-s)} \sum_{q=1}^{s} K_{2q-1} G'_{2(s-q)+1} \Big] + \sum_{s=1}^{n} \Big[ F_{2(n-s)+1}$$

$$\sum_{q=1}^{s} (2q-1)\, K_{2q-1} G_{2(s-q)+1} \Big]$$

$$- l_o \sum_{q=1}^{n-1} G''_{2q-1} K_{2(n-q)+1} - \sum_{s=2}^{n} \Big[ G''_{2(n-s)+1} \sum_{q=2}^{s} l_{2(q-1)} K_{2(s-q)+1} \Big] \Big] \Big] \quad (3\text{-}127)$$

After comparison of coefficients of $x_1^{*2n-1}$ in the continuity equation we obtain

$$H'_{2(n-1)} = \frac{-1}{K_1 l_o} \Big[ \sum_{q=1}^{n} F_{2(n-q)+1} (2q-1)\, K_{2q-1} + \sum_{q=1}^{n} K_{2(n-q)+1} (2q-1) F_{2q-1}$$

$$+ l_o \sum_{q=1}^{n-1} H'_{2(q-1)} K_{2(n-q)+1} + \sum_{s=1}^{n-1} \Big[ H'_{2(n-s-1)} \sum_{q=1}^{s} l_{2q} K_{2(s-q)+1} \Big] \Big] \quad (3\text{-}128)$$

The equations (3-126) to (3-128) with the boundary conditions (3-122) are now in such a form as to make their solution by numerical techniques straightforward. The method of solution of these equations will be dealt with in chapter 4.

### 3.4.2 Mass or Heat Transfer Boundary Layer Equation

In order to differentiate the case of heat or mass transport in axial flow from heat or mass transport in a quiescent fluid we define the dimensionless transport function x* by

$$X^* = \sum_{n=1}^{\infty} J_{2(n-1)} x_1^{*2(n-1)} \quad (3\text{-}129)$$

Here the definition of the transport function $X^*$ is the same as (3-97) only here J replaces $\mathcal{H}$, the boundary conditions for J being

at $\alpha = 0$ $\quad J_o = 1$ ; $J_{2(i-1)} = 0$ $\quad$ all $i \geq 2$

$$\text{as } \alpha \longrightarrow \infty \; J_{2(i-1)} \longrightarrow 0 \qquad \text{all } i \tag{3-130}$$

the mass or heat transport equation is given by

$$\frac{V_1^*}{h_{1,0}^*}(X^*)_{x_1^*} + V_N^*(X^*)_{N^*} = \frac{1}{\overline{Pr}.R_s}(X^*)_{N,N^*} \tag{3-131}$$

Substitution of the previously defined power series expressions (3-119), (3-121) and (3-129) into (3-131) leads to the summation equation,

$$\sum F_{2n-1} x_1^{*2n-1} \cdot \sum 2(n-1) J_{2(n-1)} x_1^{*2n-3} + \sum 1_{2(n-1)} x_1^{*2(n-1)} \cdot \sum H_{2(n-1)} x_1^{*2(n-1)} \cdot \sum J'_{2(n-1)} x_1^{*2(n-1)}$$

$$= \frac{1}{\overline{Pr}} \sum 1_{2(n-1)} x_1^{*2(n-1)} \cdot \sum J''_{2(n-1)} x_1^{*2(n-1)} \tag{3-132}$$

Once again we use the Cauchy product theorem and identity theorem and obtain after comparing coefficients of $x_1^{*2(n-1)}$

$$J''_{2(n-1)} = \frac{\overline{Pr}}{1_o}\left[\sum_{r=1}^{n-1} F_{2r-1}.2(n-r)J_{2(n-r)} + \sum_{r=1}^{n} H_{2(r-1)}J'_{2(n-r)} + \sum_{s=1}^{n-1}\left[J'_{2(n-s-1)} \sum_{r=1}^{s} 1_{2r} H_{2(s-r)}\right]\right] - \frac{1}{1_o}\sum_{r=1}^{n-1} 1_{2r} J''_{2(n-r-1)} \tag{3-133}$$

here the differentiation (') is with respect to $\alpha$. Equation (3-133) is now in a form that is amenable to solution by computer - the method of solution is discussed in chapter 4.

## 3.5 POINT MASS TRANSFER FUNCTIONS

### 3.5.1 Body with Constant Surface Concentration or Constant Surface Temperature

The flux of heat or mass per unit area $q(x_1^*)$ at a point $P(x_1^*)$ on the surface S of our body of revolution is given by Fourier's equation

$$q(x_1^*) = -\alpha_\nu \frac{\partial X}{\partial N}\bigg|_{N=0} \tag{3-134}$$

where $\alpha_v$ is the diffusivity for mass transfer or thermal conductivity of the fluid in the case of heat transfer, $\left.\frac{\partial X}{\partial N}\right|_{N=0}$ is the gradient of the concentration or temperature distribution at the surface of the body in the normal direction N.

We may also define the mass or heat flux in terms of the local mass or heat transfer coefficient $h_c(x_1^*)$

i.e. $$q(x_1^*) = h_c(x_1)(X_s - X_m) \tag{3-135}$$

Equating the two equations (3-134) and (3-135) we obtain

$$\frac{h_c(x_1)}{\alpha_v} = \frac{-1}{(X_s - X_m)} \left.\frac{\partial X}{\partial N}\right|_{N=0} \tag{3-136}$$

We have already defined the dimensionless transfer function $X^*$ and the dimensionless normal co-ordinates $\eta$ and $\alpha$ as:

$$X^* = \frac{X - X_m}{X_s - X_m}$$

$$\eta = \frac{N}{L_c} Re^{\frac{1}{2}} \tag{3-137}$$

$$\alpha = \frac{N}{L_c} R_s^{\frac{1}{2}}$$

Substitution of (3-137) yields:

for case of body in axial flow

$$\frac{h_c(x_1^*)L_c}{\alpha \Big/ Re^{\frac{1}{2}}} = -\left.\frac{\partial X^*}{\partial \eta}\right|_{\eta=0} \tag{3-138}$$

for case of body in quiescent fluid

$$\frac{h_c(x_1^*)L_c}{\alpha \Big/ R_s^{\frac{1}{2}}} = -\left.\frac{\partial X^*}{\partial \alpha}\right|_{\alpha=0} \tag{3-139}$$

In order that comparison may be made with the results of Green (1968) for local mass or heat transfer rates we define two more Reynolds numbers as follows:

$$\overline{Re} = (2L_c \cdot U_c/\nu) \text{ and } \overline{R_s} = \left(\frac{2L_c \cdot L_c \Omega}{\nu}\right) \qquad (3\text{-}140)$$

thus we have for a body in axial flow

$$\frac{\overline{Nu}(x_1^*)}{\overline{Re}^{\frac{1}{2}}} = \frac{-1}{\sqrt{2}} \left.\frac{\partial X^*}{\partial \eta}\right|_{\eta=0}$$

and

$$\frac{\overline{Nu}(x_1^*)}{\overline{R_s}^{\frac{1}{2}}} = \frac{-1}{\sqrt{2}} \left.\frac{\partial X^*}{\partial \alpha}\right|_{\alpha=0}$$

where $\overline{Nu}(x_1^*)$ is the local Nusselt or Sherwood number given by:

$$\overline{Nu}(x_1^*) = \frac{h_c(x_1^*)L_c}{\alpha_v} \qquad (3\text{-}141)$$

We have already defined $X^*$ to be

$$X^* = \sum_{n=1}^{\infty} \mathcal{H}_{2(n-1)}(\eta) x_1^{*2(n-1)} \qquad (3\text{-}142)$$

for the case of axial flow with rotation and

$$X^* = \sum_{n=1}^{\infty} J_{2(n-1)}(\alpha) x_1^{*2(n-1)} \qquad (3\text{-}143)$$

It has been shown by Frossling that as the Prandtl number (Pr) or the Schmidt number (Sc) tend to infinity then the local Nusselt and Sherwood numbers become proportional to $Pr^{\frac{1}{3}}$ and $Sc^{\frac{1}{3}}$ respectively. It would hence be expected that functions

$$M_H^A = \frac{Nu(x_1^*)}{\overline{Re}^{\frac{1}{2}} Pr^{\frac{1}{3}}} ; \quad M_H^q = \frac{Nu(x_1^*)}{\overline{R_s}^{\frac{1}{2}} Pr^{\frac{1}{3}}} \qquad (3\text{-}144)$$

$$M_M^A = \frac{Sh(x_1^*)}{\overline{Re}^{\frac{1}{2}} Sc^{\frac{1}{3}}} ; \quad M_M^q = \frac{Sh(x_1^*)}{\overline{R_s}^{\frac{1}{2}} Sc^{\frac{1}{3}}} \qquad (3\text{-}145)$$

are weak functions of Schmidt or Prandtl number. Here the mass transfer numbers M are suffixed by A for the case of spin in axial

flow, q for the case of spin in quiescent fluid, H for heat transfer and M for mass transfer. Thus we have

$$M_H^A = \frac{-1}{Pr^{\frac{1}{3}}\sqrt{2}} \sum_{n=1}^{\infty} \mathcal{H}'_{2(n-1)}(0) x_1^{*2(n-1)} \qquad (3\text{-}146)$$

$$M_H^q = \frac{-1}{Pr^{\frac{1}{3}}\sqrt{2}} \sum_{n=1}^{\infty} J'_{2(n-1)}(0) x_1^{*2(n-1)} \qquad (3\text{-}147)$$

with similar equations for mass transfer. These mass transfer numbers will be used to determine the effect of spin on local transfer rates.

### 3.5.2 Body with Non-uniform Surface Temperature or Concentration

The theory previously presented has dealt with an isothermal body or body with a constant surface concentration thus the transfer function $X^*$ is constant along the body surface

i.e. at surface of body $X^* = X_s^*$ (constant)

and in boundary layer $X^* = X^*(x_1^*, \eta)$

In the case when the surface value of $X^*$ is arbitrary all have:

at the surface $X^* = X^*(x_1^*)$

in the boundary layer $X^* = X^*(x_1^*, \eta)$

Now: $$X = X_m + (X_s - X_\infty) \qquad (3\text{-}148)$$

and $X_s - X_\infty$ is a function of $x_1^*$.

Substitution of (3-143) into

$$\frac{V_1^*}{h_{1,0}^*}(X)_{x_1^*} + V_\eta^{**}(X)_\eta = \frac{1}{Pr}(X)_{\eta,\eta} \qquad (3\text{-}149)$$

yields

$$\frac{V_1^*}{h_{1,0}^*}(X^*)_{x_1^*} + V_\eta^{**}(X^*)_\eta + \frac{V_1^*}{h_{1,0}^*}\frac{X^*}{(X_s - X_\infty)}(X_s - X_\infty)_{x_1^*} = \frac{1}{Pr}(X^*)_{\eta,\eta} \qquad (3\text{-}150)$$

Hence if the surface temperature or concentration can be expressed as a power series in $x_1^*$ the same approach as before is used to reduce the boundary layer equations to ordinary differential equations, only this time there are the added terms due to surface temperature or concentration variation.

As the term $X_s - X_m$ is a function of $x_1^*$ only the point mass or heat flux expression remains

$$\frac{Nu(x_1^*)}{\overline{Re}^{\frac{1}{2}}} = -\frac{1}{\sqrt{2}}\left[(X^*)_\eta\right]_{\eta=0} \qquad (3\text{-}151)$$

## 3.6 POINT MASS TRANSFER NUMBER FOR LIMIT AS $\overline{Pr} \to \infty$ AND $\overline{Pr} \to 0$

### 3.6.1 Axisymmetric Body Rotating in Axial Flow as $\overline{Pr} \to \infty$

From section 3.2.1 we have the following boundary layer equations

momentum meridional direction

$$\frac{V_1^*}{h_{1,0}^*}(V_1^*)_{x_1^*} - \frac{V_2^{*2}}{h_{1,0}^* h_{2,0}^*}(h_2^*)_{x_1^*} + V_\eta^{**}(V_1^*)_\eta = \frac{U^*}{h_{1,0}^*}(U^*)_{x_1^*} + (V_1^*)_{\eta,\eta} \qquad (3\text{-}152)$$

momentum azimuthal direction

$$\frac{V_1^*}{h_{1,0}^*}(V_2^*)_{x_1^*} + \frac{V_1^* V_2^*}{h_{1,0}^* h_{2,0}^*}(h_{2,0}^*)_{x_1^*} + V_\eta^{**}(V_2^*)_\eta = (V_2^*)_{\eta,\eta} \qquad (3\text{-}153)$$

continuity equation

$$\frac{1}{h_{1,0}^* h_{2,0}^*}(V_1^* h_{2,0}^*)_{x_1^*} + (V_\eta^{**})_\eta = 0 \qquad (3\text{-}154)$$

mass or heat transport

$$\frac{V_1^*}{h_{1,0}^*}(X^*)_{x_1^*} + V_\eta^{**}(X^*)_\eta = \frac{1}{\overline{Pr}}(X^*)_{\eta,\eta} \qquad (3\text{-}155)$$

Point flux

$$\frac{\overline{Nu}(x_1^*)}{\overline{Re}^{\frac{1}{2}}} = -\frac{1}{\sqrt{2}}\left[(X^*)_\eta\right]_{\eta=0} \qquad (3\text{-}156)$$

where $V_\eta^{**}$ is the dimensionless velocity component in the direction of our previously defined normal co-ordinate $\eta$. Our boundary conditions are:

$$\left.\begin{array}{llllll} \text{at } \eta = 0 & X^* = 1 & (V_2^*) = (V_2^*)_s & V_\eta^{**} = 0 & V_1^* = 0 \\ \text{as } \eta \longrightarrow \infty & X^* \longrightarrow 0 & V_2^* \longrightarrow 0 & & V_1^* \Rightarrow U_1^* \end{array}\right\} \qquad (3\text{-}157)$$

In the limit as the Schmidt or Prandtl number tends to infinity the mass or heat transfer boundary layer thickness tends to zero. Taking the Taylor series representation of $V_1^*$ expanded from the body surface, i.e.

$$V_1^* = V_1^*/_{\eta=0} + (V_1^*)_\eta /_{\eta=0}\,\eta + (V_1^*)_{\eta,\eta}/_{\eta=0}\,\eta^2 \ldots . \qquad (3\text{-}158)$$

then for an extremely thin thermal (or mass) boundary layer very little error is introduced by taking only the first two terms in the expansion, now as $V_1^*/_{\eta=0}$ then to a good approximation:

$$V_1^* = \beta(x_1^*). \quad \text{where } \beta(x_1^*) = (V_1^*)_\eta /_{\eta=0} \qquad (3\text{-}159)$$

Substitution for $V_1^*$ in the continuity equation yields, after integration:

$$V_\eta^{**} = -\frac{\eta^2}{2h_{1,0}^* h_{2,0}^*}(\beta(x_1^*)h_{2,0}^*)_{x_1^*} \qquad (3\text{-}160)$$

If we define a new variable $\xi$ where

$$\xi = \eta \overline{Pr}^{\frac{1}{3}} \qquad (3\text{-}161)$$

and using expressions (3-159) and (3-160) in the heat (or mass) transport equation leads us to obtain

$$\frac{\beta(x_1^*)}{h_{1,0}^*}\xi (X^*)_{x_1^*} - \frac{\xi^2}{2h_{1,0}^* h_{2,0}^*}(\beta(x_1^*)h_{2,0}^*)_{x_1^*}(X^*)_\xi = (X^*)_{\xi,\xi} \qquad (3\text{-}162)$$

also

$$\frac{Nu(x_1^*)}{Re^{\frac{1}{2}}Pr^{\frac{1}{3}}} = \frac{-1}{\sqrt{2}}\left[(X^*)_{\hat{\xi}}\right]_{\hat{\xi}=0} \tag{3-163}$$

Acrivos (1960) suggested the similarity type substitution

$$X^* = X^*(\hat{\xi}) \tag{3-164}$$

where

$$\hat{\xi} = \xi\ 9^{-\frac{1}{3}}\ (\beta(x_1^*)h_{2,0}^*)^{\frac{1}{2}}\left[\int_0^{x_1^*}(\beta(x_1^*)\chi)^{\frac{1}{2}}dx_1^*\right]^{-\frac{1}{3}} \tag{3-165}$$

and $\chi$ is a function of $x_1^*$ to be determined.

If $\chi$ is defined by

$$\chi = h_{2,0}^3 h_{1,0}^2 \tag{3-166}$$

then we obtain, after substitution of $\hat{\xi}$ into (3-162), the ordinary differential equation

$$\frac{d^2X^*}{d\hat{\xi}^2} + 3\hat{\xi}^2\frac{dX^*}{d\hat{\xi}} = 0 \tag{3-167}$$

The solution of which is

$$X^* = 1 - \frac{1}{\Gamma(4/3)}\int_0^{\hat{\xi}^3} e^{-z}z^{-\frac{2}{3}}dz \tag{3-168}$$

the local mass (or heat) transfer number being

$$M_H^A \text{ or } M = \frac{Nu(x_1^*)}{Re^{\frac{1}{2}}Pr^{\frac{1}{3}}} = \frac{1}{2\Gamma(4/3)9^{\frac{1}{3}}}\ \frac{\sqrt{\beta(x_1^*)h_{2,0}^*}}{\left[\int_0^{x_1^*}\sqrt{\beta(x_1^*)h_{2,0}^*\cdot h_{1,0}^* h_{2,0}^*}dx_1^*\right]^{\frac{1}{3}}} \tag{3-169}$$

where $\Gamma(\ )$ is the Gamma function

and $\beta(x_1^*) = \sum_{n=1}^{\infty} U_{2n-1}f''_{2n-1}(0)x_1^{*2n-1}$

Hence for the case of infinite Schmidt or Prandtl number we obtain our

local mass (or heat transfer) number direct from hydrodynamic boundary layer solutions.

3.6.2 Axisymmetric Body Rotating in a Quiescent Fluid as $\overline{Pr} \to \infty$

Again the same method of analysis is used as in section 3.7.1. Our results being in different form however

$$M_H^q = \frac{Nu(x_1^*)}{R_s^{\frac{1}{2}} Pr^{\frac{1}{3}}} = \frac{1}{\sqrt{2}\Gamma(4/3)9^{\frac{1}{3}}} \frac{\sqrt{\beta(x_1^*)h_{2,0}^*}}{\left[\int_0^{x_1^*} \sqrt{\beta(x_1^*)h_{2,0}^*}\, h_{1,0}^* h_{2,0}^*\right]^{\frac{1}{3}}} \qquad (3\text{-}170)$$

where $$\beta(x_1^*) = \sum_{n=1}^{\infty} F'_{2n-1}(0) x_1^{*2n-1} \qquad (3\text{-}171)$$

3.6.3 Axisymmetric Body Rotating in Axial Flow as $\overline{Pr} \to 0$

The continuity equation may be written

$$\frac{1}{h_{1,0}^* h_{2,0}^*}(V_1 h_{2,0}^*)_{x_1^*} + (V_\eta^{**})_\eta = 0 \qquad (3\text{-}172)$$

As $\overline{Pr} \to 0$ the hydrodynamic boundary layer thickness tends to zero (here we are assuming that the Kinematic viscosity is tending to zero) hence the velocity in the mass or heat transport boundary layer may be taken as that of the potential flow

hence $$V_1^* = U^* \qquad (3\text{-}173)$$

On substitution into the continuity equation we achieve an integration

$$V_\eta^{**} = -\frac{\eta}{h_{1,0}^* h_{2,0}^*}(U^* h_{2,0}^*)_{x_1^*} \qquad (3\text{-}174)$$

Substitution of $V_1^*$ and $V_\eta^*$ into the mass (or heat) transport equation together with the substitution of the variable $\tau$ where

$$\tau = \overline{Pr}^{\frac{1}{2}} \eta \qquad (3\text{-}175)$$

gives

$$\frac{U^*}{h^*_{1,0}}(X^*)_{x^*_1} - \frac{\tau}{h^*_{1,0}h^*_{2,0}}(U^* h^*_{2,0})_{x^*_1}(X^*)_\tau = (X^*)_{\tau,\tau} \tag{3-176}$$

and

$$\frac{Nu(x^*_1)}{Re^{\frac{1}{2}}Pr^{\frac{1}{2}}} = -\frac{1}{\sqrt{2}}\left[(X^*)_\tau\right]_{\tau=0} \tag{3-177}$$

If we now substitute the variable $\zeta$ which is defined as:

$$\zeta = \frac{\tau U^* h^*_{2,0}}{2\sqrt{\int_0^{x^*_1} h^*_{1,0}h^{*2}_{2,0}U^* dx^*_1}} \tag{3-178}$$

into equation (3-176) and assume the similarity type transformation

$$X^* = X^*(\zeta)$$

we obtain the ordinary differential equation

$$\frac{d^2X^*}{d\zeta^2} + 2\zeta\frac{dX^*}{d\zeta} = 0 \tag{3-179}$$

for which the solution is

$$X^* = \text{erfc}(\zeta) \tag{3-180}$$

erfc being the complimentary error function, the local mass (or heat) transfer number being

$$M^A_H \text{ or } M = \frac{Nu(x^*_1)}{Re^{\frac{1}{2}}Pr^{\frac{1}{2}}} = U^* h^*_{2,0}\left[\pi\int_0^{x^*_1} h^*_{1,0}h^{*2}_{2,0}U^* dx^*_1\right]^{-\frac{1}{2}} \tag{3-181}$$

It can be seen that the local transfer number is independent on the rotational spin of the body, the potential flow being the factor which primarily determines the mass or heat transfer rate. One can hence assume that as the Prandtl or Schmidt number approaches zero then the effect of spin on mass transfer diminishes.

### 3.6.4 Axisymmetric Body Rotating in a Quiescent Fluid as $\overline{Pr} \to 0$

Because in this case we can assume that the Kinematic viscosity of the system tends to zero then no velocity components exist in the

fluid. This particular case is hence a pure diffusional problem a boundary layer not being in existence, our equations are valid for the boundary layer region in forced convective conditions only and are not valid for this case.

## 3.7 APPLICATION OF METHOD TO THE OBLATE SPHEROID

We shall now use the general theory that has been developed to predict local heat or mass transfer rates from oblate spheroid bodies rotating in axial flow or quiescent fluid.

We shall work with the oblate spheroidal co-ordinate system $(\xi, \theta, \phi)$ which can be defined in terms of the Cartesian co-ordinate system $(x, y, z)$ as follows:

$$\begin{aligned} x &= c \cosh \xi \sin \theta \cos \phi \\ y &= c \cosh \xi \sin \theta \sin \phi \\ z &= c \sinh \xi \cos \theta \end{aligned} \tag{3-182}$$

where $\xi \geq 0$; $0 \leq \theta \leq \pi$; $0 \leq \phi \leq 2\pi$ and c is the distance of the focii of the spheroid from the spheroid centre. It can further be shown (see Green (1968) or Spiegel (1959)) that the scale factors are given by

$$\begin{aligned} h_\xi = h_\theta &= c\,(\sinh^2 \xi + \cos^2 \theta)^{\frac{1}{2}} \\ h_\phi &= c \cosh \xi \sin \theta \end{aligned} \tag{3-183}$$

consequently on the body surface where $\xi = \xi_s$

$$\begin{aligned} h_{\xi,0} = h_{\theta,0} &= c\,(\sinh^2 \xi_s + \cos^2 \theta)^{\frac{1}{2}} \\ h_{\phi,0} &= c \cosh \xi_s \sin \theta \end{aligned} \tag{3-184}$$

Now the semi-major axis, a, and the semi-minor axis, b, are given by

$$\begin{aligned} a &= c \cosh \xi_s \\ b &= c \sinh \xi_s \end{aligned} \tag{3-185}$$

Consequently the equations (3-184) become, on rearrangement:

$$h_{\xi,0} = h_{\theta,0} = a(1-(\sin\theta/\cosh\xi_s)^2)^{\frac{1}{2}}$$

$$h_{\phi,0} = a\sin\theta$$

we thus have for the scale factor $h_{\phi,0}$

$$h_{\phi,0} = a(1-\frac{\theta^3}{3!}+\frac{\theta^5}{5!}-\ldots\ldots+(-1)^{n-1}\frac{\theta^{2n-1}}{(2n-1)!}+\ldots) \quad (3\text{-}186)$$

It should here be noted that $\theta$ is dimensionless, it hence follows from (3-85) that the characteristic dimension for the oblate spheroid is the semi-major axis, a. It follows that the coefficients in the dimensionless scale factor expansion $h^*_{\phi,0} = \sum K_{2n-1}\theta^{2n-1}$ are given by:

$$K_1 = 1\ ;\quad K_3 = -\frac{1}{3!}\ ;\ \ldots\ldots\ ;\quad K_{2n-1} = (-1)^{n-1}/(2n-1)! \quad (3\text{-}187)$$

The expansion in power series form of $h_{\theta,0}$ is very complicated the first terms in the expansion being

$$h_{\theta,0} = a(1-(\frac{1-e^2}{2})\theta^2+\left\{4(1-\frac{e-3(1-e^2)^2}{4!}\right\}\theta^4+\ldots) \quad (3\text{-}188)$$

where $e = b/a$. It follows that the coefficients $l_{2(n-1)}$ in $h^*_{\theta,0} = \sum l_{2(n-1)}\theta^{2(n-1)}$ are given by

$$l_0 = 1\ ;\quad l_2 = -(\frac{1-e^2}{2!})\ ;\quad l_4 = \frac{4(1-e^2)-4(1-e^2)^2}{4!}\ ;\ \ldots(3\text{-}189)$$

further terms become increasingly difficult to obtain, the remainder of the terms up to $l_{2(n-1)}$ are obtained by a numerical method explained in chapter 4. In our general analysis $x_2$ is the same as $\phi$ and $x_1$ is the same as $\theta$ it follows that $h_{1,0} \equiv h_{\theta,0}$ and $h_{2,0} \equiv h_{\phi,0}$.

The expression for potential flow around a stationary oblate spheroid in axial flow has previously been determined by Milne-

Thomson (1938). In terms of the oblate spheroidal co-ordinate system ($\xi$, $\theta$, $\phi$) it is given by

$$U = K(e)\, U_\infty \sin\theta \left(1 - \sin^2\theta/\cosh^2\xi_s\right)^{-\frac{1}{2}} \qquad (3\text{-}190)$$

where

$$K(e) = \frac{1 - e^2}{\frac{1}{(1-e^2)^{\frac{1}{2}}}\cot^{-1}\frac{e}{(1-e^2)^{\frac{1}{2}}} - e} \qquad (3\text{-}191)$$

The expansion of (3-190) into a power series form presents even more difficulties than that of the scale factor $h_{\theta,0}$, again this is done by numerical techniques as explained in chapter 4. We hence have from (3-190) the characteristic velocity dimension is $K(e)U_\infty$ and consequently dimensionless potential flow is given by

$$U^* = 1 + \left(\frac{2-3e^2}{3!}\right)\theta^3 + \ldots\ldots \qquad (3\text{-}192)$$

and therefore coefficients $U_{2i-1}$ in the expansion $U^* = \sum U_{2n-1}\theta^{2n-1}$ are given by:

$$U_1 = 1 \; ; \; U_3 = \left(\frac{2-3e^2}{3!}\right) \; ; \; \ldots\ldots \qquad (3\text{-}193)$$

# CHAPTER IV

## NUMERICAL TECHNIQUES

### 4.1 INTRODUCTION

We have shown in chapter 3 that substitution of suitable power series forms for the velocity components, scale factors and potential flow into the non-linear partial differential boundary layer equations reduces them to infinite sets of ordinary differential equations which are more amenable to analysis. These ordinary differential equations are linear except for the first pair of hydrodynamic equations (the hydrodynamic stagnation point equations).

The two original partial differential hydrodynamic equations were coupled; consequently, the two infinite sets of ordinary differential equations obtained from power series substitution are coupled. The hydrodynamic ordinary differential equations do not contain any mass or heat transfer functions and as a consequence can be integrated independently of the mass or heat transfer equations. The mass or heat transfer equations, however, do contain hydrodynamic functions and subsequently can only be integrated simultaneously with the hydrodynamic equations.

In order to determine the effect of spin on mass or heat transfer it is necessary for us to determine the boundary values $\mathcal{H}'_{2(i-1)}(0)$ in the case of a body rotating in axial flow and $J'_{2(i-1)}(0)$ for the case of a body rotating in a quiescent fluid. Because of the complexity of our equations it is not possible to determine these analytically,

a numerical technique must be used.

When integrating our equations for $\mathcal{H}''_{2(i-1)}(\eta)$ and $J''_{2(i-1)}(\alpha)$ we can supply the values of the hydrodynamic functions either explicitly in tabular form or use an implicit method, i.e. integrate the hydrodynamic equations simultaneously. The explicit form of approach is limited by the computer storage facility, however the implicit method requires only the boundary values $\bar{f}''_{2i-1}(0)$, $\bar{g}'_{2i-1}(0)$ (in the case of a body rotating in an axial flow) to be supplied, the implicit approach was chosen as being the most economical in computer storage.

The general approach in the numerical solution of boundary value problems is to guess the unknown boundary values, integrate the simultaneous ordinary differential equations with respect to the independent variable $\eta$ over the range $0 \leqslant \eta \leqslant \infty$ where $\infty$ is some large finite number, at infinity comparisons between calculated and known boundary values can be made - these comparisons leading to better guesses of the unknown initial boundary values.

For the stagnation point equations a special technique of quasilinearisation introduced by Lee and Fan (1968) is used, this is a powerful tool in the solution of non-linear boundary value problems, all of the linear differential equations can be solved using the principle of superposition.

## 4.2 SOLUTION OF THE NON-LINEAR HYDRODYNAMIC STAGNATION POINT EQUATIONS FOR A BODY ROTATING IN AXIAL FLOW

### 4.2.1 Theoretical

Substitution of $U_1 = 1$ in (3-78) yields for $n = 1$

$$\bar{f}'''_1 = (-2\bar{f}_1\bar{f}''_1 + \bar{f}'^2_1 - \lambda\,\bar{g}^2_1 - 1)\,/l_o \qquad (4\text{-}1)$$

$$\bar{g}''_1 = (2\bar{g}_1\bar{f}'_1 - 2\bar{g}'_1\bar{f}_1)\,/l_o \qquad (4\text{-}2)$$

the pertinent boundary values of the functional coefficients being

$$\left.\begin{array}{lll} \text{at } \eta = 0 & \bar{f}_1 = \bar{f}_1' = 0 & \bar{g}_1 = K_1 \\ \text{as } \eta \longrightarrow \infty & \bar{f}_1 \longrightarrow 1 & \bar{g}_1 \longrightarrow 0 \end{array}\right\} \qquad (4\text{-}3)$$

The order of the differential system is five, there are also five distinct boundary values and so the system is fully defined, the boundary values, however, are not all stipulated at the same boundary and we hence have a two point boundary value problem with split boundary values.

If we now define five new variables

$$\left.\begin{array}{l} Y(1) = \bar{f}_1 \\ Y(2) = \bar{f}_1' \\ Y(3) = \bar{f}_1'' \\ Y(4) = \bar{g}_1 \\ Y(5) = \bar{g}_1' \end{array}\right\} \qquad (4\text{-}4)$$

and define $YG(N) \equiv Y'(N) \qquad N = 1, \ldots, 5 \qquad (4\text{-}5)$

it is possible to reduce our fifth order ordinary differential equation system to five simultaneous first order differential equations. Substitution of (4-4) into (4-1) and (4-2) yields the five first order simultaneous differential equations,

$$\left.\begin{array}{l} YG(1) = Y(2) \\ YG(2) = Y(3) \\ YG(3) = (-2Y(1)\,Y(3)+Y(2)^2-\lambda Y(4)^2-1)/l_o \\ YG(4) = Y(5) \\ YG(5) = (2Y(4)\,Y(2)-2Y(5)\,Y(1))/l_o \end{array}\right\} \qquad (4\text{-}6)$$

with boundary values:

$$\left.\begin{array}{lll} \text{at } \eta = 0 & Y(1) = Y(2) = 0 & Y(4) = K_1 \\ \text{as } \eta \longrightarrow \infty & Y(2) \longrightarrow 1 & Y(4) \longrightarrow 0 \end{array}\right\} \qquad (4\text{-}7)$$

Hoskin (1955) has already solved equations (4-1) and (4-2) for seven values of $\lambda$, the spin parameter in the region $0 < \lambda < 10$, his method of solution was to expand known boundary values in Taylor series forms the partial differential coefficients being determined by a finite difference procedure, this type of procedure is reproduced in Appendix B. The method unfortunately was found to be very difficult to use in practice as guesses of the unknown boundary values had to be correct to two decimal places for the method to produce a better estimate, usually because of the high non-linearity of the system and the inability to give an accurate enough initial estimate calculated values of the unknown functions rapidly become infinite and unmanageable.

A much more effective method and a very powerful tool in general for the solution of non-linear boundary value problems with split boundary values is the quasilinearisation procedure of Lee and Fan (1968) which we shall describe.

Because an n'th order differential equation may be represented by n first order simultaneous ordinary differential equations we can here discuss the general case of a system of simultaneous first order ordinary differential equations given by

$$\frac{dZ_i}{dt} = \phi_i(Z_1, Z_2, Z_3, \ldots . Z_n, t) \quad i = 1,2,\ldots .n \qquad (4\text{-}8)$$

where $Z_i$ are functions of the independent variable t. These equations may be represented in vector form as:

$$\frac{d\underline{Z}}{dt} = f(\underline{Z}, t) \qquad (4\text{-}9)$$

where f and $\underline{Z}$ are n-dimensional vectors, the boundary values for the system being,

$$\begin{aligned} Z_j(0) &= Z_{jo} \qquad j = 1,2,\ldots.m \\ Z_q(t_f) &= Z_{qf} \qquad q = m+1,\ldots.n \end{aligned} \tag{4-10}$$

where $t_f$ represents the final value of t.

If we know an approximate solution $\underline{Z}^o$ of equation (4-9) we can use the Taylor series expansion around $\underline{Z}^o$ to obtain (on neglect of non-linear terms)

$$\frac{d\underline{Z}}{dt} = f(\underline{Z}^o, t) + J(\underline{Z}^o)\,(\underline{Z} - \underline{Z}^o) \tag{4-11}$$

where $J(\underline{Z}^o)$ the Jacobi matrix is defined as:

$$J(\underline{Z}^o) = \begin{bmatrix} \frac{\partial \phi_1}{\partial Z_1}^o & \frac{\partial \phi_1}{\partial Z_2}^o & \cdots\cdots & \frac{\partial \phi_1}{\partial Z_n}^o \\ \cdots\cdots & \cdots\cdots & \cdots\cdots & \cdots\cdots \\ \frac{\partial \phi_n}{\partial Z_1}^o & \frac{\partial \phi_n}{\partial Z_2}^o & \cdots\cdots & \frac{\partial \phi_n}{\partial Z_n}^o \end{bmatrix} \tag{4-12}$$

Now $\underline{Z}^o$ is a known function and so (4-11) represents a system of linear equations with variable coefficients $\underline{Z}^o$, hence the set can be solved numerically using the principle of superposition.

If the solution of (4-11) is $\underline{Z}^1$ we can expand equation (4-9) again to obtain

$$\frac{d\underline{Z}}{dt} = f(\underline{Z}^1, t) + J(\underline{Z}^1)(\underline{Z} - \underline{Z}^1) \tag{4-13}$$

which again can be solved by the superposition principle, if we continue the procedure to the k'th iteration we obtain

$$\frac{d\underline{Z}^{k+1}}{dt} = f(\underline{Z}^k, t) + J(\underline{Z}^k)(\underline{Z}^{k+1} - Z^k) \tag{4-14}$$

for which the homogeneous part is

$$\frac{d\underline{Z}^{k+1}}{dt} = J(\underline{Z}^{k})\ \underline{Z}^{k+1} \qquad (4\text{-}15)$$

The boundary values for our recurrence relationship (4-14) and (4-15) are:

$$\left.\begin{aligned} Z_j^{k+1}(0) &= Z_{j0} \qquad j = 1,2,\ldots.m \\ Z_q^{k+1}(t_f) &= Z_{qf} \qquad q = m+1,\ldots.n \end{aligned}\right\} \qquad (4\text{-}16)$$

In non-vector terms equations (4-14) and (4-15) can be written respectively for the n'th component of the vector

$$\frac{dZ_n^{k+1}}{dt} = f_n(Z_n^k,t)+(Z_1^{k+1}-Z_1^k)\frac{\partial f_n}{\partial Z_1^k}+\ldots+(Z_n^{k+1}-Z_n^k)\frac{\partial f_n}{\partial Z_n^k}$$

$$\frac{dZ_n^{k+1}}{dt} = Z_1^{k+1}\frac{\partial f_n}{\partial Z_1^k}+\ldots\ldots+Z_n^{k+1}\frac{\partial f_n}{\partial Z_n^k}$$

In our problem we let $\underline{Y}^{k+1}(P)$ be the current value of the k+1'th iteration, i.e. $\underline{Y}^{k+1}(P) \equiv \underline{Z}^{k+1}$ in equations (4-14) and (4-15) and $\underline{Y}^{k}(P) \equiv \underline{Z}^{k}$. We can use the recurrence relationship (4-14) on (4-6) to obtain the following equations

$$\left.\begin{aligned} YG(1) &= Y^{k+1}(2) \\ YG(2) &= Y^{k+1}(3) \\ YG(3) &= (-2Y^{k}(1)\ Y^{k+1}(3) - 2Y^{k}(3)\ Y^{k+1}(1) + 2Y^{k}(2)\ Y^{k+1}(2) + 2Y^{k}(1)\ Y^{k}(3) \\ &\quad -Y^{k}(2)\ Y^{k}(2) - 1 - 2\lambda\ Y^{k}(4)\ Y^{k+1}(4) + \lambda\ Y^{k}(4)\ Y^{k}(4))/l_o \\ YG(4) &= Y^{k+1}(5) \\ YG(5) &= (2Y^{k}(4)\ Y^{k+1}(2) + 2Y^{k}(2)\ Y^{k+1}(4) - 2Y^{k}(5)\ Y^{k+1}(1) - 2Y^{k}(1)\ Y^{k+1}(5) \\ &\quad +2Y^{k}(5)\ Y^{k}(1) - 2Y^{k}(2)\ Y^{k}(4))/l_o \end{aligned}\right\} \qquad (4\text{-}17)$$

with their pertinent boundary values being

$$\left.\begin{aligned} &\text{at } \eta = 0 \quad Y^{k+1}(1) = Y^{k+1}(2) = 0 \quad Y^{k+1}(4) = k_1 \\ &\text{as } \eta \longrightarrow \infty \quad Y^{k+1}(2) \longrightarrow 1 \quad Y^{k+1}(4) \longrightarrow 0 \end{aligned}\right\} \qquad (4\text{-}18)$$

The equations (4-17) are our linearised set of equations the homogeneous equivalents of these linearised equations are obtained by using the recurrance relationship (4-15) on (4-6) to obtain

$$\left.\begin{aligned} YG(1) &= Y(2)^{k+1} \\ YG(2) &= Y(3)^{k+1} \\ YG(3) &= (-2Y(1)^{k+1}\, Y(3)^{k} - 2Y(1)^{k}\, Y(3)^{k+1} + 2Y(2)^{k+1}\, Y(2)^{k} - 2\lambda\, Y(4)^{k+1}\, Y(4)^{k})/1_o \\ YG(4) &= Y(5)^{k+1} \\ YG(5) &= (2Y(4)^{k+1}\, Y(2)^{k} + 2Y(4)^{k}\, Y(2)^{k+1} - 2Y(5)^{k}\, Y(1)^{k+1} - 2Y(5)^{k+1}\, Y(1)^{k})/1_o \end{aligned}\right\} \quad (4\text{-}19)$$

it should be noted that in equation sets (4-17) and (4-19) we have used the notation $YG(i) = \frac{d}{d\eta}\left[Y(i)^{k+1}\right]$.

If we let $Y(1)^{k+1}_p$, $Y(2)^{k+1}_p$, ....., $Y(5)^{k+1}_p$ be any set of solutions of (4-17) and $Y(1)^{k+1}_{hj}$, $Y(2)^{k+1}_{hj}$, ....., $Y(5)^{k+1}_{hj}$ be any five sets of non-trivial and distinct solutions of the homogeneous equations (4-19) then the solution of (4-17) can be written

$$Y(i)^{k+1} = Y(i)^{k+1}_p + \sum_{j=1}^{5} a_j^{k+1}\, Y(i)^{k+1}_{hj} \qquad i = 1,2,\ldots 5 \qquad (4\text{-}20)$$

Since equations (4-17) are a system of differential equations of order five, then five integration constants $a_j^{k+1}$ ; j = 1,2,...5 are required for their general solution.

The five sets of homogeneous solutions can be obtained by numerically integrating (4-19) five times with any five sets of distinct and non-trivial initial conditions, similarly the required one set of particular solutions can be obtained by integrating equations (4-17) with any initial conditions. By using the three initial conditions in (4-18) we are able to reduce the number of homogeneous equations required by three, i.e. two homogeneous equations are now required to determine the two remaining unknown constants. If the following initial conditions

are used then the three initial conditions in (4-18) are satisfied

$$\underline{Y}(i)^{k+1}_{p}\Big|_{\eta=0} = \begin{bmatrix} Y(1)^{k+1}_{p} \\ Y(2)^{k+1}_{p} \\ . \\ . \\ Y(5)^{k+1}_{p} \end{bmatrix} = \begin{bmatrix} 0 \\ 0 \\ 0 \\ k_1 \\ 0 \end{bmatrix} \qquad (4\text{-}21)$$

$$\underline{Y}(i)_{h1}\Big|_{\eta=0} = \begin{bmatrix} Y(1)^{k+1}_{h1} \\ . \\ . \\ . \\ Y(5)^{k+1}_{h1} \end{bmatrix} = \begin{bmatrix} 0 \\ 0 \\ 1 \\ 0 \\ 0 \end{bmatrix} \qquad (4\text{-}22)$$

$$\underline{Y}(i)^{k+1}_{h2}\Big|_{\eta=0} = \begin{bmatrix} Y(1)^{k+1}_{h2} \\ . \\ . \\ . \\ Y(5)^{k+1}_{h2} \end{bmatrix} = \begin{bmatrix} 0 \\ 0 \\ 0 \\ 0 \\ 1 \end{bmatrix} \qquad (4\text{-}23)$$

and equation (4-20) reduces to:

$$Y(i)^{k+1} = Y(i)^{k+1}_{p} + \sum_{j=1}^{2} a_j^{k+1}\, Y(i)^{k+1}_{hj} \qquad i = 1,2,\ldots.5 \qquad (4\text{-}24)$$

We can determine the two remaining constants by making use of the two conditions at infinity in (4-18)

i.e.

$$Y(2)^{k+1}_{p}\Big|_{\eta=\infty} + a_1^{k+1}\cdot Y(2)^{k+1}_{h1}\Big|_{\eta=\infty} + a_2^{k+1}\cdot Y(2)^{k+1}_{h2}\Big|_{\eta=\infty} = Y(2)^{k+1}\Big|_{\eta=\infty} = 1 \qquad (4\text{-}25)$$

$$Y(4)^{k+1}_{p}\Big|_{\eta=\infty} + a_1^{k+1}\cdot Y(4)^{k+1}_{h1}\Big|_{\eta=\infty} + a_2^{k+1}\cdot Y(4)^{k+1}_{h2}\Big|_{\eta=\infty} = Y(4)^{k+1}\Big|_{\eta=\infty} = 0 \qquad (4\text{-}26)$$

From (4-25) and (4-26) we obtain:

$$a_1^{k+1} = \left[\frac{Y(4)^{k+1}_{h2}(1-Y(2)^{k+1}_{p}) + Y(4)^{k+1}_{p}\cdot Y(2)^{k+1}_{h2}}{Y(2)^{k+1}_{h2}\cdot Y(4)^{k+1}_{h1} - Y(4)^{k+1}_{h2}\cdot Y(2)^{k+1}_{h1}}\right]_{\eta=\infty} \qquad (4\text{-}27)$$

$$a_2^{k+1} = \left[\frac{Y(4)^{k+1}_{h1}(1-Y(2)^{k+1}_{p}) + Y(4)^{k+1}_{p}\cdot Y(2)^{k+1}_{h1}}{Y(2)^{k+1}_{h2}\cdot Y(4)^{k+1}_{h1} - Y(4)^{k+1}_{h2}\cdot Y(2)^{k+1}_{h1}}\right]_{\eta=\infty} \qquad (4\text{-}28)$$

hence we are now able to determine $a_1^{k+1}$ and $a_2^{k+1}$ and hence we are able to determine $\bar{f}_1''(0)$ (or Y(3)) and $\bar{g}_1'(0)$ (or Y(5)).

### 4.2.2 Numerical Technique

In order to start the numerical calculations we need to know all the values of Y(i), i = 1,2,...,5 for the previous iteration, i.e. all $Y^{k}(i)$ must be known. For the first iteration we have no previous values of $Y^{k}(i)$ and hence we must supply initial approximations to these values. Guesses were made at the average values of these unknown $Y^{k}(i)$, it was found that choosing

$$\left.\begin{aligned} Y(1)^{k=0} &= 3 \\ Y(2)^{k=0} &= 0.5 \\ Y(3)^{k=0} &= 0.3 \\ Y(4)^{k=0} &= 0.3 \\ Y(5)^{k=0} &= -0.5 \end{aligned}\right\} \qquad (4\text{-}29)$$

for all $\eta$ , our system behaved well over the range $0 < \lambda < 100$ which was the range tested for spin parameter $\lambda$.

It should be remembered that the boundary values of our functions Y(1) to Y(5) are given at $\eta = 0$ and $\eta = \infty$ which is their asymptotic value. It was found however that these functions rapidly approach their asymptotic values and at approximately $\eta = 4$ they differ from their asymptotic values only in the sixth place of decimals. The numerical values of the boundary values determined by the quasilinearisation technique were found to be independent of the value of $\eta$ taken as infinity as long as it is greater than five. In order to have a safety margin the value of the 'effective' infinity for $\eta$ was taken as six.

The method of calculation was as follows: equation (4-17) with initial conditions (4-21) was integrated from $\eta = 0$ to $\eta = 6$ by a Runge-Kutta integration procedure the stored values of the previous iteration being used for the functions $Y(i)^{k}$. From the Runge-Kutta integration we are able to determine $Y(i)^{k+1}_{p}$ at each $\eta$ and $Y(2)^{k+1}_{p}|_{\eta=\infty}$ and $Y(4)^{k+1}_{p}|_{\eta=\infty}$ at $\eta = 6$. Similarly integrating equations (4-19) with boundary conditions (4-22) we obtain $Y(i)^{k+1}_{h1}$ at each $\eta$ and $Y(2)^{k+1}_{h1}|_{\eta=\infty}$ and $Y(4)^{k+1}_{h1}|_{\eta=\infty}$ at $\eta = 6$, integration of (4-19) with boundary conditions (4-23) yields $Y(i)^{k+1}_{h2}$ at each $\eta$ and $Y(2)^{k+1}_{h2}|_{\eta=\infty}$ and $Y(4)^{k+1}_{h2}|_{\eta=\infty}$ at $\eta = 6$. Substitution of these values of Y(2) and Y(4) at infinity into equations (4-27) and (4-28) yields the values of $a_1^{k+1}$ and $a_2^{k+1}$. Substitution of $a_1^{k+1}$, $a_2^{k+1}$ and $Y(i)^{k+1}_{p}$, $Y(i)^{k+1}_{h1}$, $Y(i)^{k+1}_{h2}$ at each $\eta$ into (4-24) thus enables us to determine $Y(2)^{k+1}$ at each $\eta$, these values become the $Y(i)^{k}$ of the next iteration.

The procedure was repeated and new values of the constants $a_1^{k+1}$, $a_2^{k+1}$ obtained, the calculation being stopped when two successive values of $a_1^{k+1}$ and $a_2^{k+1}$ differed by a value less than or equal to $1 \times 10^{-6}$.

From (4-24) it can be seen that the values $\bar{f}_1''(0)$ and $\bar{g}_1'(0)$ are

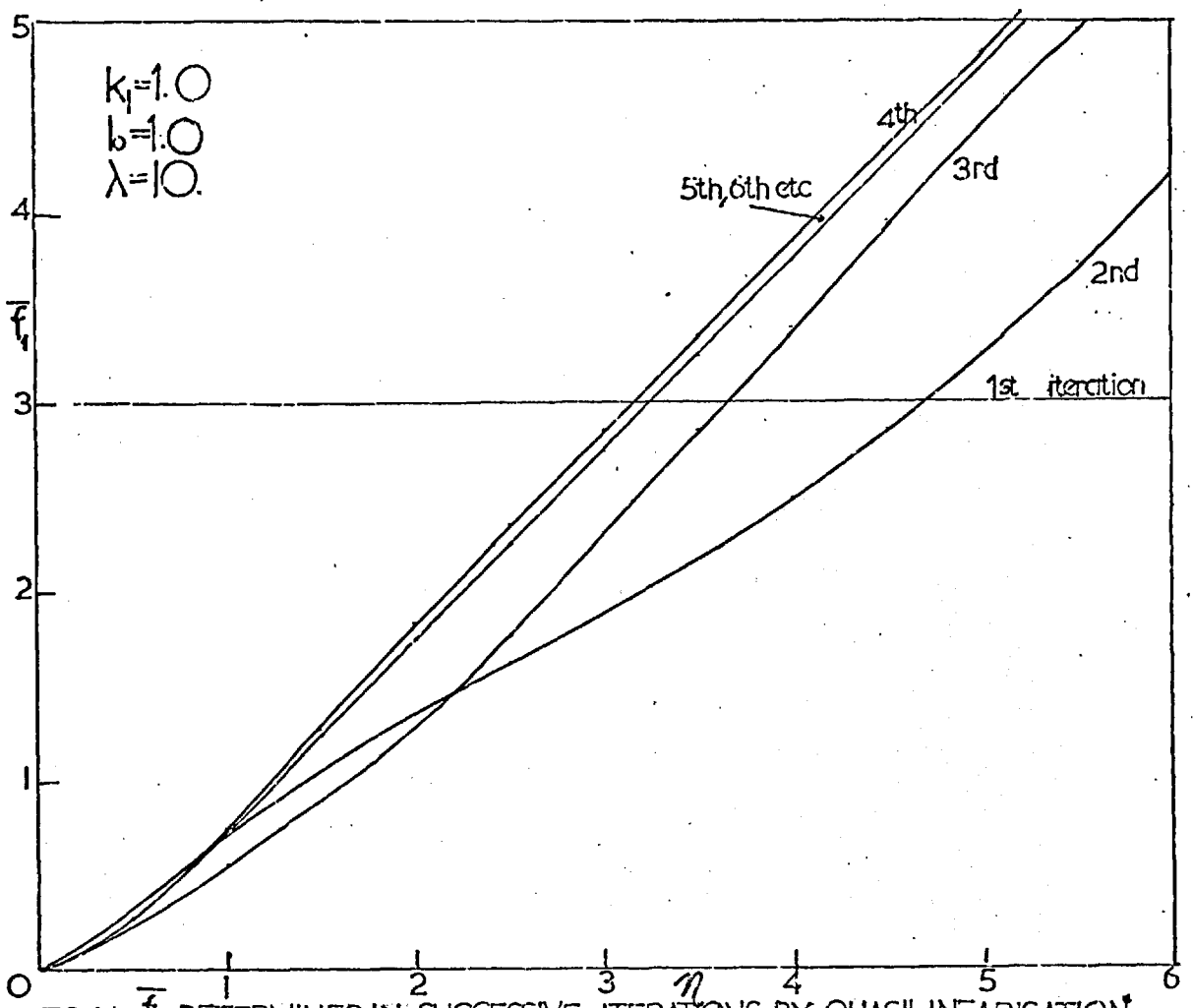



FIG 4.1 $\bar{f}_1$ DETERMINED IN SUCCESSIVE ITERATIONS BY QUASILINEARISATION

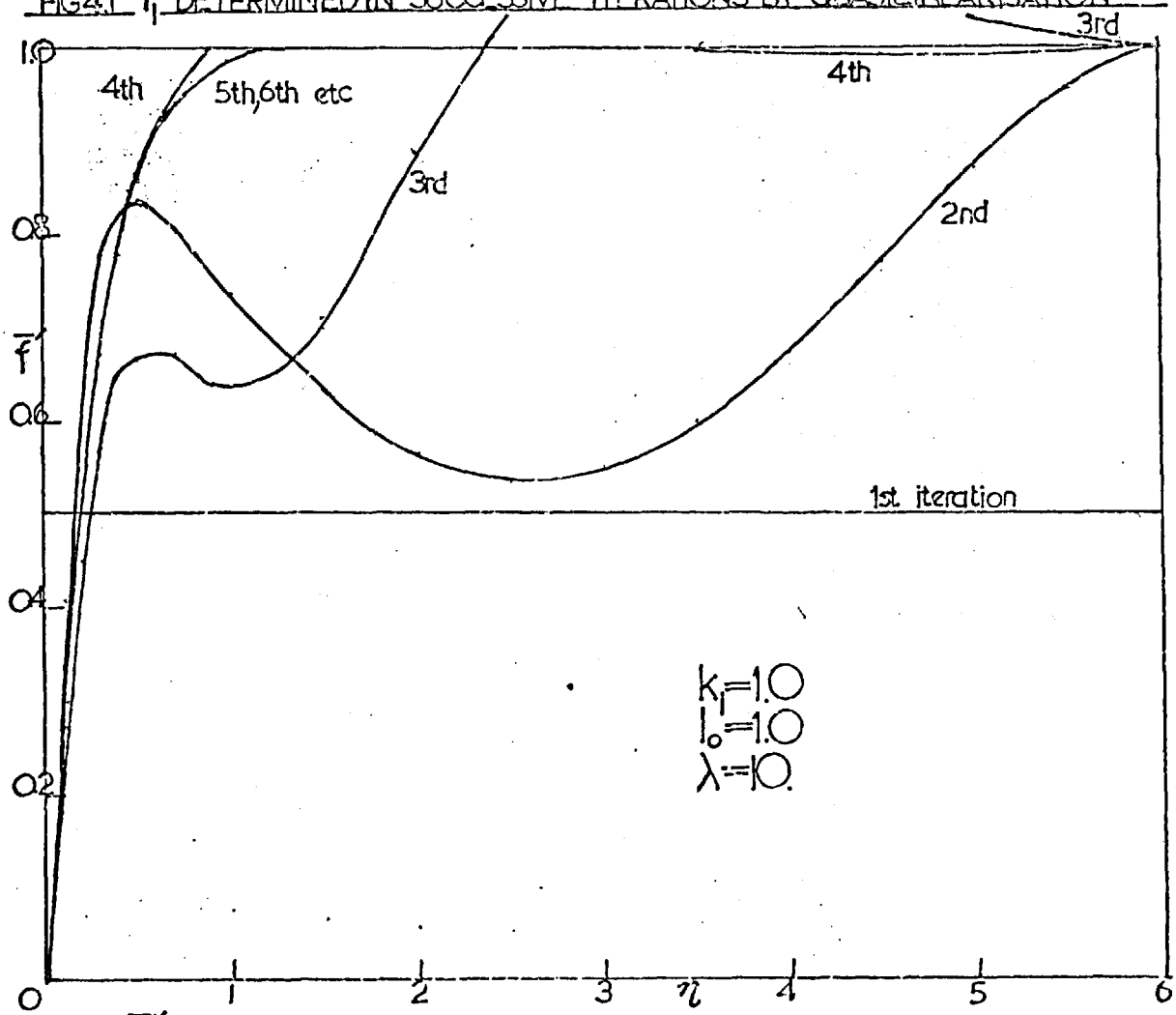



FIG 4.2 $\bar{f}_1'$ DETERMINATION BY QUASILINEARISATION

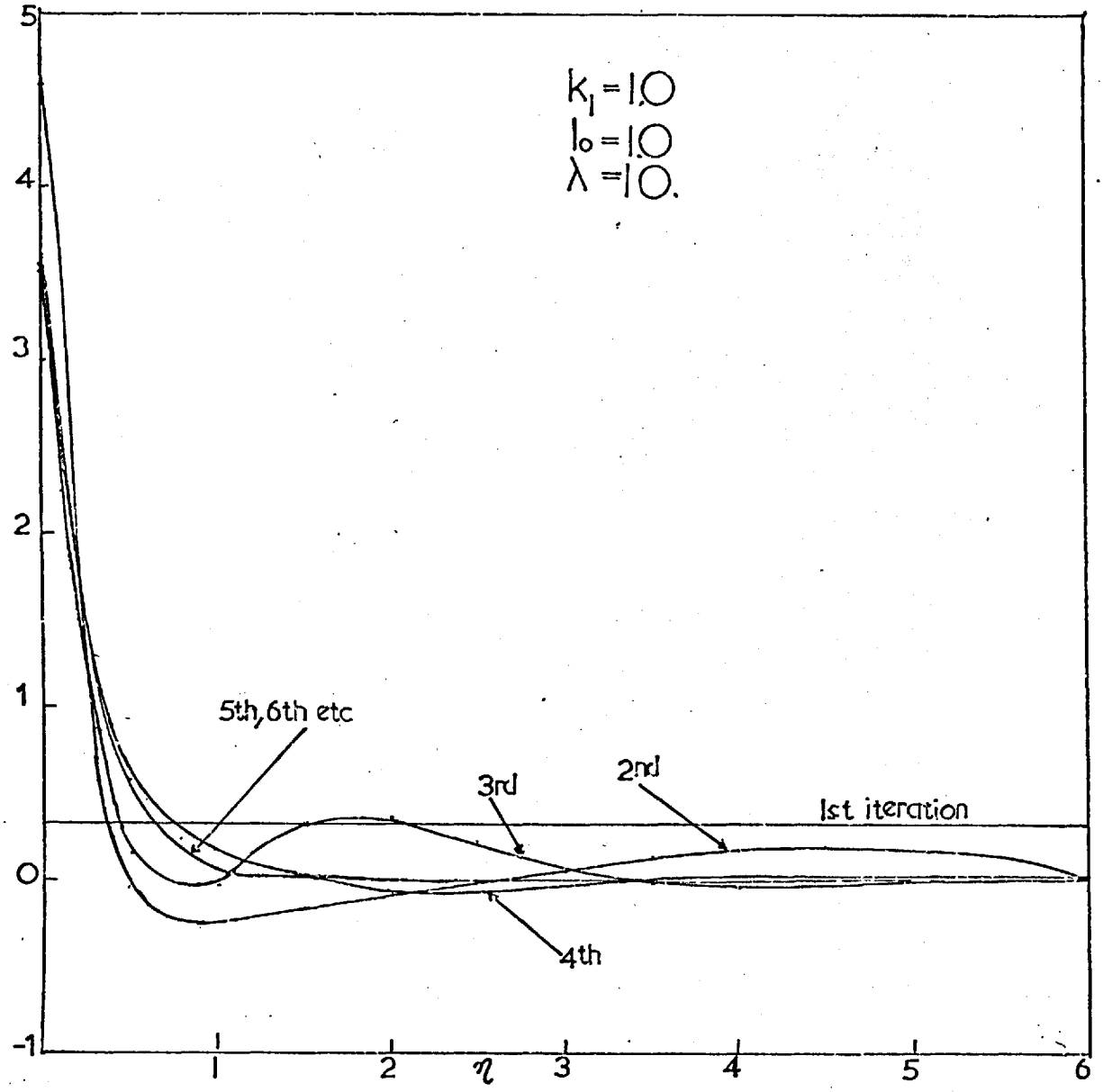



FIG4.3 $\overline{f_1}''$ DETERMINED BY QUASILINEARISATION

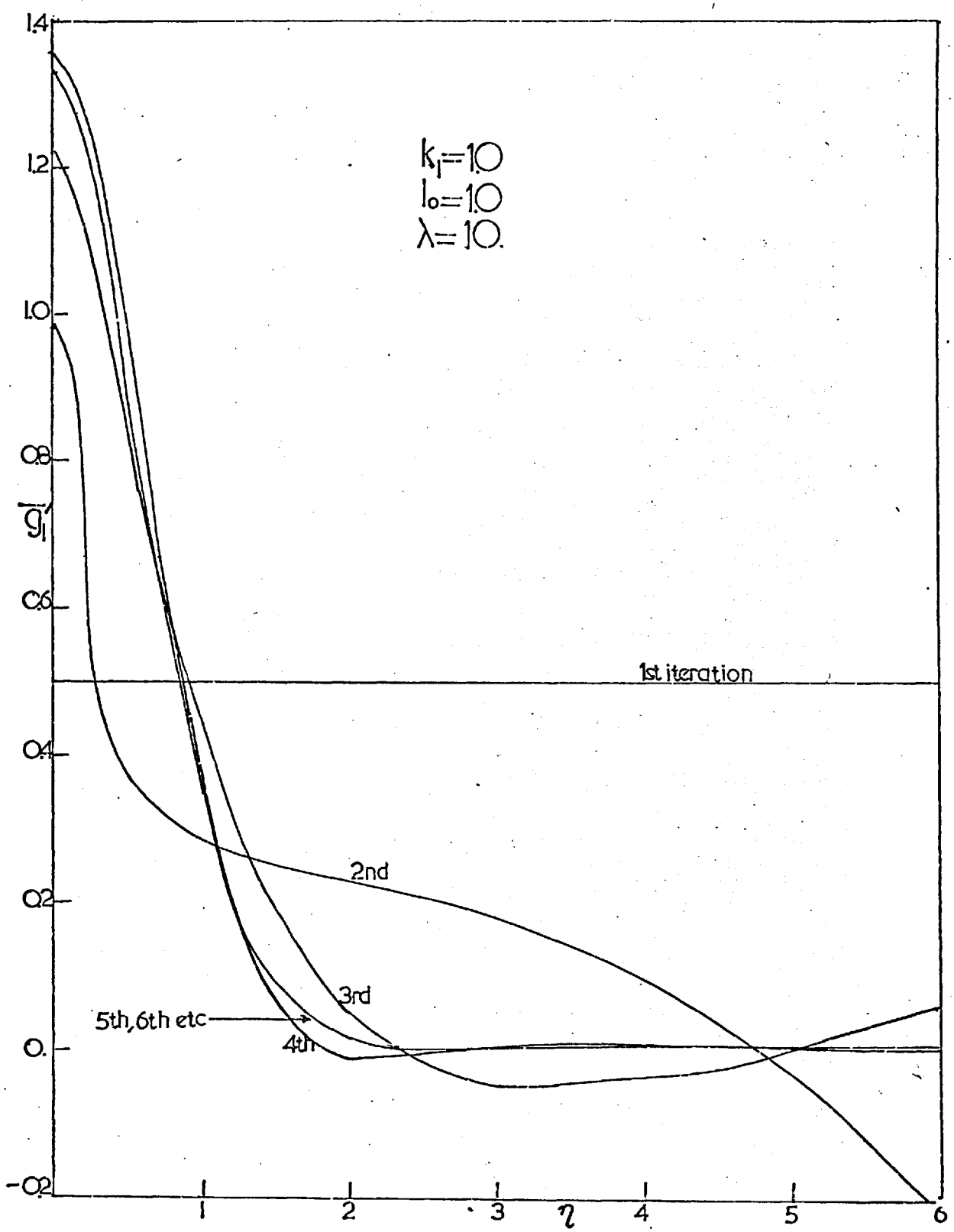



FIG4.4 $\bar{g}_1'$ DETERMINATION BY QUASILINEARISATION

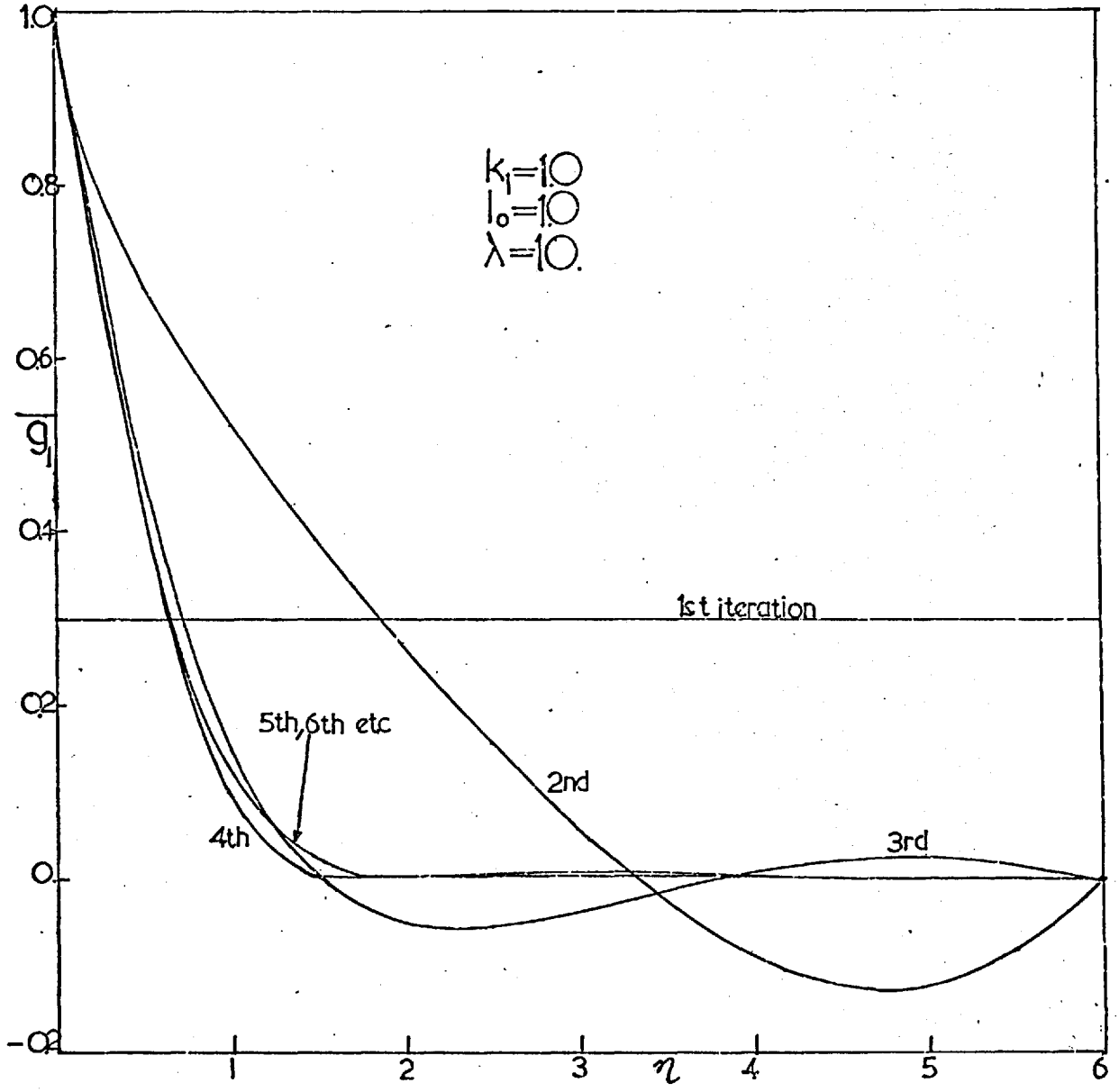



FIG 4.5 $\bar{g}_1$ DETERMINATION BY QUAZILINEARISATION

numerically equal to $a_1^{k+1}$ and $a_2^{k+1}$ respectively.

As can be seen in the graphs, fig.4.1 to fig.4.5, using the most crude of guesses (4-29) we have a numerically stable system that converges to the correct results rapidly.

The step length used for the Runge-Kutta integration procedure was found to have a decisive influence on the values obtained for $a_1^{k+1}$ and $a_2^{k+1}$ as can be seen from the table below

| step length h | 0.1 | 0.05 | 0.025 | 0.01 |
|---|---|---|---|---|
| $a_1^{k+1}(=\bar{f}_1''(0))$ | 3.554284 | 3.563224 | 3.565408 | 3.566016 |
| $a_2^{k+1}(=\bar{g}_1'(0))$ | -1.330536 | -1.325602 | -1.324339 | -1.323983 |

for which $k_1 = l_o = 1$ and spin parameter $\lambda = 10$. The results show that the boundary values obtained by using a step length of 0.01 differ from those obtained by using a step length of 0.025 by approximately $5\times10^{-4}$ consequently the boundary value obtained by using the step length of 0.01 is probably correct to three places of decimals.

A more elaborate system of solution could be used to acheive even more accurate results, now because the functions have an extremely high rate of change of value near $\eta$ =0 it would be advantageous to choose an even smaller step length in that vicinity and a larger step length in $\eta$ further out from the body surface where the rate of change in the value of the functions is very small.

## 4.3 SOLUTION OF THE LINEAR HYDRODYNAMIC EQUATIONS

In order to solve the linear differential sets of equations use is made of the superposition principle, i.e. if $\phi_1$ and $\phi_2$ are solutions of a linear differential equation then $A\phi_1 + B\phi_2$ is also a solution

to the differential equation where A and B are arbitrary constants.

Let us consider the general equations (3-105) and (3-106) with the pertinent boundary values (3-107), if we integrate these equations with three separate values for the boundary conditions $\bar{f}''_{2n-1}(0)$ and $\bar{g}'_{2n-1}(0)$, i.e. $(a_1,b_1)$ ; $(a_2,b_2)$ ; $(a_3,b_3)$ we obtain the three solutions

$$\left[\bar{f}_{2n-1}(\eta)\right]_i \quad , \quad \left[\bar{g}_{2n-1}(\eta)\right]_i \qquad i=1,2,3,$$

hence the functions given by

$$\bar{f}_{2n-1}(\eta) = \frac{\alpha_c\left[\bar{f}_{2n-1}(\eta)\right]_1 + \beta_c\left[\bar{f}_{2n-1}(\eta)\right]_2 + \left[\bar{f}_{2n-1}(\eta)\right]_3}{\alpha_c + \beta_c + 1} \tag{4-30}$$

and

$$\bar{g}_{2n-1}(\eta) = \frac{\alpha_c\left[\bar{g}_{2n-1}(\eta)\right]_1 + \beta_c\left[\bar{g}_{2n-1}(\eta)\right]_2 + \left[g_{2n-1}(\eta)\right]_3}{\alpha_c + \beta_c + 1} \tag{4-31}$$

must also be solutions (by the superposition principle), here $\alpha_c$ and $\beta_c$ are any constants. The two functions given by (4-30) and (4-31) also satisfy the boundary conditions for the system of an axisymmetric body rotating in axial flow if,

$$\alpha_c\left[\bar{f}'_{2n-1}(\infty)\right]_1 + \beta_c\left[\bar{f}'_{2n-1}(\infty)\right]_2 + \left[\bar{f}'_{2n-1}(\infty)\right]_3 = U_{2n-1}(\alpha+\beta+1)$$

and

$$\alpha_c\left[\bar{g}_{2n-1}(\infty)\right]_1 + \beta_c\left[\bar{g}_{2n-1}(\infty)\right]_2 + \left[\bar{g}_{2n-1}(\infty)\right]_3 = 0 \tag{4-32}$$

From equation (4-32) we obtain the following expressions for $\alpha_c$ and $\beta_c$:

$$\alpha_c = \frac{\left[\bar{g}_{2n-1}(\infty)\right]_3\cdot\left(\left[\bar{f}'_{2n-1}(\infty)\right]_2 - U_{2n-1}\right) - \left[\bar{g}_{2n-1}(\infty)\right]_2\cdot\left(\left[\bar{f}'_{2n-1}(\infty)\right]_3 - U_{2n-1}\right)}{\left[\bar{g}_{2n-1}(\infty)\right]_2\cdot\left(\left[\bar{f}_{2n-1}(\infty)\right]_1 - U_{2n-1}\right) - \left[\bar{g}_{2n-1}(\infty)\right]_1\cdot\left(\left[\bar{f}'_{2n-1}(\infty)\right]_2 - U_{2n-1}\right)} \tag{4-33}$$

$$\beta_c = \frac{\left[\bar{g}_{2n-1}(\infty)\right]_1 \cdot \left(\left[\bar{f}_{2n-1}(\infty)\right]_3 - U_{2n-1}\right) - \left[\bar{g}_{2n-1}(\infty)\right]_3 \cdot \left(\left[\bar{f}'_{2n-1}(\infty)\right]_1 - U_{2n-1}\right)}{\left[\bar{g}_{2n-1}(\infty)\right]_2 \cdot \left(\left[\bar{f}'_{2n-1}(\infty)\right]_1 - U_{2n-1}\right) - \left[\bar{g}_{2n-1}(\infty)\right]_1 \cdot \left(\left[\bar{f}'_{2n-1}(\infty)\right]_2 - U_{2n-1}\right)} \tag{4-34}$$

these values of $\alpha_c$ and $\beta_c$ are used to obtain better approximations of $\bar{f}''_{2n-1}(0)$ and $\bar{g}'_{2n-1}(0)$.

As explained previously in 4.2 it is possible to achieve the value of the functions by integrating (in this case equations (3-105) and (3-106)) to $\eta$ =6 where the asymptotic values of the functions have effectively been reached.

The method of solution of the general equations (3-105) and (3-106) is as follows. First three guesses at the boundary values $\bar{f}''_{2n-1}(0)$, $\bar{g}'_{2n-1}(0)$ are made, i.e. $(a_1,b_1)$ ; $(a_2,b_2)$ ; $(a_3,b_3)$ the boundary values $\bar{f}''_{2n-3}(0)$, $\bar{g}'_{2n-3}(0)$, $\bar{f}''_{2n-5}(0)$, $\bar{g}''_{2n-5}(0)$,....., $\bar{f}''_1(0)$, $\bar{g}'_1(0)$ having previously been determined and all other boundary values known to us being given in (3-107). The equations are then integrated to $\eta$ =6 to obtain the three sets $\left[\bar{f}'_{2n-1}(\infty)\right]_i$, $\left[\bar{g}_{2n-1}(\infty)\right]_i$ i = 1,2,3 and thus to determine $\alpha_c$ and $\beta_c$.

We now have from (4-30) and (4-31)

$$\bar{f}''_{2n-1}(0) = \frac{\alpha_c \left[\bar{f}''_{2n-1}(0)\right]_1 + \beta_c \left[\bar{f}''_{2n-1}(0)\right]_2 + \left[\bar{f}''_{2n-1}(0)\right]_3}{\alpha_c + \beta_c + 1} \tag{4-35}$$

$$\bar{g}'_{2n-1}(0) = \frac{\alpha_c \left[\bar{g}'_{2n-1}(0)\right]_1 + \beta_c \left[\bar{g}'_{2n-1}(0)\right]_2 + \left[\bar{g}'_{2n-1}(0)\right]_3}{\alpha_c + \beta_c + 1} \tag{4-36}$$

these values of $\bar{f}''_{2n-1}(0)$, $\bar{g}'_{2n-1}(0)$ are in fact better approximations to the actual values, they may be alternatively written:

$$\left[\bar{f}''_{2n-1}(0)\right]_{IMP} = \frac{\alpha_c a_1 + \beta_c a_2 + a_3}{\alpha_c + \beta_c + 1} \tag{4-37}$$

$$\left[\bar{g}'_{2n-1}(0)\right]_{IMP} = \frac{\alpha_c b_1 + \beta_c b_2 + b_3}{\alpha_c + \beta_c + 1} \qquad (4\text{-}38)$$

The two improved values of $\bar{f}''_{2n-1}(0)$, $\bar{g}'_{2n-1}(0)$ given by (4-37) and (4-38) are chosen together with the two pairs of the set $(a_1,b_1)$ ; $(a_2,b_2)$ ; $(a_3,b_3)$ which are closest to them in value. These three pairs are then used to evaluate further improved approximations of $\bar{f}''_{2n-1}(0)$ and $\bar{g}'_{2n-1}(0)$, the procedure being stopped when to successive approximations differ by $0.5\times10^{-7}$.

For the case of a body rotating in a quiescent fluid the pertinent boundary value equations are (3-126), (3-127) and (3-128) with known boundary values given in (3-122). The procedure for determining the unknown boundary values $F'_{2n-1}(0)$, $G'_{2n-1}(0)$ follows an analogous procedure to that previously explained in case of a body rotating in axial flow. Here three guesses are made for the boundary values $(F'_{2n-1}(0), G'_{2n-1}(0))$, i.e. $(c_1,d_1)$ ; $(c_2,d_2)$ ; $(c_3,d_3)$ integration of the pertinent boundary value equations with the known boundary values leads to three solutions of $F_{2n-1}(\alpha)$, $G_{2n-1}(\alpha)$, i.e. one solution for each guessed pair of boundary values used. The three solutions obtained may be denoted by $F_{2n-1}(\alpha)_i$, $G_{2n-1}(\alpha)_i$ $i = 1,2,3$, it follows from the superposition principle that the functions

$$F_{2n-1}(\alpha) = \frac{\gamma_c \left[F_{2n-1}(\alpha)\right]_1 + \rho_c \left[F_{2n-1}(\alpha)\right]_2 + \left[F_{2n-1}(\alpha)\right]_3}{\gamma_c + \rho_c + 1} \qquad (4\text{-}39)$$

and

$$G_{2n-1}(\alpha) = \frac{\gamma_c \left[G_{2n-1}(\alpha)\right]_1 + \rho_c \left[G_{2n-1}(\alpha)\right]_2 + \left[G_{2n-1}(\alpha)\right]_3}{\gamma_c + \rho_c + 1} \qquad (4\text{-}40)$$

are also solutions of the boundary value equations. Here $\gamma_c$ and $\rho_c$

are arbitrary constants. These functions satisfy the boundary conditions (3-122) if

$$\gamma_c \left[F_{2n-1}(\infty)\right]_1 + \rho_c \left[F_{2n-1}(\infty)\right]_2 + \left[F_{2n-1}(\infty)\right]_3 = 0 \qquad (4\text{-}41)$$

and

$$\gamma_c \left[G_{2n-1}(\infty)\right]_1 + \rho_c \left[G_{2n-1}(\infty)\right]_2 + \left[G_{2n-1}(\infty)\right]_3 = 0 \qquad (4\text{-}42)$$

Solving (4-41) and (4-42) for $\gamma_c$ and $\rho_c$ we obtain:

$$\gamma_c = \frac{\left[G_{2n-1}(\infty)\right]_3 \left[F_{2n-1}(\infty)\right]_2 - \left[G_{2n-1}(\infty)\right]_2 \left[F_{2n-1}(\infty)\right]_3}{\left[G_{2n-1}(\infty)\right]_2 \left[F_{2n-1}(\infty)\right]_1 - \left[G_{2n-1}(\infty)\right]_1 \left[F_{2n-1}(\infty)\right]_2} \qquad (4\text{-}43)$$

$$\rho_c = \frac{\left[G_{2n-1}(\infty)\right]_1 \left[F_{2n-1}(\infty)\right]_3 - \left[G_{2n-1}(\infty)\right]_3 \left[F_{2n-1}(\infty)\right]_1}{\left[G_{2n-1}(\infty)\right]_2 \left[F_{2n-1}(\infty)\right]_1 - \left[G_{2n-1}(\infty)\right]_1 \left[F_{2n-1}(\infty)\right]_2} \qquad (4\text{-}44)$$

Using expressions for $\gamma_c$ and $\rho_c$ above we are able to obtain improved approximations to the two boundary values $F'_{2n-1}(0)$ and $G'_{2n-1}(0)$ by using the relationships

$$\left[F'_{2n-1}(0)\right]_{IMP} = \frac{\gamma_c c_1 + \rho_c c_2 + c_3}{\gamma_c + \rho_c + 1} \qquad (4\text{-}45)$$

$$\left[G'_{2n-1}(0)\right]_{IMP} = \frac{\gamma_c d_1 + \rho_c d_2 + d_3}{\gamma_c + \rho_c + 1} \qquad (4\text{-}46)$$

The procedure for solution of the boundary value problems is the same as that described for a body rotating in axial flow. It should be noted here, however, that the numerical integration of the boundary value problems was carried out over a range $0 < \alpha < 20$ where $\alpha$ is the dimensionless perpendicular distance from the body surface already defined in chapter 3. It was found that the 'effective' infinity for this case was able to be represented by $\alpha$ equal to twenty, numerical

calculations showed this to be well within the range where functions had reached their asymptotic values to within six places of decimals. The procedure of determination of the unknown boundary values was discontinued when two successively calculated values of $(F'_{2n-1}(0), G'_{2n-1}(0))$ are within $0.5\times10^{-7}$ of each other.

## 4.4 SOLUTION OF MASS TRANSFER EQUATIONS

In both cases: a) a body rotating in axial flow, b) a body rotating in a quiescent fluid, the mass transport (or heat transport) equations are all linear including the stagnation point equations, thus these also can be solved by means of a method utilising the superposition principle.

The boundary value problem for the case of a body rotating in axial flow is given by (3-108) with the pertinent boundary values being given by (3-109).

If we supply two initial guesses to the boundary value $\mathcal{H}'_{2(n-1)}(0)$ i.e. $e_1$ and $e_2$, it being assumed that $\mathcal{H}'_{2(n-2)}(0), \ldots, \mathcal{H}'_0(0)$ are known, then we obtain on integration of equation (3-108) two solutions $\left[\mathcal{H}_{2(n-1)}(\eta)\right]_1$ and $\left[\mathcal{H}_{2(n-1)}(\eta)\right]_2$. Using the principle of superposition then $\left[\mathcal{H}_{2(n-1)}(\eta)\right]$ must also be a solution, where

$$\left[\mathcal{H}_{2(n-1)}(\eta)\right] = \frac{\epsilon_c \left[\mathcal{H}_{2(n-1)}(\eta)\right]_1 + \left[\mathcal{H}_{2(n-1)}(\eta)\right]_2}{\epsilon_c + 1} \qquad (4\text{-}47)$$

$\epsilon_c$ being an arbitrary constant.

Now $\left[\mathcal{H}_{2(n-1)}(\eta)\right]$ satisfies the boundary conditions for a body rotating in axial flow if

$$\epsilon_c \left[\mathcal{H}_{2(n-1)}(\eta)\right]_1 + \left[\mathcal{H}_{2(n-1)}(\eta)\right]_2 = 0 \qquad (4\text{-}48)$$

i.e.

$$\epsilon_c = - \left[\mathcal{H}_{2(n-1)}(\infty)\right]_1 \Big/ \left[\mathcal{H}_{2(n-1)}(\infty)\right]_2 \qquad (4\text{-}49)$$

Once again the derived constant $\epsilon_c$ was used to make a better guess at the correct value of $\mathcal{H}'_{2(n-1)}(0)$, i.e.

$$\left[\mathcal{H}'_{2(n-1)}(0)\right]_{IMP} = \frac{\epsilon_c e_1 + e_2}{\epsilon_c + 1} \tag{4-50}$$

This improved approximation to $\mathcal{H}'_{2(n-1)}(0)$ was used together with the better guess out of $e_1$ and $e_2$ to obtain a new value for $\epsilon_c$ and consequently a new $\left[\mathcal{H}'_{2(n-1)}(0)\right]_{IMP}$. The method was terminated when two successive values of $\left[\mathcal{H}'_{2(n-1)}(0)\right]_{IMP}$ were within $0.5\times10^{-7}$ of each other.

For the case of a body rotating in a quiescent fluid an exactly analogous approach is used. This time we have

$$\left[J'_{2(n-1)}(0)\right]_{IMP} = \frac{\epsilon'_c e'_1 + e'_2}{\epsilon'_c + 1} \tag{4-51}$$

where $\left[J'_{2(n-1)}(0)\right]_{IMP}$ is the improved guess at $J_{2(n-1)}(0)$ $e'_1$ and $e'_2$ are guesses at $J'_{2(n-1)}(0)$ and

$$\epsilon'_c = -\left[J_{2(n-1)}(\infty)\right]_2 \Big/ \left[J_{2(n-1)}(\infty)\right]_1 \tag{4-52}$$

## 4.5 GENERAL METHOD OF SOLUTION OF EQUATIONS

### 4.5.1 Body Rotating in Axial Flow

The functional forms of our hydrodynamic and mass (or heat) transfer equations may be written:

$$\bar{f}'''_{2n-1} = FD3_n(\bar{f}'''_{2i-3}, \bar{f}''_{2i-1}, \bar{f}'_{2i-1}, \bar{f}_{2i-1}, \bar{g}'_{2i-1}, \bar{g}_{2i-1}, k_{2i-1}, l_{2(i-1)}, \lambda) \tag{4-53}$$

$$\bar{g}''_{2n-1} = GD2_n(\bar{g}''_{2i-3}, \bar{g}'_{2i-1}, \bar{g}_{2i-1}, \bar{f}'_{2i-1}, \bar{f}_{2i-1}, k_{2i-1}, l_{2(i-1)}) \tag{4-54}$$

$$\mathcal{H}''_{2(n-1)} = HD2_n(\mathcal{H}''_{2(i-2)}, \mathcal{H}'_{2(i-1)}, \mathcal{H}_{2(i-1)}, \bar{f}'_{2i-1}, \bar{f}_{2i-1}, k_{2i-1}, l_{2(i-1)}, \overline{Pr}) \tag{4-55}$$

where i = 1,2,....n and FD3, GD2 and HD2 are the right-hand sides of equations (3-105) ; (3-106) and (3-108) respectively.

We can transform equation (4-53) into three first ordinary differential equations and each equation of (4-54) and (4-55) into two ordinary differential equations by the following substitutions:

$$\begin{aligned} Y(7n-6) &= \bar{f}_{2n-1} \\ Y(7n-5) &= \bar{f}'_{2n-1} \\ Y(7n-4) &= \bar{f}''_{2n-1} \\ Y(7n-3) &= \bar{g}_{2n-1} \\ Y(7n-2) &= \bar{g}'_{2n-1} \\ Y(7n-1) &= \mathcal{H}_{2(n-1)} \\ Y(7n) &= \mathcal{H}'_{2(n-1)} \end{aligned} \qquad (4\text{-}56)$$

where each left-hand side of equations (4-56) are elements of the column $\underline{Y}$.

The system of equations (4-53) to (4-55) which is of order seven is transformed to the seven first order equations:

$$\left.\begin{aligned} YG(7n-6) &= Y(7n-5) \\ YG(7n-5) &= Y(7n-4) \\ YG(7n-4) &= FD3(n) \\ YG(7n-3) &= Y(7n-2) \end{aligned}\right\} \qquad (4\text{-}57)$$

$$\left.\begin{aligned} YG(7n-2) &= GD2(n) \\ YG(7n-1) &= Y(7n) \\ YG(7n) &= HD2(n) \end{aligned}\right\} \qquad (4\text{-}58)$$

where $YG(\ ) = \frac{d}{d\eta} Y(\ )$.

It will be noted that to determine $\mathcal{H}'_{2(n-1)}(\eta)$ we have to solve 7n differential equations. The pertinent boundary values become:

$$\left.\begin{array}{lll} \text{at } \eta = 0 & Y(7n-6) = Y(7n-5) = 0\ ; \quad Y(7n-3) = K_{2n-1} & n=1,2,\ldots \\ & Y(6) = 1;\ Y(7n-1) = 0 & n=2,3,\ldots \\ \text{as } \eta \to \infty & Y(7n-5) \to U_{2n-1};\ Y(7n-3) \to 0;\ Y(7n-1) \to 0 & n=1,2,\ldots \end{array}\right\} \quad (4\text{-}59)$$

It has been explained previously that the hydrodynamic equations (4-57) can be solved independently of the mass or heat transfer equations (4-58), the functional form of the hydrodynamic equations (4-53) and (4-54) shows that these hydrodynamic equations do not contain any mass or heat transfer functions - their independence from (4-55) is thus obvious. The first five hydrodynamic equations YG(1) to YG(5) are a non-linear set for which the unknown boundary values Y(3) and Y(5) at $\eta$ =0 are determined by the quasilinearisation technique. The next and all subsequent sets of hydrodynamic equations, i.e. YG(7I-6) to YG(7I-2), I = 2,3,... are all linear for which the boundary values Y(7I-4) and Y(7I-2) can be determined by means of the superposition principle (4.3).

When determining the unknown boundary values Y(7n-4) and Y(7n-2) at $\eta$ =0 in the n'th set of hydrodynamic equations it is necessary to know all the previous Y(7I-4) and Y(7I-2), I = 1,2,...,(n-1) in order to supply the values of the hydrodynamic functions in FD3(n) and GD2(n) as a function of $\eta$.

In the case of the mass (or heat) transfer equations it can be seen that the n'th set is dependent on all previous sets of hydrodynamic equations, i.e. sets 1,2,...,n-1, thus to determine the unknown boundary value Y(7n) at $\eta$ =0 all previous sets of hydrodynamic equations as well as all previous mass (or heat) transfer equations must be supplied as functions of $\eta$, again this is accomplished by simultaneous integration of all previous equations with respect to $\eta$. Because the mass (or heat) transfer equations are all linear the

unknown boundary values Y(7I) at $\eta$ =0, I = 1,2,3... are determined by using the principle of superposition.

In the computer programme that was written to determine numerically the unknown boundary values the value of $\eta$ taken as infinity for the hydrodynamic boundary layer was XMAX. XMAX was maintained at 6 for the range of spin parameter $\lambda$ investigated, i.e. $0 < \lambda < 20$. Frossling (1958) has shown that the ratio of the mass (or heat) transfer boundary layer thickness to the hydrodynamic thickness is of order $\overline{Pr}^{\frac{1}{3}}$. Consequently the value of $\eta$ taken as infinity for the solution of the mass transfer equations was $XMAX/\overline{Pr}^{\frac{1}{3}}$, this value of the effective infinity was found to be large enough for the functions $f_{2(n-1)}(\eta)$ and $f'_{2(n-1)}(\eta)$ to have reached their asymptotic values within six places of decimals. The procedure adopted in the computer programme was to calculate the unknown boundary values of the first unknown set of hydrodynamic equations and use these to determine the unknown boundary value in the first set of mass or heat transfer equations, then the second set was solved and so on.

The number of sets that can be solved is obviously limited by the computer time available, the time required for solving each set rapidly increasing with the number of the set. It was decided that the first five sets of the mass transfer equations would be solved.

From our definition of mass transfer number M it follows that

$$M^A = \frac{-1}{\sqrt{2}.\overline{Pr}^{\frac{1}{3}}} \left(Y(7)\Big|_{\eta=0} + Y(14)\Big|_{\eta=0} x_1^{*2} + \ldots + Y(7n)\Big|_{\eta=0} x_1^{*2(n-1)} + \ldots\right) \qquad (4\text{-}60)$$

consequently $M^A$ is known at each value of $x_1^*$ these values being printed by the computer up to $90^\circ$ around the body in steps of $5^\circ$.

4.5.2 Body Rotating in a Quiescent Fluid

Here again we may define the functional forms of our hydrodynamic and mass transfer boundary value equation as follows:

$$F''_{2n-1} = SFD2_n(F''_{2i-3}, F'_{2i-1}, F_{2i-1}, H_{2(i-1)}, G_{2i-1}, k_{2i-1}, l_{2(i-1)}) \quad (4\text{-}61)$$

$$G''_{2n-1} = SGD2_n(G''_{2i-3}, G'_{2i-1}, G_{2i-1}, F_{2i-1}, H_{2(i-1)}, k_{2i-1}, l_{2(i-1)}) \quad (4\text{-}62)$$

$$H'_{2(n-1)} = SHD1_n(H'_{2(i-2)}, F_{2i-1}, k_{2i-1}, l_{2(i-1)}) \quad (4\text{-}63)$$

$$J''_{2(n-1)} = SJD2_n(J''_{2(i-2)}, F_{2i-1}, k_{2i-1}, l_{2(i-1)}) \quad (4\text{-}64)$$

$$i = 1,2,\ldots.n$$

For $l_o = k_1 = 1$ the stagnation point equation for this system becomes

$$\left.\begin{aligned} F''_1 &= F_1^2 + H_0 F'_1 - G_1^2 \\ G''_1 &= 2F_1 G_1 + H_0 G'_1 \\ H'_0 &= -2F_1 \end{aligned}\right\} \quad (4\text{-}65)$$

$$J''_0 = Pr\, J'_0\, H_0 \quad (4\text{-}66)$$

with boundary values for the functional coefficients being

$$\begin{aligned} &\text{at } \eta = 0 \quad H_o = F_1 = 0 \;;\; G_1 = 1 \;;\; J_0 = 1 \\ &\text{as } \eta \to \infty \quad F_1 \longrightarrow 0 \;;\; G_1 \longrightarrow 0 \;;\; J_0 \longrightarrow 0 \end{aligned} \quad (4\text{-}67)$$

The stagnation point equations, as a set, are non-linear and as such the unknown boundary values $F'_1(0)$ and $G'_1(0)$ could be determined by the technique of quasilinearisation, however, their values have already been determined by Rogers and Lance (1960)

i.e.

$$\begin{aligned} F'_1(0) &= 0.510233 \\ G'_1(0) &= -0.615922 \end{aligned} \quad (4\text{-}68)$$

The determination of all the boundary values $J'_{2(i-1)}(0)$ is possible by

use of the superposition principle as the mass transfer equations are all linear.

A method analogous to that used in section (4.5.1) transforms our equations into simultaneous first order differential equations i.e.,

$$\left.\begin{aligned} Y(7n-6) &= F_{2n-1} \\ Y(7n-5) &= F'_{2n-1} \\ Y(7n-4) &= G_{2n-1} \\ Y(7n-3) &= G'_{2n-1} \\ Y(7n-2) &= H_{2(n-1)} \\ Y(7n-1) &= J_{2(n-1)} \\ Y(7n) &= J'_{2(n-1)} \end{aligned}\right\} \qquad (4\text{-}69)$$

the pertinent boundary values being:

$$\left.\begin{aligned} &\text{at } \alpha = 0 \quad Y(7n-2) = Y(7n-6) = 0 \;;\; Y(7n-4) = K_{2n-1} && n=1,2,3\ldots \\ &\qquad\qquad Y(6) = 1 \;;\; Y(7n-1) = 0 && n=2,3\ldots\ldots \\ &\text{as } \alpha \to \infty \quad Y(7n-6) \to 0 \;;\; Y(7n-4) \to 0 \;;\; Y(7n-1) \to 0 && n=1,2,3\ldots \end{aligned}\right\} \qquad (4\text{-}70)$$

Our system of differential equations (4-61) to (4-64) becomes:

$$\left.\begin{aligned} YG(7n-6) &= Y(7n-5) \\ YG(7n-5) &= SFD2(n) \\ YG(7n-4) &= Y(7n-3) \\ YG(7n-3) &= SGD2(n) \\ YG(7n-2) &= SHD1(n) \\ YG(7n-1) &= Y(7n) \\ YG(7n) &= SJD2(n) \end{aligned}\right\} \qquad (4\text{-}71)$$

An exactly analogous procedure to that used in (4.5.1) may be used

to determine the unknown boundary values Y(7n-5); Y(7n-3); Y(7n) at $\alpha=0$. Finally the computer as in (4.5.1) prints out the local $M^q$ numbers at intervals of $5^o$ around the body up to a parametric angle of $90^o$ for the oblate spheroid, here $M^q$ is given by

$$M^q = \frac{-1}{\sqrt{2}.\overline{Pr}^{\frac{1}{2}}}\left(Y(7)\Big|_{\alpha=0} + Y(14)\Big|_{\alpha=0} X_1^{*2} + \ldots + Y(7n)\Big|_{\alpha=0} X_1^{*2(n-1)} + \ldots\right) \qquad (4\text{-}72)$$

It was found that the effective infinity for the dimensionless distance $\alpha$ was 20, consequently in computer time the integration is a lengthy procedure, only the first four sets of equations were hence solved.

4.5.3 Flow Diagram for Solution of all Linear Equations

The flow diagram shown is the flow diagram of the computer programme in the case of a body rotating in axial flow. The flow diagram of the computer programme in the solution of the linear boundary value problems for a body rotating in a quiescent fluid has the following modifications:

1) as shown in (4.5.2) there are different boundary values associated with this case.

2) Y(7n-5) and Y(7n-3) n=1,2,3 now become the functions which are required at $\alpha=0$.

3) the boundary value equations are of course different.

4) the expressions for determining better approximations are different.

With these modifications the flow diagram becomes identical with that of the one pertaining to rotation in axial flow (shown).

In the flow diagram the nomenclature used is

U(2I-1) - I'th coefficient in the potential flow series expression previously denoted by $U_{2I-1}$.

CL(2(I-1)) - I'th coefficient in the scale factor series expression for the meridional direction, i.e. $l_{2(I-1)}$.

CK(2I-1) - I'th coefficient in the scale factor series for the azimuthal direction, i.e. $K_{2i-1}$.

PRNDTL - Prandtl number for heat transfer problem or Schmidt number for mass transfer problem.

SPIN - Spin parameter.

H - Step length for Runge-Kutta integration procedure.

XMAX - Limit of integration with regard to the dimensionless perpendicular distance $\eta$, i.e. this is the effective infinity for the system.

BXMAX - is the limit of integration with regard to $\eta$ in the case of mass (or heat) transfer equations, this is the 'effective' infinity and as already explained is given by BXMAX = XMAX/$\overline{Pr^{\frac{1}{3}}}$.

The actual step length used for the integration of the mass transport boundary value equations was taken as BXMAX/60, which is a smaller step length than the 0.1 step used in the integration of hydrodynamic boundary value equations. This step length was used because of the fact that the 'effective' infinity for the mass transport functions BXMAX is smaller than that of the hydrodynamic effective infinity XMAX.

ALP(1) - is the initial guess at the unknown boundary value Y(7I-4) at $\eta$ =0.

BET(1) - is the initial guess at the unknown boundary value Y(7I-2) at $\eta$ =0.

GAM(1) - is the initial guess at the unknown boundary value Y(7I) at $\eta$ =0.

ALPHA(I) - is the determined value of Y(7I-4) at $\eta$ =0.

BETA(I) - is the determined value of Y(7I-2) at $\eta$=0.

GAMMA(I)- is the determined value of Y(7I) at $\eta$=0.

ERMINA - is the accuracy to which ALPHA(I) and BETA(I) have been determined.

ERMINB - is the accuracy to which GAMMA(I) has been determined.

NS - is the order of the first set of boundary value equations to be solved (NS must be greater than unity this being the non-linear first set).

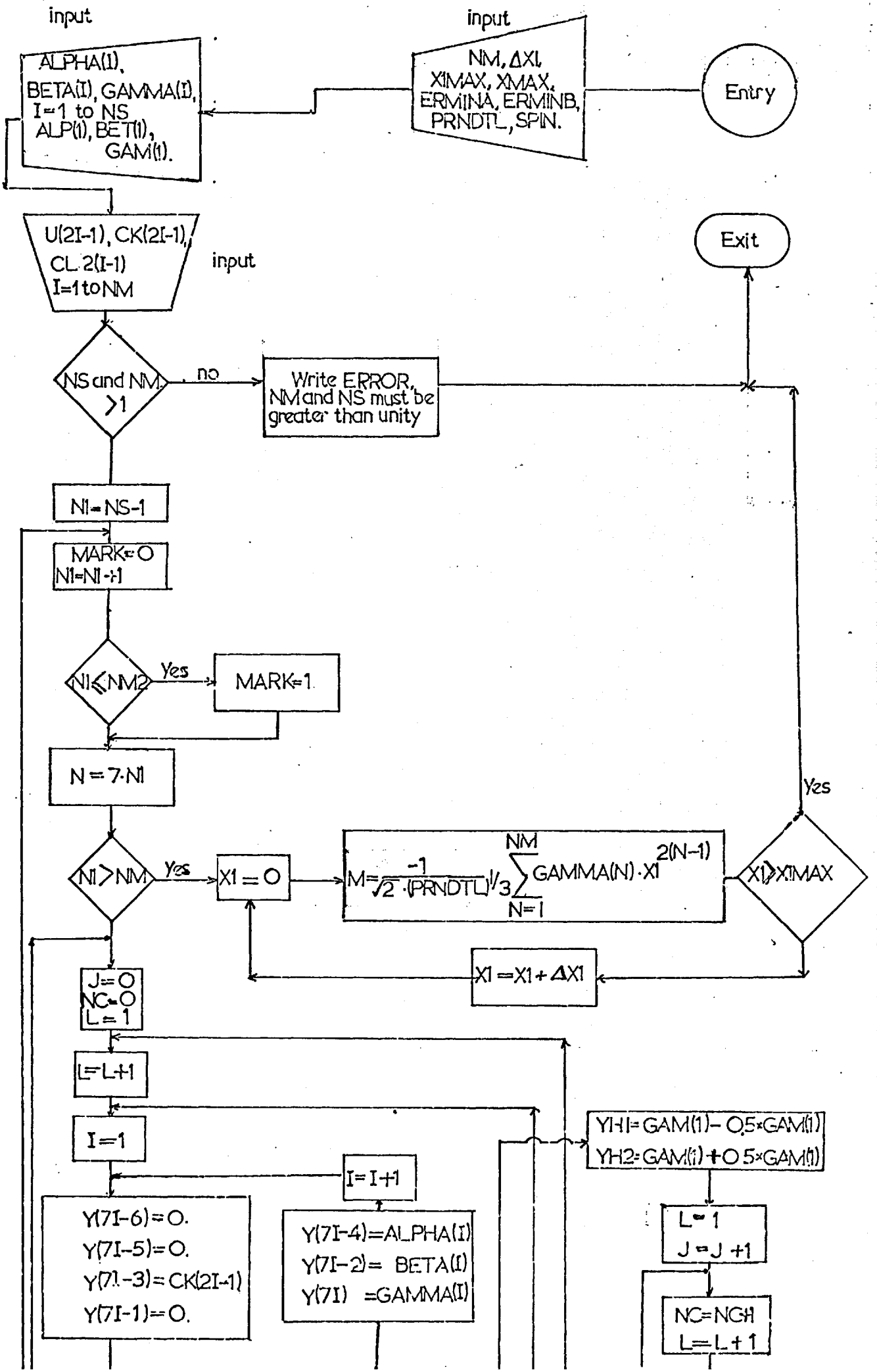
NM - maximum order of equations to be solved.

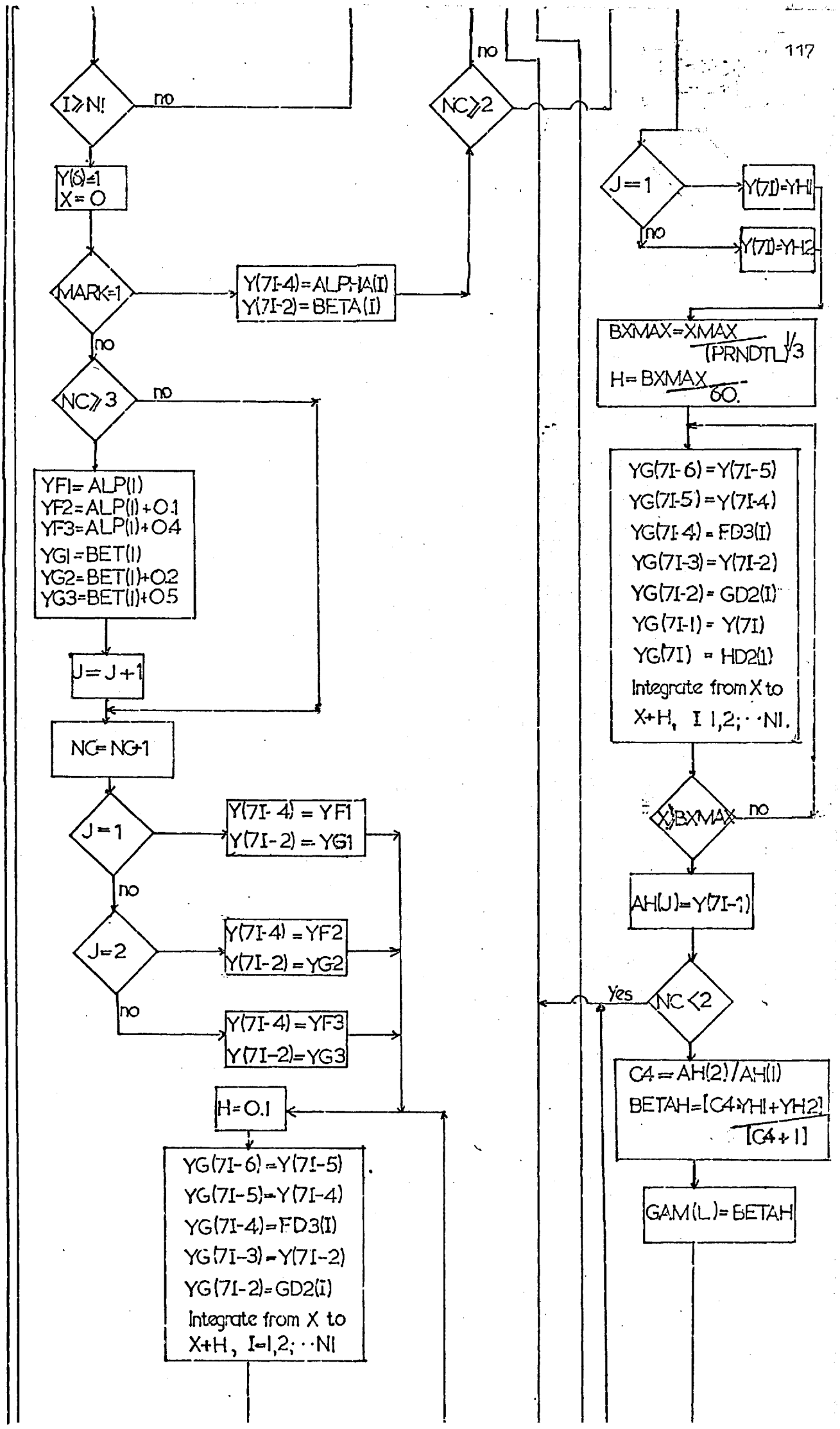
The final results for the local mass transfer number M are printed out as point values in the azimuthal co-ordinate $x_1$ at intervals of $\Delta x_1$, which was chosen as $5^\circ$ for the oblate spheroid, to a maximum value of X1MAX, which was chosen as $90^\circ$ for the oblate spheroid.

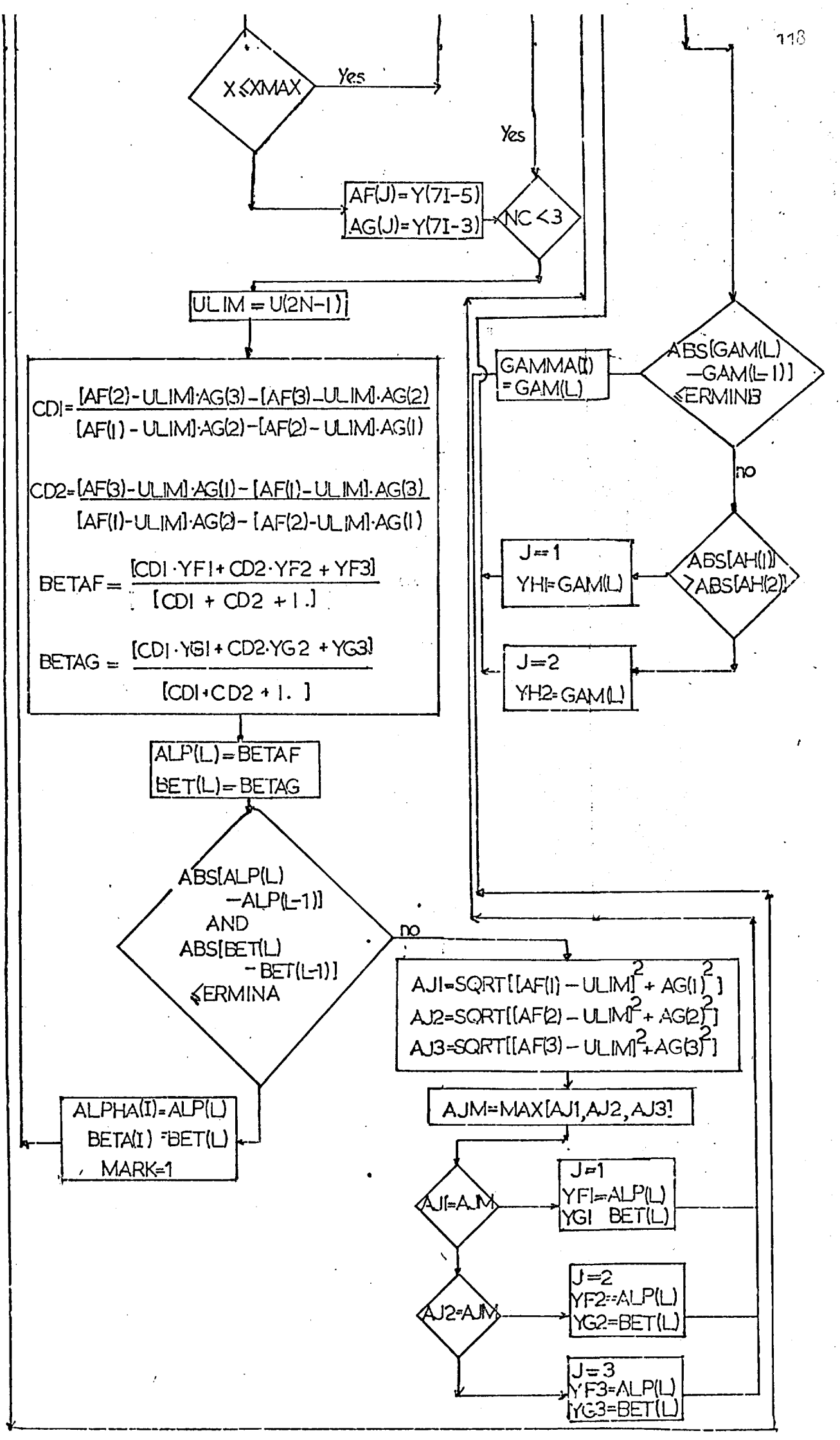
Once the unknown hydrodynamic boundary values have been determined for a particular body shape and a particular spin parameter they may be used to determine the unknown mass transfer boundary values for each Schmidt number, the number of hydrodynamic boundary value sets, i.e. ALPHA(I), BETA(I) supplied initially to the programme being NM2.

The actual computer programme is set out fully in appendix D.

# COMPUTER PROGRAMME FLOW-DIAGRAM




I≥N!
no
Y(6)=1
X=0
MARK=1
Y(7I-4)=ALPHA(I)
Y(7I-2)=BETA(I)
no
NC≥3
no
YF1=ALP(1)
YF2=ALP(1)+0.1
YF3=ALP(1)+0.4
YG1=BET(1)
YG2=BET(1)+0.2
YG3=BET(1)+0.5
J=J+1
NC=NC+1
J=1
Y(7I-4)=YF1
Y(7I-2)=YG1
no
J=2
Y(7I-4)=YF2
Y(7I-2)=YG2
no
Y(7I-4)=YF3
Y(7I-2)=YG3
H=0.1
YG(7I-6)=Y(7I-5)
YG(7I-5)=Y(7I-4)
YG(7I-4)=FD3(I)
YG(7I-3)=Y(7I-2)
YG(7I-2)=GD2(I)
Integrate from X to X+H, I=1,2;··NI
no
NC≥2
J=1
Y(7I)=YH1
no
Y(7I)=YH2
BXMAX=XMAX/(PRNDTL)^1/3
H=BXMAX/60.
YG(7I-6)=Y(7I-5)
YG(7I-5)=Y(7I-4)
YG(7I-4)=FD3(I)
YG(7I-3)=Y(7I-2)
YG(7I-2)=GD2(I)
YG(7I-1)=Y(7I)
YG(7I)=HD2(1)
Integrate from X to X+H, I=1,2;··NI.
X≥BXMAX
no
AH(J)=Y(7I-1)
Yes
NC<2
C4=AH(2)/AH(1)
BETAH=[C4*YH1+YH2]/[C4+1]
GAM(L)=BETAH


X≤XMAX
Yes
AF(J)=Y(7I-5)
AG(J)=Y(7I-3)
Yes
NC<3
ULIM=U(2N-1)
CD1=[AF(2)-ULIM]·AG(3)-[AF(3)-ULIM]·AG(2) / [AF(1)-ULIM]·AG(2)-[AF(2)-ULIM]·AG(1)
CD2=[AF(3)-ULIM]·AG(1)-[AF(1)-ULIM]·AG(3) / [AF(1)-ULIM]·AG(2)-[AF(2)-ULIM]·AG(1)
BETAF=[CD1·YF1+CD2·YF2+YF3] / [CD1+CD2+1.]
BETAG=[CD1·YG1+CD2·YG2+YG3] / [CD1+CD2+1.]
ALP(L)=BETAF
BET(L)=BETAG
ABS[ALP(L)-ALP(L-1)] AND ABS[BET(L)-BET(L-1)] ≤ERMINA
ALPHA(I)=ALP(L)
BETA(I)=BET(L)
MARK=1
GAMMA(I)=GAM(L)
ABS[GAM(L)-GAM(L-1)] ≤ERMINB
no
ABS[AH(1)]>ABS[AH(2)]
J=1
YH1=GAM(L)
J=2
YH2=GAM(L)
no
AJ1=SQRT[[AF(1)-ULIM]^2+AG(1)^2]
AJ2=SQRT[[AF(2)-ULIM]^2+AG(2)^2]
AJ3=SQRT[[AF(3)-ULIM]^2+AG(3)^2]
AJM=MAX[AJ1,AJ2,AJ3]
AJ1=AJM
J=1
YF1=ALP(L)
YG1 BET(L)
AJ2=AJM
J=2
YF2=ALP(L)
YG2=BET(L)
J=3
YF3=ALP(L)
YG3=BET(L)

## 4.6 NUMERICAL DETERMINATION OF COEFFICIENTS IN THE POWER SERIES EXPANSION FOR POTENTIAL FLOW AND SCALE FACTORS FOR OBLATE SPHEROIDS

We have shown that to obtain the values of the coefficients in the expansion for the scale factor $h_{\theta,0}$ and potential flow U becomes progressively more difficult as the power of the variable increases, it is hence necessary to determine the coefficients by a numerical procedure.

### 4.6.1 Exansion of $h_{\theta,0}$

Green (1968) previously expanded the following form of $h_{\theta,0}$ in a power series of $\theta$

$$h_{\theta,0} = a \cos\theta \, (1 + e^2\tan^2\theta)^{\frac{1}{2}} \qquad (4\text{-}73)$$

This method of obtaining the coefficients will not be used, however, because in order to exapnd the square root term $\theta$ becomes restricted in magnitude by convergence requirements,

i.e. $e^2\tan^2\theta < 1$ for convergence.

This restriction is not present when $h_{\theta,0}$ is expanded in the form

$$h_{\theta,0} = a(1 - (\sin\theta/\cosh\xi_o)^2)^{\frac{1}{2}} \qquad (4\text{-}74)$$

Now $$\cosh\xi_o = (1-e^2)^{-\frac{1}{2}} \qquad (4\text{-}75)$$

and hence $$h_{\theta,0} = a(1 - ((1-e^2)^{\frac{1}{2}} \sin\theta)^2)^{\frac{1}{2}} \qquad (4\text{-}76)$$

which on expansion yields:

$$h_{\theta,0} = a(1 + (\frac{e^2-1}{2})\sin^2\theta - (\frac{e^2-1}{8})\sin^4\theta + \ldots\ldots + B_n \sin\theta^{2(n-1)} + \ldots\ldots\ldots) \qquad (4\text{-}77)$$

We can obtain the following recurrence relationship for $B_n$ the coefficient of $\sin\theta^{2(n-1)}$.

$$\left.\begin{aligned} B_n &= \frac{(n - 5/2)}{(n - 1)} (1 - e^2)\, B_{n-1} \qquad n > 1 \\ B_1 &= 1 \end{aligned}\right\} \tag{4-78}$$

We hence have

$$h_{\theta,0} = a \sum_{m=0}^{\infty} B_{m+1}(\theta^2 + \ldots\ldots + S2_n \theta^{2n})^m \tag{4-79}$$

where $S2_n$ is the coefficient of $\theta^{2n}$ in the expansion of $\mathrm{Sin}^2\theta$, it follows that

$$h_{\theta,0} = a \sum_{m=0}^{\infty} B_{m+1}(\theta^{2m} + \ldots\ldots + X_{n,m}\theta^{2n} + \ldots) \tag{4-80}$$

here $X_{n,m}$ is the coefficient of $\theta^{2n}$ in $\mathrm{Sin}^{2m}\theta$.

The coefficient L(2n) in the power series

$$h_{\theta,0} = a(1 + (\frac{e^2-1}{2})\theta^2 + \ldots\ldots + L(2n)\theta^{2n} + \ldots) \tag{4-81}$$

is thus given by

$$L(2n) = \sum_{m=0}^{n} B_{m+1}\, X_{n,m} \tag{4-82}$$

Now $S2_n$ is given by

$$S_{2n} = (-1)^{n+1} \frac{2^{2n-1}}{(2n)!} \tag{4-83}$$

It can further be shown that

$$X_{n,m} = \sum_{J_{m-1}=1}^{J_{m-1}=n-m+1} S2_{(n-j_{m-1}-m+2)} \sum_{J_{m-2}}^{J_{m-2}=J_{m-1}} S2_{(j_{m-1}-j_{m-2}+1)} \cdots$$

$$\cdots \sum_{j_1=1}^{j_1=j_2} S2_{j_1}\; S2_{j2-j1+1} \tag{4-84}$$

for n-m+1 $\geq$ 1, i.e. n=m,m+1,.....and m $\geq$ 2

because

$$X_{n,2} = \sum_{j_1=1}^{j_1=n-1} Sj_1 \cdot S_{n-j_1}$$

also

$$\left.\begin{array}{lll} \text{for } m=1 & X_{n,1}=S2n & n=1,2..... \\ m=0 & X_{0,0}=1 & X_{n,0}=0 \end{array}\right\} \qquad (4\text{-}85)$$

Thus as both coefficients B and X may be determined it is also possible to determine the coefficient L(2n). The method of application by computer programme has been explained previously by Green (1968).

4.6.2 Potential Flow Expansion

Once again we change the basic representation of the power series expansion used by Green

i.e. $$U = k(e)\, U \tan\theta(1+e^2\tan^2\theta)^{-\frac{1}{2}} \qquad (4\text{-}86)$$

which is limited by the convergence requirements on $\theta$. In order to remove the limitations on $\theta$ we use the form

$$U = k(e)\, U \sin\theta(1-((1-e^2)\sin\theta))^{-\frac{1}{2}} \qquad (4\text{-}87)$$

Expanding (4-87) in powers of sin $\theta$ we obtain

$$U = k(e)\, U \sin\theta\left(1+\left(\frac{1-e^2}{2}\right)\sin^2\theta + ..... \right.$$

$$\left. +...BU_n \sin\theta^{2(n-1)} + .....\right) \qquad (4\text{-}88)$$

where

$$\left.\begin{array}{ll} BU_n = \dfrac{(n-3/2)}{(n-1)}(1-e^2)\, BU_{n-1} & n>1 \\ BU_1 = 1 & \end{array}\right\} \qquad (4\text{-}89)$$

is the pertinent recurrence relationship for the coefficients $BU_n$. Hence,

$$U = k(e)U \sin\theta\left(\sum_{m=0}^{\infty} BU_{m+1}(\theta^2+...+S2_n\theta^{2n})^m\right) \qquad (4\text{-}90)$$

or

$$U = k(e)U \sin\theta\left(1-\frac{e^2}{2}\theta^2+...+ \sum_{m=0}^{m=n} BU_{m+1}X_{n,m}\right)\theta^{2n}+...) \qquad (4\text{-}91)$$

If $S1_n$ is the coefficient of $\theta^{2n}$ in the expansion of $\sin\theta$ we have,

$$U = k(e)U_{\infty}\left(\theta - \left(\frac{2-3e^2}{6}\right)\theta^3 + \ldots + U_{2n+1}\,\theta^{2n+1} + \ldots\right) \qquad (4\text{-}92)$$

where $$U_{2n+1} = \sum_{j=0}^{j=n} S1_{n-j+1} \sum_{m=0}^{m=j} BU_{m+1}\, X_{j,m} \qquad (4\text{-}93)$$

This form of the coefficient in the power series expansion is analogous to that obtained by Green; it is hence treatable by the same method as used by Green. Because our series representation does not need Bernoulli numbers and also because our analysis does not put any restrictions on $\theta$ it is obviously more advantageous to use; however, we find in practice that the values of the coefficients that are obtained by both methods differ by less than $1\times10^{-7}$.

Once again the computer programme for obtaining these coefficients is to be found in appendix D, it takes the form of the subroutine COEFFS in the main computer programme, the computer language being Fortran IV.

# CHAPTER V

# RESULTS

## 5.1 INTRODUCTION

The present work was started and carried out in order to determine the effects of secondary motions on mass or heat transfer rates from droplets and solid bodies in laminar flow, the particular secondary motion studied was that of axial rotation.

A general method of analysis of the boundary layer equations has been presented in Chapter 3 which is applicable to all axisymmetric shapes rotating in axial flow. It was decided that the analysis presented would be used to study in particular the effect of rotation on local mass transfer rates from spheres and oblate spheroids - these shapes being very good approximations to the shapes often exhibited by droplets in a continuous phase. The body shapes studied were the sphere, the 10/16 spheroid, 7/16 spheroid and the disk.

The study of these rotating bodies covered the range of spin parameter $0 \leq \lambda \leq 20$ and Schmidt numbers of 0.7, 1.0, 2.4 and 10.0. By means of the expression developed in (3.6.1) it was also possible to predict local mass transfer numbers at infinite Schmidt number.

The analysis was further extended to determine the effects of rotation on the rates of mass transfer from axisymmetric bodies rotating in a quiescent fluid. In this case the sphere, the 13/16 spheroid and the 10/16 spheroid were studied at Schmidt numbers of 0.7, 1.0, 2.4, 5.0, 10.0 and 100.0. Using the expression developed in (3.6.2) it was also possible to study the effects of rotation on local

mass transfer numbers at infinite Schmidt number.

In both analyses the Runge-Kutta method of numerical integration was used, as already described in Chapter 4, integration of the hydrodynamic functions was carried out over the range $0 \leqslant \eta (\text{or } \alpha) \leqslant \text{XMAX}$ where XMAX = 6.0 in the case of a body rotating in axial flow and XMAX = 20.0 in the case of a body rotating in a quiescent fluid.

These ranges were found to be high enough for the hydrodynamic functions to have reached their asymptotic values to at least six significant figures.

In the case of the integration of mass transfer functions the approximate relationship of Frossling (1958), i.e.

$$\underset{Pr \to \infty}{\text{limit}} \; S_H^* / S_M^* \longrightarrow \overline{Pr}^{\frac{1}{3}}$$

where $S_H^*$ is the dimensionless hydrodynamic boundary layer thickness and $S_M^*$ is the dimensionless mass transfer boundary layer thickness, was used to calculate the range of integration for finite Schmidt numbers.

It was found that the integration range $0 \leqslant \eta (\text{or } \alpha) \leqslant \text{XMAX}/\overline{Pr}^{\frac{1}{3}}$ was sufficiently high for all mass transfer functions to have reached their asymptotic values to at least six significant places.

In the description of the results comment is also made on the accuracy of the boundary values that have been determined, the accuracy being very dependent on the numerical methods used.

## 5.2 STAGNATION POINT SOLUTIONS FOR AN AXISYMMETRIC BODY ROTATING IN AXIAL FLOW

### 5.2.1 The Hydrodynamic Stagnation Point Solutions

The hydrodynamic equations which describe flow conditions at the front stagnation point of a body rotating in axial flow, i.e. (4-1)

and (4-2) have been solved for spin parameters up to one-hundred for bluff bodies ($K_1 = l_o = 1$). Up to spin parameters of ten the method of solution of the hydrodynamic boundary value problem (i.e. determination of $\bar{f}_1''(0)$ and $\bar{g}_1'(0)$) was the finite difference method as outlined in appendix B, this method of solution was found to need initial guesses of $\bar{f}_1''(0)$ and $\bar{g}_1'(0)$ correct to two significant figures to give satisfactory results - this limited greatly the usefulness of the method.

For the finite difference method the integration of the equations was carried out at different step lengths in $\eta$ in order that the step length required for the desired accuracy could be calculated. In table 1, appendix E are set out the boundary values $\bar{f}_1''(0)$ and $\bar{g}_1'(0)$ determined by the finite difference method at integration step lengths in $\eta$ of 0.1 and 0.05. At spin parameter $\lambda = 0$ the difference in magnitude in the boundary values at these two step lengths is of order $5.0 \times 10^{-7}$, at $\lambda = 10$ the difference is of the order $1.0 \times 10^{-5}$, consequently it is expected that the boundary values $\bar{f}_1''(0)$ and $\bar{g}_1'(0)$ estimated at step length 0.1 are correct to at least five significant figures.

For spin parameters above ten the method of quasilinearisation was used, this method, as has been explained in Chapter 4, requires only crude initial estimates of the boundary values in order to obtain useable results. Lee and Fan (1968) stated that the technique of quasilinearisation is not suitable for the solution of all boundary value problems; for some problems the method does not give better estimates of the unknown boundary values. With the finite difference method of solution the technique uses the stagnation point equations in an unmodified form: the results obtained by this method can hence be considered to be the correct ones (within, of course, the accuracy

of $1.0 \times 10^{-5}$). Results obtained by quasilinearisation, which uses the linearised forms of the equations, must hence be compared with the finite difference procedure in order to determine the suitability of the technique. For an integration step length in $\eta$ of 0.01 (and a spin parameter of ten) the quasilinearisation technique yielded:

$$\bar{f}_1''(0) = 3.566016 \; ; \; \bar{g}_1'(0) = -1.323983$$

At the same spin parameter and an integration step length in of 0.1 the finite difference technique yielded:

$$\bar{f}_1''(0) = 3.5661108; \; \bar{g}_1'(0) = -1.3238863$$

Because of the close agreement of the results yielded by both techniques it was assumed that the method of quasilinearisation was capable of yielding correct results for this particular boundary value problem.

The integration step length required by the method of quasilinearisation was found to be much smaller than that required by the finite difference method for the same accuracy of solution. The effect of step length in $\eta$ on the results obtained by the quasilinearisation technique is given in the table below:

| STEP LENGTH IN $\eta$ | $\lambda = 10$ | | $\lambda = 20$ | |
|---|---|---|---|---|
| | $\bar{f}_1''(0)$ | $\bar{g}_1'(0)$ | $\bar{f}_1''(0)$ | $\bar{g}_1'(0)$ |
| 0.01 | 3.566016 | -1.323983 | 5.411517 | -1.473409 |
| 0.025 | 3.565408 | -1.324339 | 5.412899 | -1.473053 |

$K_1 = 1o = 1.$

In fig.5.2 plots of $\bar{f}_1''(\eta)$ across the boundary layer are given for different spin parameters $\lambda$, it can be seen that as the spin parameter $\lambda$ increases the most abrupt changes in magnitude of $\bar{f}_1''(\eta)$

became confined to ever smaller regions near the body surface.

It would seem from the above discussion that the method of quasilinearisation yields results that are sensitive to abrupt changes in the hydrodynamic functions, this sensitivity being probably due to the inaccuracy of the linearised forms of the stagnation point equations. From the above table it would be expected that the boundary values obtained by the quasilinearisation technique at a step length in $\eta$ of 0.01 and a spin parameter of ten would be accurate to within $\pm 0.0005$ and for a spin parameter of twenty to within $\pm 0.001$.

From a comparison of the results obtained by both the described techniques of solution it is seen that if sufficiently accurate initial estimates are supplied to the finite difference procedure it is capable of yielding more accurate results than the quasilinearisation procedure at the same step length; the disadvantage of the finite difference procedure is, as stated previously, the requirement that the accuracy of the initial estimates of the unknown boundary values must be high if the method is to work.

The computer programme used in the determination of the hydrodynamic boundary values is shown in appendix D. The accuracy of the determined boundary value is limited by the magnitude of the integration step length which in turn is limited by the storage facility of the I.B.M. 7094 machine used in the numerical calculations. The present technique of solution limits the smallness of the integration step length used in this problem to 0.01. Consequently the accuracy of the stagnation point boundary values $\bar{f}_1''(0)$ and $\bar{g}_1'(0)$ are limited to $\pm 0.001$ for a spin parameter of twenty.

Because of the sensitivity of the quasilinearisation technique to abrupt changes in $\bar{f}_1''(\eta)$ an improvement in the numerical technique

would be to have small step lengths in $\eta$ when integrating the hydrodynamic functions near to $\eta=0$ and larger step lengths at higher values of $\eta$ where abrupt changes in the hydrodynamic functions do not occur. Thus, for the same computer storage facility much smaller step lengths could be used in the most important regions of the integration range thus enabling greater accuracy to be obtained. A different approach would be to use the quasilinearisation procedure to supply the required accurate initial estimates for the finite difference technique.

In fig.5.1 plots of $\bar{f}_1'(\eta)$ across the boundary layer are given for spin parameters up to one hundred. The plots of $\bar{f}_1'(\eta)$ for $\lambda=20$ and $\lambda=100$ were obtained by the quasilinearisation method using an integration step length of 0.01. Although the accuracy of the solution at a spin parameter of $\lambda=100$ is not expected to be as high as for the smaller values of $\lambda$ due to the relatively large integration step length used, it is expected that the solution does give a good representation of the behaviour of $\bar{f}_1'(\eta)$ at high values of $\lambda$. It is worthy of note that even at this high value of $\lambda$ the spin parameter $\lambda$ the quasilinearisation technique was numerically stable - even though the initial estimates were very approximate.

From equations (3-59) and (3-60) the following expression for the meridional velocity component $V_1^*$ is obtained:

$$V_1^* = \sum_{n=1}^{\infty} U_{2n-1} f'_{2n-1}(\eta) X_1^{*2n-1} \qquad (5\text{-}1)$$

where $V_1^* = V_1 / \bar{U}_1$, $\bar{U}_1$ being the first coefficient in the series expression for potential flow given by (3-87). Near to the front stagnation point, where all powers of $X_1^*$ other than unity may be neglected we have

$$V_1^* = U_1 f_1'(\eta)\, X_1^* \tag{5-2}$$

or

$$V_1^* = \bar{f}_1'(\eta)\, X_1^* \tag{5-3}$$

consequently because $V_1^*$ is directly proportional to $\bar{f}_1'(\eta)$ near the front stagnation point the plots in fig.5.1 can be used to describe the velocity profiles in the meridional direction in the boundary layer. From these plots it is interesting to note that at some points in the boundary layer the meridional component of velocity becomes greater than that in the main stream, i.e. U, this is shown most strikingly in the $\lambda$=100 plot where at certain points in the boundary layer the meridional component of velocity becomes nearly twice as large as the corresponding velocity in the main stream. From fig.5.9, where the sphere is used as an example, it can be seen that this phenomenon occurs at all points in the boundary layer.

As explained in Chapter 2, Schlichting (1956) found that at a value of $(\Omega/\tilde{a}) > 0.815$ his stagnation point solutions broke down. For the meridional component of velocity Schlichting presented a Pohlhausen type polynomial in terms of a form parameter K. The value of $(\Omega/\tilde{a}) > 0.815$ for which the stagnation point solutions broke down was found to correspond to a form parameter of K=12 which was also found to correspond to the apparent onset of greater meridional components of velocity in the boundary layer than in the main stream. Schlichting stated that it was entirely possible to obtain such a phenomenon due to the effect of centrifugal forces set up in the boundary layer by rotation. This prediction of Schlichting is shown to be correct by fig.5.1. It is interesting to note that Schlichting's spin parameter $(\Omega/\tilde{a})$ corresponds to $\lambda^{\frac{1}{2}}$, consequently Schlichting's approximate solution predicts that the onset of the described

phenomenon at $\lambda=0.664$ whereas from fig.5.1 it can be seen that the results of this work suggest that the phenomenon should initially occur in the region of $\lambda=10$.

Fig.5.4 shows the variation of $\bar{g}_1'(\eta)$ in the boundary layer; from these plots it can be seen that $\bar{g}_1'(0)$ does not vary as much in magnitude with spin parameter $\lambda$ as does the boundary value $\bar{f}_1''(0)$.

From equation (3-73) the dimensionless Azimuthal velocity component $V_2^*$ is:

$$V_2^* = \lambda^{\frac{1}{2}} \sum_{n=1}^{\infty} \bar{g}_{2n-1}(\eta)\, X_1^{*2n-1} \tag{5-4}$$

and near to the front stagnation point

$$V_2^* = \lambda^{\frac{1}{2}}\, \bar{g}_1(\eta)\, X_1^* \tag{5-5}$$

It can be seen from fig.5.3 that the azimuthal velocity component (to which $\bar{g}_1(\eta)$ is directly proportional), reaches its asymptotic value ($\lim_{\eta\to\infty} \bar{g}_1(\eta)$) nearer to the body surface with increasing spin parameter. In effect the boundary layer thickness for the azimuthal velocity component decreases with increasing spin parameter.

## 5.2.2 Mass Transfer Stagnation Point Solutions

Because of the linearity of the stagnation point equations for mass transfer (3-100) the solution of the pertinent boundary value problem (i.e. determination of $\mathcal{H}_0'(0)$) was solved by use of the superposition principle. The boundary values that have been determined for different values of Schmidt number for bluff bodies ($K_1 = l_o = 1$) are shown in tables A10 to A23 in appendix E.

As already explained, the range of integration in $\eta$ of the mass transfer functions was $0 < \eta < \mathrm{XMAX}/\overline{Pr}^{\frac{1}{3}}$, where XMAX = 6.0 was the 'effective' infinity for the hydrodynamic functions. The mass transfer boundary layer thickness for Schmidt numbers greater than

thirty is smaller than the hydrodynamic boundary layer thickness and consequently the integration step length was'scaled'. The step length used was XMAX/(60 x $\overline{Pr}^{\frac{1}{3}}$), thus for a $\overline{Pr}$ of unity (i.e. when the mass transfer boundary layer thickness is the same order of magnitude as the hydrodynamic boundary layer thickness) the value of the integration step length for XMAX = 6.0 is 0.1 which is the same step length as that used in the integration of the hydrodynamic functions.

The accuracy of the values obtained for $\mathcal{H}'_0(0)$ is dependent on the accuracy of the hydrodynamic boundary values. For spin parameter $\lambda$=20 it has been stated that the accuracy of the solution obtained by the quasilinearisation technique is $\pm$0.001. In table A2 in appendix E a perturbation on the boundary values $\overline{f}''_1(0)$, $\overline{g}'_1(0)$ of $1.0 \times 10^{-3}$ at $\overline{Pr}$ = 0.7 produces a change in the magnitude of $\mathcal{H}'_0(0)$ of $6.0 \times 10^{-4}$. In general it is expected that the values of the mass transfer boundary layer functions at the front stagnation point are more accurate than the hydrodynamic boundary values from which they are derived.

From equation (3-97) it can be seen that in the region of the front stagnation point the dimensionless concentration $X^*$ is given by $X^* = \mathcal{H}_0(\eta)$; consequently fig.5.5 is in effect a plot of the dimensionless concentration distribution near to the front stagnation point. From the plots it can be seen that the mass transfer boundary layer thickness diminishes with

1) increase in spin parameter $\lambda$

2) increase in Schmidt number

In the region of the front stagnation point the local mass transfer number is given by $-\mathcal{H}'_0(0)/\sqrt{2}\,\overline{Pr}^{\frac{1}{3}}$, from fig.5.6 it can be seen that the value of the local mass transfer number increases with both Schmidt number and spin parameter.

5.2.3 Boundary Values for Oblate Spheroids Rotating in Axial Flow

From table A1 it can be seen that the values obtained for $\bar{f}_1''(0)$ and $\bar{g}_1'(0)$ at a step length in $\eta$ of 0.1 differ from those obtained at a step length of 0.05 in the fifth significant figure at most. Similarly in the determination of higher order boundary values it can be seen in table A2B the effect of this halving of step length is to effect the fifth significant figure only. During the computation of the unknown boundary values a step length of 0.1 was used, this was considered to yield results of acceptable accuracy.

From table A2A it can be seen that a small perturbation of order $1.0 \times 10^{-3}$ applied to the stagnation point hydrodynamic boundary values does not cause large errors in subsequent sets of hydrodynamic boundary values. The higher order sets, which are dependent on the lower order sets, are affected less by the perturbation as their order increases. Consequently it would be expected that the higher order sets are determined to a greater accuracy than the stagnation point equations from which they were derived.

From the above considerations it would be expected that the hydrodynamic boundary values obtained in this work (see tables A3 to A6, appendix E) are correct to at least five significant figures for spin parameters up to ten and three for the spin parameter of twenty.

Hoskin has presented values of $f''_{2n-1}(0)$ and $g'_{2n-1}(0)$ for a sphere rotating in axial flow at spin parameters up to ten, from these results the modified boundary values $\bar{f}''_{2n-1}(0)$ and $\bar{g}'_{2n-1}(0)$ have been obtained and reproduced in table A7 appendix E. Comparison with the values obtained in this work shows that agreement is reached to at least five significant figures.

For the non-rotating body (i.e. a spin parameter of zero), Green has presented the first five sets of the hydrodynamic boundary values $\bar{f}''_{2n-1}(0)$. The results in tables A8 and A9 have been derived from the results presented by Green taking into account the different form of Blasius series used for the stream function. It can be seen that agreement is reached to at least five significant figures for the sphere and 10/16 spheroid; the same agreement was also found for the boundary values of all the other spheroidal shapes that were studied by Green.

As in the case of the stagnation point equations, the step length used in the determination of higher order mass transfer boundary values was scaled down in order that the relative sizes of the hydrodynamic and mass transfer boundary layers would be taken into account. The integration step length was $(XMAX/(60 \times \overline{Pr}^{\frac{1}{3}}))$ in $\eta$ for integration of the mass transfer functions.

From table A2A it can be seen that a perturbation applied to the values of $\bar{f}''_1(0)$ and $\bar{g}'_1(0)$ results in smaller changes in the mass transfer boundary values. The results obtained in this work for $\mathcal{H}'_{2(n-1)}(0)$ (tables A10 to A23) are hence expected to be more accurate than the hydrodynamic boundary values from which they were derived.

Again comparison can be made with the results of other workers. The results of Siekmann for the rotating sphere can be compared with the results obtained in this work; tables A24 and A25 contain values of $\mathcal{H}'_{2(n-1)}(0)$ derived from Siekmann's results. It should be noted that Siekmann's results are based on different series representations of the mass transfer functions. The results for spin parameters $\lambda$=0 and 4 and $\overline{Pr}$ numbers of 0.7 and 1.0 can be compared with the results obtained in this work, tables A10 and A11,

once again agreement is obtained to five significant figures.

In table A26 appendix E are presented values of $f''_{2(n-1)}(0)$ obtained from the results of Green for non-rotation spheroids ($\lambda=0$) at a $\overline{Pr}$ number of 2.4. The results obtained in this work are again in excellent agreement for all five sets of the boundary values $f''_0(0), \ldots f''_8(0)$.

5.2.4 Local Mass Transfer Numbers for Oblate Spheroids Rotating in Axial Flow

The computer programme used in determining the unknown hydrodynamic and mass (or heat) transfer boundary values uses the values obtained for $f''_{2n-1}(0)$ (of which the first five sets are determined) in equation (3-146) to obtain point mass transfer numbers at $5^o$ intervals of the parametric angle around the spheroid. Examples of the results are plotted in figs.5.10 to 5.18.

From these plots it can be seen that the effect of spin is to increase the values of the local mass transfer numbers, it can also be seen that for any spin parameter and body shape the values of the point mass transfer numbers increase with Schmidt number.

The effect of spin on local mass transfer numbers is seen to be quite substantial; the maximum effect being at the front stagnation point region and the minimum effect being in the region of the equator. For example, for a sphere at Schmidt number of unity, (see fig.5.11) an increase in the spin parameter from zero (non-rotating body) to twenty gives a 30% increase in the value of the mass transfer number.

The effect of rotation is also seen to be greatest at high Schmidt numbers; for the sphere when the Schmidt number is very large (i.e. $Sc \rightarrow \infty$) the value of the stagnation point mass transfer number at a

spin parameter of ten is approximately 40% greater than at a spin parameter of zero; for a Schmidt number of unity the corresponding value is 20%.

The accuracy of the values obtained for point mass transfer numbers are dependent on

1) the accuracy of the boundary values $\mathcal{H}'_{2(n-1)}(0)$

2) the rate of convergence of the power series for $M_A$, equation (3-146).

The accuracy of the terms $\mathcal{H}'_{2(n-1)}(0)$ has already been discussed, it was calculated that values of $\mathcal{H}'_{2(n-1)}(0)$ would be accurate to at least five significant figures for spin parameters up to ten and accurate to at least three significant figures for a spin parameter of twenty.

The rate of convergence of the power series for $M_A$ is dependent on the rate of convergence of the power series which represents the potential flow and the scale factor $h_{\theta,0}$. Green has shown that both these power series converge more rapidly for the sphere than for oblate spheroids - the rate of convergence decreasing with increasing oblateness.

In tables A10 to A23 the values of $\mathcal{H}'_{2(n-1)}(0)$ that have been obtained in this work have been presented. On examination of the rate at which the magnitudes of $\mathcal{H}'_{2(n-1)}(0)$ decrease with order (i.e. value of n) it would seem that the rate of convergence of the power series for $M_A$:

1) decreases with increasing spin parameter;

2) decreases with increasing Schmidt number.

The first five coefficients in the power series for $M_A$ have been determined, i.e. $\mathcal{H}'_0(0)$ to $\mathcal{H}'_8(0)$, but because the remainder of the coefficients remain unknown it is not possible to state the accuracy

of the point mass transfer numbers that have been determined. It is assumed, however, that the magnitude of the higher order mass transfer boundary values, i.e. $f'_{10}(0)$ etc. will be small enough to have only a minor effect on the values of $M_A$ that have been obtained. The convergence properties of $M_A$ are shown in fig.5 in which plots are shown of $M_A$ using an increasing number of coefficients in the power series expansion.

Green (1968) compared his theoretical results for local mass transfer number with the experimental results of Beg (1966); he found that for non-rotating bodies boundary layer theory gave good predictions of local mass transfer numbers up to angles of $70^\circ$ from the front stagnation point for the sphere and up to $50^\circ$ from the front stagnation point for oblate spheroids of all eccentricities. At higher angles he found that boundary layer theory over-predicted the local mass transfer numbers by increasingly large values. Green came to the conclusion that the difference between the results given by boundary layer theory and experiments at larger angles was due to the failure of the potential flow theory used to predict the pressure distributions satisfactorily. No series representations exist which give reliable pressure distributions at large angles around spheroidal bodies. Thus the accuracy of the power series expansion for $M_A$, i.e. (3-146) is not increased if higher order boundary values are calculated using potential flow theory. The first five coefficients in the series for $M_A$ have already been obtained, the sixth coefficient $f'_{10}(0)$ would probably only have a significant effect on $M_A$ at large angles which may well be in the region in which the pressure distribution is no longer adequately predicted from potential flow. If, however, it is desired to obtain forms of higher order than $f'_8(0)$ the computer routine should be programmed in double precision arithmetic,

also the modifications to the quasilinearisation technique already suggested should be used in order to obtain more accurate stagnation point solutions.

## 5.3 STAGNATION POINT SOLUTIONS FOR AN AXIALLY SYMMETRIC BODY ROTATING IN A QUIESCENT FLUID

### 5.3.1 Hydrodynamic Stagnation Point Solution

The hydrodynamic stagnation point equations (4-65) have been presented in Chapter 4 together with the pertinent boundary conditions (4-67). The boundary value problem of the calculation of $F_1'(0)$ and $G_1'(0)$ has already been solved by Rogers and Lance (1960) and Banks (1965) - both results are in agreement to five significant figures. In this work the results of Rogers and Lance were used, their results being published to six significant figures

$$\text{i.e.} \quad F_1'(0) = 0.510233$$

$$G_1'(0) = -0.615922$$

### 5.3.2 Mass Transfer Stagnation Point Solutions

The mass transfer stagnation point equation (4-66) with pertinent boundary conditions (4-67) has been solved for different values of Schmidt number: the solutions are plotted in figs.5.7 and 5.8.

As in the case of a body rotating in axial flow the step length used in the integration of the mass transfer functions has been 'scaled' in order to take into account the differences in magnitude of the mass transfer and hydrodynamic boundary layer thicknesses, the step length in $\alpha$ was taken as XMAX/(200 x $\overline{Pr}^{\frac{1}{3}}$) where XMAX was 20. It was found for the case of $\overline{Pr}$ unity that when the step length was halved only the sixth significant figure was changed. Hence, it is expected that the boundary values $Jo'(0)$ tabulated in tables Q2 to Q4, appendix E, are accurate to at least five significant figures.

At the front stagnation point, the dimensionless concentration $X^*(\alpha)$ is identical to the function $Jo(\alpha)$. From fig.5.7 it can be seen that the Schmidt number has a marked effect on the mass transfer

boundary layer thickness; the higher the Schmidt number the smaller the boundary layer thickness. It may therefore be expected that higher mass transfer numbers would be obtained at higher Schmidt numbers. This conclusion is shown to be correct by fig.5.8 in which the mass transfer number at the front stagnation point (which is given by $-Jo(0)/\sqrt{2} \times \overline{Pr}^{\frac{1}{3}}$) can be seen to increase with increased Schmidt number.

5.3.3 Boundary Values for an Oblate Spheroid Rotating in a Quiescent Fluid

The numerical technique used to determine the unknown boundary values $F'_{2n-1}(0)$, $G'_{2n-1}(0)$ and $J'_{2n-1}(0)$ has been explained in Chapter 4. The computer programme used to carry out the calculations is shown in appendix D.

As already described the integration of the hydrodynamic functions was carried out with a step length in $\alpha$ of 0.1. In table Q8 it can be seen that the boundary values obtained when using a step length of 0.05 differ from those using a step length of 0.1 in the sixth significant figure, hence it is expected that the hydrodynamic boundary values obtained in this work (see table Q1 appendix E) are correct to at least five significant figures.

The integration step length in $\alpha$ for the case of mass transfer functions was, as already explained scaled; the value being taken as $XMAX/(\overline{Pr}^{\frac{1}{3}} \times 200)$. It was found that a change in XMAX from 20 to 25 produced only a change in the sixth significant figure of the values of $J'_{2(n-1)}(0)$: once again it is expected that the values of $J'_{2(n-1)}(0)$ obtained in this work are accurate to at least five significant figures.

As in the case of a body rotating in axial flow, the solution

of the n'th set of equations is dependent on the results obtained from the previous (n-1) sets, hence, it might be expected that the errors in any particular set of the boundary values might have an accumulative effect and make significant changes in the magnitude of the higher order boundary values. This was found not to be the case in practice; perturbations applied to the stagnation point boundary values were found to have a diminishing effect on other boundary values as their order increased, it would be expected, therefore, that all boundary values $F'_{2n-1}(0)$, $G'_{2n-1}(0)$ and $J'_{2(n-1)}(0)$ are more accurate than the stagnation point boundary values from which they were derived, i.e. accurate to at least five significant figures.

It is interesting to compare the values obtained in this work with the results obtained by W.H.H. Banks (1965)[1,2]. As can be seen in tables Q6 and Q7 appendix E agreement in all boundary values is obtained to five significant figures.

The first four sets of the hydrodynamic boundary values $F'_{2n-1}(0)$ and $G'_{2n-1}(0)$, n = 1 to 4, are given in table Q1 appendix E for the sphere, 13/16 spheroid and the 10/16 spheroid. The values of $J'_{2(n-1)}(0)$ for the same bodies at six $\overline{Pr}$ numbers are given in tables Q2 to Q4.

## 5.3.4 Local and Overall Mass Transfer Numbers for Oblate Spheroids Rotating in a Quiescent Fluid

The computer programme automatically substitutes the values of $J'_{2(n-1)}(0)$ that have been determined into equation (3-147) to produce point or local values of the mass transfer number at intervals of $5^{\circ}$ in the parametric meridional co-ordinate $\theta$ up to a maximum value of $90^{\circ}$. In figs.5.19 and 5.20 these values of local mass transfer number have been plotted for the sphere and 10/16 oblate spheroid, respectively, at various Schmidt numbers in the range of 0.7 to 100.0.

Using the values obtained for $F'_{2n-1}(0)$ the local mass transfer numbers at infinite Schmidt number have also been plotted (see section 3.6.2).

The rate of convergence of the series representation of the local mass transfer number $M_Q$, i.e. (3-147) is dependent on the rate of convergence of the power series which represent the scale factor $h_{\theta,0}$ and the velocity components (which are also dependent on the rate of convergence of $h_{\theta,0}$). As explained previously, the rate of convergence of the scale factor $h_{\theta,0}$ decreases with the oblateness of the body, it would hence be expected that as the order of the set increases (i.e. as n increases) the values obtained for $F'_{2n-1}(0)$ and $G'_{2n-1}(0)$ would diminish most rapidly for the sphere and least rapidly for the 10/16 oblate spheroid. This trend does not manifest itself in the first four sets of the hydrodynamic boundary values shown in table Q1 appendix E; as can be seen the magnitudes of the fourth set of boundary values are far from negligible and the rate of convergence for both the sphere and the spheroids is very poor.

The effect of this poor rate of convergence of the hydrodynamic series representations on the convergence of the power series for local mass transfer number $M_Q$ can be seen in tables Q2 to Q4, appendix E; here the first four sets of the values $J'_{2(n-1)}(0)$ are given for Schmidt numbers of 0.7 to 100.0. It can be seen that the values of $J'_{2(n-1)}(0)$ diminish most rapidly for the sphere as the order of the set, n, increases and least rapidly for the 10/16 spheroid. It can be seen that this rate also is highest for low Schmidt numbers. The rate of convergence of the power series representing $M_Q$ can be seen from fig.52in which plots of $M_Q$ against angle around the body are shown for an increasing number of terms in the series. It can be seen that when the first four terms in the

series expression for $M_Q$ are given, the values obtained for $M_Q$ will be good over much of the body surface, the poorest agreement is seen to be in the vicinity of the equator.

Local values of mass transfer numbers are plotted in figs.5.19 and 5.20. From the definition of the local mass transfer number given in (3-145) it follows that at the front stagnation point, local mass transfer numbers are independent of shape and dependent on Schmidt number only, this can be seen from the two sets of curves.

The shapes of the two curves for the sphere and 10/16 body also show that the values of local mass transfer number vary little with shape, the two sets of curves being very similar. If more terms had been determined in series (3-147) the similarity of the shapes of the curves may have been greater. This similarity of shape of the curves might be due to the velocity profiles in the induced boundary layers for both the sphere and 10/16 spheroid being similar. Further work is obviously required and more terms $F'_{2n-1}(0)$, $G'_{2n-1}(0)$ obtained in order that these flow fields can be thoroughly investigated. The curves also show that in general the value of $M_Q$ increases with increasing Schmidt number and increasing oblateness of the body.

It has been previously explained in Chapter 2 that a boundary layer is induced on both hemispheres of a sphere rotating in a quiescent fluid, similarly it is expected that all enclosed bodies such as oblate spheroids will induce a 'double' boundary layer. Based on the assumption that the area of eruption of these two boundary layers was negligible, values of the overall mass transfer numbers were obtained by integration of the local mass transfer number values over the body surface

i.e.
$$M_O = \iint_{\bar{A}} M_{LOC}\, dA/\bar{A} \qquad (5\text{-}7)$$

where $M_0$ is the overall mass transfer number, $M_{LOC}$ is the local mass transfer number, dA is an elemental area on the spheroid surface, and $\bar{A}$ is the total spheroid surface area. Overall values of $M_0$ are given in table Q5 and plots of the values of overall mass transfer number at particular Schmidt numbers for the sphere, 13/16 spheroid, and 10/16 spheroid are given in fig.5.21. From the plots it can be seen that the overall mass transfer numbers increase in magnitude with increasing Schmidt number and increasing oblateness of the body. The values of the overall mass transfer numbers at infinite Schmidt number are shown as asymptotes. It can be seen that for a spheroid rotating in a quiescent fluid a Schmidt number of 100 is still a few orders of magnitude below those Schmidt numbers which are effectively infinite.

Banks (1965)[2] from his study of the rotating sphere at Prandtl numbers of 0.7 and 1.0 gave values for the overall coefficients as follows:

$$\frac{Nu_o}{R^{\frac{1}{2}}} = 0.25 \text{ for } Pr = 0.7, \quad \frac{Nu_o}{R^{\frac{1}{2}}} = 0.30 \text{ for } Pr = 1 \qquad (5\text{-}8)$$

where R is his spin Reynolds number $\frac{4d^2\Omega}{\nu}$ and $Nu_o = h_o 2d/K_T$.

Conversion of Banks definitions to those used herein (spin Reynolds number, $\bar{R}_S = 2d.\frac{\Omega d}{\nu}$ and $\overline{Nu}_o = hd/K$) gives:

$$\frac{\overline{Nu}_o}{\bar{R}_S^{\frac{1}{2}}\overline{Pr}^{\frac{1}{3}}} = 0.196 \text{ for } \overline{Pr} = 0.7; \quad \frac{\overline{Nu}_o}{\bar{R}_S^{\frac{1}{2}}\overline{Pr}^{\frac{1}{3}}} = 0.212 \text{ for } \overline{Pr} = 1.0 \qquad (5\text{-}9)$$

These expressions compare well with the results of this work (see table Q5, appendix E).

The semi-empirical equation of Kreith et al (1963) i.e.

$$\frac{Nu_o}{R^{\frac{1}{2}}} = 0.43\,\overline{Pr}^{0.4} \qquad (5\text{-}10)$$

correlates their experimental results within 15%. Substitution of $\overline{Pr}$ = 0.7 and 1.0 into Kreiths results yields:

$$\frac{Nu_o}{R^{\frac{1}{2}}} = 0.37 \text{ for } \overline{Pr} = 0.7; \quad \frac{Nu_o}{R^{\frac{1}{2}}} = 0.43 \text{ for } \overline{Pr} = 1.0 \qquad (5\text{-}11)$$

These results can be seen to differ quite substantially from our predicted values and those of Banks, i.e. equation (5-8). Banks has commented that it is highly unlikely that the poor convergence of the series representation for local heat or mass transfer numbers is the cause of such poor agreement. For the case of a sphere rotating in a quiescent fluid of $\overline{Pr} = 0.7$ it was found in the present work that the first five boundary values are:

$$\left.\begin{aligned} J_0'(0) &= -0.3231282 \\ J_2'(0) &= 0.06263696 \\ J_4'(0) &= 0.00131540 \\ J_6'(0) &= 0.00064938 \\ J_8'(0) &= 0.00017788 \end{aligned}\right\} \qquad (5\text{-}12)$$

It is consequently unlikely that additional terms in the determination of the overall mass (or heat) transfer number would in fact contribute much towards the difference between the theoretical results and Kreith's experimental results.

However, Nordlie and Kreith (1961-62) measured the rates of heat transfer from a rotating sphere in air over the spin Reynolds number range $1.8 \times 10^4 < R < 1.3 \times 10^5$. They presented the expression

$$Nu_o = 0.29\, R^{0.527} \qquad (5\text{-}13)$$

which correlated their experimental data to $\pm 12\%$.

If the exponent of the spin Reynolds number R is taken to be 0.5 instead of 0.527, the $\overline{Pr}$ number in their work taken as 0.7, and if their definitions are converted to those used in the present work, equation (5-13) becomes:

$$M_O = \frac{\overline{Nu}_o}{\overline{R}_S^{0.5}\,\overline{Pr}^{\frac{1}{3}}} = 0.231 \qquad (5\text{-}14)$$

The value obtained in this work for the right hand side of (5-14) i.e. 0.196 deviates from Nordlie and Kreith's value by 15%. This represents good agreement despite the fact that the exponent of R was taken to be 0.5 instead of 0.527 and despite the fact that the precise value of their $\overline{Pr}$ is not known.

Because of the fact that boundary layer theory does give good agreement with the data of Nordlie and Kreith (1961-62) but poor agreement with the data of Kreith et al (1963), more experimental data is required in order that conclusions may be made regarding the accuracy of mass or heat transfer number predictions made using boundary layer theory.

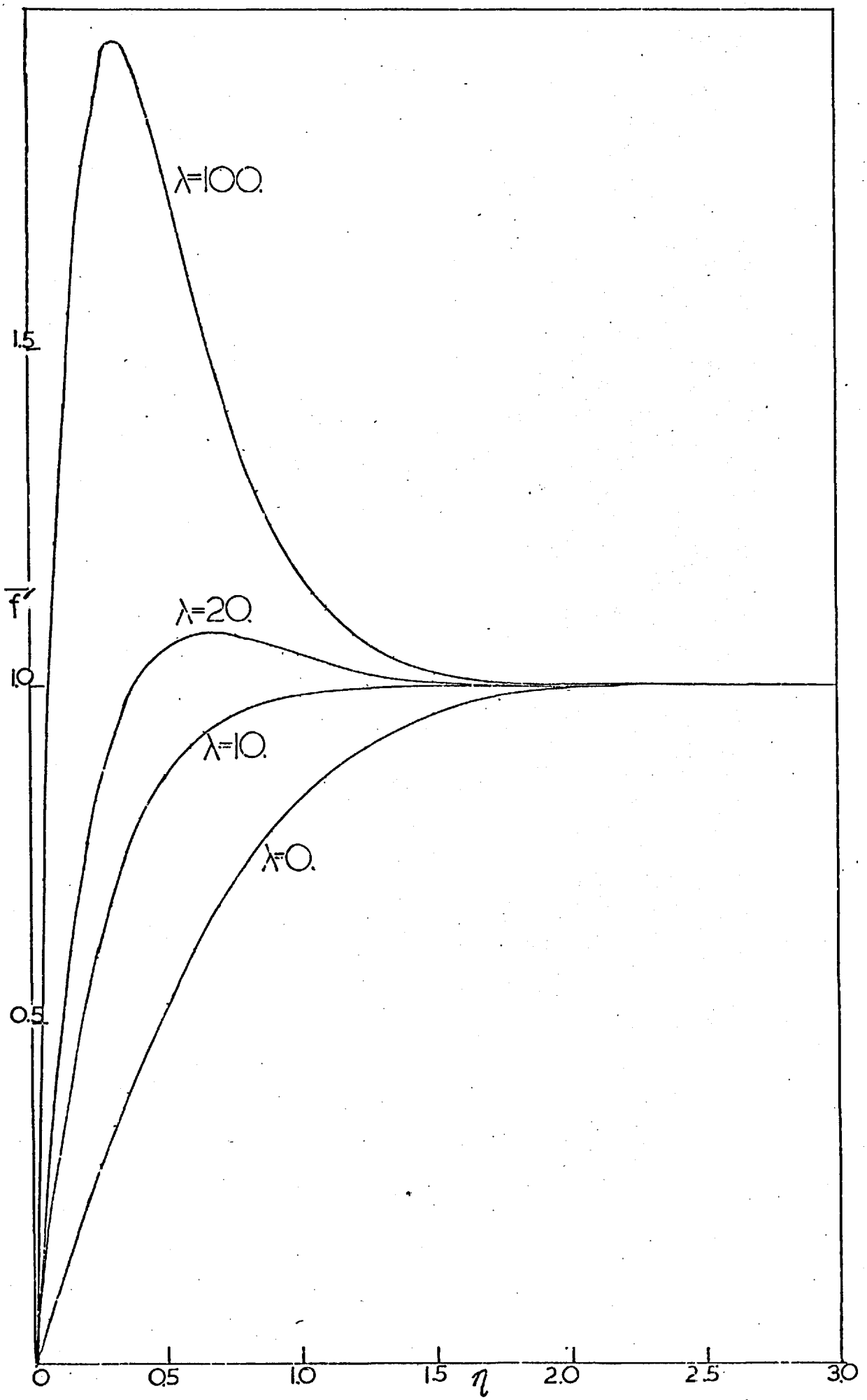



FIG 5.1 EFFECT OF SPIN PARAMETER λ ON $\bar{f}'$

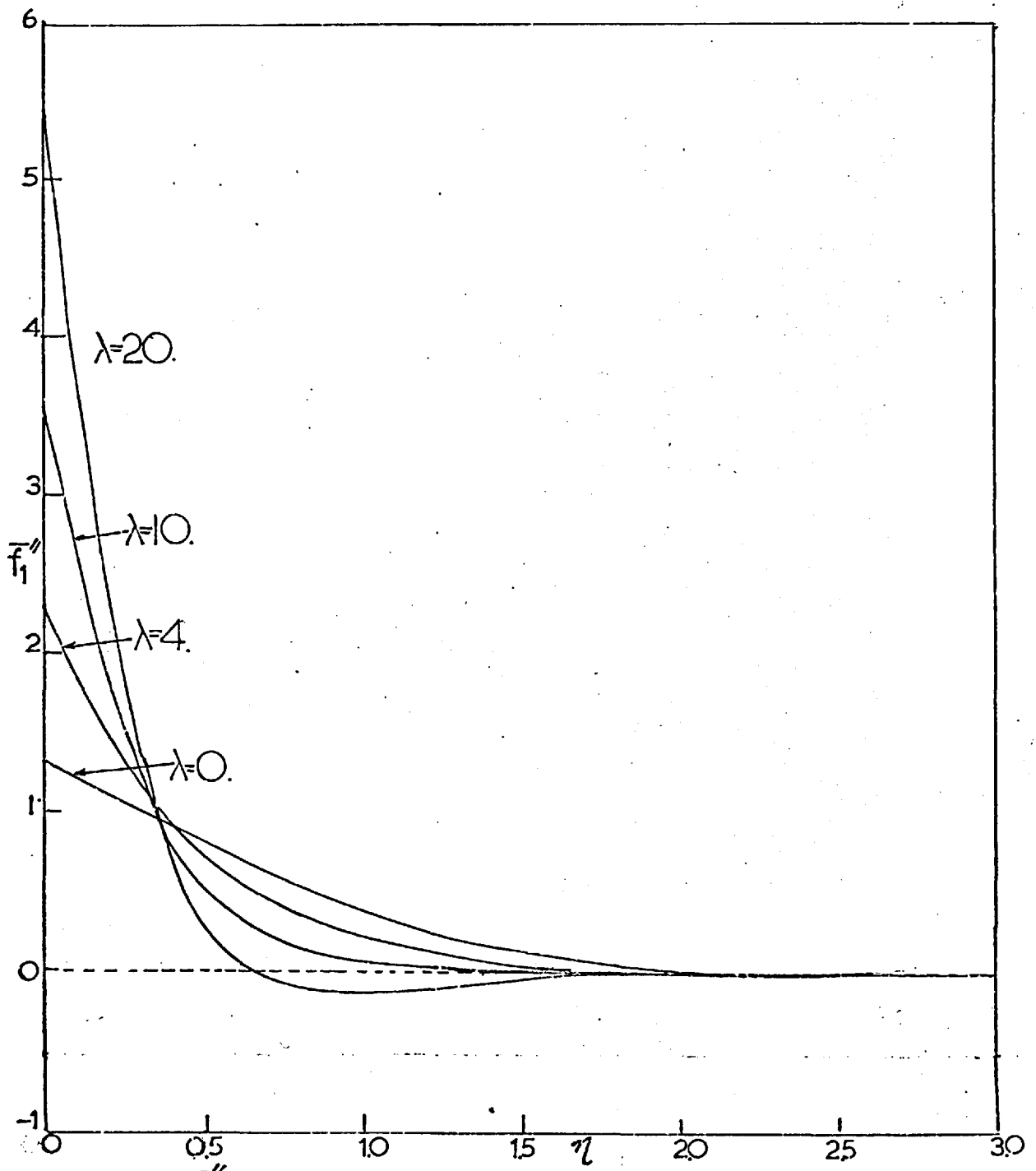



FIG 5.2 $\bar{f}_1''$ SHOWN AS A FUNCTION OF $\eta$ FOR SPIN PARAMETERS 0. TO 20.

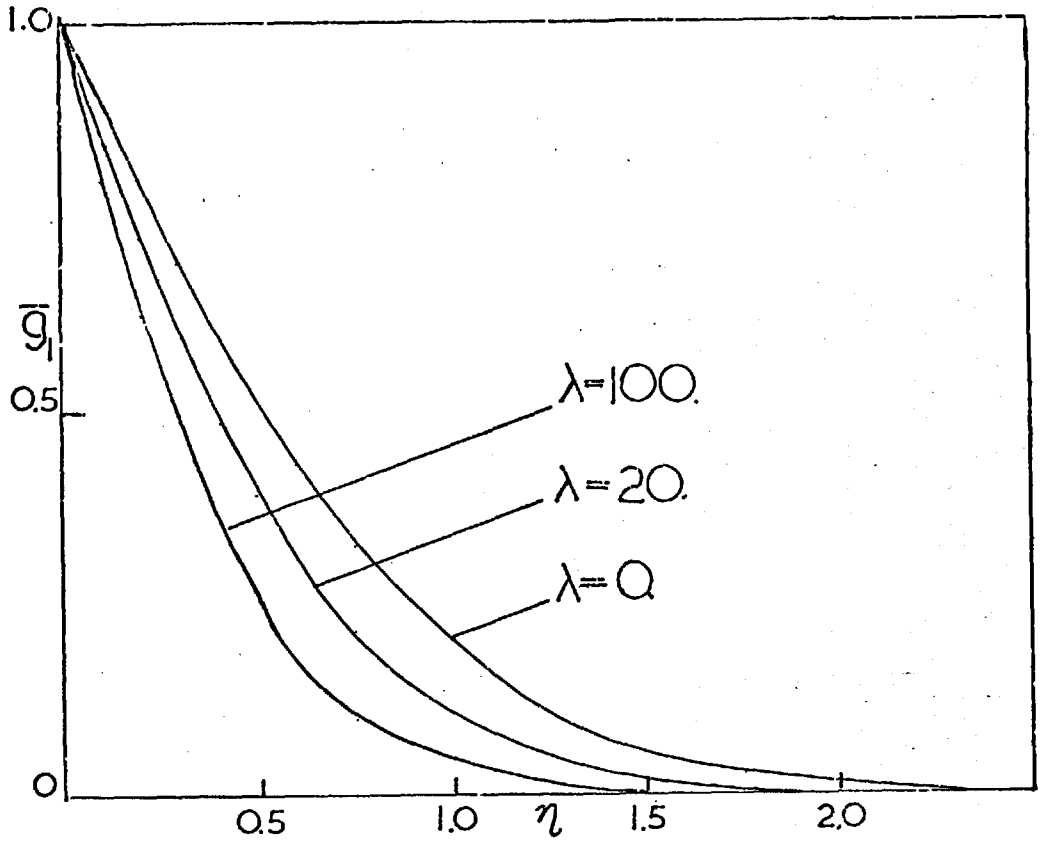



FIG 5.3 EFFECT OF SPIN PARAMETER λ ON $\bar{g}_1$

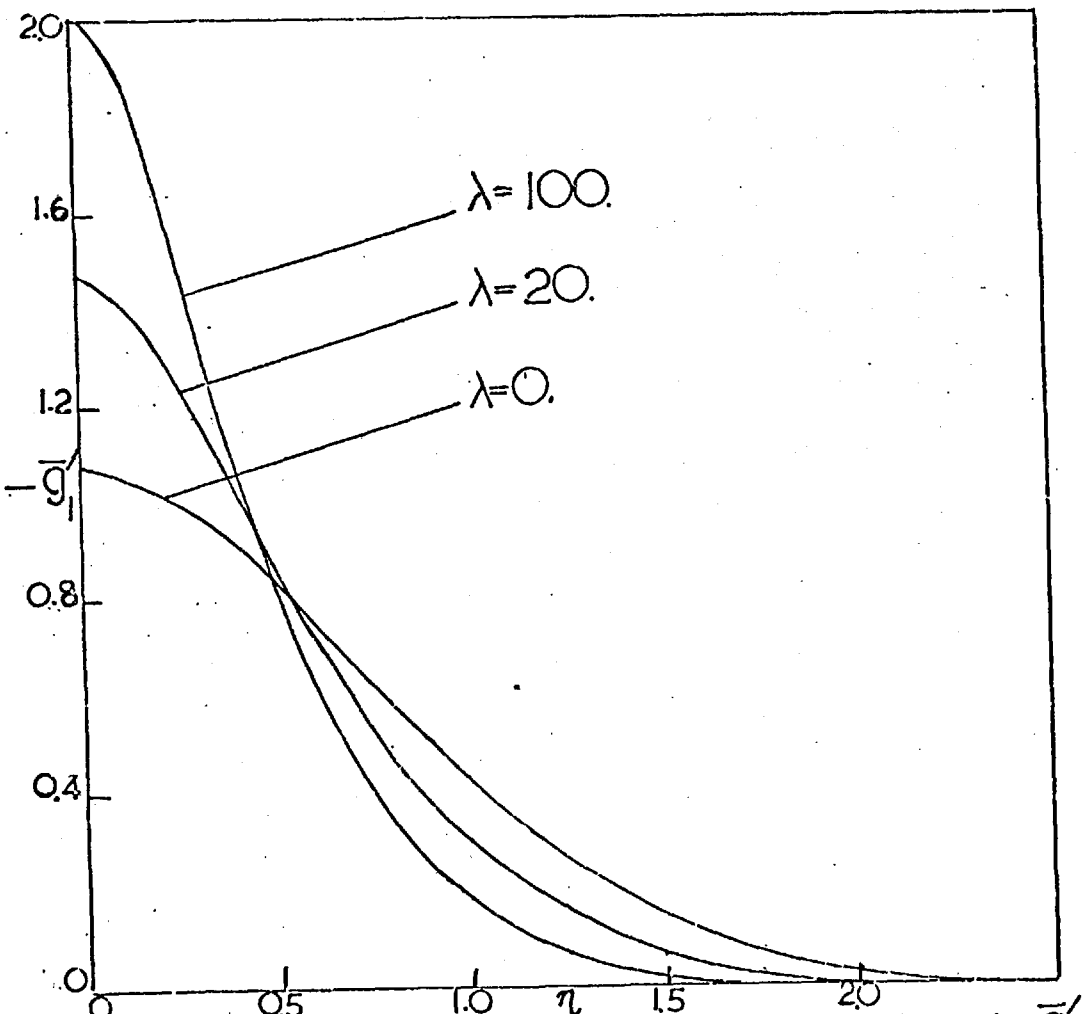



FIG 5.4 EFFECT OF SPIN PARAMETER λ ON $-\bar{g}_1'$

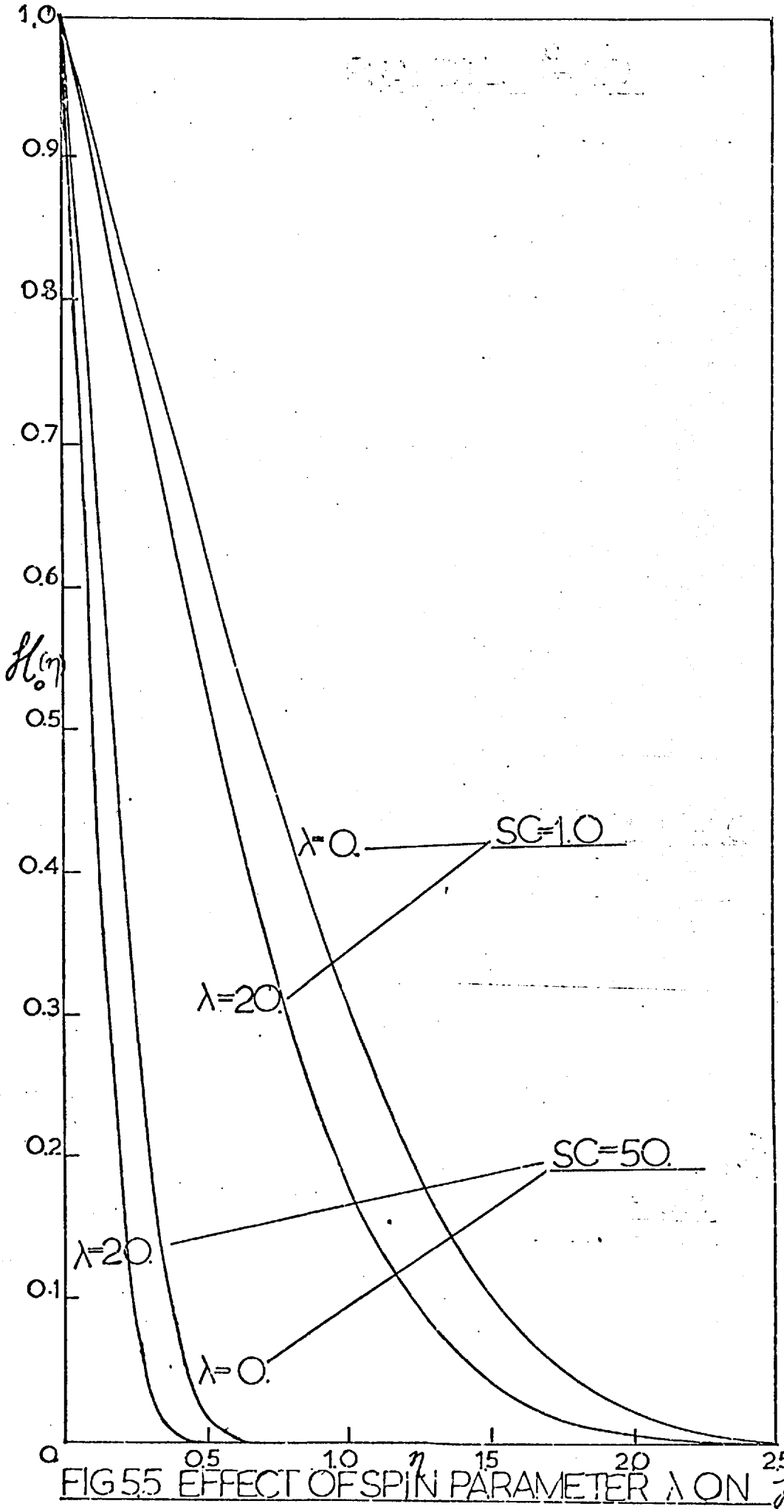



FIG 5.5 EFFECT OF SPIN PARAMETER λ ON $f_0(\eta)$.

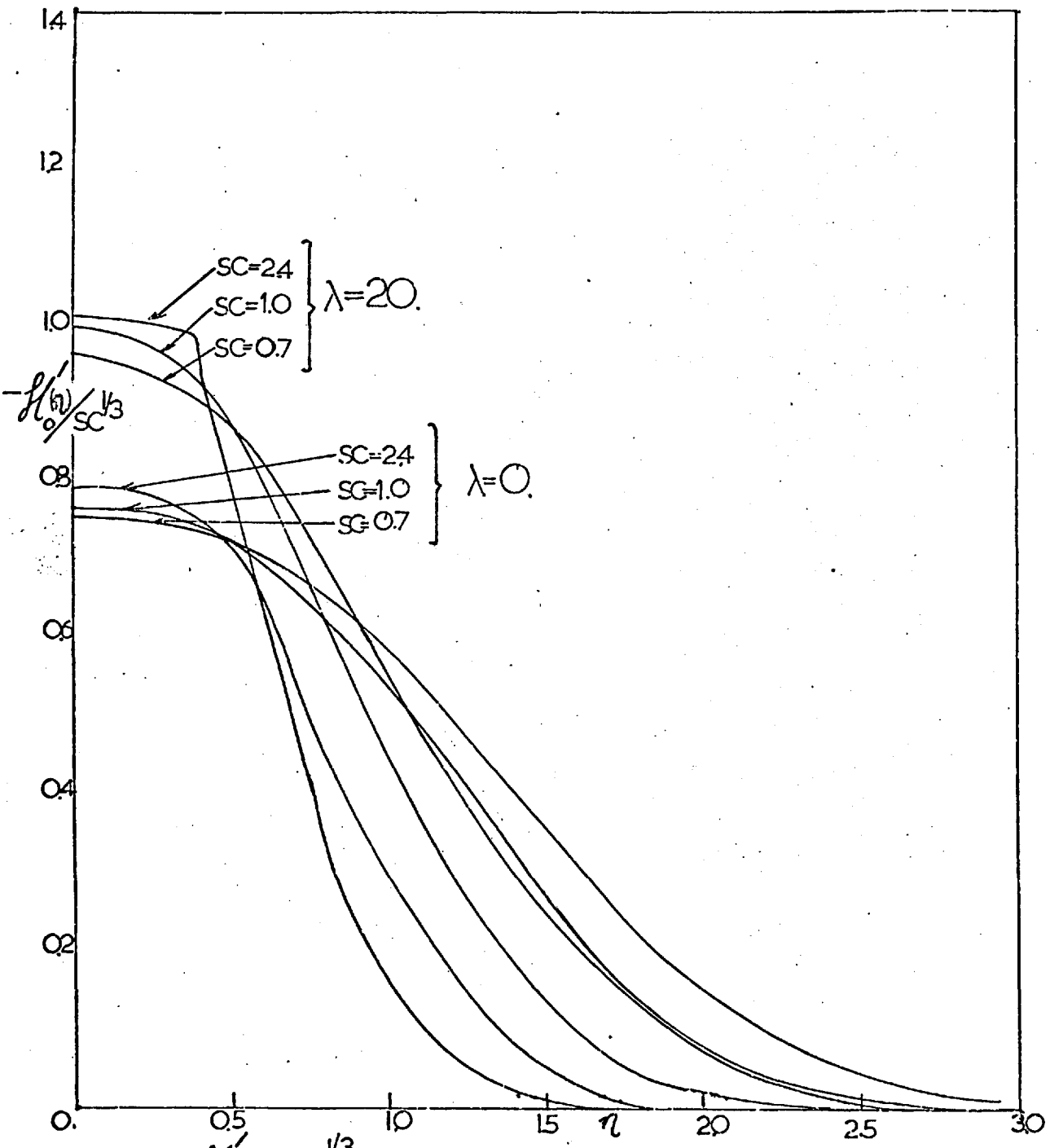



FIG 5.6 $f_0'(\eta)/SC^{1/3}$ SHOWN AS A FUNCTION OF $\eta$ FOR SPIN PARAMETERS OF 2.0 AND 0.

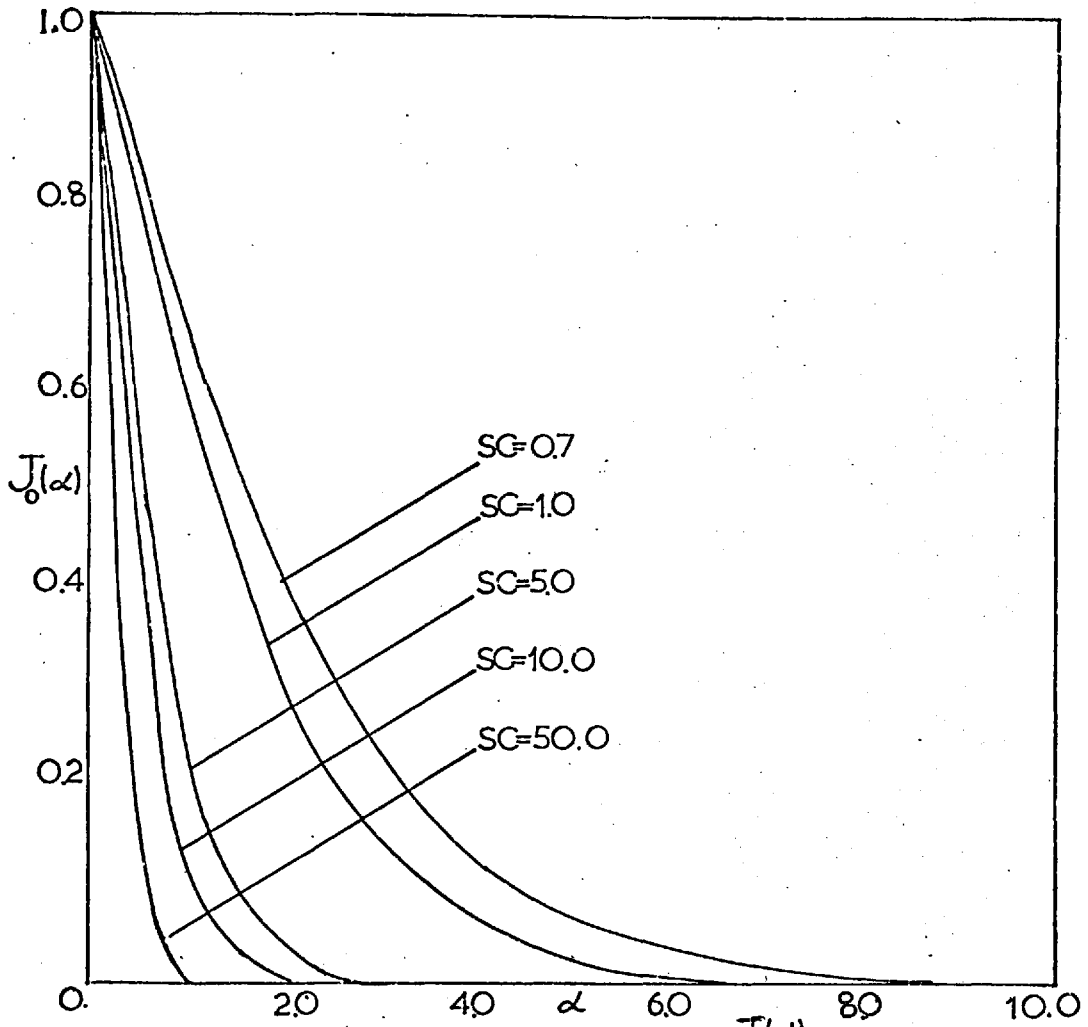



FIG 5.7 EFFECT OF SCHMIDT NUMBER ON $J_0(\alpha)$.

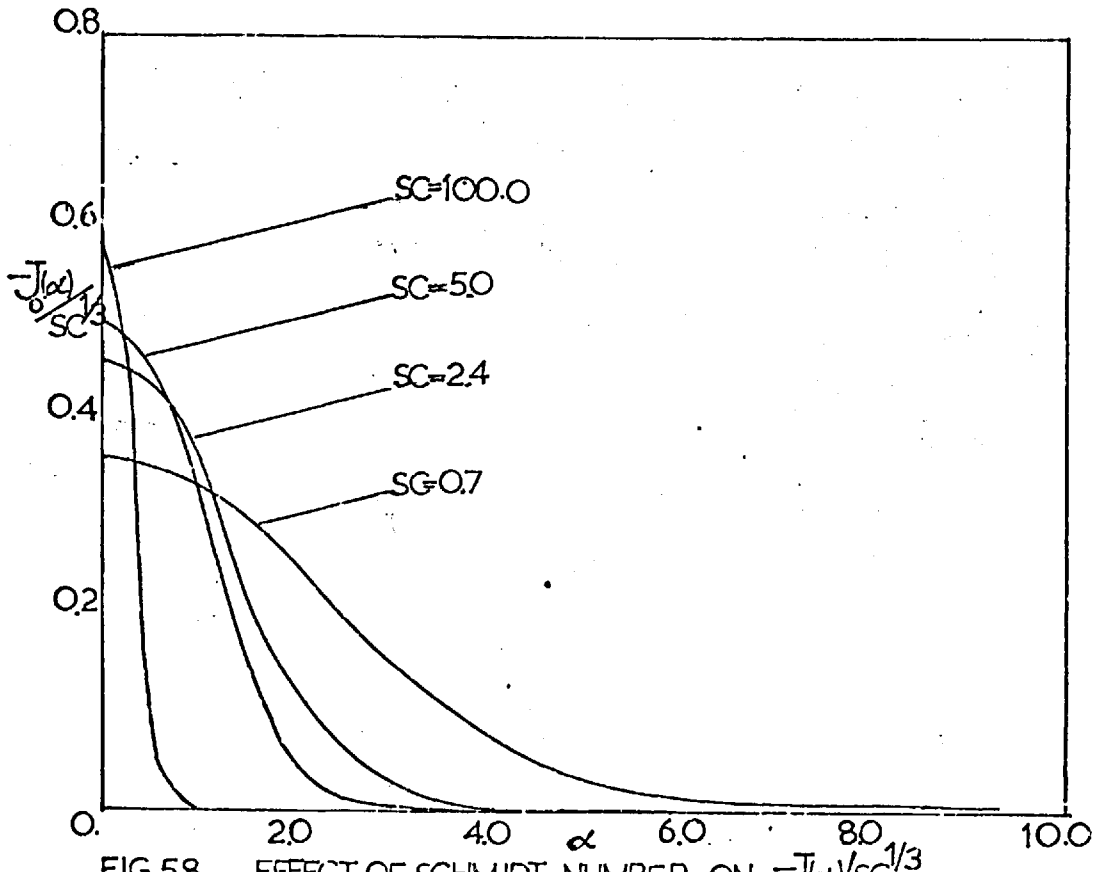



FIG 5.8 EFFECT OF SCHMIDT NUMBER ON $-J_0(\alpha)/SC^{1/3}$.

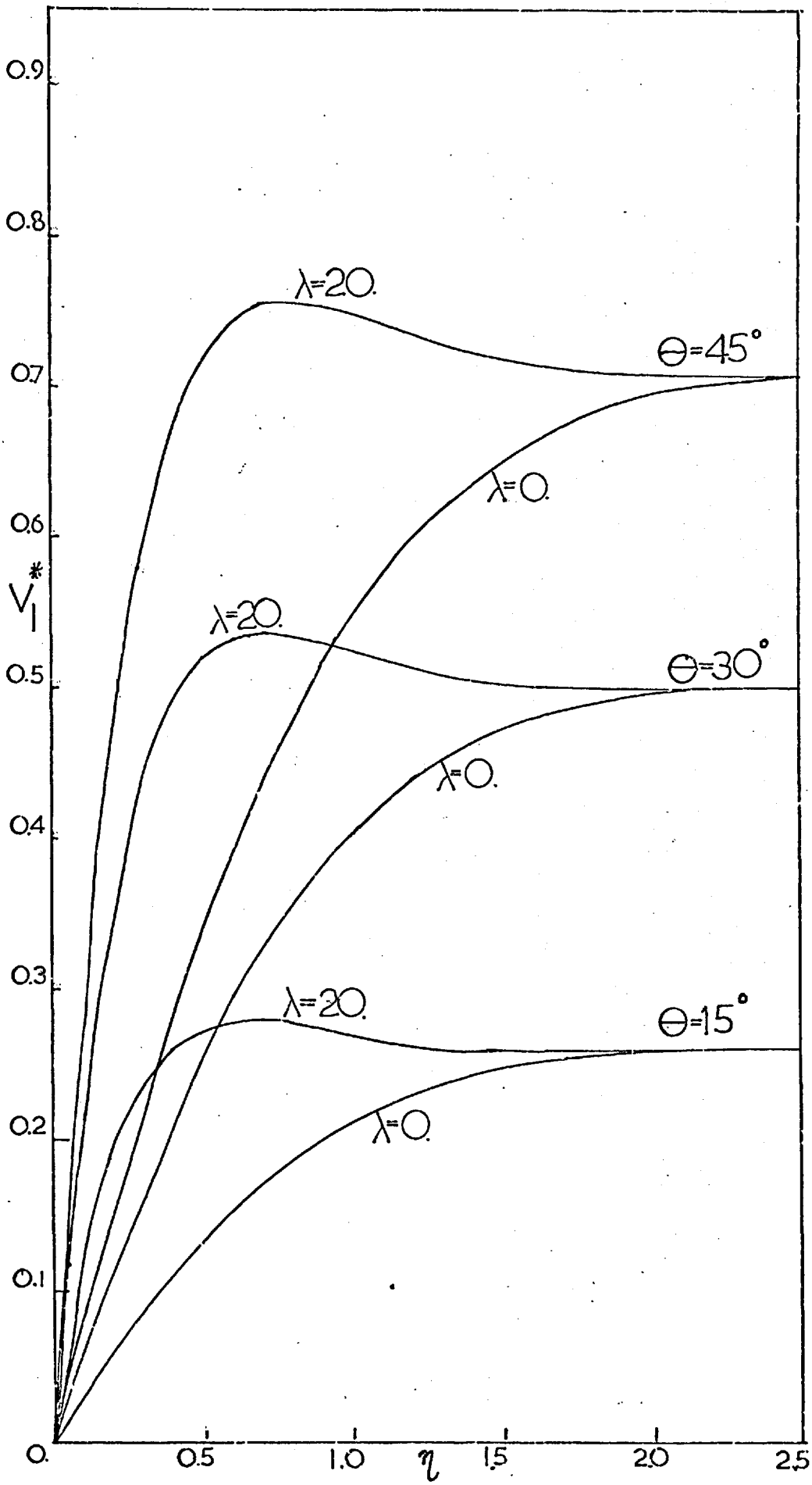



FIG 5.9 DIMENSIONLESS MERIDIONAL VELOCITY COMPONENT DISTRIBUTIONS FOR THE SPHERE.

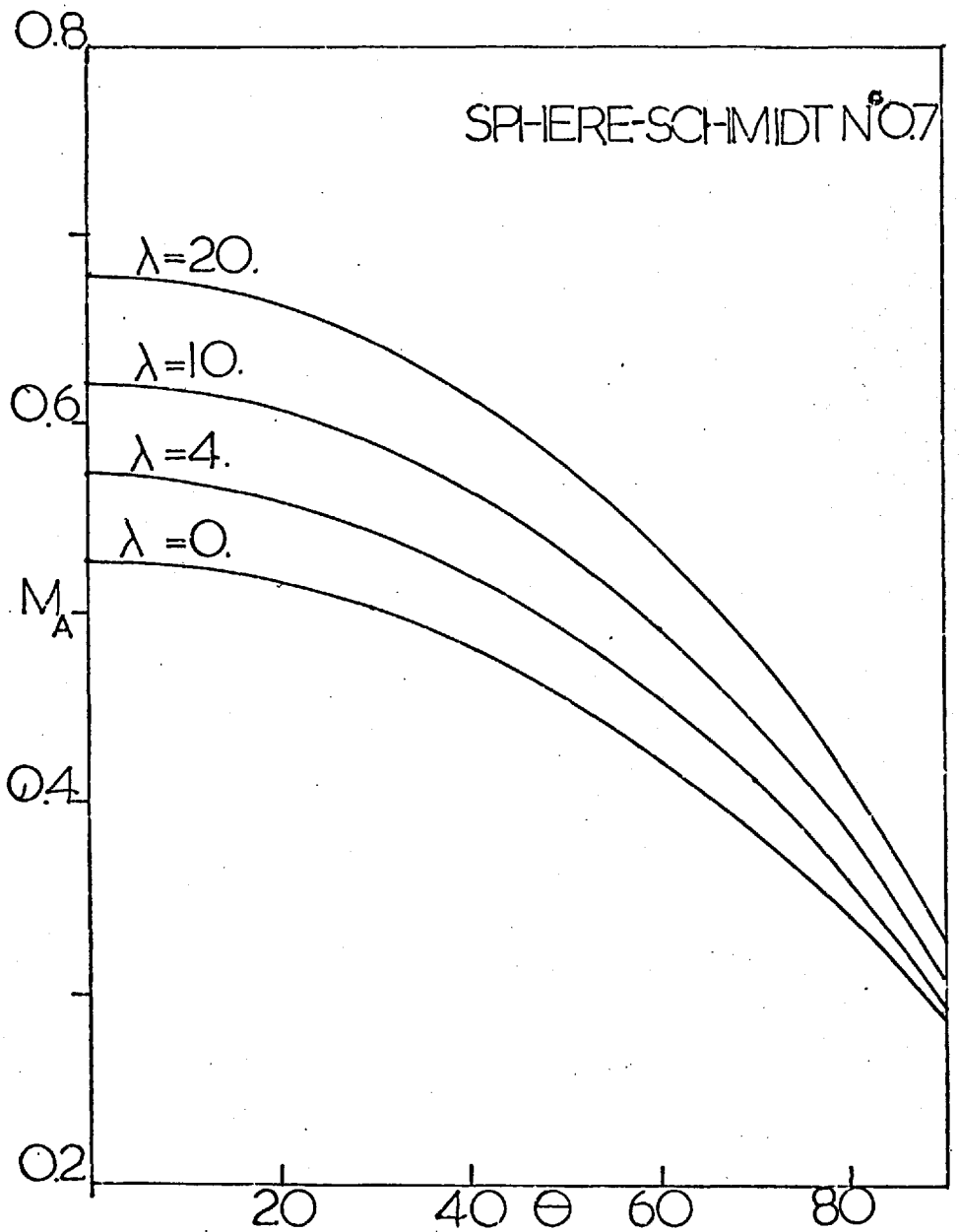



FIG 5.10 EFFECT OF SPIN PARAMETER λ ON $M_A$ FOR THE SPHERE AT SCHMIDT N° 0.7

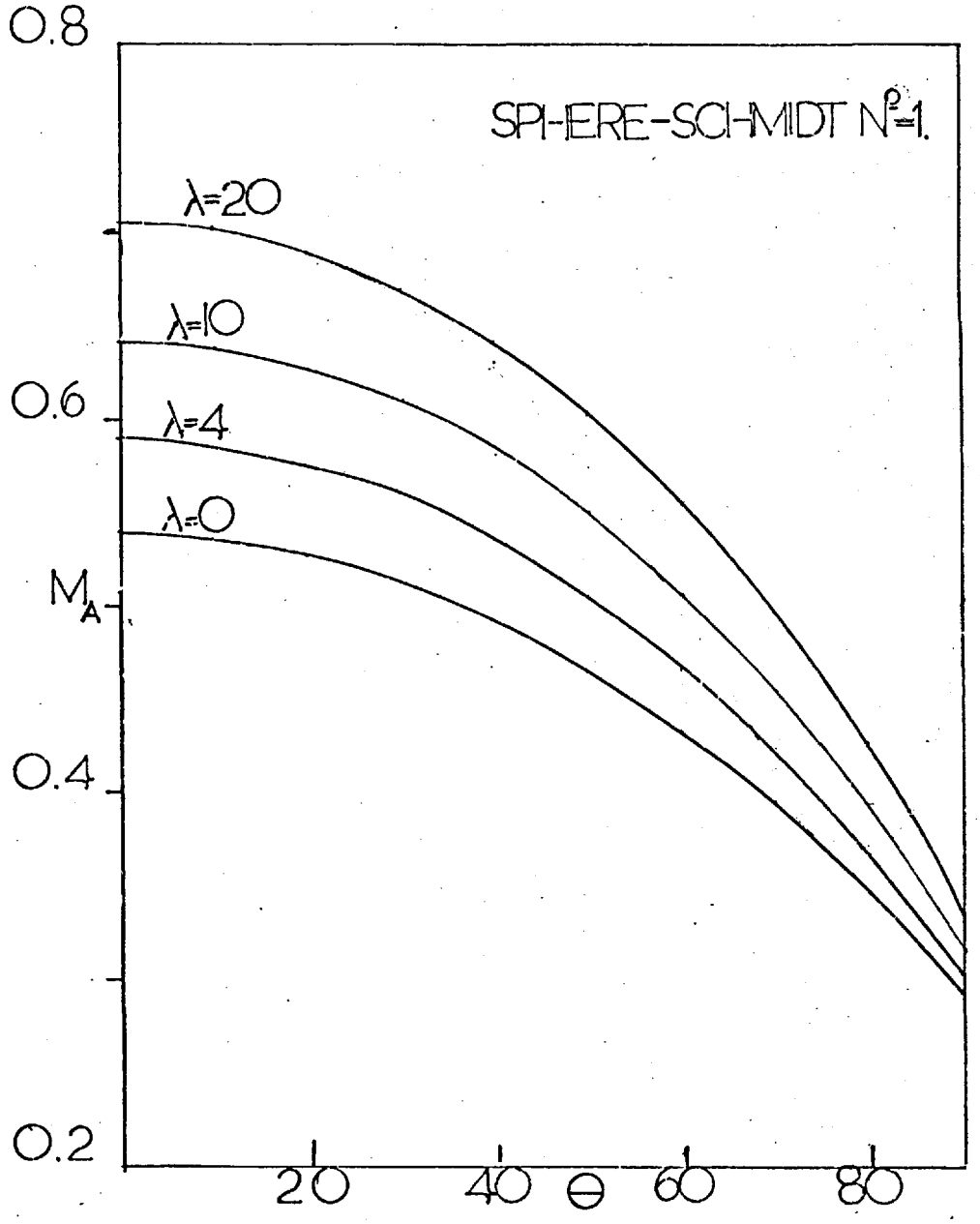



FIG 5.11 EFFECT OF SPIN PARAMETER λ ON $M_A$ FOR THE SPHERE AT SCHMIDT N$^o$ 1.0

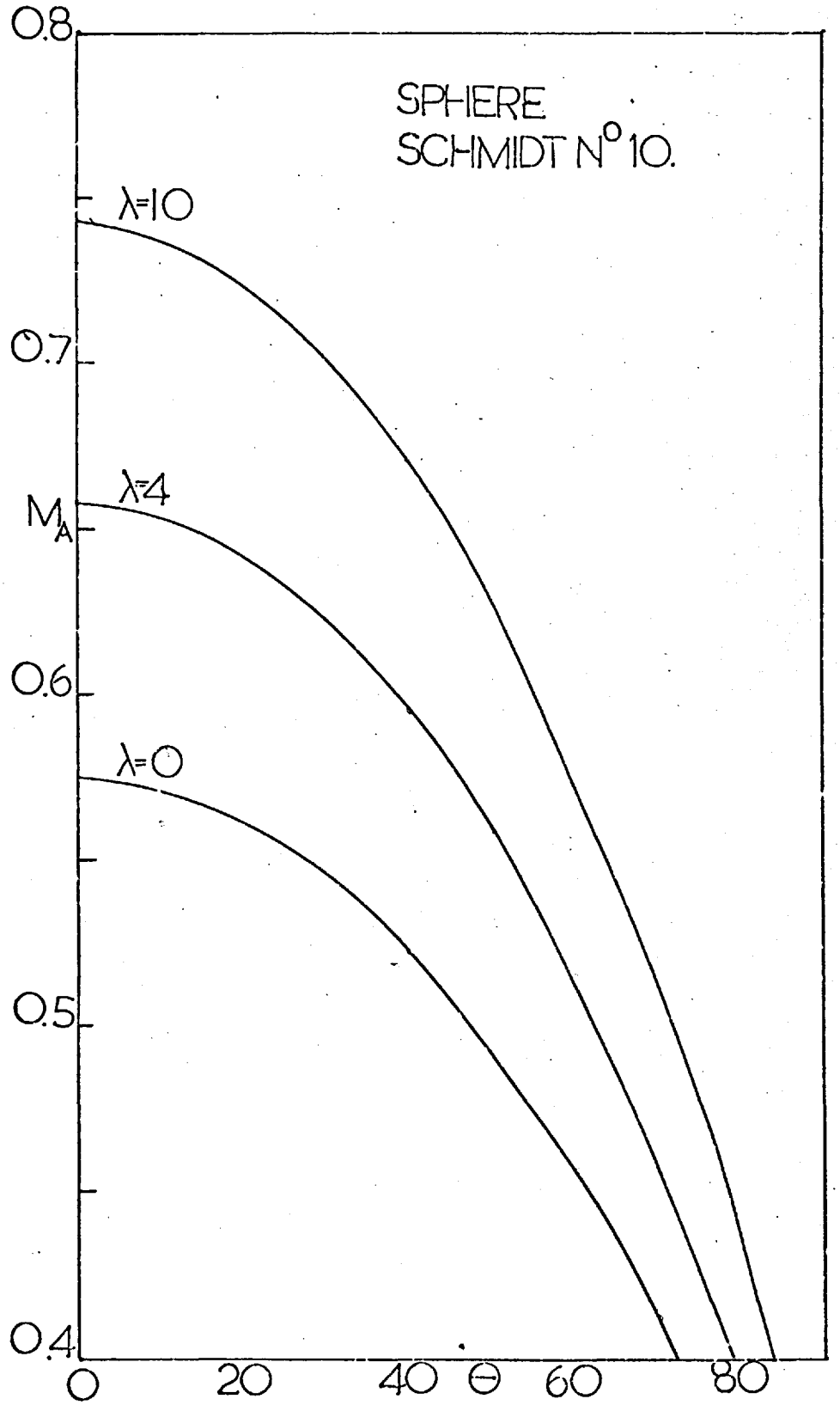



FIG 5.12 EFFECT OF SPIN PARAMETER λ ON $M_A$ FOR THE SPHERE AT SCHMIDT N° 10.

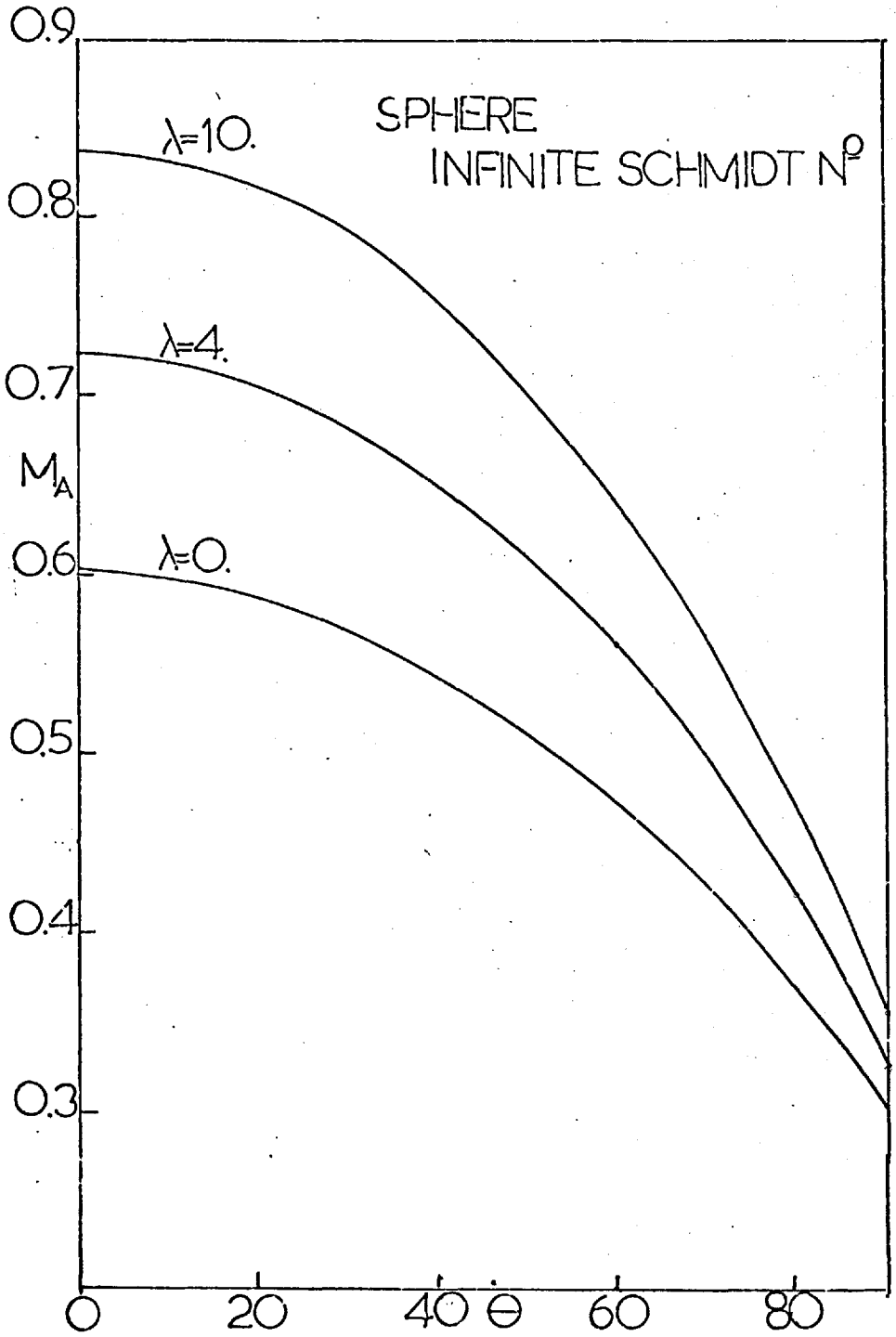



FIG 5.13 EFFECT OF SPIN PARAMETER λ ON $M_A$ FOR INFINITE SCHMIDT NUMBER

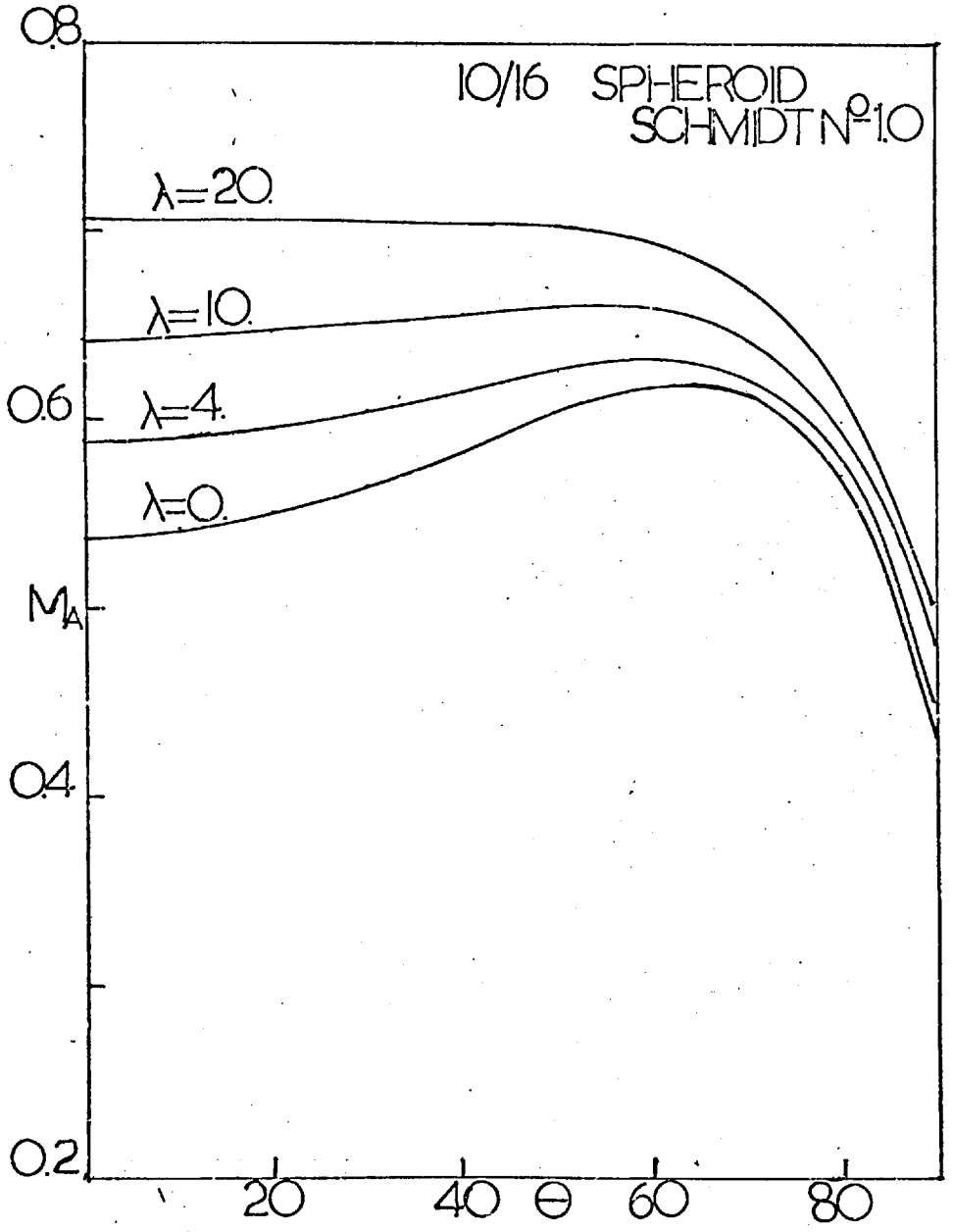



FIG 5.14 EFFECT OF SPIN PARAMER λ ON $M_A$ FOR 10/16 SPHEROID SCHMIDT Nº 1.0

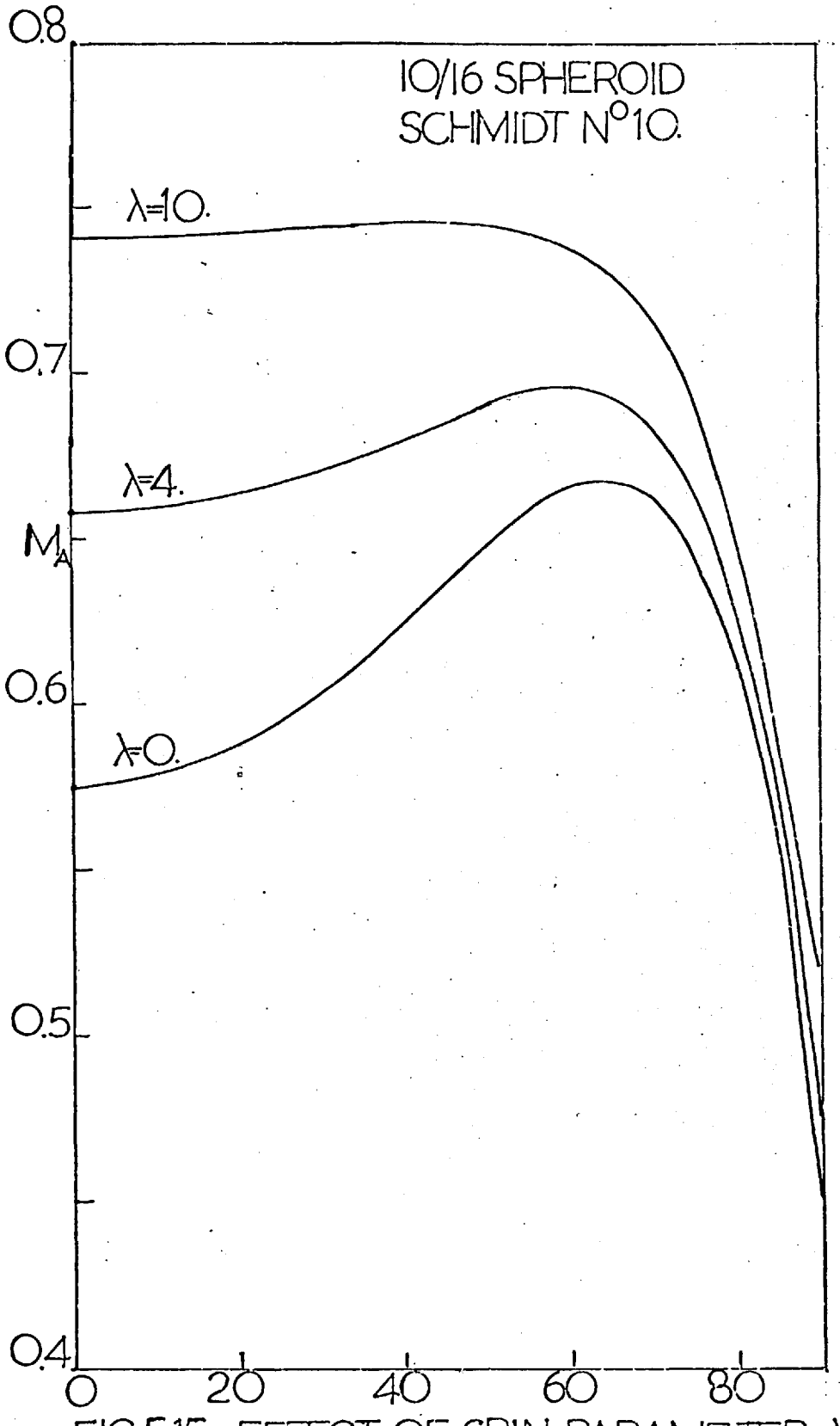



FIG 5.15 EFFECT OF SPIN PARAMETER λ ON $M_A$ FOR 10/16 SPHEROID AT SCHMIDT N° 10.

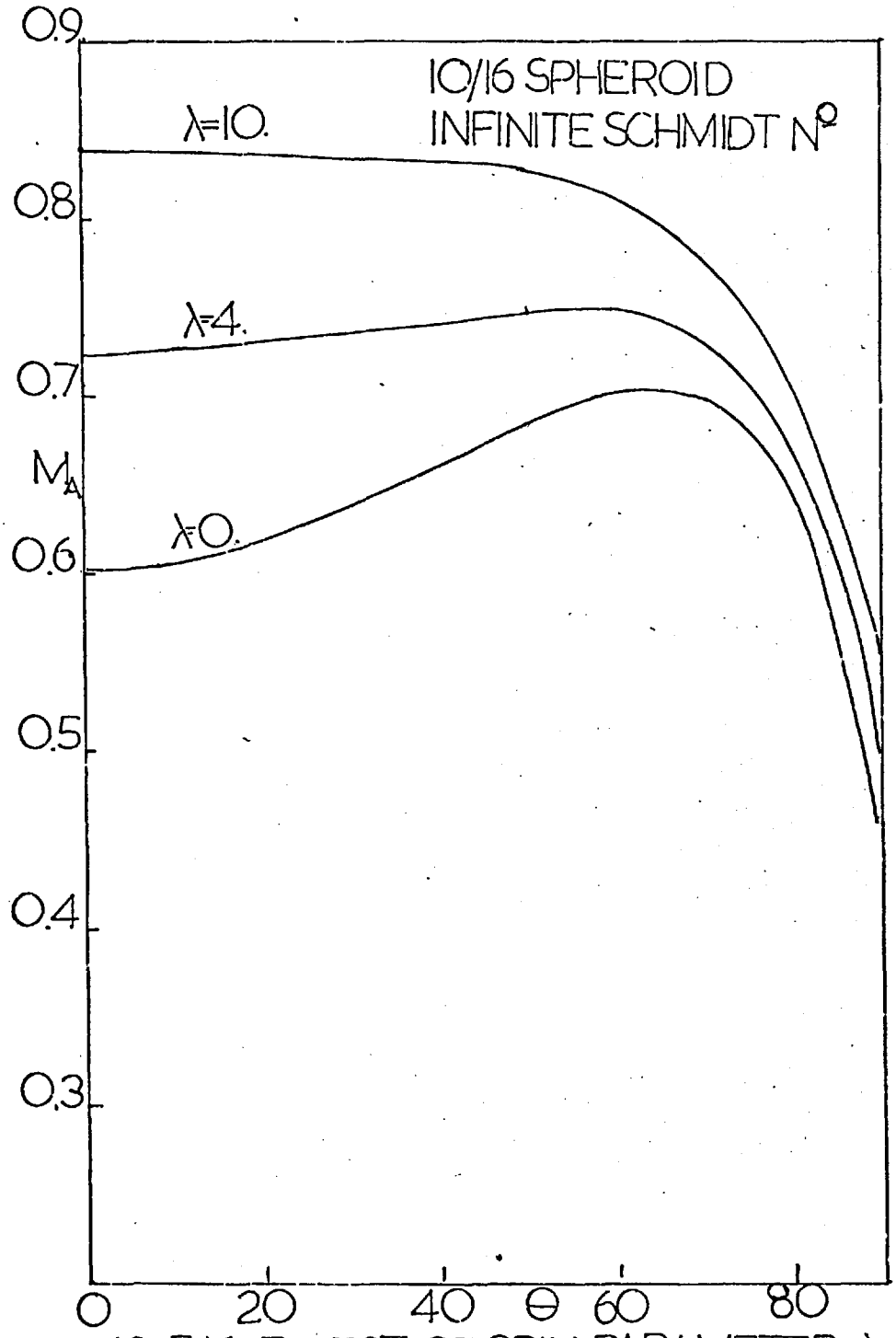



FIG 5.16 EFFECT OF SPIN PARAMETER λ ON $M_A$ FOR 10/16 SPHEROID AT INFINITE SCHMIDT Nº

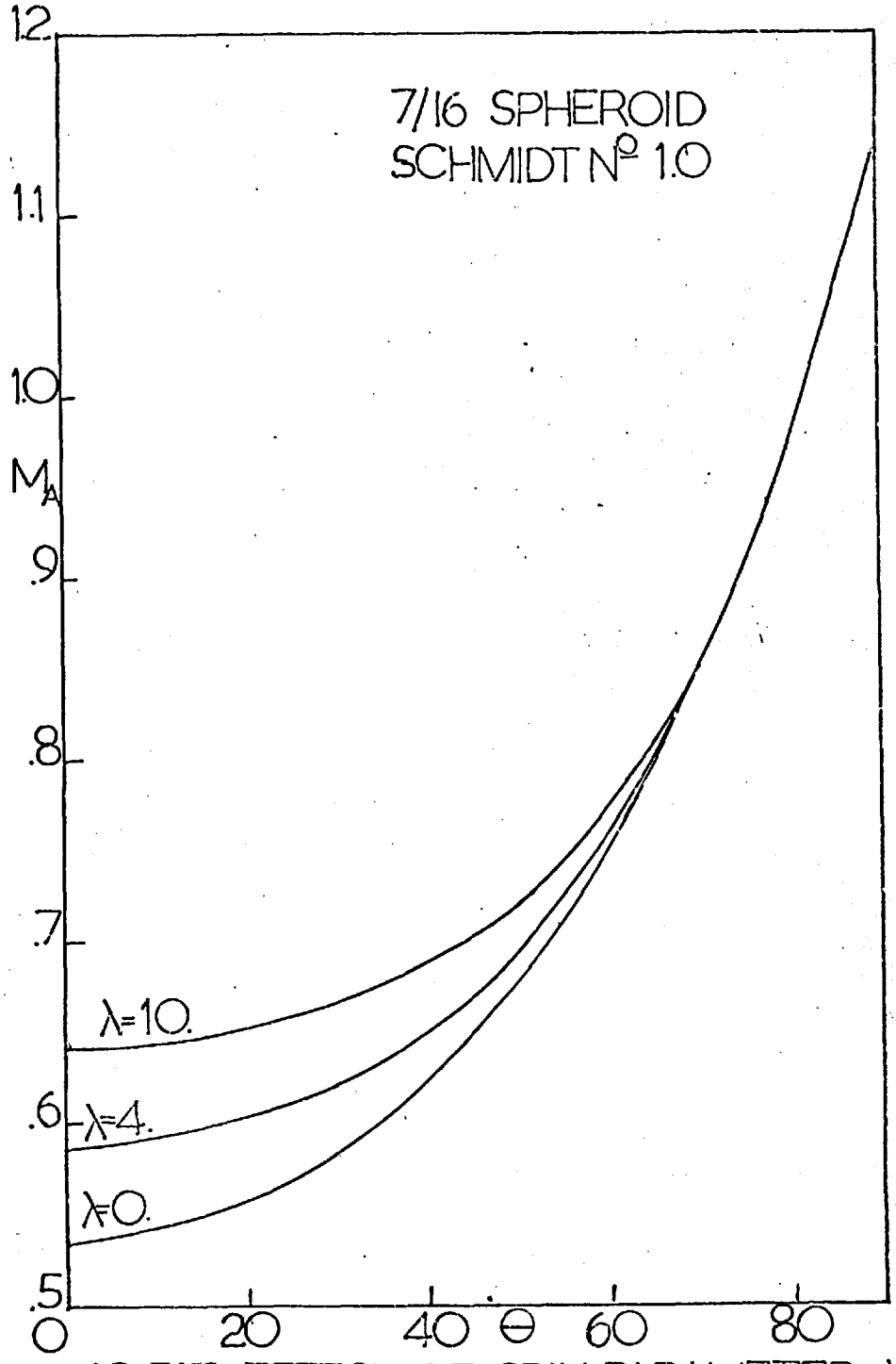



FIG 5.17 EFFECT OF SPIN PARAMETER λ ON $M_A$ --- FOR 7/16 SPHEROID AT SCHMIDT Nº 1.0

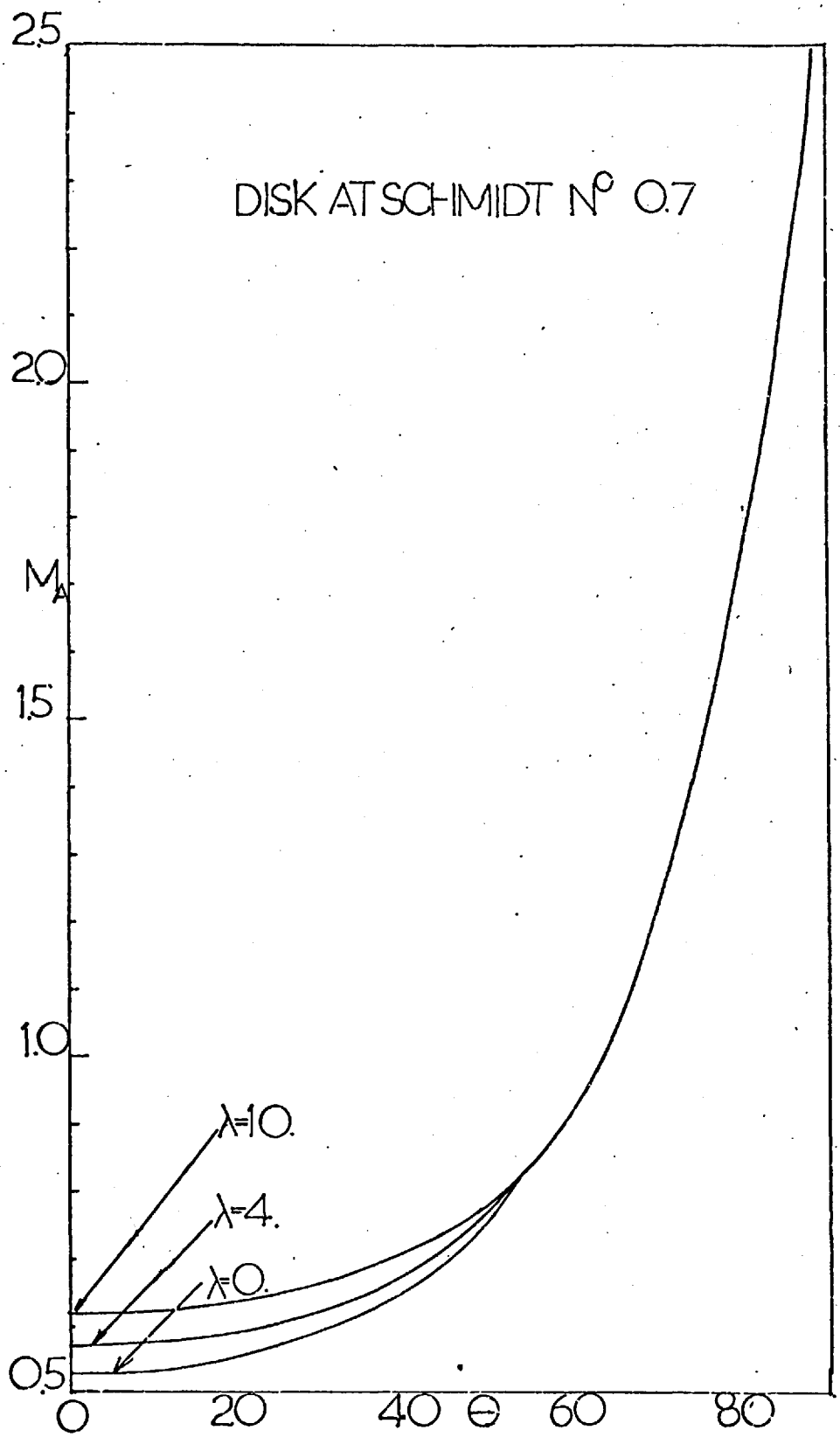



FIG 5.18 EFFECT OF SPIN PARAMETER λ ON $M_A$ FOR DISK AT SCHMIDT N° 0.7

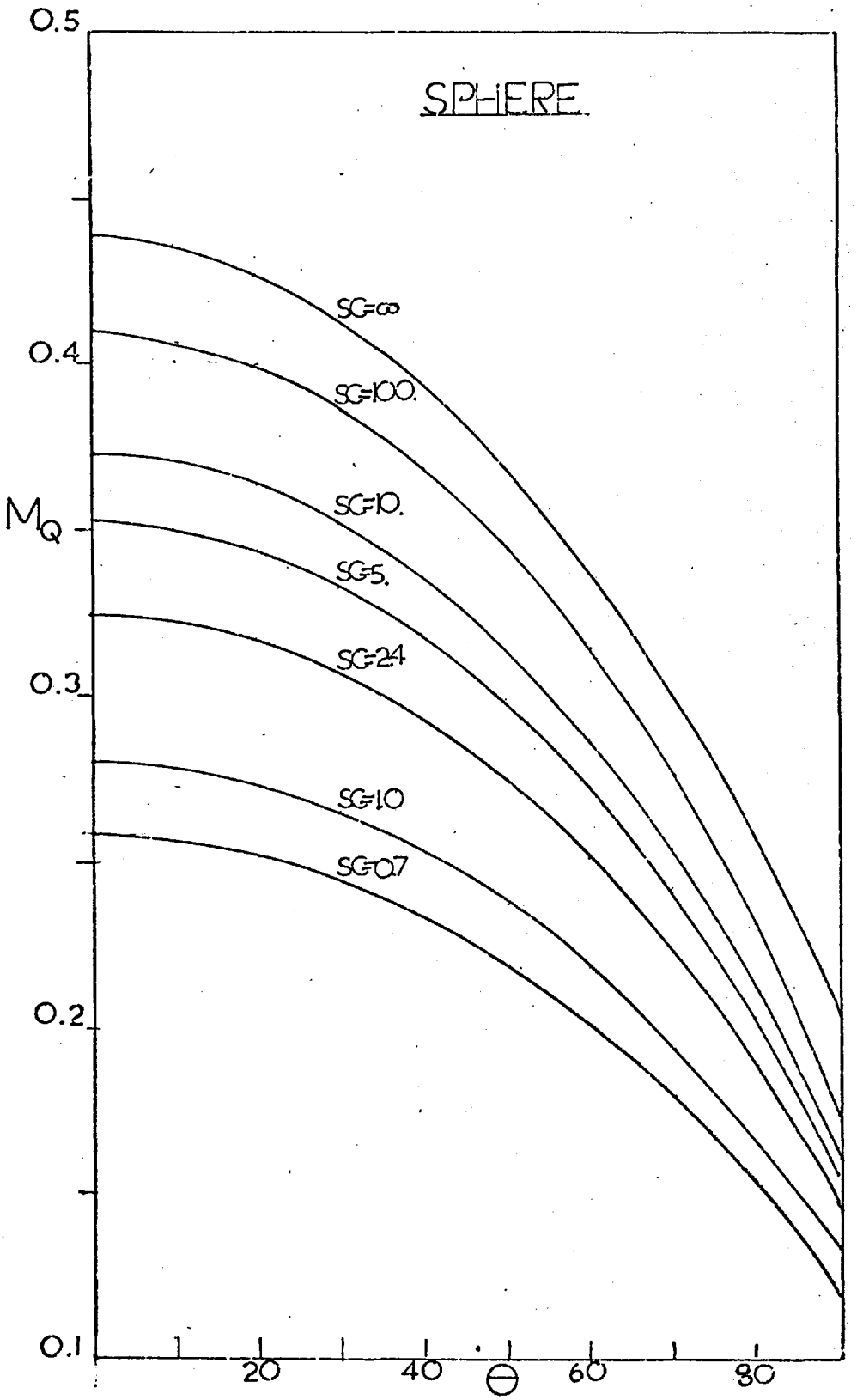



FIG 5.19 PLOTS OF $M_Q$ AGAINST $\theta$ FOR THE SPHERE AT SCHMIDT NUMBERS 0.7 TO ∞

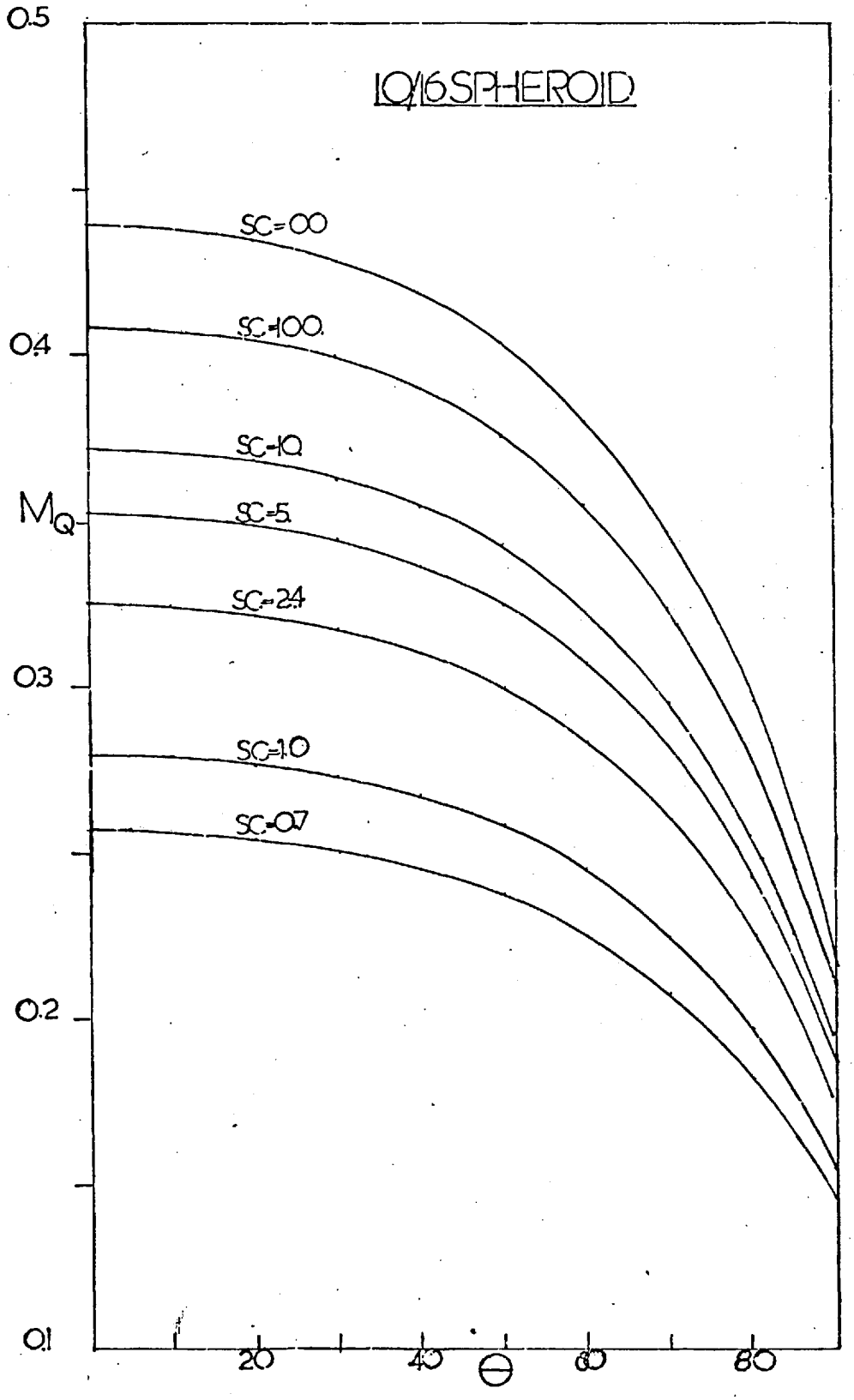
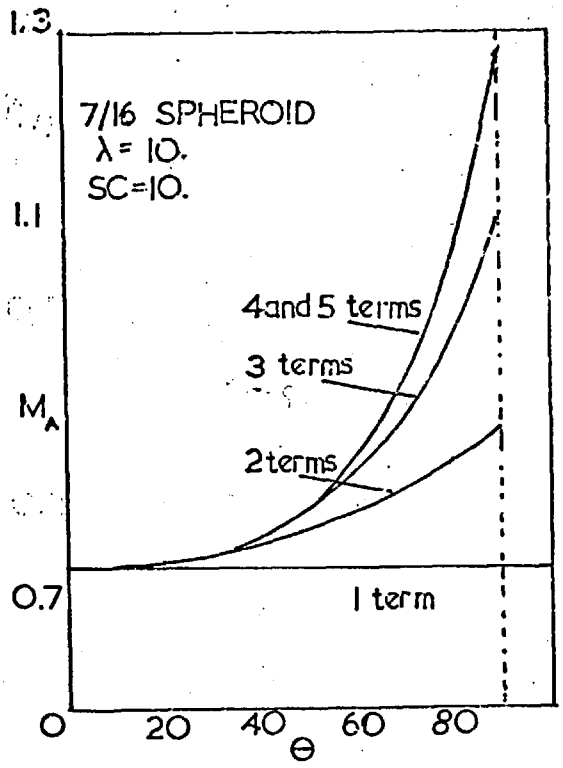
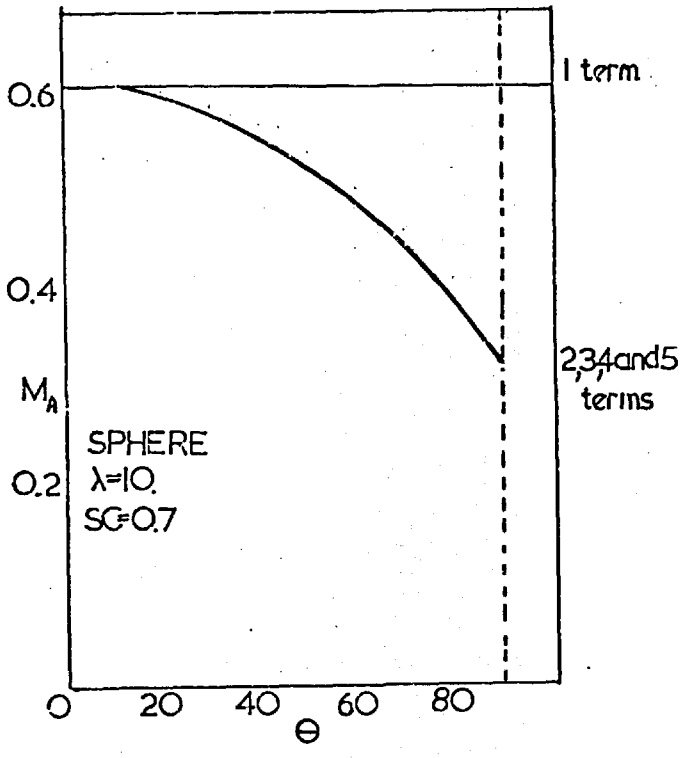
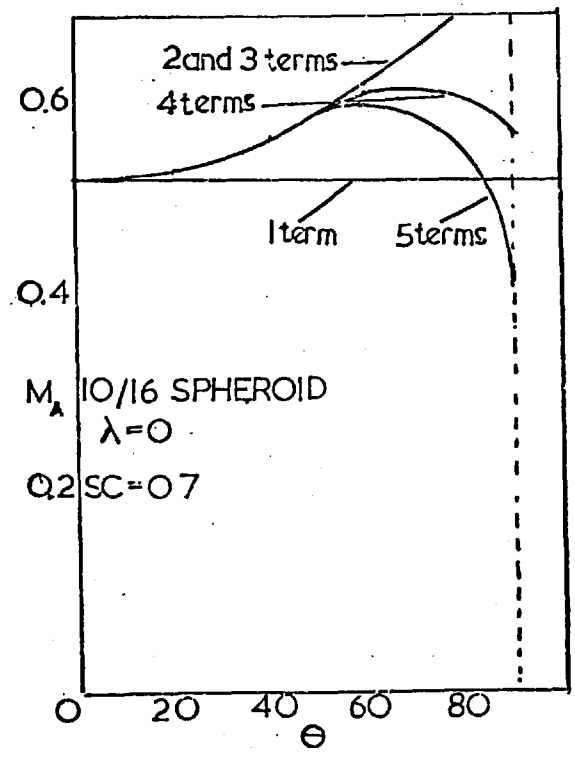



FIG 5.20 PLOTS OF $M_Q$ AGAINST $\theta$ FOR THE 10/16 SPHEROID AT SCHMDT NUMBERS 0.7 TO ∞



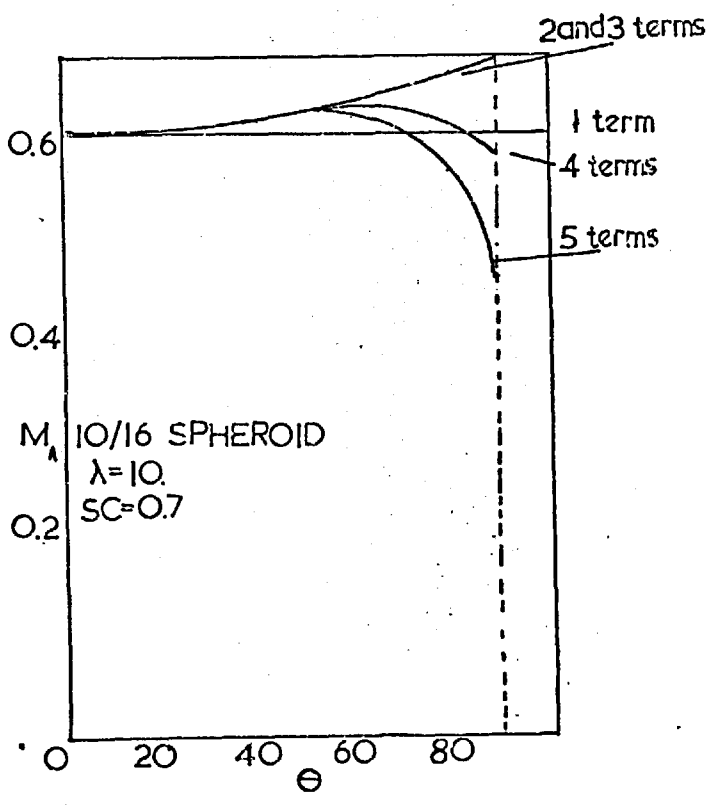




FIG 5.22 EFFECT OF THE NUMBER OF TERMS IN SERIES FOR $M_A$

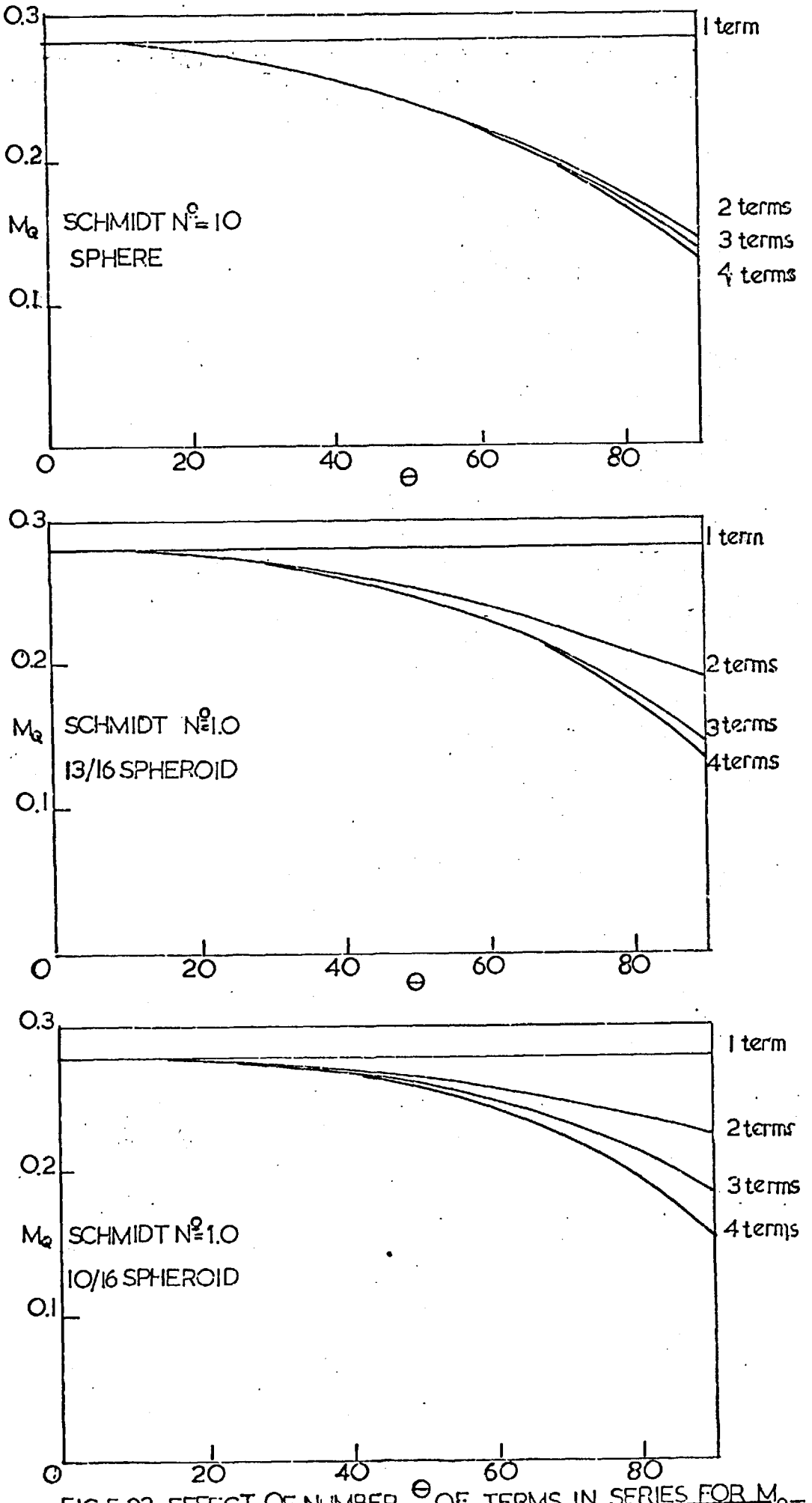
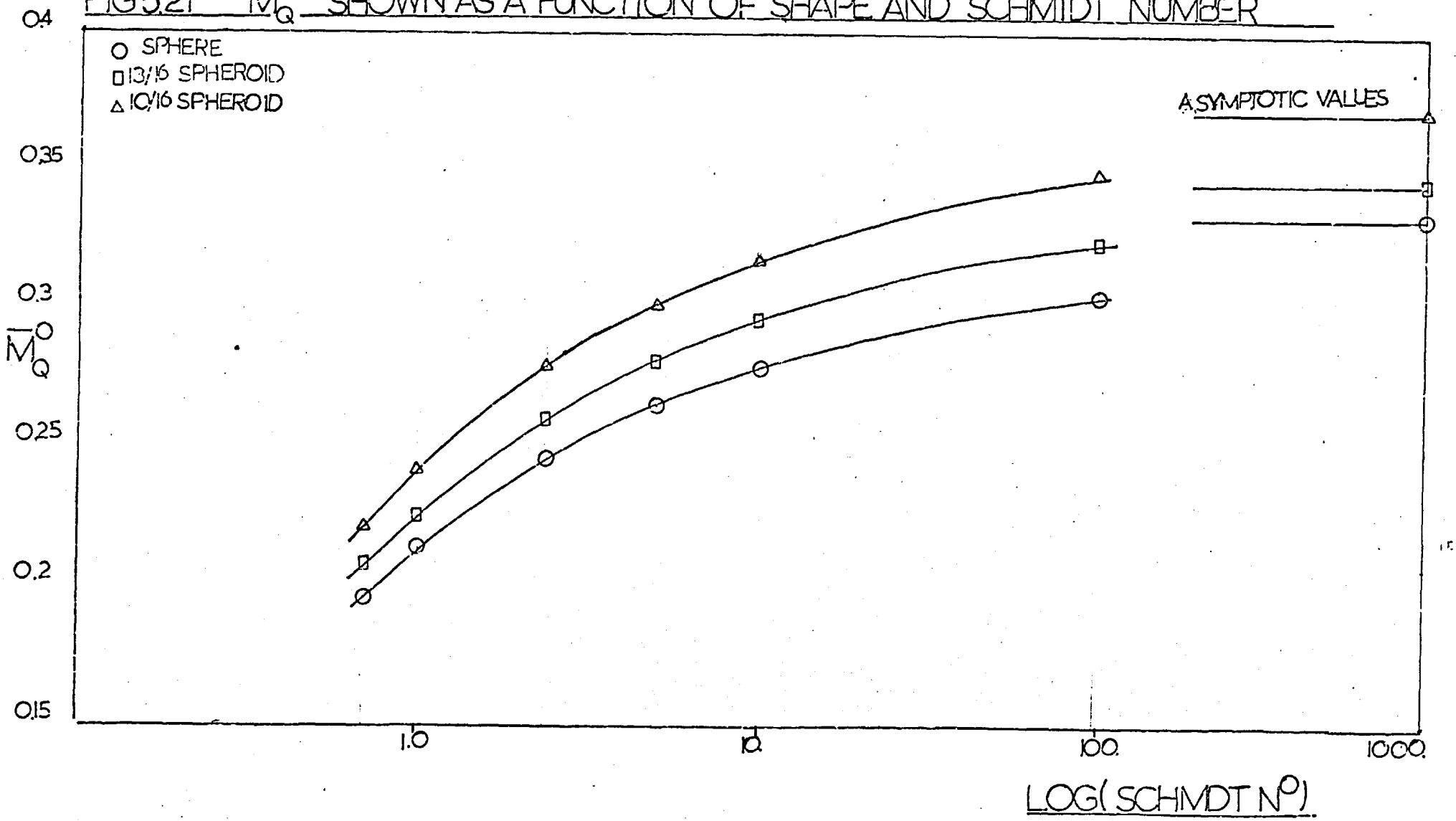



FIG 5.23 EFFECT OF NUMBER OF TERMS IN SERIES FOR $M_Q$

FIG 5.21 $\bar{M}_Q^o$ SHOWN AS A FUNCTION OF SHAPE AND SCHMIDT NUMBER



# CHAPTER VI

## CONCLUSIONS

The results of the present study may be summarised as follows:

1) The boundary layer equations for forced convective heat or mass transfer from a general axisymmetric body rotating in axial flow have been derived in terms of a general orthogonal curvilinear co-ordinate system. By substitution of suitable power series representations for velocity components potential flow, scale factors and temperature or concentration distributions the three boundary layer equations were reduced to three infinite sets of ordinary differential equations. Two of these sets, the hydrodynamic sets were coupled and were solved independently of the third set, i.e. the transfer set. All of the ordinary differential equations except the first hydrodynamic set were found to be linear, the first hydrodynamic set - the stagnation point equations-being non-linear.

2) The solution of the non-linear hydrodynamic stagnation point equations was obtained for spin parameters in the range $0 < \lambda < 10$ by a finite difference technique, for higher spin parameters a quasilinearisation technique was successfully used. For the finite difference technique very accurate guesses of the unknown boundary values $\bar{f}_1''(0)$ and $\bar{g}_1'(0)$ were needed; in the quasilinearisation technique, however, only crude initial guesses were required. It was found that when the finite difference technique was supplied with accurate initial guesses it was capable of yielding more accurate

results than the quasilinearisation technique using the same integration step length. It is to be concluded that the most appropriate method of solution of the stagnation point equations would be to use the quasilinearisation technique to supply accurate initial estimates which would then be used in the finite difference method to obtain even more accurate results.

3) A computer programme was developed to generate and solve the general linear equations of each set of ordinary differential equations for any axisymmetric body, any spin parameter and any Schmidt or Prandtl number. This programme was used to obtain the first five sets of unknown boundary values $\bar{f}''_{2n-1}(0)$, $\bar{g}'_{2n-1}(0)$ and $\mathcal{H}'_{2(n-1)}(0)$ for mass transfer from the sphere, the disk, the 10/16 and the 7/16 oblate spheroids in the spin parameter range $0 < \lambda < 20$ and for Schmidt numbers 0.7, 1.0, 2.4 and 10.0. The boundary values obtained in this study were expected to be accurate to at least five significant figures for spin parameters below ten and to three significant figures for the spin parameter of twenty. The programme utilised the mass transfer boundary values that were obtained to generate point mass transfer values up to the equator of the body where the boundary layer assumptions would break down due to the formation of a wake. The work was also extended to cover the case of rotation at infinite Schmidt numbers.

4) It was found that the effect of rotation on oblate spheroids was to increase the values of the local mass transfer number. It was found that for increasing spin parameter the maximum effect on local mass transfer numbers was at the front stagnation point, the effect decreased to a minimum in the region of the equator. The increase in the values of local mass transfer number for increasing spin parameter

was also found to be a maximum for infinite Schmidt number the effect decreasing with decreasing Schmidt number until at zero Schmidt number the effect was non-existant.

5) A further analysis was presented to cover the case of axisymmetric bodies rotating in a quiescent fluid. Once again a computer programme was developed to generate and solve any number of the infinite sets of ordinary differential equations for any axisymmetric body at any Schmidt number. This programme was used to obtain the first four sets of boundary values for the sphere, 13/16 and 10/16 oblate spheroids in a Schmidt number range of 0.7 to 100. Once again the boundary values obtained in this study were expected to be accurate to at least five significant figures. The programme generated the values of local mass transfer number up to the equator of the body under study. Because the rotation of the body induces a boundary layer on both its halves it was expected that the boundary layer simplifications were capable of predicting local values of mass transfer number all round the body except in a small region - the region of the equator where the boundary layers collide. Consequently on making the assumption that the area of collision was negligible overall values of mass transfer number were obtained by integration of the local values over the total body surface.

6) For the case of a body rotating in a quiescent fluid it was found that the local mass transfer numbers increased with increasing Schmidt number. At the front stagnation the mass transfer number was independent of body shape, however, at all other places around the body it was found that the local value of mass transfer number was higher the more oblate the body. Similarly it was found that overall values of the mass transfer number increased with increasing Schmidt

number and increasing oblateness of the body.

7) It would be hoped that future work would be directed towards obtaining experimental data on local values of mass (or heat) transfer number for bodies rotating in axial flow in order that comparisons could be made with the results of the present analysis. Similarly in the case of the body rotating in a quiescent fluid experimental data is required in order that conditions as to the validity of the boundary layer assumptions may be made.

# APPENDIX A

## NAVIER-STOKES EQUATIONS

Our steady state equations governing mass (or heat) and momentum transfer for an incompressible fluid for which viscous heat dissipation is negligible were shown in Chapter 3 to be

$$(\underline{V}.\nabla)\underline{V} = \frac{-1}{\rho}\nabla P + \nu\nabla^2\underline{V} \tag{A-1}$$

$$\nabla.\underline{V} = 0 \tag{A-2}$$

$$\underline{V}.\nabla X = \alpha_v \nabla^2 X \tag{A-3}$$

We are able to put these equations into a more manageable form by utilising the following relationships $\underline{A}$, $\underline{B}$ and scalar $\phi$ derived by Spiegel (1959) as well as many other authors.

1. $\nabla(\underline{A}.\underline{B}) = (\underline{B}.\nabla)\underline{A} + (\underline{A}.\nabla)\underline{B} + \underline{B}x(\nabla x\underline{A}) + \underline{A}x(\nabla x\underline{B})$

2. $(\nabla.\underline{A}) = \nabla^2\underline{A} + \nabla x(\nabla x\underline{A})$

3. $(\underline{A}.\nabla)\phi = \underline{A}.\nabla\phi$

Equations can thus be transformed to

$$\tfrac{1}{2}\nabla(\underline{V}.\underline{V}) - \underline{V}x(\nabla x\underline{V}) = \frac{-1}{\rho}\nabla P - \nu\nabla x(\nabla x\underline{V}) \tag{A-4}$$

$$\nabla.\underline{V} = 0 \tag{A-5}$$

$$\underline{V}.\nabla X = \alpha_v\nabla^2 X \tag{A-6}$$

Curvilinear Co-ordinates

Defining the curvilinear co-ordinates $(x_1, x_2, x_3)$ with $(\underline{e}_1, \underline{e}_2, \underline{e}_3)$ being their respective unit vectors Spiegel has defined the grad operator $\nabla$ as

4. $$\nabla \equiv \frac{\underline{e}_1}{h_1}\frac{\partial}{\partial x_1} + \frac{\underline{e}_2}{h_2}\frac{\partial}{\partial x_2} + \frac{\underline{e}_3}{h_3}\frac{\partial}{\partial x_3}$$

where $(h_1,h_2,h_3)$ are the scale factors in the directions of unit vectors $(\underline{e}_1,\underline{e}_2,\underline{e}_3)$ respectively. Using this operator Spiegel has shown that the following relationships are true

$$5.\quad \nabla\cdot\underline{A} = \text{div}\,\underline{A} = \frac{1}{h_1h_2h_3}\left[(h_2h_3A_1)_{x_1} + (h_3h_1A_2)_{x_2} + (h_1h_2A_3)_{x_3}\right]$$

$$6.\quad \nabla \times \underline{A} = \text{curl}\,\underline{A} = \frac{1}{h_1h_2h_3}\begin{bmatrix} h_1\underline{e}_1 & h_2\underline{e}_2 & h_3\underline{e}_3 \\ \frac{\partial}{\partial x_1} & \frac{\partial}{\partial x_2} & \frac{\partial}{\partial x_3} \\ h_1A_1 & h_2A_2 & h_3A_3 \end{bmatrix}$$

$$7.\quad \nabla^2\phi = \text{Laplacian}\,\phi = \left[\frac{1}{h_1h_2h_3}\left(\frac{h_2h_3}{h_1}(\phi)_{x_1}\right)_{x_1} + \left(\frac{h_3h_1}{h_2}(\phi)_{x_2}\right)_{x_2} + \left(\frac{h_1h_2}{h_3}(\phi)_{x_3}\right)_{x_3}\right]$$

here vector $\underline{A}$ is defined

$$\underline{A} = A_1\underline{e}_1 + A_2\underline{e}_2 + A_3\underline{e}_3$$

and the convention for partial differentiation is

$$\frac{\partial}{\partial x_i} \equiv (\quad)_{x_i} \qquad \frac{\partial^2}{\partial x_i^2} \equiv (\quad)_{x_i,x_i}$$

Using the above relationships we are able to derive the three dimensional Navier-Stokes equations in their curvilinear co-ordinate form for incompressible flow.

$$\frac{V_1}{h_1}(V_1)_{x_1} + \frac{V_2}{h_1}(V_2)_{x_1} + \frac{V_3}{h_1}(V_3)_{x_1} - \frac{V_2}{h_1h_2}\left\{(V_2h_2)_{x_1} - (V_1h_1)_{x_1}\right\}$$

$$+ \frac{V_3}{h_3h_1}\left\{(V_1h_1)_{x_3} - (V_3h_3)_{x_1}\right\} = -\frac{1}{\rho h_1}\frac{\partial P}{\partial x_1} - \frac{\nu}{h_2h_3}\left[\left(\frac{h_3}{h_1h_2}\left\{(V_2h_2)_{x_1}\right.\right.\right.$$

$$- (V_1 h_1)_{x_2} \Big\} \Big)_{x_2} - \Big(\frac{h_2}{h_3 h_1} \Big\{ (V_1 h_1)_{x_3} - (V_3 h_3)_{x_1} \Big\} \Big)_{x_3} \Big] \qquad \text{(A-7)}$$

$$\frac{V_1}{h_2}(V_1)_{x_2} + \frac{V_2}{h_2}(V_2)_{x_2} + \frac{V_3}{h_2}(V_3)_{x_2} - \frac{V_3}{h_2 h_3} \Big\{ (V_3 h_3)_{x_2} - (V_2 h_2)_{x_3} \Big\}$$

$$+ \frac{V_1}{h_1 h_2} \Big\{ (V_2 h_2)_{x_1} - (V_1 h_1)_{x_2} \Big\} = - \frac{1}{\rho h_2}(P)_{x_2} - \frac{\nu}{h_1 h_3} \Big[ \Big(\frac{h_1}{h_2 h_3}$$

$$\Big\{ (V_3 h_3)_{x_2} - (V_2 h_2)_{x_3} \Big\} \Big)_{x_3} - \Big(\frac{h_3}{h_1 h_2} \Big\{ (V_2 h_2)_{x_1} - (V_1 h_1)_{x_2} \Big\} \Big)_{x_1} \Big] \qquad \text{(A-8)}$$

$$\frac{V_1}{h_3}(V_1)_{x_3} + \frac{V_2}{h_3}(V_2)_{x_3} + \frac{V_3}{h_3}(V_3)_{x_3} - \frac{V_1}{h_3 h_1} \Big\{ (V_1 h_1)_{x_3} - (V_3 h_3)_{x_1} \Big\}$$

$$+ \frac{V_2}{h_2 h_3} \Big\{ (V_3 h_3)_{x_2} - (V_2 h_2)_{x_3} \Big\} = - \frac{1}{\rho h_3}(P)_{x_3} - \frac{\nu}{h_1 h_2} \Big[ \Big(\frac{h_2}{h_3 h_1}$$

$$\Big\{ (V_1 h_1)_{x_3} - (V_3 h_3)_{x_1} \Big\} \Big)_{x_1} - \Big(\frac{h_1}{h_2 h_3} \Big\{ (V_3 h_3)_{x_2} - (V_2 h_2)_{x_3} \Big\} \Big)_{x_2} \Big] \qquad \text{(A-9)}$$

The <u>continuity equation</u> is the divergence of the velocity vector and is given by

$$\frac{1}{h_1 h_2 h_3} \Big[ (h_2 h_3 V_1)_{x_1} + (h_3 h_1 V_2)_{x_2} + (h_1 h_2 V_3)_{x_3} \Big] = 0 \qquad \text{(A-10)}$$

The <u>heat or mass transport equation</u> is

$$\frac{V_1}{h_1}(X)_{x_1} + \frac{V_2}{h_2}(X)_{x_2} + \frac{V_3}{h_3}(X)_{x_3} = \frac{\alpha_v}{h_1 h_2 h_3} \Big[ \Big(\frac{h_2 h_3}{h_1}(X)_{x_1}\Big)_{x_1} + \Big(\frac{h_3 h_1}{h_2}(X)_{x_2}\Big)_{x_2}$$

$$+ \Big(\frac{h_1 h_2}{h_3}(X)_{x_3}\Big)_{x_3} \Big] \qquad \text{(A-11)}$$

# APPENDIX B

## METHOD OF SOLUTION OF HYDRODYNAMIC STAGNATION POINT EQUATIONS UTILISING FINITE DIFFERENCE TECHNIQUE AND TAYLOR EXPANSION

This method was employed by Hoskin (1955).

The basic equations to be solved are

$$\left.\begin{aligned} YG(1) &= Y(2) \\ YG(2) &= Y(3) \\ YG(3) &= Y(2)^2 - 2Y(1)\,Y(3) - \lambda\, Y(4)^2 - 1 \\ YG(4) &= Y(5) \\ YG(5) &= 2Y(4)\,Y(2) - 2Y(5)\,Y(1) \end{aligned}\right\} \qquad \text{(B-1)}$$

where $YG(\ ) \equiv Y'(\ )$

with the pertinent boundary values

$$\begin{aligned} &\text{at } \eta = 0 && Y(1) = Y(2) = 0 && Y(4) = 1 \\ &\text{as } \eta \to \infty && Y(2) \to 1 && Y(4) \to 0 \end{aligned} \qquad \text{(B-2)}$$

it being necessary for us to determine Y(3) and Y(5) at $\eta = 0$.

Let us define the actual values of Y(3) and Y(5) at $\eta = 0$ as $\alpha$ and $\beta$ respectively

i.e.
$$\left.\begin{aligned} Y(3) &= \alpha \\ Y(5) &= \beta \end{aligned}\right\} \quad \text{at } \eta = 0 \qquad \text{(B-3)}$$

We make a guess at $\alpha$ and $\beta$, i.e. $\alpha o$ and $\beta o$ respectively, using $\alpha o$ and $\beta o$ as our boundary values we integrate (B-1) numerically across the boundary layer (i.e. with respect to $\eta$) and obtain the values of Y(2) and Y(4) at 'infinity', here 'infinity' is O(6) the value of $\eta$ where values (Y1),.....Y(5) should have reached their asymptotes.

Let these values at 'infinity' be defined by

$$Y(2) = Y2(\alpha o, \beta o, \infty)$$
$$Y(4) = Y4(\alpha o, \beta o, \infty) \qquad \text{(B-4)}$$

Now since the values of Y(2) and Y(4) at infinity are functions of $\alpha$ and $\beta$ we can expand the true values of Y(2) and Y(4) at infinity, i.e. $Y2(\alpha,\beta,\infty)$ and $Y4(\alpha,\beta,\infty)$ in a Taylor series as follows

$$Y2(\alpha,\beta,\infty) = Y2(\alpha o,\beta o,\infty) + (\alpha-\alpha o)\frac{\partial}{\partial\alpha} Y2(\alpha o,\beta o,\infty) + (\beta-\beta o)\frac{\partial}{\partial\beta} Y2(\alpha o,\beta o,\infty) + \frac{1}{2!}\left[(\alpha-\alpha o)^2 \frac{\partial^2 Y2(\alpha o,\beta o,\infty)}{\partial\alpha^2} + 2(\alpha-\alpha o)(\beta-\beta o)\frac{\partial^2 Y2(\alpha o,\beta o,\infty)}{\partial\alpha\partial\beta} + (\beta-\beta o)^2 \frac{\partial^2 Y2(\alpha o,\beta o,\infty)}{\partial\beta^2}\right] + \cdots \qquad \text{(B-5)}$$

$$Y4(\alpha,\beta,\infty) = Y4(\alpha o,\beta o,\infty) + (\alpha-\alpha o)\frac{\partial Y4}{\partial\alpha}(\alpha o,\beta o,\infty) + (\beta-\beta o)\frac{\partial Y4}{\partial\beta}(\alpha o,\beta o,\infty) + \frac{1}{2!}\left[(\alpha-\alpha o)^2\frac{\partial Y4}{\partial\alpha^2}(\alpha o,\beta o,\infty) + 2(\alpha-\alpha o)(\beta-\beta o)\frac{\partial^2 Y4}{\partial\alpha\partial\beta}(\alpha o,\beta o,\infty) + (\beta-\beta o)^2 \frac{\partial^2 Y4}{\partial\beta^2}(\alpha o,\beta o,\infty)\right] + \cdots \qquad \text{(B-6)}$$

Further approximations of $\alpha$ and $\beta$ are made with initial values of Y(3) and Y(5) at $\eta = 0$ being $(\alpha o + \Delta\alpha o, \beta o)$ and $(\alpha o, \beta o + \Delta\beta o)$ once again these initial values are used to integrate equations (B-1) to'infinity', we obtain then the values

$$Y2(\alpha o + \Delta\alpha o, \beta o, \infty);\ Y4(\alpha o, \beta o + \Delta\beta o, \infty)$$
$$Y2(\alpha o, \beta o + \Delta\beta o, \infty);\ Y4(\alpha o + \Delta\alpha o, \beta o, \infty)$$

for Y(2) and Y(4) where $\Delta\alpha o$ and $\Delta\beta o$ are movements of $\alpha o$ and $\beta o$ respectively.

If we take only the linear terms in (B-5) and (B-6) we can

represent the partial differential forms infinite difference terms as follows

$$\left.\begin{aligned}
\frac{\partial Y2}{\partial \alpha}(\alpha o,\beta o,\infty) &= \frac{Y2(\alpha o + \Delta\alpha o,\beta o,\infty) - Y2(\alpha o,\beta o,\infty)}{\Delta\alpha o} \\
\frac{\partial Y2}{\partial \beta}(\alpha o,\beta o,\infty) &= \frac{Y2(\alpha o,\beta o + \Delta\beta o,\infty) - Y2(\alpha o,\beta o,\infty)}{\Delta\beta o} \\
\frac{\partial Y4}{\partial \alpha}(\alpha o,\beta o,\infty) &= \frac{Y4(\alpha o + \Delta\alpha o,\beta o,\infty) - Y4(\alpha o,\beta o,\infty)}{\Delta\alpha o} \\
\frac{\partial Y4}{\partial \beta}(\alpha o,\beta o,\infty) &= \frac{Y4(\alpha o,\beta o + \Delta\beta o,\infty) - Y4(\alpha o,\beta o,\infty)}{\Delta\beta o}
\end{aligned}\right\} \quad \text{(B-7)}$$

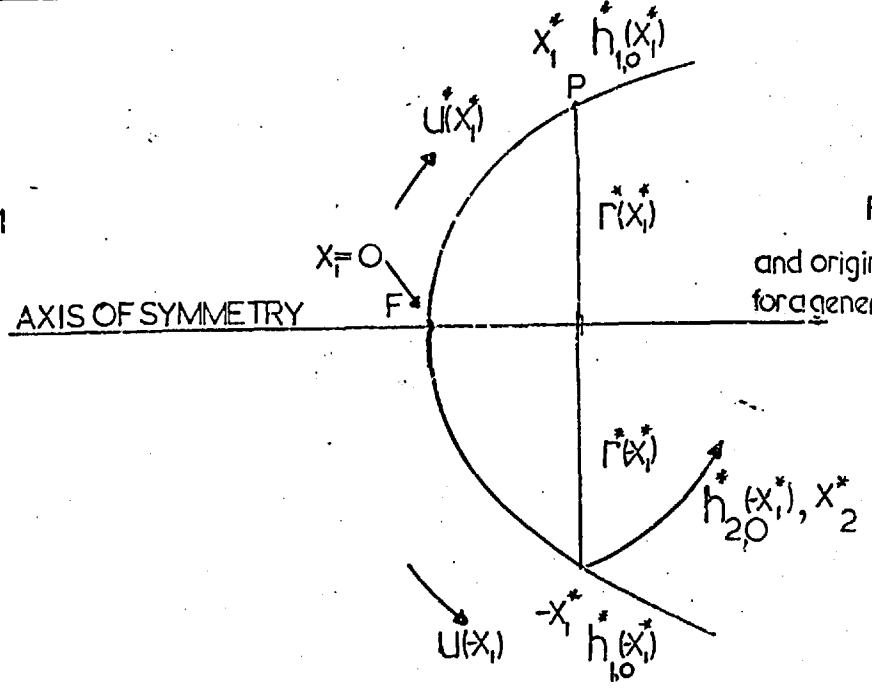
$$\left.\begin{aligned}
\text{Now } Y2(\alpha,\beta,\infty) &= 1 \\
\text{and } Y4(\alpha,\beta,\infty) &= 0
\end{aligned}\right\} \quad \text{(B-8)}$$

and because all other values in equations (B-5) and (B-6) are known we can find the approximate values of $\alpha$ and $\beta$. For the method to work these determined values of $\alpha$ and $\beta$ must be closer to the real $\alpha$ and $\beta$ than $\alpha o$ and $\beta o$ otherwise the method diverges.

A more precise method which would give better convergence would be to keep all terms in equations (B-5) and (B-6) not just the linear ones.

# APPENDIX C
## DEFINITION OF CO-ORDINATE SYSTEM

FIG.1




F - Front stagnation point and origin of co-ordinate system for a general axisymmetric body.

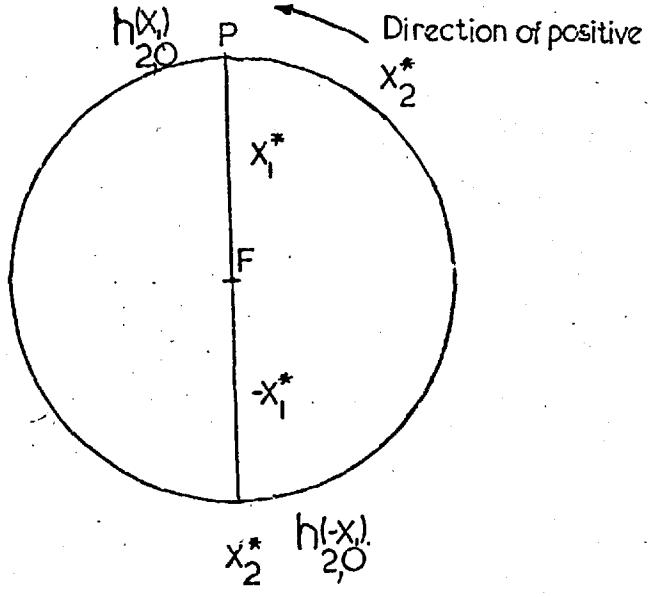
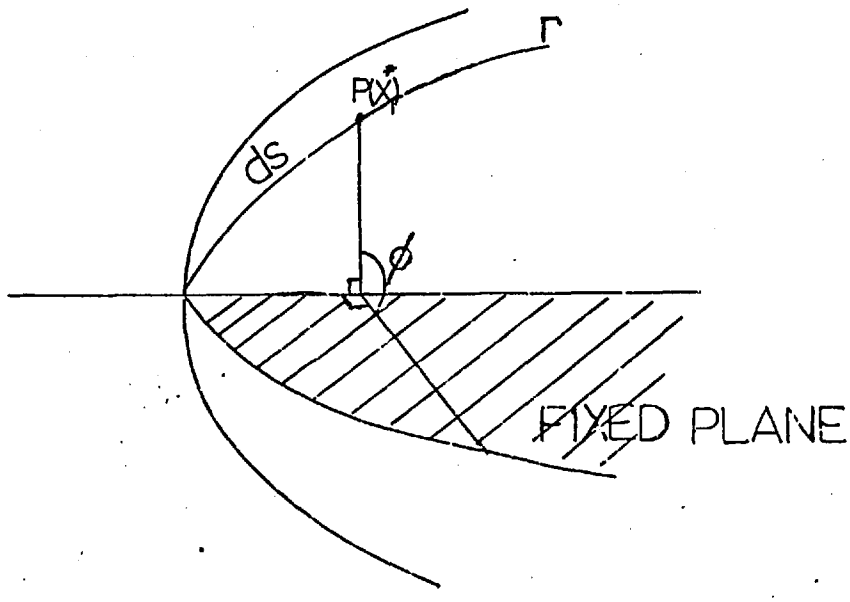



FIG. 2



# APPENDIX D

## COMPUTER PROGRAMMES

Programme 1 is the programme used to determine the unknown hydrodynamic boundary values $\bar{f}_1''(0)$ and $\bar{g}_1'(0)$ by the quasilinearisation technique. Five initial estimates AVPA1, AVPA2,..., AVPA5 have to be supplied in the main programme, these are the guesses for the average values of Y(1), Y(2),..., Y(5) respectively (i.e. $\bar{f}_1$, $\bar{f}_1'$, $\bar{f}_1''$, $\bar{g}_1$, $\bar{g}_1'$) over the boundary layer. The values used as shown were found to be accurate enough to obtain results over the spin parameter range $0 \leqslant \lambda \leqslant 100$ (see Chapter 4). The main programme calls the subroutine METHOD which in turn calls the subroutine RKINT, the general subroutine for the Runge-Kutta integration procedure used in all programmes. RKINT in turn calls the subroutine YGRD1, which contains the linearised forms of the non-linear stagnation point equations, and subroutine YGRD2 which contains the homogeneous equivalents of these linearised equations. In subroutines YGRD1 and YGRD2 the variables Y(1), Y(2),...,Y(5) denote values at the K+1'th iteration whilst YK(1), YK(2),..., YK(5) denote the values of Y(1), Y(2),..., Y(5) at the previous or K'th iteration. The iteration procedure stops when two successive estimates of the boundary values are within $1.0 \times 10^{-6}$ of each other, the programme then prints out the values of all the functions $\bar{f}_1$, $\bar{f}_1'$, $\bar{f}_1''$, $\bar{g}_1$, $\bar{g}_1'$ as functions of $\eta$ across the hydrodynamic boundary layer. The particular programme shown allows a minimum integration step length in $\eta$ of 0.01. In this programme XMAX is the value of 'effective' infinity for $\eta$

i.e. $\eta_\infty = 6$

H is the integration step length in $\eta$ for the Runge-Kutta integration procedure.

ERMINA is the difference in two successively obtained values of $\bar{f}_1''(0)$ for the procedure to finish.

ERMINB is the difference in two successively obtained values of $\bar{g}_1'(0)$ for the procedure to finish.

Programme 2 is the programme to solve the general linear equation or n'th equation for the case of a body rotating in axial flow. The flow diagram for this programme is shown in 4.5.3. The particular programme shown is typical of the programmes used in the study, the two boundary values $\bar{f}_1''(0)$ and $\bar{g}_1'(0)$ (here defined as ALPHA(1) and BETA(1) are supplied to obtain point mass transfer number for a rotating sphere (ER=1) at a spin parameter of 20 and a Schmidt number (here denoted PRNDTL) of 0.7. In this programme the main subroutine calls the subroutines COEFFS and METHOD. Subroutine COEFFS supplies the coefficients in the power series expansions for the potential flow and scale factors for the oblate spheroid with the ratio of minor to major axis of ER. Subroutine METHOD calls the subroutine RKINT which in turn calls the subroutine YGRD where the general equations are set out in the form given in equations (4-57) and (4-58). Subroutine PROCES is the subroutine which uses the principle of superposition as described in 4.3 and 4.4 to obtain better estimates of the unknown boundary values.

Programme 3 is the programme to solve the general linear equation or n'th equation for the case of a body rotating in a quiescent fluid. Once again a typical example of the use of the programme is shown. Four values of $F'_{2n-1}(0)$, $G'_{2n-1}(0)$ and $J'_{2(n-1)}(0)$ (i.e., ALPHA(N),

BETA(N) and GAMMA(N)) N=1,4 have been supplied to the programme in order that the fifth set ALPHA(5), BETA(5) and GAMMA(5) may be determined for the sphere (ER=1) at a Schmidt number of 0.7.

Programme 3 is a modification of Programme 2 (see 4.5.3). The major modification being in the subroutine YGRD which generates the n'th equations as set out in (4-71).

# PROGRAMME 1



```
$JOB  10013074    .T.G.SANDERS IBJOB    3.0   3000
$*    NAME CARD
$EXECUTE        IBJOB
$IBJOB
$IBFTC MAIN
      COMMON PE1(700),PE2(700),PE3(700),PE4(700),PE5(700)
      COMMON AVPA1,AVPA2,AVPA3,AVPA4,AVPA5,PA1(700),PA2(700),PA3(700),
     1PA4(700),PA5(700),PB1(700),PB2(700),PB3(700),PB4(700),PB5(700),
     2PC1(700),PC2(700),PC3(700),PC4(700),PC5(700),PD1(700),PD2(700),
     3PD3(700),PD4(700),PD5(700),YK(5),PRNDTL,ERMINA,ERMINB
      COMMON CONST1(20),CONST2(20)
      COMMON SPIN
C
C
C
C*************************************************************************
C       QUASI-LINEARISATION TECHNIQUE
C*************************************************************************
C
C
C
      AVPA1=3.
      AVPA2=.5
      AVPA3=.3
      AVPA4=.3
      AVPA5=-.5
      SPIN=20.
      ERMINB=1.E-6
      ERMINA=1.E-6
      CALL METHOD
      STOP
      END
```

```
$IBFTC ARKNT
      SUBROUTINE RKINT(X,H,N,Y,YG,YH,YD,YGRD)
      DIMENSION Y(N),YG(N),YH(N),YD(N)
      DO 1J=1,N
    1 YD(J) = Y(J)
      CALL YGRD(X,N,Y,YG)
      DO2 J=1,N
      YG(J)=YG(J)*H
    2 YH(J)=YG(J)
      X=X 0.5*H
      DO4I=1,2
      DO3J=1,N
    3 Y(J)=YD(J)+.5*YG(J)
      CALL YGRD(X,N,Y,YG)
      DO4J=1,N
      YG(J)=YG(J)*H
    4 YH(J)=YH(J)+2.*YG(J)
      X=X 0.5*H
      DO5J=1,N
    5 Y(J)=YD(J)+YG(J)
      CALL YGRD(X,N,Y,YG)
      DO6J=1,N
      YH(J)=(YH(J)+H*YG(J))/6.
      YD(J)=YD(J)+YH(J)
    6 Y(J)=YD(J)
      RETURN
      END
```

```
$IBFTC AMETH
      SUBROUTINE METHOD
      DIMENSION Y(5),YG(5),YH(5),YD(5)
      COMMON PE1(700),PE2(700),PE3(700),PE4(700),PE5(700)
      COMMON AVPA1,AVPA2,AVPA3,AVPA4,AVPA5,PA1(700),PA2(700),PA3(700),
     1PA4(700),PA5(700),PB1(700),PB2(700),PB3(700),PB4(700),PB5(700),
     2PC1(700),PC2(700),PC3(700),PC4(700),PC5(700),PD1(700),PD2(700),
     3PD3(700),PD4(700),PD5(700),YK(5),PRNDTL,ERMINA,ERMINB
      COMMON CONST1(20),CONST2(20)
      COMMON SPIN
      EXTERNAL YGRD1,YGRD2
      N=5
      H=0.025
      XMAX=6.
      MMAX=((XMAX+1.E-5)/H)+1.00001
      NC=1
      GO TO 2
    1 NC=NC+1
      GO TO 4
    2 PA1(1)=0.
      PA2(1)=0.
      PA3(1)=0.
      PA4(1)=1.
      PA5(1)=0.
      DO 3 M=2,MMAX
      PA1(M)=AVPA1
      PA2(M)=AVPA2
      PA3(M)=AVPA3
      PA4(M)=AVPA4
    3 PA5(M)=AVPA5
      GO TO 6
    4 DO 5 M=1,MMAX
      PA1(M)=PE1(M)
      PA2(M)=PE2(M)
      PA3(M)=PE3(M)
      PA4(M)=PE4(M)
    5 PA5(M)=PE5(M)
    6 M=1
      Y(1)=0.
      Y(2)=0.
      Y(3)=0.
      Y(4)=1.
      Y(5)=0.
      X=0.
    7 YK(1)=PA1(M)
      YK(2)=PA2(M)
      YK(3)=PA3(M)
      YK(4)=PA4(M)
      YK(5)=PA5(M)
      CALL RKINT(X,H,N,Y,YG,YH,YD,YGRD1)
      M=M+1
      PB1(M)=Y(1)
      PB2(M)=Y(2)
      PB3(M)=Y(3)
      PB4(M)=Y(4)
      PB5(M)=Y(5)
      IF(ABS(X-XMAX).GT.1.E-5) GO TO 7
      PY2INF=Y(2)
      PY4INF=Y(4)
```

```
    9 M1=1
      Y(1)=0.
      Y(2)=0.
      Y(3)=1.
      Y(4)=0.
      Y(5)=0.
      X=0.
   10 YK(1)=PA1(M1)
      YK(2)=PA2(M1)
      YK(3)=PA3(M1)
      YK(4)=PA4(M1)
      YK(5)=PA5(M1)
      CALL RKINT (X,H,N,Y,YG,YH,YD,YGRD2)
      M1=M1+1
      PC1(M1)=Y(1)
      PC2(M1)=Y(2)
      PC3(M1)=Y(3)
      PC4(M1)=Y(4)
      PC5(M1)=Y(5)
      IF(ABS(X-XMAX).GT.1.E-5) GO TO 10
      H1Y2IN=Y(2)
      H1Y4IN=Y(4)
   12 M2=1
      Y(1)=0.
      Y(2)=0.
      Y(3)=0.
      Y(4)=0.
      Y(5)=1.
      X=0.
   13 YK(1)=PA1(M2)
      YK(2)=PA2(M2)
      YK(3)=PA3(M2)
      YK(4)=PA4(M2)
      YK(5)=PA5(M2)
      CALL RKINT(X,H,N,Y,YG,YH,YD,YGRD2)
      M2=M2+1
      PD1(M2)=Y(1)
      PD2(M2)=Y(2)
      PD3(M2)=Y(3)
      PD4(M2)=Y(4)
      PD5(M2)=Y(5)
      IF(ABS(X-XMAX).GT.1.E-5) GO TO 13
      H2Y2IN=Y(2)
      H2Y4IN=Y(4)
      CONST1(NC)=(H2Y4IN*(1.-PY2INF)+PY4INF*H2Y2IN)/(H1Y2IN*H2Y4IN
     1-H1Y4IN*H2Y2IN)
      CONST2(NC)=(H1Y4IN*(1.-PY2INF)+PY4INF*H1Y2IN)/(H2Y2IN*H1Y4IN
     1-H2Y4IN*H1Y2IN)
      MM=0
      IF(NC.EQ.1) GO TO 20
      A=CONST1(NC)-CONST1(NC-1)
      B=CONST2(NC)-CONST2(NC-1)
      A=ABS(A)
      B=ABS(B)
      IF(A.LE.ERMINA.AND.B.LE.ERMINB) MM=1
   20 CONTINUE
      WRITE(6,1000) NC
 1000 FORMAT(1X,25HTHIS IS ITERATION NUMBER,I3)
      X=0.
```

```
      Y(1)=0.
      PE1(1)=Y(1)
      Y(2)=0.
      PE2(1)=Y(2)
      Y(3)=CONST1(NC)
      PE3(1)=Y(3)
      Y(4)=1.
      PE4(1)=Y(4)
      Y(5)=CONST2(NC)
      PE5(1)=Y(5)
      WRITE(6,1001)
      WRITE(6,1002) X,Y(1),Y(2),Y(3),Y(4),Y(5)
 1001 FORMAT(1X,62H   X          Y(1)          Y(2)          Y(3)          Y(4)
     1      Y(5))
 1002 FORMAT(1X,F4.1,5(3X,F9.6))
      DO 16 M=2,MMAX
      Y(1)=PB1(M)+CONST1(NC)*PC1(M)+CONST2(NC)*PD1(M)
      PE1(M)=Y(1)
      Y(2)=PB2(M)+CONST1(NC)*PC2(M)+CONST2(NC)*PD2(M)
      PE2(M)=Y(2)
      Y(3)=PB3(M)+CONST1(NC)*PC3(M)+CONST2(NC)*PD3(M)
      PE3(M)=Y(3)
      Y(4)=PB4(M)+CONST1(NC)*PC4(M)+CONST2(NC)*PD4(M)
      PE4(M)=Y(4)
      Y(5)=PB5(M)+CONST1(NC)*PC5(M)+CONST2(NC)*PD5(M)
      PE5(M)=Y(5)
      AA=M-1
      X=AA*H
   16 IF(MM.EQ.1)WRITE(6,1002)X,Y(1),Y(2),Y(3),Y(4),Y(5)
      IF(MM.EQ.1) GO TO 15
   14 GO TO 1
   15 RETURN
      END
```

```
$IBFTC AYGRD
      SUBROUTINE YGRD1(X,N,Y,YG)
      DIMENSION Y(5),YG(5)
      COMMON PE1(700),PE2(700),PE3(700),PE4(700),PE5(700)
      COMMON AVPA1,AVPA2,AVPA3,AVPA4,AVPA5,PA1(700),PA2(700),PA3(700),
     1PA4(700),PA5(700),PB1(700),PB2(700),PB3(700),PB4(700),PB5(700),
     2PC1(700),PC2(700),PC3(700),PC4(700),PC5(700),PD1(700),PD2(700),
     3PD3(700),PD4(700),PD5(700),YK(5),PRNDTL,ERMINA,ERMINB
      COMMON CONST1(20),CONST2(20)
      COMMON SPIN
C     THESE ARE THE LINEARISED NON HOMOGENEOUS EQUATIONS
      YG(1)=Y(2)
      YG(2)=Y(3)
      YG(3)=-2.*YK(1)*Y(3)-2.*YK(3)*Y(1)+2.*YK(2)*Y(2)+2.*YK(1)*YK(3)
     1-YK(2)*YK(2)-1.-2.*SPIN*YK(4)*Y(4)+SPIN*YK(4)*YK(4)
      YG(4)=Y(5)
      YG(5)=2.*YK(4)*Y(2)+2.*YK(2)*Y(4)-2.*YK(5)*Y(1)-2.*YK(1)*Y(5)
     1+2.*YK(5)*YK(1)-2.*YK(2)*YK(4)
      RETURN
      END
```

```
$IBFTC BYGRD
      SUBROUTINE YGRD2(X,N,Y,YG)
      DIMENSION Y(5), YG(5)
      COMMON PE1(700),PE2(700),PE3(700),PE4(700),PE5(700)
      COMMON AVPA1,AVPA2,AVPA3,AVPA4,AVPA5,PA1(700),PA2(700),PA3(700),
     1PA4(700),PA5(700),PB1(700),PB2(700),PB3(700),PB4(700),PB5(700),
     2PC1(700),PC2(700),PC3(700),PC4(700),PC5(700),PD1(700),PD2(700),
     3PD3(700),PD4(700),PD5(700),YK(5),PRNDTL,ERMINA,ERMINB
      COMMON CONST1(20),CONST2(20)
      COMMON SPIN
C     THESE ARE THE HOMOGENEOUS EQUIVILENTS OF THE LINEARISED EQUATIC
      YG(1)=Y(2)
      YG(2)=Y(3)
      YG(3)=-2.*Y(1)*YK(3)-2.*YK(1)*Y(3)+2.*Y(2)*YK(2)-2.*SPIN*YK(4)
     1*Y(4)
      YG(4)=Y(5)
      YG(5)=2.*Y(4)*YK(2)+2.*YK(4)*Y(2)-2.*YK(5)*Y(1)-2.*Y(5)*YK(1)
      RETURN
      END
```

# PROGRAMME 2



```
$*      NAME CARD
$EXECUTE        IBJOB
$IBJOB
$IBFTC MAIN
C---------
C THIS MAIN PROGRAMME SETS THE FOLLOWING VALUES
C NM IS THE MAXIMUM NUMBER OF THE LINEAR DIFF EQUN TO BE SOLVED
C---------
C ERMINA IS THE CONVERGENCE ERROR FOR VELOCITY EQUNS
C*************************************************************************
      DIMENSION Y(100),YG(100),YH(100),YD(100)
      COMMON/COMN1/U(20),CL(20),CK(20),FD3(10),GD2(10),HD2(10),ULIM
      COMMON/COMN2/N1,BETAF,BETAG,BETAH,AF(3),AG(3),AH(2),NM,ERMINA
      COMMON/COMN3/ERMINB,NS,PRNDTL,SPIN,H,X1MAX,DX1,NM7,NM2,ALPHA(10)
      COMMON/COMN4/BETA(10),GAMMA(10),ALP(20),BET(20),GAM(20),DELTA
      COMMON/COMN5/YF1,YF2,YF3,YG1,YG2,YG3,YH1,YH2,MARK,XMAX,ER
C ERMINB IS THE CONVERGENCE ERROR FOR TRANSFER EQUN
C NS IS THE MINIMUM EQUN TO BE STARTED
C PRNDTL IS THE PRANDTL OR SCHMIDT NUMBER OF THE SYSTEM TO BE ANALYSED
C SPIN IS THE SPIN PARAMETER  OF THE SYSTEM TO BE ANALYSED
C H IS THE INTEGRATION STEP FOR THE RUNGE-KUTTA INTEGRATION PROCEDURE
C X1MAX IS THE MAXIMUM ANGLE AROUND THE BODY TO BE ANALYSED
C DX1 IS THE INTERVAL AROUND THEBODY FOR WHICH POINT MASS TRANSFER VALUES
C ARE REQUIRED
C ALPHA(NS-1),BETA(NS-1),GAMMA(NS-1) FROM NS EQ TO 2 TO NS ARE THE KNOWN
C SUPPLIED VALUES OF Y(7*I 4),Y(7*I-2),Y(7*I)
C ALP (1),BET(1),GAM(1) ARE THE SUPPLIED VALUES OF INITIAL GUESSES OF THE
C FUNCTIONS Y(7*I 4),Y(7*I 2),Y(7*I)
CDELTA IS APERTURBATION STEP FOR THESE INITIAL GUESSES
C
C
C*************************************************************************
CC      SOLUTION OF GENERAL LINEAR EQATION
C       BODY ROTATING IN A AXIAL FLOW
C*************************************************************************
C
C
      ALPHA(1)=5.412899
      BETA(1)=-1.473053
      GAMMA(1)=-0.8544438
      ALP(1)=-.5
      BET(1)=-1.
      GAM(1)=-1.
      PRNDTL=0.7
      SPIN=20.
      ER=1.
C     NS IS THE ORDER OF THE FIRST SET OF EQUATIONS TO BE SOLVED
      NS=2
C     NM IS THE MAXIMUM ORDER OF EQUATIONS TO BE SOLVED
      NM=5
      NM2=1
C     NM7 IS THE NUMBER OF MASS TRANSFER BOUNDARY VALUES SUPPLIED
      NM7=1
C*************************************************************************
      WRITE(6,8186) ER
 8186 FORMAT(1X,23HRATIO OF  MIN/MAJ AXIS=,F7.4/////1X)
      WRITE(6,8184) NM2,NM7
 8184 FORMAT(1X, 9HTHE FIRST,I2,51HPAIRS OF HYDRODYNAMIC BOUNDARY VALUES
     1 WERE SUPPLIED/1X,10HTHE FIRST ,I1,47HBOUNDARY VALUES FOR MASS TRA
```

```
     2NSFER WERE SUPPLIED)
      ERMINA=.5E-7
      ERMINB=.5E-7
      X1MAX=3.14159265/2.
      DX1=5.*X1MAX/90.
      XMAX=6.
      WRITE(6,8182) PRNDTL,SPIN,NM
      WRITE(6,8185) XMAX
      WRITE(6,8183) ERMINA,ERMINB
 8182 FORMAT(1X,15HPRANDTL NUMBER=,F6.2,5X,15HSPIN PARAMETER=F6.2,5X
     127HMAX NO OF INTEGRATED EQUNS=,I1)
 8183 FORMAT(1X,40HERMINA(MAX ERROR FOR HYDRODYNAMIC CASE)=,E9.2,5X,
     141HERMINB(MAX ERROR FOR MASS TRANSFER CASE)=,E9.2)
 8185 FORMAT(1X,6H XMAX=,F6.4)
      CALL COEFFS
      DELTA=.5
      CALL METHOD
      STOP
      END
```

```
$IBFTC ACOEF
      SUBROUTINE COEFFS
      DOUBLE PRECISION S1(30),S2(30),ERD, B(30),SUM1,SUM2,SUM3,SUM4,
     1BU(30),YE(20),Y(20),A(20,20),X(20,20)
      INTEGER   E,EE,DD,D
      COMMON/COMN1/U(20),CL(20),CK(20),FD3(10),GD2(10),HD2(10),ULIM
      COMMON/COMN2/N1,BETAF,BETAG,BETAH,AF(3),AG(3),AH(2),NM,ERMINA
      COMMON/COMN3/ERMINB,NS,PRNDTL,SPIN,H,X1MAX,DX1,NM7,NM2,ALPHA(10)
      COMMON/COMN4/BETA(10),GAMMA(10),ALP(20),BET(20),GAM(20),DELTA
      COMMON/COMN5/YF1,YF2,YF3,YG1,YG2,YG3,YH1,YH2,MARK,XMAX,ER
C*************************************************************************
C THIS SUBROUTINE SUPPLIES THE VALUES OF COEFFS FOR OBLATE SPHEROIDS
C*************************************************************************
      U(1)=1.
      S1(1)=1.D0
      S2(1)=1.D0
      DO 50 N=2,NM
   50 S1(N)=-S1(N-1)/FLOAT(2*(N-1)*(2*N-1))
      DO 1 I=1,NM
    1 CK(2*I-1)=S1(I)
C     S1(I) AND S2(I) ARE COEFFS OF SIN(O) AND SIN(O)**2 RESP
      DO 2 N=2,NM
    2 S2(N)=-4.*S2(N-1)/FLOAT(2*N*(2*N-1))
      ERD=ER
      B(1)=1.D0
      BU(1)=1.D0
      NMA=NM-1
      DO 3 E=2,NM
      B(E)=B(E-1)*(1.D0-ERD**2)*FLOAT(2*E-5)/FLOAT(E-1)/2.D0
    3  BU(E)=BU(E-1)*(1.D0-ERD**2)*FLOAT(2*E-3)/FLOAT(E-1)/2.D0
C     MAIN LOOP DETERMINATION OF CL( ),U( )
      DO 13 N=1,NMA
       SUM3=0.D0
       SUM4=0.D0
      DO 14 K=1,N
      IF(K-2) 15,16,17
   15 X(N,1)=S2(N)
      GO TO 30
   16 SUM1=0.D0
      N2=N-1
      DO 18 E=1,N2
      EE=N-E
   18 SUM1=S2(EE)*S2(E)+SUM1
       X(N,2)=SUM1
       GO TO 30
   17 N2=K-1
      DO 19 KK=2,N2
      N3=N-K+1
       DO 20 D=1,N3
      SUM2=0.D0
       SUM1=0.D0
       IF(KK-2) 21,21,22
   21 DO 23 E=1,D
       EE=D-E+1
   23  SUM1=S2(EE)*S2(E)+SUM1
      A(2,D)=SUM1
   22  DO 24 E=1,D
       DD=D-E+1
   24  SUM2=S2(DD)*A(KK,E) SUM2
```

```
   20  A(KK+1,D)=SUM2
   19  CONTINUE
       X(N,K)=A(N2+1,N3)
   30  SUM3=SUM3+B(K+1)*X(N,K)
   14 SUM4=SUM4+BU(K+1)*X(N,K)
       YE(N+1)=SUM4
       YE(1)=1.D0
       N2=N+1
       SUM4=0.D0
       DO 26 L=1,N2
       E=N L+2
   26 SUM4=YE(L)*S1(E)+SUM4
       U(2*N+1)=SUM4
   13 CL(2*N)=SUM3
       NMS=2*NM-1
       WRITE(6,27)(N,U(N),N=1,NMS,2)
   27 FORMAT(1X,(1X,4(2X,2HU(,I2,1H),E20.8)))
       NMT=2*NM
       WRITE(6,28)(N,CL(N),N=2,NMT,2)
   28 FORMAT(1X,(1X,4(2X,3HCL(,I2,1H),E20.8)))
       WRITE(6,29)(N,CK(N),N=1,NMS,2)
   29 FORMAT(1X,(1X,4(2X,3HCK(,I2,1H),E20.8)))
        RETURN
        END
  $IBFTC AMETH
       SUBROUTINE METHOD
       DIMENSION Y(100),YG(100),YH(100),YD(100)
       COMMON/COMN1/U(20),CL(20),CK(20),FD3(10),GD2(10),HD2(10),ULIM
       COMMON/COMN2/N1,BETAF,BETAG,BETAH,AF(3),AG(3),AH(2),NM,ERMINA
       COMMON/COMN3/ERMINB,NS,PRNDTL,SPIN,H,XIMAX,DX1,NM7,NM2,ALPHA(10)
       COMMON/COMN4/BETA(10),GAMMA(10),ALP(20),BET(20),GAM(20),DELTA
       COMMON/COMN5/YF1,YF2,YF3,YG1,YG2,YG3,YH1,YH2,MARK,XMAX,ER
  C--------
  C      N1 IS THE ORDER OF THE EQUATION BEING SOLVED
  C       NM IS THE HIGHEST VALUE OF N1
  C       NS IS THE STARTING VALUE OF N1
  C       N IS THE NUMBER OF DIFFERENTIAL EQUATIONS BEING SOLVED
  C--------
       IF(LIST.EQ.1) N1=NS+1
       IF(LIST.EQ.1) GO TO 444
       IF(NS.LE.1.OR.NM.LE.1) WRITE(6,5000)
  5000 FORMAT(1X46HNS AND NM MUST BE GREATER THAN UNITY-----ERROR)
       IF(NS.LE.1.OR.NM.LE.1) GO TO 1
  C  NS CAN NOT BE UNITY (THIS IS THE NON-LINEAR CASE)
       N1=NS-1
    21 N1=N1+1
       MARK=0
       IF(N1.LE.NM2) MARK=1
       N=7*N1
       IF(N1.GT.NM) GO TO 2
    16 J=0
       NC=0
       L=1
    15 L=L 1
   444 CONTINUE
       I=1
    25 Y(7*I-6)=0.
       Y(7*I-5)=0.
       Y(7*I-3)=CK(2*I-1)
```

```
      Y(7*I-1)=0.
      IF(I.GE.N1) GO TO 3
      Y(7*I-4)=ALPHA(I)
      Y(7*I-2)=BETA(I)
      Y(7*I)=GAMMA(I)
      I=I 1
      GO TO 25
    3 Y(6)=1.
      X=0.
      IF(LIST.EQ.1) N1=5
      IF(LIST.EQ.1) N=7*N1
      IF(LIST.EQ.1) WRITE(6,101) X,(Y(K),K=1,35)
  101 FORMAT(1X,F3.1,5X,8(E12.4,2X)/3(9(E12.4,2X)/))
      IF(LIST.EQ.1) GO TO 9
      IF(MARK.EQ.1) GO TO 4
      IF(NC.GE.3) GO TO 5
C     YG1,YG2,YG3, ARE INITIAL GUESSES FOR COMPUTER-
C     YF1,YF2,YF3, ARE INITIAL GUESSES FOR COMPUTER
      YF1=ALP(1)
      YF2=ALP(1)+.1
      YF3=ALP(1)+.4
       YG1=BET(1)
      YG2=BET(1)+.2
      YG3=BET(1)+.5
   10 J=J 1
    5 NC=NC+1
      GO TO (6,7,40) ,J
   40 Y(7*I-4)=YF3
      Y(7*I-2)=YG3
      GO TO 8
    6 Y(7*I-4)=YF1
      Y(7*I-2)=YG1
      GO TO 8
    7 Y(7*I-4)=YF2
      Y(7*I-2)=YG2
    8 CONTINUE
    9 CONTINUE
      H=0.1
      CALL RKINT(X,H,N,Y,YG,YH,YD)
      IF(LIST.EQ.1) WRITE(6,101) X,(Y(K),K=1,35)
      IF (X.LE.XMAX) GO TO 9
      IF(LIST.EQ.1)STOP
      AF(J)=Y(7*I-5)
      AG(J)=Y(7*I-3)
      IF(NC.LT.3) GO TO 444
      ULIM=U(2*N1-1)
      WRITE(6,3993) (J,AF(J),J,AG(J),J=1,3)
 3993 FORMAT(1X,3HAF(,I1,2H)=,F12.8,3HAG(,I1,2H)=,F12.8)
      WRITE(6,3994) ULIM
 3994 FORMAT(1X,5HULIM=,F12.8)
      CALL PROCES
      ALP(L)=BETAF
      BET(L)=BETAG
      A1=ALP(L)-ALP(L-1)
      A2=BET(L)-BET(L-1)
      L1=L+1
      IF(ABS(A1).LE.ERMINA.AND.ABS(A2).LE.ERMINA) WRITE(6,8888)
     1N1,BETAF,N1,BETAG,L1
 8888 FORMAT(1X,4HF2D(,I1,1H),1H=,F16.8,5X,4HGD1(,I1,1H),1H=,F16.8,5X,
```

```
     1 21HNUMBER OF ITERATIONS=,I3)
       IF(ABS(A1).LE.ERMINA.AND.ABS(A2).LE.ERMINA) GO TO 11
       IF(L.LT.3) GO TO 30
       A3=ALP(L)-ALP(L-2)
       A4=BET(L)-BET(L-2)
       IF(ABS(A3).LE.0.5E-7.AND.ABS(A1).LE.0.5E-7) WRITE(6,9999)
       IF(ABS(A4).LE.0.5E-7.AND.ABS(A2).LE.0.5E-7) WRITE(6,9998)
  9999 FORMAT(1X,71HOSCILLATION OF RESULT WAS OBTAINED-F2D( ) WITHIN ERMI
      1NA GD1 OSCILLATING,1X///1X)
  9998 FORMAT(1X,71HOSCILLATION OF RESULT WAS OBTAINED-GD1( ) WITHIN ERMI
      1NA F2D OSCILLATING,1X///1X)
       IF(ABS(A3).LE.0.5E-7.AND.ABS(A1).LE.0.5E-7) WRITE(6,8888)
      1N1,BETAF,N1,BETAG,L1
       IF(ABS(A4).LE.0.5E-7.AND.ABS(A2).LE.0.5E-7) WRITE(6,8888)
      1N1,BETAF,N1,BETAG,L1
       IF(ABS(A3).LE.0.5E-7.AND.ABS(A1).LE.ERMINA) GO TO 11
       IF(ABS(A4).LE.0.5E-7.AND.ABS(A2).LE.ERMINA) GO TO 11
    30 CONTINUE
       AJ1=SQRT((AF(1)-ULIM)*(AF(1)-ULIM)+AG(1)*AG(1))
       AJ2=SQRT((AF(2)-ULIM)*(AF(2)-ULIM)+AG(2)*AG(2))
       AJ3=SQRT((AF(3)-ULIM)*(AF(3)-ULIM)+AG(3)*AG(3))
       AJM=AMAX1(AJ1,AJ2,AJ3)
       IF(ABS(AJ1-AJM).LE.0.5E-7) GO TO 12
       IF(ABS(AJ2-AJM).LE.0.5E-7) GO TO 13
       J=3
       YF3=ALP(L)
       YG3=BET(L)
       GO TO 14
    12 J=1
       YF1=ALP(L)
       YG1=BET(L)
       GO TO 14
    13 J=2
       YF2=ALP(L)
       YG2=BET(L)
    14 CONTINUE
       GO TO 15
    11 ALPHA(I)=ALP(L)
       BETA(I)=BET(L)
       MARK=1
       GO TO 16
     4 CONTINUE
       Y(7*I-4)=ALPHA(I)
       Y(7*I-2)=BETA(I)
       IF(NC.GE.2) GO TO 23
       YH1=GAM(1)-DELTA*GAM(1)
       YH2=GAM(1)+DELTA*GAM(1)
       L=1
    20 J=J 1
    23 NC=NC+1
       L=L 1
       IF(J.EQ.1) GO TO 17
       Y(7*I)=YH2
       GO TO 18
    17 Y(7*I)=YH1
    18 BXMAX=XMAX/(PRNDTL)**.3333
    19 CONTINUE
       H=BXMAX/60.
       CALL RKINT(X,H,N,Y,YG,YH,YD)
```

```
      IF (X.LE.BXMAX) GO TO 19
      AH(J)=Y(7*I-1)
      IF(NC.LT.2) GO TO 444
      CALL PROCES
      GAM(L)=BETAH
      A3=GAM(L)-GAM(L-1)
      IF(ABS(A3).LE.ERMINB) WRITE(6,8887) N1,BETAH,NC
 8887 FORMAT(1X,4HHD1(,I1,1H),1H=,F12.8,5X,21HNUMBER OF ITERATIONS=,I3)
      IF(ABS(A3).LE.ERMINB) GAMMA(I)=GAM(L)
      IF(ABS(A3).LE.ERMINB) GO TO 21
      IF(ABS(AH(1)).GT.ABS(AH(2))) GO TO 22
      J=2
      YH2=GAM(L)
      GO TO 444
   22 J=1
      YH1=GAM(L)
      GO TO 444
    2 X1=0.
   24 SUM=-GAMMA(1)
      DO 26 I=2,NM
   26 SUM=SUM-GAMMA(I)*X1**(2*I-2)
      AMTN=SUM/((PRNDTL**.3333)*SQRT(2.))
      DEGX1=X1*180./3.14159265
      WRITE(6,5001)DEGX1,AMTN
 5001 FORMAT(1X,5HDEGS=,F5.1,5X,7HM.T.N.=,F10.7)
      IF(ABS(X1-X1MAX).LT.1.E-6) GO TO 1
      X1=X1+DX1
      GO TO 24
    1 CONTINUE
      RETURN
      END
```

```
$IBFTC APROC
      SUBROUTINE PROCES
       DOUBLE PRECISION C1,C2,C3,AG1,AG2,AG3,YF1D,YF2D,YF3D,CD1,CD2,
     1YG1D,YG2D,YG3D
      COMMON/COMN1/U(20),CL(20),CK(20),FD3(10),GD2(10),HD2(10),ULIM
      COMMON/COMN2/N1,BETAF,BETAG,BETAH,AF(3),AG(3),AH(2),NM,ERMINA
      COMMON/COMN3/ERMINB,NS,PRNDTL,SPIN,H,XMAX,DX1,NM7,NM2,ALPHA(10)
      COMMON/COMN4/BETA(10),GAMMA(10),ALP(20),BET(20),GAM(20),DELTA
      COMMON/COMN5/YF1,YF2,YF3,YG1,YG2,YG3,YH1,YH2,MARK,XMAX,ER
      IF(MARK.EQ.1) GO TO 30
C     THIS SECTION GIVES A BETTER APPROX OF VELOCITY BOUNDARY VALUES
      AG1=AG(1)
      AG2=AG(2)
      AG3=AG(3)
      C1=AF(1)-ULIM
      C2=AF(2)-ULIM
      C3=AF(3)-ULIM
      CD1=(C2*AG3-C3*AG2)/(C1*AG2-C2*AG1)
      CD2=(C3*AG1-C1*AG3)/(C1*AG2-C2*AG1)
       YF1D=YF1
       YF2D=YF2
       YF3D=YF3
       YG1D=YG1
       YG2D=YG2
      YG2D=YG2
      YG3D=YG3
      BETAF=(CD1*YF1D+CD2*YF2D+YF3D)/(CD1+CD2+1.D0)
      BETAG=(CD1*YG1D+CD2*YG2D+YG3D)/(CD1+CD2+1.D0)
      WRITE(6,3999) BETAF,BETAG
 3999 FORMAT(1X,20H STILL TRYING BETAF=,F16.8,5X,7H BETAG=,F16.8)
      GO TO 31
C     THIS SECTION GIVES A BETTER APPROX OF TRANSFER BOUNDARY VALUES
   30 C4= AH(2)/AH(1)
      BETAH=(C4*YH1+YH2)/(C4+1.)
      WRITE(6,1212) BETAH
 1212 FORMAT(1X,20H STILL TRYING BETAH=,F12.8)
   31 CONTINUE
      RETURN
      END
```

```
$IBFTC PRKIN
      SUBROUTINE RKINT(X,H,N,Y,YG,YH,YD)
C     RUNGE KUTTA INTEGRATION ROUTINE
C*****************************************************************************
C     ARGUMENT LIST DEFINITIONS
C     X= INDEPENDENT VARIABLE
C     H= CURRENT INTEGRATION INTERVAL
C     N= NUMBER OF DIFFERENTIAL EQUATIONS
C     Y = DEPENDENT VARIABLES
C     YG= THE DERIVATIVES OF Y WITH RESPECT TO X
C     YH= WORKING SPACE
C     YD = WORKING SPACE
C     YGRD(------  ) NAME AND ARGUMENTS OF THE SUBROUTINE TO FIND THE
C     DERIVATIVES OF THE DEPENDENT VARIABLES Y WITH RESPECT TO X
C*****************************************************************************
C     THE FOLLOWING TWO   TYPE STATEMENTS ARE VERY IMPORTANT
C     NOTE THEM CAREFULLY
      DIMENSION Y(N),YG(N),YH(N),YD(N)
C*****************************************************************************
      DO 1 J=1,N
    1 YD(J) = Y(J)
      CALL YGRD(X,N,Y,YG)
      DO2 J=1,N
      YG(J)=YG(J)*H
    2 YH(J)=YG(J)
      X=X 0.5*H
      DO4I=1,2
      DO3J=1,N
    3 Y(J)=YD(J)+.5*YG(J)
      CALL YGRD(X,N,Y,YG)
      DO4J=1,N
      YG(J)=YG(J)*H
    4 YH(J)=YH(J)+2.*YG(J)
      X=X 0.5*H
      DO5J=1,N
    5 Y(J)=YD(J)+YG(J)
      CALL YGRD(X,N,Y,YG)
      DO6J=1,N
      YH(J)=(YH(J)+H*YG(J))/6.
      YD(J)=YD(J)+YH(J)
    6 Y(J)=YD(J)
      RETURN
      END
```

```
$IBFTC AHGRD
      SUBROUTINE YGRD(X,N,Y,YG)
      DIMENSION Y(100),YG(100),
      COMMON/COMN1/U(20),CL(20),CK(20),FD3(10),GD2(10),HD2(10),ULIM
      COMMON/COMN2/N1,BETAF,BETAG,BETAH,AF(3),AG(3),AH(2),NM,ERMINA
      COMMON/COMN3/ERMINB,NS,PRNDTL,SPIN,H,X1MAX,DX1,NM7,NM2,ALPHA(10)
      COMMON/COMN4/BETA(10),GAMMA(10),ALP(20),BET(20),GAM(20),DELTA
      COMMON/COMN5/YF1,YF2,YF3,YG1,YG2,YG3,YH1,YH2,MARK,XMAX,ER
C     WHERE N IS THE NUMBER OF  DIFFERENTIAL EQUATIONS
C     AND N1 IS THE N1,TH BOUNDARY FUNCTION FOR TRANSFER
      DO 40 I=1,N1
      I1=I
      YG(7*I-6)=Y(7*I-5)
      YG(7*I-5)=Y(7*I-4)
C*************************************************************
C    THESE OPERATIONS DEDUCE THE VALUE OF FD3(I)
      SUM1=0.
      DO 50 M=1,I1
      COUNT=0.
      DO 51 K=1,M
      M1=M-K
   51 COUNT=COUNT+CK(2*M1+1)*Y(7*K-5)
      A=2*(I1-M)+1
      M2=I1-M
   50 SUM1=SUM1+A*Y(7*M2+2)*COUNT
      SUM2=0.
      DO 52 M=1,I1
      COUNT=0.
      DO 53 K=1,M
      A=2*K-1
      M1=M-K
   53 COUNT=COUNT+A*Y(7*K-6)*CK(2*M1+1)
      M2=I1-M
   52 SUM2=SUM2+Y(7*M2+3)*COUNT
      SUM3=0.
      DO 54 M=1,I1
      COUNT=0.
      DO 55 K=1,M
      A=2*K-1
      M1=M-K
   55 COUNT=COUNT+A*CK(2*K-1)*Y(7*M1+1)
      M2=I1-M
   54 SUM3=SUM3+Y(7*M2+3)*COUNT
      SUM4=0.
      DO 56M=1,I1
      COUNT=0.
      DO 57 K=1,M
      A=2*K-1
      M1=M-K
   57 COUNT=COUNT+A*CK(2*K-1)*Y(7*M1+4)
      M2=I1-M
   56 SUM4=SUM4+Y(7*M2+4)*COUNT
      SUM5=0.
      DO 58 M=1,I1
      COUNT=0.
      DO 59 K=1,M
      M1=M-K
   59 COUNT=COUNT+U(2*M1+1)*CK(2*K-1)
      A=2*(I1-M)+1
```

```
      M2=I1-M
   58 SUM5=SUM5+U(2*M2+1)*COUNT*A
      SUM6=0.
      IF(I1.LE.1) GO TO 60
      DO 61 M=2,I1
      COUNT=0.
      DO 62 K=1,M
      M1=M-K
      IF(M1.LE.0) GO TO 162
      COUNT=COUNT+CK(2*K-1)*CL(2*M1)
      GO TO 62
  162 COUNT=COUNT+CK(2*K-1)
   62 CONTINUE
      M2=I1-M
   61 SUM6=SUM6+FD3(M2+1)*COUNT
   60 FD3(I)=SUM1-SUM2-SUM3-SPIN*SUM4-SUM5-SUM6
C*****************************************************************************
      YG(7*I-4)=FD3(I)
      YG(7*I-3)=Y(7*I-2)
C     THESE OPERATIONS DEDUCE THE VALUE OF GD2(I)
C*****************************************************************************
      SUM7=0.
      DO63 M=1,I1
      COUNT=0.
      DO 64 K=1,M
      M1=M-K
   64 COUNT=COUNT+CK(2*M1+1)*Y(7*K-5)
      A=2*(I1-M)+1
      M2=I1-M
   63 SUM7=SUM7+A*Y(7*M2+4)*COUNT
      SUM8=0.
      DO 65 M=1,I1
      COUNT=0.
      DO 66 K=1,M
      A=2*K-1
      M1=M-K
   66 COUNT=COUNT+A*CK(2*K-1)*Y(7*M1+1)
      M2=I1-M
   65 SUM8=SUM8+Y(7*M2+5)*COUNT
      SUM9=0.
      DO 67 M=1,I1
      COUNT=0.
      DO 68 K=1,M
      A=2*K-1
      M1=M-K
   68 COUNT=COUNT+CK(2*M1+1)*Y(7*K-6)*A
      M2=I1-M
   67 SUM9=SUM9+Y(7*M2+5)*COUNT
      SUM10=0.
      DO 69 M=1,I1
      COUNT=0.
      DO 70 K=1,M
      A=2*K-1
      M1=M-K
   70 COUNT=COUNT+A*CK(2*K-1)*Y(7*M1+2)
      M2=I1-M
   69 SUM10=SUM10+Y(7*M2+4)*COUNT
      SUM11=0.
      IF(I1.LE.1) GO TO 71
```

```
      DO 72 M=2,I1
      COUNT=0.
      DO 73 K=1,M
      M1=M-K
      IF(M1.LE.0) GO TO 173
      COUNT=COUNT+CK(2*K-1)*CL(2*M1)
      GO TO 73
  173 COUNT=COUNT+CK(2*K-1)
   73 CONTINUE
      M2=I1-M
   72 SUM11=SUM11+GD2(M2+1)*COUNT
   71 GD2(I)=SUM7-SUM8-SUM9+SUM10-SUM11
C*****************************************************************
      YG(7*I-2)=GD2(I)
      IF(MARK.EQ.0) GO TO 41
      YG(7*I-1)=Y(7*I)
C*****************************************************************
C    THESE OPERATIONS DEDUCE THE VALUE OF HD2(I)
      SUM12=0.
      IF(I1.LE.1) GO TO 74
      DO 75 M=2,I1
      COUNT=0.
      DO 76 K=2,M
      M1=M-K
      K1=K-1
   76 COUNT =COUNT+CK(2*M1+1)*Y(7*K1-5)
      A=2*(I1-M+1)
      M2=I1-M
   75 SUM12=SUM12+A*Y(7*M2+13)*COUNT
   74 SUM13=0.
      DO 77 M=1,I1
      COUNT=0.
      DO78 K=1,M
      A=2*K-1
      M1=M-K
   78 COUNT=COUNT+A*CK(2*K-1)*Y(7*M1+1)
      M2=I1-M
   77 SUM13=SUM13+Y(7*M2+7)*COUNT
      SUM14=0.
      DO 79 M=1,I1
      COUNT=0.
      DO 80 K=1,M
      A=2*K-1
      M1=M-K
   80 COUNT=COUNT+CK(2*M1+1)*Y(7*K-6)*A
      M2=I1-M
   79 SUM14=SUM14+Y(7*M2+7)*COUNT
      SUM15=0.
      SUM16=0.
      IF(I1.LE.1) GO TO 81
      DO 82 M=2,I1
      COUNT=0.
      DO 83 K=2,M
      M1=M-K
   83 COUNT=COUNT+CK(2*M1+1)*CL(2*K-2)
      M2=I1-M
   82 SUM15=SUM15+HD2(M2+1)*COUNT
      DO 84 M=2,I1
      M2=I1-M
```

```
   84 SUM16=SUM16 CK(2*M-1)*HD2(M2 1)
   81 HD2(I)=(SUM12-SUM13-SUM14)*PRNDTL -(SUM15+SUM16)
C*****************************************************************
      YG(7*I)=HD2(I)
      GO TO 40
   41 YG(7*I-1)=0.
      YG(7*I)=0.
   40 CONTINUE
      RETURN
      END
```

```
$JOB  10013074    T.G.SANDERS IBJOB    10.0   2000
$*    NAME CARD
$EXECUTE        IBJOB
$IBJOB
$IBFTC MAIN
      DIMENSION Y(100),YG(100),YH(100),YD(100)
      COMMON U(20),CL(20),CK(20),FD3(10),GD2(10),HD2(10),ULIM,N1,BETAF,
     1BETAG,BETAJ,AF(3),AG(3),AH(2),NM,ERMINA,ERMINB,NS,PRNDTL,SPIN,H,
     2X1MAX,DX1,NM7,NM2,ALPHA(10),BETA(10),GAMMA(10),ALP(20),BET(20),
     3GAM(20),DELTA,YF1,YF2,YF3,YG1,YG2,YG3,YH1,YH2,MARK,XMAX,ER
C--------
C
C
C*************************************************************************
CC      SOLUTION OF GENERAL LINEAR EQATION
C       BODY ROTATING IN A QUIESCENT FLUID
C*************************************************************************
C
C
      ALPHA(1)=.510233
      ALPHA(2)=-0.22128535
      ALPHA(3)=0.02071030
      ALPHA(4)=-0.00189041
      BETA(1)=-.615922
      BETA(2)=0.24764359
      BETA(3)=-0.02568883
      BETA(4)=0.00181337
      GAMMA(1)=-0.3231282
      GAMMA(2)=0.06263696
      GAMMA(3)=0.00131540
      GAMMA(4)=0.00064938
      PRNDTL=0.7
      ALP(1)=-.5
      BET(1)=-1.
      GAM(1)=-1.
      ER=1.
C     NS IS THE ORDER OF THE FIRST SET OF EQUATIONS TO BE SOLVED
      NS=5
C     NM IS THE MAXIMUM ORDER OF EQUATIONS TO BE SOLVED
      NM=5
C      NM2 IS THE NUMBER OF PAIRS OF HYDRODYNAMIC BOUNDARY VALUES SUPPLIED
      NM2=4
C     NM7 IS THE NUMBER OF MASS TRANSFER BOUNDARY VALUES SUPPLIED
      NM7=4
C*************************************************************************
      WRITE(6,8186) ER
 8186 FORMAT(1X,23HRATIO OF  MIN/MAJ AXIS=,F7.4/////1X)
      WRITE(6,8184) NM2,NM7
 8184 FORMAT(1X, 9HTHE FIRST,I2,51HPAIRS OF HYDRODYNAMIC BOUNDARY VALUES
     1 WERE SUPPLIED/1X,10HTHE FIRST ,I1,47HBOUNDARY VALUES FOR MASS TRA
     2NSFER WERE SUPPLIED)
      ERMINA=.5E-7
      ERMINB=.5E-7
      X1MAX=3.14159265/2.
      DX1=5.*X1MAX/90.
      XMAX=20.
      WRITE(6,8182) PRNDTL,NM
      WRITE(6,8185) XMAX
      WRITE(6,8183) ERMINA,ERMINB
```

```
 8182 FORMAT(1X,15HPRANDTL NUMBER=,F6.2,5X,19HSPIN PARAMETER=INF ,5X
     127HMAX NO OF INTEGRATED EQUNS=,I1)
 8183 FORMAT(1X,40HERMINA(MAX ERROR FOR HYDRODYNAMIC CASE)=,E9.2,5X,
     141HERMINB(MAX ERROR FOR MASS TRANSFER CASE)=,E9.2)
 8185 FORMAT(1X,6H XMAX=,F8.4)
      WRITE(6,8187)
 8187 FORMAT(1X,37H HERE THE SPIN PARAMETER IS INFINITE /////1X)
      CALL COEFFS
      DELTA=.5
      CALL METHOD
      STOP
      END
```

```
$IBFTC AMETH
      SUBROUTINE METHOD
      DIMENSION Y(100),YG(100),YH(100),YD(100)
      COMMON U(20),CL(20),CK(20),FD3(10),GD2(10),HD2(10),ULIM,N1,BETAF,
     1BETAG,BETAJ,AF(3),AG(3),AH(2),NM,ERMINA,ERMINB,NS,PRNDTL,SPIN,H,
     2X1MAX,DX1,NM7,NM2,ALPHA(10),BETA(10),GAMMA(10),ALP(20),BET(20),
     3GAM(20),DELTA,YF1,YF2,YF3,YG1,YG2,YG3,YH1,YH2,MARK,XMAX,ER
C--------
C     N1 IS THE ORDER OF THE EQUATION BEING SOLVED
C      NM IS THE HIGHEST VALUE OF N1
C      NS IS THE STARTING VALUE OF N1
C      N IS THE NUMBER OF DIFFERENTIAL EQUATIONS BEING SOLVED BY
C      RUNG-KUTTA
      IF(NS.LE.1.OR.NM.LE.1) WRITE(6,5000)
 5000 FORMAT(1X,52HNS AND NM MUST BE GREATER THAN UNITY---------, ERROR)
      IF(NS.LE.1.OR.NM.LE.1) GO TO 1
C     NS CAN NOT BE UNITY (THIS IS THE NON-LINEAR CASE)
      N1=NS-1
   21 N1=N1+1
      MARK=0
      IF(N1.LE.NM2) MARK=1
      N=7*N1
      IF(N1.GT.NM) GO TO 2
   16 J=0
      NC=0
      L=1
   15 L=L+1
  444 CONTINUE
      I=1
   25 Y(7*I-6)=0.
      Y(7*I-4)=CK(2*I-1)
      Y(7*I-2)=0.
      Y(7*I-1)=0.
      IF(I.GE.N1) GO TO 3
      Y(7*I-5)=ALPHA(I)
      Y(7*I-3)=BETA(I)
      Y(7*I)=GAMMA(I)
      I=I 1
      GO TO 25
    3 Y(6)=1.
      X=0.
      IF(MARK.EQ.1) GO TO 4
      IF(NC.GE.3) GO TO 5
C     YG1,YG2,YG3, ARE INITIAL GUESSES FOR COMPUTER-
C     YF1,YF2,YF3. ARE INITIAL GUESSES FOR COMPUTER.
      YF1=ALP(1)
      YF2=ALP(1)+.1
      YF3=ALP(1)+.4
       YG1=BET(1)
      YG2=BET(1)+.2
      YG3=BET(1)+.5
   10 J=J 1
    5 NC=NC+1
      GO TO (6,7,40) ,J
   40 Y(7*I-5)=YF3
      Y(7*I-3)=YG3
      GO TO 8
    6 Y(7*I-5)=YF1
      Y(7*I-3)=YG1
```

```
      GO TO 8
    7 Y(7*I-5)=YF2
      Y(7*I-3)=YG2
    8 CONTINUE
    9 CONTINUE
      H=0.1
      CALL RKINT(X,H,N,Y,YG,YH,YD)
      IF (X.LE.XMAX) GO TO 9
      AF(J)=Y(7*I-6)
      AG(J)=Y(7*I-4)
      IF(NC.LT.3) GO TO 444
      WRITE(6,3993) (J,AF(J),J,AG(J),J=1,3)
 3993 FORMAT(1X,3HAF(,I1,2H)=,F12.8,3HAG(,I1,2H)=,F12.8)
      CALL PROCES
      ALP(L)=BETAF
      BET(L)=BETAG
      A1=ALP(L)-ALP(L-1)
      A2=BET(L)-BET(L-1)
      L1=L+1
      IF(ABS(A1).LE.ERMINA.AND.ABS(A2).LE.ERMINA) WRITE(6,8888)
     1N1,BETAF,N1,BETAG,L1
 8888 FORMAT(1X,4HF1D(,I1,1H),1H=,F12.8,5X,4HGD1(,I1,1H),1H=,F12.8,5X,
     1 21HNUMBER OF ITERATIONS=,I3)
      IF(ABS(A1).LE.ERMINA.AND.ABS(A2).LE.ERMINA) GO TO 11
      IF(L.LT.3) GO TO 30
      A3=ALP(L)-ALP(L-2)
      A4=BET(L)-BET(L-2)
      IF(ABS(A3).LE.0.5E-7.AND.ABS(A1).LE.0.5E-7) WRITE(6,9999)
      IF(ABS(A4).LE.0.5E-7.AND.ABS(A2).LE.0.5E-7) WRITE(6,9998)
 9999 FORMAT(1X,71HOSCILLATION OF RESULT WAS OBTAINED-F1D( ) WITHIN ERMI
     1NA GD1 OSCILLATING,1X///1X)
 9998 FORMAT(1X,71HOSCILLATION OF RESULT WAS OBTAINED-GD1( ) WITHIN ERMI
     1NA F1D OSCILLATING,1X///1X)
      IF(ABS(A3).LE.0.5E-7.AND.ABS(A1).LE.0.5E-7) WRITE(6,8888)
     1N1,BETAF,N1,BETAG,L1
      IF(ABS(A4).LE.0.5E-7.AND.ABS(A2).LE.0.5E-7) WRITE(6,8888)
     1N1,BETAF,N1,BETAG,L1
      IF(ABS(A3).LE.0.5E-7.AND.ABS(A1).LE.ERMINA) GO TO 11
      IF(ABS(A4).LE.0.5E-7.AND.ABS(A2).LE.ERMINA) GO TO 11
   30 CONTINUE
      AJ1=SQRT(AF(1)*AF(1)+AG(1)*AG(1))
      AJ2=SQRT(AF(2)*AF(2)+AG(2)*AG(2))
      AJ3=SQRT(AF(3)*AF(3)+AG(3)*AG(3))
      AJM=AMAX1(AJ1,AJ2,AJ3)
      IF(ABS(AJ1-AJM).LE.0.5E-7) GO TO 12
      IF(ABS(AJ2-AJM).LE.0.5E-7) GO TO 13
      J=3
      YF3=ALP(L)
      YG3=BET(L)
      GO TO 14
   12 J=1
      YF1=ALP(L)
      YG1=BET(L)
      GO TO 14
   13 J=2
      YF2=ALP(L)
      YG2=BET(L)
   14 CONTINUE
      GO TO 15
```

```
   11 ALPHA(I)=ALP(L)
      BETA(I)=BET(L)
      MARK=1
      GO TO 16
    4 CONTINUE
      Y(7*I-5)=ALPHA(I)
      Y(7*I-3)=BETA(I)
      IF(NC.GE.2) GO TO 23
      YH1=GAM(1)-DELTA*GAM(1)
      YH2=GAM(1)+DELTA*GAM(1)
      L=1
   20 J=J+1
   23 NC=NC+1
      L=L+1
      IF(J.EQ.1) GO TO 17
      Y(7*I)=YH2
      GO TO 18
   17 Y(7*I)=YH1
   18 BXMAX=XMAX/(PRNDTL)**.3333
   19 CONTINUE
      H=BXMAX/200.
      CALL RKINT(X,H,N,Y,YG,YH,YD)
      IF (X.LE.BXMAX) GO TO 19
      AH(J)=Y(7*I-1)
      IF(NC.LT.2) GO TO 444
      CALL PROCES
      GAM(L)=BETAJ
      A3=GAM(L)-GAM(L-1)
      IF(ABS(A3).LE.ERMINB) WRITE(6,8887) N1,BETAJ,NC
 8887 FORMAT(1X,4HHDI(,I1,1H),1H=,F12.8,5X,21HNUMBER OF ITERATIONS=,I3)
      IF(ABS(A3).LE.ERMINB) GAMMA(I)=GAM(L)
      IF(ABS(A3).LE.ERMINB) GO TO 21
      IF(ABS(AH(1)).GT.ABS(AH(2))) GO TO 22
      J=2
      YH2=GAM(L)
      GO TO 444
   22 J=1
      YH1=GAM(L)
      GO TO 444
    2 X1=0.
   24 SUM=-GAMMA(1)
      DO 26 I=2,NM
   26 SUM=SUM-GAMMA(I)*X1**(2*I-2)
      AMTN=SUM/((PRNDTL**.3333)*SQRT(2.))
      DEGX1=X1*180./3.14159265
      WRITE(6,5001)DEGX1,AMTN
 5001 FORMAT(1X,5HDEGS=,F5.1,5X,7HM.T.N.=,F10.7)
      IF(ABS(X1-X1MAX).LT.1.E-6) GO TO 1
      X1=X1+DX1
      GO TO 24
    1 CONTINUE
      RETURN
      END
```

```
$IBFTC APROC
      SUBROUTINE PROCES
       DOUBLE PRECISION C1,C2,C3,AG1,AG2,AG3,YF1D,YF2D,YF3D,CD1,CD2,
     1YG1D,YG2D,YG3D
       COMMON U(20),CL(20),CK(20),FD3(10),GD2(10),HD2(10),ULIM,N1,BETAF,
     1BETAG,BETAJ,AF(3),AG(3),AH(2),NM,ERMINA,ERMINB,NS,PRNDTL,SPIN,H,
     2X1MAX,DX1,NM7,NM2,ALPHA(10),BETA(10),GAMMA(10),ALP(20),BET(20),
     3GAM(20),DELTA,YF1,YF2,YF3,YG1,YG2,YG3,YH1,YH2,MARK,XMAX,ER
       IF(MARK.EQ.1) GO TO 30
C      THIS SECTION GIVES A BETTER APPROX OF VELOCITY BOUNDARY VALUES
       AG1=AG(1)
       AG2=AG(2)
       AG3=AG(3)
       C1=AF(1)
       C2=AF(2)
       C3=AF(3)
       CD1=(C2*AG3-C3*AG2)/(C1*AG2-C2*AG1)
       CD2=(C3*AG1-C1*AG3)/(C1*AG2-C2*AG1)
       YF1D=YF1
       YF2D=YF2
       YF3D=YF3
       YG1D=YG1
       YG2D=YG2
       YG3D=YG3
       BETAF=(CD1*YF1D+CD2*YF2D+YF3D)/(CD1+CD2+1.D0)
       BETAG=(CD1*YG1D+CD2*YG2D+YG3D)/(CD1+CD2+1.D0)
       WRITE(6,3999) BETAF,BETAG
 3999  FORMAT(1X,20H STILL TRYING BETAF=,F12.8,5X,7H BETAG=,F12.8)
       GO TO 31
C      THIS SECTION GIVES A BETTER APPROX OF TRANSFER BOUNDARY VALUES
   30  C4= AH(2)/AH(1)
       BETAJ=(C4*YH1+YH2)/(C4+1.)
       WRITE(6,1212) BETAJ
 1212  FORMAT(1X,20H STILL TRYING BETAJ=,F12.8)
   31  CONTINUE
       RETURN
       END
```

```
$IBFTC AYGRD
      SUBROUTINE YGRD(X,N,Y,YG)
      INTEGER R,S,R1,S1,T1,S2,R2,T
      DIMENSION Y(100),YG(100),SFD2(20),SGD2(20),SHD1(20),SJD2(20)
      DIMENSION SFG2(20)
      COMMON U(20),CL(20),CK(20),FD3(10),GD2(10),HD2(10),ULIM,N1,BETAF,
     1BETAG,BETAJ,AF(3),AG(3),AH(2),NM,ERMINA,ERMINB,NS,PRNDTL,SPIN,H,
     2X1MAX,DX1,NM7,NM2,ALPHA(10),BETA(10),GAMMA(10),ALP(20),BET(20),
     3GAM(20),DELTA,YF1,YF2,YF3,YG1,YG2,YG3,YH1,YH2,MARK,XMAX,ER
      DO 1 I=1,N1
      YG(7*I-6)=Y(7*I-5)
C*****************************************************************
C     THESE OPERATIONS DEDUCE THE VALUE OF SFD2(I)
      SUM1=0.
      DO 2 S=1,I
      COUNT=0.
      DO3 R=1,S
      A=2*R-1
      R1=S-R+1
    3 COUNT=COUNT+A*Y(7*R1-6)*Y(7*R-6)
      S1=I-S
    2 SUM1=SUM1+CK(2*S1+1)*COUNT
      SUM2=0.
      DO 4 S=1,I
      COUNT=0.
      DO 5R=1,S
      R1=S-R+1
    5 COUNT=COUNT+CK(2*R-1)*Y(7*R1-5)
      S2=I-S+1
    4 SUM2=SUM2+Y(7*S2-2)*COUNT
      SUM3=0.
      IF(I.LE.1) GO TO 40
      IL=I-1
      DO 6 T=1,IL
      COUNT=0.
      DO 7 S=1,T
      TOLL=0.
      DO 8 R=1,S
      R1=S-R+1
    8 TOLL=TOLL+CK(2*R-1)*Y(7*R1-5)
      T1=T-S+1
    7 COUNT=COUNT+Y(7*T1-2)*TOLL
      R2=I-T
    6 SUM3=SUM3+CL(2*R2)*COUNT
   40  CONTINUE
      SUM4=0.
      DO 9 S=1,I
      COUNT=0.
      DO 10 R=1,S
      A=2*R-1
      R1=S-R+1
   10 COUNT=COUNT+A*CK(2*R-1)*Y(7*R1-4)
      S2=I-S+1
    9 SUM4=SUM4+Y(7*S2-4)*COUNT
      SUM5=0.
      IF(I.LE.1) GO TO 41
      IL=I-1
      DO 11 R=1,IL
      NC=I-R
```

```
   11 SUM5=SUM5+CK(2*NC+1)*SFD2(R)
   41  CONTINUE
       SUM6=0.
       IF(I.LE.1) GO TO 42
       DO 12 S=2.I
       COUNT=0.
       DO 13 R=2.S
       J=S R
   13 COUNT =COUNT+CL(2*R-2)*CK(2*J+1)
       S2=I-S+1
   12 SUM6=SUM6+SFD2(S2)*COUNT
   42  CONTINUE
       SFD2(I)=SUM1+SUM2+SUM3-SUM4-SUM5-SUM6
C*************************************************************************
       YG(7*I-5)=SFD2(I)
       YG(7*I-4)=Y(7*I-3)
C*************************************************************************
C      THESE OPERATIONS DEDUCE THE VALUES OF SGD2(I)
       SUM7=0.
       DO 14 S=1.I
       COUNT=0.
       DO 15 R=1.S
       A=2*R-1
       R1=S-R+1
   15 COUNT=COUNT+A*Y(7*R1-6)*Y(7*R-4)
       S1=I-S
   14 SUM7=SUM7+CK(2*S1+1)*COUNT
       SUM8=0.
       DO 16 S=1.I
       COUNT=0.
       DO 17 R=1.S
       R1=S-R+1
   17 COUNT=COUNT+CK(2*R-1)*Y(7*R1-3)
       S2=I-S+1
   16 SUM8=SUM8+Y(7*S2-2)*COUNT
       SUM9=0.
       IF(I.LE.1) GO TO 43
       IL=I-1
       DO 18 T=1.IL
       COUNT=0
       DO 19 S=1.T
       TOLL=0.
       DO 20 R=1.S
       R1=S-R+1
   20 TOLL=TOLL+CK(2*R-1)*Y(7*R1-3)
       T1=T-S+1
   19 COUNT=COUNT+Y(7*T1-2)*TOLL
       R2=I-T
   18 SUM9=SUM9+CL(2*R2)*COUNT
   43  CONTINUE
       SUM10=0.
       DO 21 S=1.I
       COUNT=0.
       DO 22 R=1.S
       A=2*R-1
       R1=S-R+1
   22 COUNT=COUNT+CK(2*R-1)*Y(7*R1-4)*A
       S2=I-S+1
   21 SUM10=SUM10+Y(7*S2-6)*COUNT
```

```
      SUM11=0.
      IF(I.LE.1) GO TO 44
      IL=I-1
      DO 23 R=1,IL
      NC=I-R
   23 SUM11=SUM11+CK(2*NC+1)*SFG2(R)
   44  CONTINUE
      SUM12=0.
      IF(I.LE.1) GO TO 45
      DO 24 S=2,I
      COUNT=0.
      DO 25 R=2,S
      J=S R
   25 COUNT=COUNT+CL(2*R-2)*CK(2*J+1)
      S2=I-S+1
   24 SUM12=SUM12 + SFG2(S2)*COUNT
   45  CONTINUE
      SGD2(I)=SUM7+SUM8+SUM9+SUM10-SUM11-SUM12
C*************************************************************************
      YG(7*I-3)=SGD2(I)
C*************************************************************************
C     THESE OPERATIONS DEDUCE THE VALUE OF SHD1(I)
      SUM13=0.
      DO 26 R=1,I
      A=2*R-1
      M=I R+1
   26 SUM13=SUM13+A*CK(2*R-1)*Y(7*M-6)
      SUM14=0.
      DO 27 R=1,I
      NC=I-R
      A=2*R-1
   27 SUM14=SUM14+A*CK(2*NC+1)*Y(7*R-6)
      SUM15=0.
      IF(I.LE.1) GO TO 46
      IL=I-1
      DO 28 R=1,IL
      NC=I-R
   28 SUM15=SUM15+CK(2*NC+1)*SHD1(R)
   46  CONTINUE
      SUM16=0.
      IF(I.LE.1) GO TO 47
      IL=I-1
      DO 29 S=1,IL
      COUNT=0.
      DO 30 R=1,S
      J=S R
   30 COUNT=COUNT+CL(2*R)*CK(2*J+1)
      NC=I-S
   29 SUM16=SUM16+SHD1(NC)*COUNT
   47  CONTINUE
      SHD1(I)=-(SUM13+SUM14+SUM15+SUM16)
C*************************************************************************
      YG(7*I-2)=SHD1(I)
      IF(MARK.EQ.0) GO TO 31
      YG(7*I-1)=Y(7*I)
C*************************************************************************
C     THESE OPERATIONS DEDUCE THE VALUE OF SJD2(I)
      SUM17=0.
      IF(I.LE.1) GO TO 48
```

```
      IL=I-1
      DO 32 R=1,IL
      M=I R+1
      A=I R
   32 SUM17=SUM17+2.*A *Y(7*M-1)*Y(7*R-6)
   48  CONTINUE
      SUM18=0.
      DO 33 R=1,I
      M=I R+1
   33 SUM18=SUM18+Y(7*R-2)*Y(7*M)
      SUM19=0.
      IF(I.LE.1) GO TO 49
      IL=I-1
      DO 34 S=1,IL
      COUNT=0.
      DO 35 R=1,S
      R1=S-R+1
   35 COUNT=COUNT+CL(2*R)*Y(7*R1-2)
      S1=I-S
   34 SUM19=SUM19+Y(7*S1)*COUNT
   49  CONTINUE
      SUM20=0.
      IF(I.LE.1) GO TO 50
      IL=I-1
      DO36 R=1,IL
      NC=I-R
   36 SUM20=SUM20+CL(2*R)*SJD2(NC)
   50  CONTINUE
      SJD2(I)=(SUM17+SUM18+SUM19)*PRNDTL-SUM20
C*****************************************************************
      YG(7*I)=SJD2(I)
      GO TO 1
   31 YG(7*I-1)=0.
      YG(7*I)=0.
    1 CONTINUE
      RETURN
      END
```

# APPENDIX E — TABLES

TABLE A1 HYDRODYNAMIC BOUNDARY VALUES DETERMINED BY THE FINITE DIFFERENCE TECHNIQUE AT DIFFERENT STEP LENGTHS IN $\eta$

| $\lambda$ | $\bar{f}''_1(0)$ | | $\bar{g}'_1(0)$ | |
|---|---|---|---|---|
| | $\Delta\eta$=0.05 | $\Delta\eta$=0.1 | $\Delta\eta$=0.05 | $\Delta\eta$=0.1 |
| 0 | 1.3119379 | 1.3119374 | -1.0746699 | -1.0746695 |
| 1 | 1.5739205 | 1.5739179 | -1.1099996 | -1.1099966 |
| 2 | 1.8237776 | 1.8237730 | -1.1416321 | -1.1416267 |
| 4 | 2.2956418 | 2.2956337 | -1.1968303 | -1.1968200 |
| 6 | 2.7392374 | 2.7392261 | -1.2442903 | -1.2442750 |
| 8 | 3.1612931 | 3.1612785 | -1.2862036 | -1.2861831 |
| 10 | 3.5661282 | 3.5661108 | -1.3239121 | -1.3238863 |

Here $\Delta\eta$ is the step length in $\eta$

TABLE A2A EFFECT OF PERTURBATION IN THE STAGNATION POINT BOUNDARY VALUES ON SUBSEQUENT SETS OF BOUNDARY VALUES

Pr=0.7 SPHERE SPIN PARAMETER =20

$\Delta\eta$=0.1

| n | $\bar{f}''_{2n-1}(0)$ | $\bar{g}'_{2n-1}(0)$ | $\mathcal{H}'_{2(n-1)}(0)$ |
|---|---|---|---|
| 1 | 5.412899+0.001 | -1.473053+0.001 | -0.8544438 |
| 2 | -2.31096518 | 0.57913570 | 0.16070610 |
| 3 | 0.22062158 | -0.06135499 | 0.00186987 |
| 4 | -0.01898456 | 0.00406639 | 0.00128056 |
| 5 | -0.00097326 | 0.00008463 | 0.00035491 |

| n | $\bar{f}''_{2n-1}(0)$ | $\bar{g}'_{2n-1}(0)$ | $\mathcal{H}'_{2(n-1)}(0)$ |
|---|---|---|---|
| 1 | 5.412899 | -1.473053 | -0.8538443 |
| 2 | -2.31059831 | 0.57925899 | 0.16053045 |
| 3 | 0.22065623 | -0.06135508 | 0.00186247 |
| 4 | -0.01897727 | 0.00406673 | 0.00127782 |
| 5 | -0.00097157 | 0.00008481 | 0.00035415 |

The perturbation of 0.001 applied to the stagnation point Hydrodynamic Boundary Values produces changes in magnitude of higher order Boundary Values that diminish with the order of the set.

TABLE A2B EFFECT OF STEP LENGTH IN THE DETERMINATION OF HYDRODYNAMIC BOUNDARY VALUES

EXAMPLE: DISK AT SPIN PARAMETER $\lambda$=10

| n | $\Delta\eta$ =0.05 | | $\Delta\eta$ =0.1 | |
|---|---|---|---|---|
| | $\bar{f}'(0)_{2n-1}$ | $\bar{g}'(0)_{2n-1}$ | $\bar{f}'(0)_{2n-1}$ | $\bar{g}'(0)_{2n-1}$ |
| 1 | 3.5661282 | -1.3239121 | 3.5661282 | -1.3239121 |
| 2 | 0.40359119 | 0.01519035 | 0.40356553 | 0.01519897 |
| 3 | 0.78632726 | -0.11760603 | 0.78627953 | -0.11760261 |
| 4 | 0.53010756 | -0.05690913 | 0.53004759 | -0.05690943 |

TABLE A3 HYDRODYNAMIC BOUNDARY VALUES OBTAINED IN THIS WORK FOR THE ROTATING SPHERE

| n | $\lambda$ =0 | | $\lambda$ =4 | |
|---|---|---|---|---|
| | $\bar{f}''(0)_{2n-1}$ | $\bar{g}'(0)_{2n-1}$ | $\bar{f}''(0)_{2n-1}$ | $\bar{g}'(0)_{2n-1}$ |
| 1 | 1.3119379 | -1.0746699 | 2.2956418 | -1.1968303 |
| 2 | -0.51493149 | 0.40904607 | -0.94961528 | 0.46275397 |
| 3 | 0.05518554 | -0.04565218 | 0.09457564 | -0.05028581 |
| 4 | -0.00340744 | 0.00249592 | -0.0072536 | 0.00305252 |
| 5 | 0.00001761 | -0.00006313 | -0.00023242 | -0.00000132 |

| n | $\lambda$ =10 | | $\lambda$ =20 | |
|---|---|---|---|---|
| | $\bar{f}''(0)_{2n-1}$ | $\bar{g}'(0)_{2n-1}$ | $\bar{f}''(0)_{2n-1}$ | $\bar{g}'(0)_{2n-1}$ |
| 1 | 3.5661282 | -1.3239121 | 5.412899 | -1.473053 |
| 2 | -1.50575806 | 0.51690354 | -2.31059831 | 0.57925899 |
| 3 | 0.14586501 | -0.05532342 | 0.22065623 | -0.06135508 |
| 4 | -0.01207448 | 0.00354708 | -0.01897727 | 0.00406673 |
| 5 | -0.00054029 | 0.00004496 | -0.00097157 | 0.00008481 |

TABLE A4 HYDRODYNAMIC BOUNDARY VALUES OBTAINED IN THIS WORK FOR THE ROTATING 10/16 SPHEROID

| n | $\lambda$=0 | | $\lambda$=4 | |
|---|---|---|---|---|
| | $\bar{f}''(0)_{2n-1}$ | $\bar{g}'(0)_{2n-1}$ | $\bar{f}''(0)_{2n-1}$ | $\bar{g}'(0)_{2n-1}$ |
| 1 | 1.3119379 | -1.0746699 | 2.295641 | -1.1968303 |
| 2 | 0,56832524 | 0.02245737 | 0.12156581 | 0.13110001 |
| 3 | 0.05633571 | 0.04060658 | 0.07410026 | 0.01114545 |
| 4 | -0.0637017 | 0,01922448 | -0.05278622 | 0.01756276 |
| 5 | -0.03982710 | -0.01741600 | -0.03933783 | 0.00552346 |

| n | $\lambda$ =10 | | $\lambda$ =20 | |
|---|---|---|---|---|
| | $\bar{f}''(0)_{2n-1}$ | $\bar{g}'(0)_{2n-1}$ | $\bar{f}''(0)_{2n-1}$ | $\bar{g}'(0)_{2n-1}$ |
| 1 | 3.5661282 | -1.3239121 | 5.412899 | -1.473053 |
| 2 | -0.34226400 | 0.2111732 | -0.93788628 | 0.28403871 |
| 3 | 0.04654178 | 0.00655384 | -0. 00160131 | 0.00828439 |

P.T.O.

TABLE A4 CONTD.

| | | | | |
|---|---|---|---|---|
| 4 | -0.4735341 | 0.01260456 | -0.05199464 | 0.00989630 |
| 5 | -0.03429896 | 0.00473313 | -0.02960490 | 0.00340387 |

TABLE A5 HYDRODYNAMIC BOUNDARY VALUES OBTAINED IN THIS WORK FOR THE ROTATING 7/16 SPHEROID

| n | $\lambda$ =0 | | $\lambda$ =4 | |
|---|---|---|---|---|
| | $\bar{f}''(0)_{2n-1}$ | $\bar{g}'(0)_{2n-1}$ | $\bar{f}''(0)_{2n-1}$ | $\bar{g}'(0)_{2n-1}$ |
| 1 | 1.3119379 | -1.0746699 | 2.2956418 | -1.1968303 |
| 2 | 0.92246687 | -0.10392741 | 0.47175962 | 0.02267467 |
| 3 | 0.40360124 | -0.01500268 | 0.40096051 | -0.04478149 |
| 4 | 0.10916821 | 0.00835195 | 0.12271956 | 0.02370544 |
| 5 | 0.0028244 | 0.00672740 | 0.00751562 | 0.00770972 |

| n | $\lambda$ =10 | |
|---|---|---|
| | $\bar{f}''(0)_{2n-1}$ | $\bar{g}'(0)_{2n-1}$ |
| 1 | 3.5661282 | -1.3239121 |
| 2 | 0.03810904 | 0.11122836 |
| 3 | 0.34538175 | -0.04077415 |
| 4 | 0.11681247 | 0.00340027 |
| 5 | 0.01527550 | 0.00433703 |

TABLE A6 HYDRODYNAMIC BOUNDARY VALUES OBTAINED IN THIS WORK FOR THE ROTATING DISK

| n | $\lambda=0$ | | $\lambda=4$ | |
|---|---|---|---|---|
| | $\bar{f}''(0)$ 2n-1 | $\bar{g}'(0)$ 2n-1 | $\bar{f}''(0)$ 2n-1 | $\bar{g}'(0)$ 2n-1 |
| 1 | 1.3119379 | -1.0746699 | 2.2956418 | -1.1968303 |
| 2 | 1.26272058 | -0.22535590 | 0.80822035 | -0.08149870 |
| 3 | 0.89825626 | -0.10733101 | 0.86982086 | -0.13379516 |
| 4 | 0.54971611 | -0.04404768 | 0.55915847 | -0.05415880 |
| 5 | 0.30789943 | -0.01816105 | 0.31623737 | -0.01883683 |

| n | $\lambda=10$ | |
|---|---|---|
| | $\bar{f}'(0)$ 2n-1 | $\bar{g}'(0)$ 2n-1 |
| 1 | 3.5661282 | -1.3239121 |
| 2 | 0.40356553 | 0.01519896 |
| 3 | 0.78627953 | -0.1160261 |
| 4 | 0.53004759 | -0.05690943 |
| 5 | 0.31858876 | -0.02467058 |

TABLE A7 HYDRODYNAMIC BOUNDARY VALUES OBTAINED FROM THE RESULTS PUBLISHED BY N.E. HOSKIN

| n | $\lambda=0$ | | $\lambda=4$ | | $\lambda=10$ | |
|---|---|---|---|---|---|---|
| | $\bar{f}''(0)$ 2n-1 | $\bar{g}'(0)$ 2n-1 | $\bar{f}''(0)$ 2n-1 | $\bar{g}'(0)$ 2n-1 | $\bar{f}'(0)$ 2n-1 | $\bar{g}'(0)$ 2n-1 |
| 1 | 1.311937 | -1.074673 | 2.295607 | -1.196812 | 3.566041 | -1.323862 |
| 2 | -0.51493 | 0.40905 | -0.94957 | 0.46274 | -1.50564 | 0.51686 |
| 3 | 0.05518 | -0.04566 | 0.09449 | -0.05028 | 0.14580 | -0.05530 |
| 4 | -0.003407 | 0.002497 | -0.007246 | 0.003051 | -0.012057 | 0.003541 |

COMPARISON OF HYDRODYNAMIC BOUNDARY VALUES OBTAINED IN THE PRESENT WORK WITH THOSE OF M.B. GREEN FOR STATIONARY BODIES ($\gamma_1=0$)

TABLE A8 SPHERE

| | Present work | GREEN |
|---|---|---|
| $\bar{f}''(0)$ | 1.3119379 | 1.31193778 |
| $\bar{f}_1''(0)$ | -0.51493149 | -0.514932 |
| $\bar{f}_3''(0)$ | 0.05518554 | 0.055191 |
| $\bar{f}_5''(0)$ | -0.00340744 | -0.0034077 |
| $\bar{f}_7''(0)$ | 0.00001761 | 0.00001766 |
| $\bar{f}_9''(0)$ | | |

TABLE A9 10/16 SPHEROID

| | Present work | GREEN |
|---|---|---|
| $\bar{f}''(0)$ | 1.3119379 | 1.31193778 |
| $\bar{f}_1''(0)$ | 0.56832524 | 0.568327 |
| $\bar{f}_3''(0)$ | 0.05633571 | 0.056338 |
| $\bar{f}_5''(0)$ | -0.0637017 | -0.0637018 |
| $\bar{f}_7''(0)$ | -0.03982710 | -0.039824 |
| $\bar{f}_9''(0)$ | | |

MASS TRANSFER BOUNDARY VALUES FROM THIS WORK FOR A BODY ROTATING IN AXIAL FLOW

ROTATING SPHERE

TABLE A10 $\lambda = 0$

| $\overline{Pr}$ | $\mathcal{H}_0'(0)$ | $\mathcal{H}_2'(0)$ | $\mathcal{H}_4'(0)$ | $\mathcal{H}_6'(0)$ | $\mathcal{H}_8'(0)$ |
|---|---|---|---|---|---|
| 0.7 | -0.6653791 | 0.12018440 | -0.00052872 | 0.00031080 | 0.00006869 |
| 1.0 | -0.7622323 | 0.13842343 | -0.00049288 | 0.00037691 | 0.00008265 |
| 2.4 | -1.0540565 | 0.19367218 | -0.00034402 | 0.00058481 | 0.00012656 |
| 10.0 | -1.7520560 | 0.32642113 | 0.00011529 | 0.00110717 | 0.00023740 |

TABLE A11 $\lambda = 4$

| $\overline{Pr}$ | $\mathcal{H}_0'(0)$ | $\mathcal{H}_2'(0)$ | $\mathcal{H}_4'(0)$ | $\mathcal{H}_6'(0)$ | $\mathcal{H}_8'(0)$ |
|---|---|---|---|---|---|
| 0.7 | -0.7222536 | 0.13302692 | 0.00048687 | 0.00070545 | 0.00018621 |
| 1.0 | -0.8339581 | 0.15475411 | 0.00078413 | 0.00086291 | 0.00022613 |
| 2.4 | -1.1752428 | 0.22175255 | 0.00177524 | 0.00136430 | 0.00035245 |
| 10.0 | -2.0052799 | 0.38617639 | 0.00438629 | 0.00263296 | 0.00067265 |

TABLE A12 $\lambda = 10$

| $\overline{Pr}$ | $\mathcal{H}_0'(0)$ | $\mathcal{H}_2'(0)$ | $\mathcal{H}_4'(0)$ | $\mathcal{H}_6'(0)$ | $\mathcal{H}_8'(0)$ |
|---|---|---|---|---|---|
| 0.7 | -0.7823546 | 0.14581080 | 0.00121761 | 0.00100230 | 0.00027449 |
| 1.0 | -0.9096637 | 0.17099313 | 0.00171362 | 0.00122819 | 0.00033431 |
| 2.4 | -1.3020224 | 0.24942729 | 0.00331703 | 0.00194831 | 0.00052316 |
| 10.0 | -2.2631296 | 0.44335406 | 0.00740639 | 0.00375817 | 0.00099952 |

TABLE A13 $\lambda = 20$

| $\overline{Pr}$ | $\mathcal{H}_0'(0)$ | $\mathcal{H}_2'(0)$ | $\mathcal{H}_4'(0)$ | $\mathcal{H}_6'(0)$ | $\mathcal{H}_8'(0)$ |
|---|---|---|---|---|---|
| 0.7 | -0.8538443 | 0.16053045 | 0.00186247 | 0.00127782 | 0.00035415 |
| 1.0 | -0.9995774 | 0.18964794 | 0.00255158 | 0.00156582 | 0.00043260 |

## ROTATING 10/16 SPHEROID

TABLE A14 $\lambda = 0$

| Pr | $\mathcal{H}_0'(0)$ | $\mathcal{H}_2'(0)$ | $\mathcal{H}_4'(0)$ | $\mathcal{H}_6'(0)$ | $\mathcal{H}_8'(0)$ |
|---|---|---|---|---|---|
| 0.7 | -0.6653791 | -0.11650395 | 0.00514005 | 0.01294637 | 0.00490551 |
| 1.0 | -0.7622323 | -0.13544257 | 0.00574065 | 0.01511480 | 0.00576784 |
| 2.4 | -1.0540565 | -0.19328449 | 0.00747577 | 0.02175746 | 0.00842837 |
| 10.0 | -1.7520560 | -0.33323211 | 0.01148315 | 0.03788391 | 0.01492877 |

TABLE A15 $\lambda = 4$

| Pr | $\mathcal{H}_0'(0)$ | $\mathcal{H}_2'(0)$ | $\mathcal{H}_4'(0)$ | $\mathcal{H}_6'(0)$ | $\mathcal{H}_8'(0)$ |
|---|---|---|---|---|---|
| 0.7 | -0.7222536 | -0.07026894 | -0.00225195 | 0.01019847 | 0.00526826 |
| 1.0 | -0.8339581 | -0.07789398 | -0.00333826 | 0.01173301 | 0.00620842 |
| 2.4 | -1.1752428 | -0.09889684 | -0.00685136 | 0.01627838 | 0.00911469 |
| 10.0 | -2.0052799 | -0.14353422 | -0.01527517 | 0.02671182 | 0.01620047 |

TABLE A16 $\lambda = 10$

| Pr | $\mathcal{H}_0'(0)$ | $\mathcal{H}_2'(0)$ | $\mathcal{H}_4'(0)$ | $\mathcal{H}_6'(0)$ | $\mathcal{H}_8'(0)$ |
|---|---|---|---|---|---|
| 0.7 | -0.7823546 | -0.03903868 | 0.00079316 | 0.00767737 | 0.00435193 |
| 1.0 | -0.9096637 | -0.03916693 | 0.0050511 | 0.00866027 | 0.00508322 |
| 2.4 | -1.3020224 | -0.03678245 | -0.00003874 | 0.01149082 | 0.00729483 |
| 5.0 | -1.7379232 | -0.03216864 | 0.00000263 | 0.01444914 | 0.00967956 |
| 10.0 | -2.2631296 | -0.02597013 | 0.00067704 | 0.01792865 | 0.01248063 |

TABLE A17 $\lambda = 20$

| Pr | $\mathcal{H}_0'(0)$ | $\mathcal{H}_2'(0)$ | $\mathcal{H}_4'(0)$ | $\mathcal{H}_6'(0)$ | $\mathcal{H}_8'(0)$ |
|---|---|---|---|---|---|
| 1.0 | -0.9995774 | -0.00751006 | 0.00721222 | 0.00760370 | 0.00395322 |
| 2.4 | -1.4512496 | 0.01281388 | 0.01122729 | 0.01005328 | 0.00553262 |

## ROTATING 7/16 SPHEROID

TABLE A18 $\lambda = 0$

| $\overline{Pr}$ | $\mathcal{H}_0'(0)$ | $\mathcal{H}_2'(0)$ | $\mathcal{H}_4'(0)$ | $\mathcal{H}_6'(0)$ | $\mathcal{H}_8'(0)$ |
|---|---|---|---|---|---|
| 0.7 | -0.6653791 | -0.19388283 | -0.04424596 | -0.00312194 | 0.00356198 |
| 1.0 | -0.7622323 | -0.22497569 | -0.05181952 | -0.00372514 | 0.00416779 |
| 2.4 | -1.0540565 | -0.31978957 | -0.07511964 | -0.00562762 | 0.00601658 |
| 10.0 | -1.7520560 | -0.54888798 | -0.13183694 | -0.01034652 | 0.01049650 |

TABLE A19 $\lambda = 4$

| $\overline{Pr}$ | $\mathcal{H}_0'(0)$ | $\mathcal{H}_2'(0)$ | $\mathcal{H}_4'(0)$ | $\mathcal{H}_6'(0)$ | $\mathcal{H}_8'(0)$ |
|---|---|---|---|---|---|
| 1.0 | -0.8339581 | -0.15395200 | -0.05822742 | -0.00964519 | 0.00371851 |
| 2.4 | -1.1752428 | -0.20372452 | -0.08500427 | -0.01515818 | 0.00525469 |
| 10.0 | -2.0052799 | -0.31670883 | -0.14905719 | -0.02952409 | 0.00876203 |

TABLE A20 $\lambda = 10.0$

| $\overline{Pr}$ | $\mathcal{H}_0'(0)$ | $\mathcal{H}_2'(0)$ | $\mathcal{H}_4'(0)$ | $\mathcal{H}_6'(0)$ | $\mathcal{H}_8'(0)$ |
|---|---|---|---|---|---|
| 0.7 | -0.7823546 | -0.09947024 | -0.04017837 | -0.0097853 | 0.00088969 |
| 1.0 | -0.9096637 | -0.10787310 | -0.04668293 | -0.01185896 | 0.00089466 |
| 2.4 | -1.3020224 | -0.13035101 | -0.06583445 | -0.01842862 | 0.00077430 |
| 10.0 | -2.2631296 | -0.17940304 | -0.10878970 | -0.03462101 | -0.00001409 |

## ROTATING DISK

TABLE A21 $\lambda = 0$

| $\overline{Pr}$ | $\mathcal{H}_0'(0)$ | $\mathcal{H}_2'(0)$ | $\mathcal{H}_4'(0)$ | $\mathcal{H}_6'(0)$ | $\mathcal{H}_8'(0)$ |
|---|---|---|---|---|---|
| 0.7 | -0.6653791 | -0.26822725 | -0.11547782 | -0.04894460 | -0.02043835 |
| 1.0 | -0.7622323 | -0.31099770 | -0.13478469 | -0.05732566 | -0.02398761 |
| 2.4 | -1.0540565 | -0.44133366 | -0.19399902 | -0.08314775 | -0.03497659 |
| 10.0 | -1.7520560 | -0.75608675 | -0.33778319 | -0.14609302 | -0.06186496 |

TABLE A22 $\lambda = 4$

| $\overline{Pr}$ | $\mathcal{H}_0'(0)$ | $\mathcal{H}_2'(0)$ | $\mathcal{H}_4'(0)$ | $\mathcal{H}_6'(0)$ | $\mathcal{H}_8'(0)$ |
|---|---|---|---|---|---|
| 0.7 | -0.7222536 | -0.20058679 | -0.11638018 | -0.05508944 | -0.02191945 |
| 1.0 | -0.8339581 | -0.22702737 | -0.13581518 | -0.06483970 | -0.02580240 |
| 2.4 | -1.1752428 | -0.30444132 | -0.19505780 | -0.09515536 | -0.03792678 |
| 10.0 | -2.0052799 | -0.48309229 | -0.33670393 | -0.17000567 | -0.06810557 |

TABLE A23 $\lambda = 10.0$

| $\overline{Pr}$ | $\mathcal{H}_0'(0)$ | $\mathcal{H}_2'(0)$ | $\mathcal{H}_4'(0)$ | $\mathcal{H}_6'(0)$ | $\mathcal{H}_8'(0)$ |
|---|---|---|---|---|---|
| 0.7 | -0.7823546 | -0.15753194 | -0.09849557 | -0.05336661 | -0.02486908 |
| 1.0 | -0.9096637 | -0.17388492 | -0.11373926 | -0.06264588 | -0.02936759 |
| 2.4 | -1.3020222 | -0.22025023 | -0.15907962 | -0.09121382 | -0.04345933 |
| 10.0 | -2.2631296 | -0.32681898 | -0.26375118 | -0.16013323 | -0.07849462 |

COMPARISON OF MASS TRANSFER BOUNDARY VALUES OBTAINED IN THIS WORK WITH THOSE OBTAINED FROM THE RESULTS OF J. SIEKMANN -

TABLE A24 $\lambda = 0$ $\mathcal{H}'^{(0)}_{2n-1}$

| n | $\overline{Pr}$ NUMBER=0.7 | | $\overline{Pr}$ NUMBER=1.0 | |
|---|---|---|---|---|
| | SIEKMANN | PRESENT WORK | SIEKMANN | PRESENT WORK |
| 1 | -0.66538 | -0.6653791 | -0.76223 | -0.7622323 |
| 2 | 0.120183 | 0.12018440 | 0.138423 | 0.13842343 |
| 3 | -0.0005278 | -0.0052872 | -0.0004925 | -0.00049288 |
| 4 | 0.0003106 | 0.00031080 | 0.0003769 | 0.00037691 |

TABLE A25 $\lambda = 4$ $\mathcal{H}'^{(0)}_{2n-1}$

| n | Pr NUMBER=0.7 | | Pr NUMBER=1.0 | |
|---|---|---|---|---|
| | SIEKMANN | PRESENT WORK | SIEKMANN | PRESENT WORK |
| 1 | -0.72225 | -0.7222536 | -0.83396 | -0.8339581 |
| 2 | 0.133023 | 0.13302692 | 0.154758 | 0.15475411 |
| 3 | 0.000488 | 0.00048687 | 0.000782 | 0.00078413 |
| 4 | 0.000705 | 0.00070545 | 0.000863 | 0.00086291 |

TABLE A26 VALUES OF $\mathcal{H}'^{(0)}_{2n-1}$ OBTAINED FROM THE RESULTS OF M.B. GREEN

NON-ROTATING BODY ($\lambda=0$) AND $\overline{Pr}=2.4$

| e | $\mathcal{H}'^{(0)}_0$ | $\mathcal{H}'^{(0)}_2$ | $\mathcal{H}'^{(0)}_4$ | $\mathcal{H}'^{(0)}_6$ | $\mathcal{H}'^{(0)}_8$ |
|---|---|---|---|---|---|
| 16/16 | -1.0540568 | 0.19367372 | -0.00034450 | 0.00058491 | 0.00012656 |
| 10/16 | -1.0540568 | -0.19328622 | 0.00747486 | 0.02175767 | 0.00842871 |
| 7/16 | -1.0540568 | -0.31980601 | -0.07512401 | -0.00563054 | 0.00601465 |
| 0 | -1.0540568 | -0.44133645 | -0.19400464 | -0.08315717 | -0.03498764 |

TABLE Q1 HYDRODYNAMIC BOUNDARY VALUES FOR SPHERES AND SPHEROIDS FOR A BODY ROTATING IN A QUIESCENT FLUID

| n | SPHERE | |
|---|---|---|
| | $F'(0)_{2n-1}$ | $G'(0)_{2n-1}$ |
| 1 | 0.510233 | -0.615922 |
| 2 | -0.22128535 | 0.24764359 |
| 3 | 0.02071030 | -0.02568883 |
| 4 | -0.00189041 | 0.00181337 |
| 5 | -0.00011500 | 0.00005874 |

| n | 13/16 spheroid | | 10/16 spheroid | |
|---|---|---|---|---|
| | $F'(0)_{2n-1}$ | $G'(0)_{2n-1}$ | $F'(0)_{2n-1}$ | $G'(0)_{2n-1}$ |
| 1 | 0.510233 | -0.615922 | 0.510233 | -0.615922 |
| 2 | -0.17498281 | 0.19836964 | -0.13826011 | 0.15929029 |
| 3 | -0.00463608 | 0.00052399 | -0.01027722 | 0.00723751 |
| 4 | 0.00022246 | -0.00087010 | -0.00351567 | 0.00246100 |
| 5 | 0.00038765 | -0.00038382 | | |

MASS TRANSFER BOUNDARY VALUES FOR A BODY ROTATING IN A QUIESCENT FLUID

TABLE Q2 SPHERE

| $\overline{Pr}$ | $J'(0)_0$ | $J'(0)_2$ | $J'(0)_4$ | $J'(0)_6$ |
|---|---|---|---|---|
| 0.7 | -0.3231282 | 0.06263696 | 0.00131540 | 0.00064938 |
| 1.0 | -0.3962497 | 0.07740489 | 0.00170243 | 0.00081600 |
| 2.4 | -0.6161803 | 0.12231316 | 0.00289547 | 0.00132705 |
| 5.0 | -0.8533008 | 0.17111046 | 0.00420973 | 0.00188554 |
| 10.0 | -1.1341205 | 0.22908211 | 0.00578016 | 0.00255053 |
| 100.0 | -2.6871403 | 0.55026723 | 0.01450176 | 0.00623599 |

TABLE Q3 13/16 SPHEROID

| $\overline{Pr}$ | $J'(0)_0$ | $J'(0)_2$ | $J'(0)_4$ | $J'(0)_6$ |
|---|---|---|---|---|
| 0.7 | -0.3231282 | 0.04135005 | 0.00820515 | 0.00084636 |
| 1.0 | -0.3962497 | 0.05109924 | 0.01025836 | 0.00107512 |
| 2.4 | -0.6161803 | 0.08074575 | 0.01656017 | 0.00177875 |
| 5.0 | -0.8533008 | 0.11295961 | 0.02345396 | 0.00255169 |
| 10.0 | -1.1341205 | 0.15122996 | 0.03166648 | 0.00347438 |
| 100.0 | -2.6871403 | 0.36326230 | 0.07723315 | 0.00859723 |

TABLE Q4 10/16 SPHEROID

| $\overline{Pr}$ | $J'(0)_0$ | $J'(0)_2$ | $J'(0)_4$ | $J'(0)_6$ |
|---|---|---|---|---|
| 0.7 | -0.3231282 | 0.02446729 | 0.00829817 | 0.00207073 |
| 1.0 | -0.3962497 | 0.03023611 | 0.01035678 | 0.00260928 |
| 2.4 | -0.6161803 | 0.04777851 | 0.01667344 | 0.00427122 |
| 5.0 | -0.8533008 | 0.06683997 | 0.02358063 | 0.00609709 |
| 10.0 | -1.1341205 | 0.08948515 | 0.03180766 | 0.00827644 |
| 100.0 | -2.6871403 | 0.21494808 | 0.07745225 | 0.02038121 |

BODY ROTATING IN A QUIESCENT FLUID. COMPARISON OF BOUNDARY VALUES OBTAINED IN THIS WORK WITH THOSE OF W.H.H. BANKS

TABLE Q6. Hydrodynamic Boundary Values

| n | Present Work | | W.H.H. BANKS | |
|---|---|---|---|---|
| | $F'(0)_{2n-1}$ | $G'(0)_{2n-1}$ | $F'(0)_{2n-1}$ | $G'(0)_{2n-1}$ |
| 1 | 0.510233 | -0.615922 | 0.51023 | -0.61592 |
| 2 | -0.22128535 | 0.24764359 | -0.22129 | 0.24765 |
| 3 | 0.02071030 | -0.02568883 | 0.02071 | -0.02569 |
| 4 | -0.00189041 | 0.00181337 | -0.00189 | 0.00181 |

TABLE Q7. Mass (or Heat Transfer Boundary Values ). $J'(0)_{2n-1}$

| n | $\overline{Pr}$=0.7 | | $\overline{Pr}$=1.0 | |
|---|---|---|---|---|
| | Present Work | BANKS | Present Work | BANKS |
| 1 | -0.3231282 | -0.32312 | -0.3962497 | -0.39625 |
| 2 | 0.06263696 | 0.06263 | 0.07740489 | 0.07741 |
| 3 | 0.00131540 | 0.00132 | 0.00170243 | 0.00170 |
| 4 | 0.00064938 | 0.00065 | 0.000816 | 0.00082 |

TABLE Q5 Overall Values of Mass Transfer Number

| $\overline{Pr}$ \ e | 16/16 | 13/16 | 10/16 |
|---|---|---|---|
| 0.7 | 0.19608 | 0.20736 | 0.22233 |
| 1.0 | 0.21285 | 0.22516 | 0.24154 |
| 2.4 | 0.24567 | 0.26007 | 0.27927 |
| 5.0 | 0.26533 | 0.28101 | 0.30196 |
| 10.0 | 0.27911 | 0.29570 | 0.31789 |
| 100.0 | 0.30533 | 0.32369 | 0.34827 |
| $\infty$ | 0.33260 | 0.34564 | 0.37215 |

TABLE Q8 EFFECT OF STEP LENGTH IN THE DETERMINATION OF HYDRODYNAMIC BOUNDARY VALUES FOR A BODY ROTATING IN A QUIESCENT FLUID

| n | $\Delta\alpha$ =0.05 | | $\Delta\alpha$ =0.1 | |
|---|---|---|---|---|
| | F'(0) 2n-1 | G'(0) 2n-1 | F'(0) 2n-1 | G'(0) 2n-1 |
| 1 | 0.510233 | -0.615922 | 0.510233 | -0.615922 |
| 2 | -0.17498281 | 0.19836964 | -0.17498281 | 0.1983694 |
| 3 | -0.00463616 | 0.00052397 | -0.00463608 | 0.00052399 |

Here $\Delta\alpha$ is the step length in $\alpha$

The above example applies to a 13/16 spheroid .

## LIST OF FIGURES


| | | Page No. |
|---|---|---|
| 4. 1 | $\bar{f}_1$ Determined in successive iterations by quasilinearisation. | 97 |
| 4. 2 | $\bar{f}_1'$ Determination by quasilinearisation. | 97 |
| 4. 3 | $\bar{f}_1''$ Determined by quasilinearisation. | 98 |
| 4. 4 | $\bar{g}_1'$ Determination by quasilinearisation. | 99 |
| 4. 5 | $\bar{g}_1$ Determination by quasilinearisation. | 100 |
| 5. 1 | Effect of spin parameter $\lambda$ on $\bar{f}_1'$ | 146 |
| 5. 2 | $\bar{f}_1''$ Shown as a function of $\eta$ for spin parameters 0 to 20. | 147 |
| 5. 3 | Effect of spin parameter $\lambda$ on $\bar{g}_1$. | 148 |
| 5. 4 | Effect of spin parameter $\lambda$ on $-\bar{g}_1'$. | 148 |
| 5. 5 | Effect of spin parameter $\lambda$ on $\mathcal{H}_0$. | 149 |
| 5. 6 | $-\mathcal{H}_0'(\eta)/Sc$ shown as a function of $\eta$ for spin parameters of 20 and 0. | 150 |
| 5. 7 | Effect of Schmidt number on $J_o(\alpha)$. | 151 |
| 5. 8 | Effect of Schmidt number on $-J_o(\alpha)/Sc^{1/3}$. | 151 |
| 5. 9 | Dimensionless meridional velocity component distributions for the sphere. | 152 |
| 5.10 | Effect of spin parameter $\lambda$ on $M_A$ for the sphere at Schmidt No. 0.7. | 153 |
| 5.11 | Effect of spin parameter $\lambda$ on $M_A$ for sphere at Schmidt No. 1.0. | 154 |
| 5.12 | Effect of spin parameter $\lambda$ on $M_A$ for the sphere at Schmidt No. 10. | 155 |
| 5.13 | Effect of spin parameter $\lambda$ on $M_A$ for infinite Schmidt number. | 156 |

Page No.


5.14 Effect of spin parameter $\lambda$ on $M_A$ for 10/16 spheroid Schmidt No. 1.0. 157

5.15 Effect of spin parameter $\lambda$ on $M_A$ for 10/16 spheroid at Schmidt No. 10. 158

5.16 Effect of spin parameter $\lambda$ on $M_A$ for 10/16 spheroid at infinite Schmidt No. 159

5.17 Effect of spin parameter $\lambda$ on $M_A$ for 7/16 spheroid at Schmidt No. 1.0. 160

5.18 Effect of spin parameter $\lambda$ on $M_A$ for disk at Schmidt No. 0.7. 161

5.19 Plots of $M_Q$ against $\theta$ for the sphere at Schmidt numbers 0.7 to $\infty$ . 162

5.20 Plots of $M_Q$ against $\theta$ for the 10/16 spheroid at Schmidt numbers 0.7 to $\infty$ . 163

5.21 $\overline{M}_Q^o$ Shown as a function of shape and Schmidt number. 166

5.22 Effect of the number of terms in series for $M_A$. 164

5.23 Effect of the number of terms in series for $M_Q$ 165

## LIST OF SYMBOLS

$a$ - Radius of sphere or semi-major axis of an oblate spheroid.

$\bar{a}$ - Value of $dU/dx$ at $x=0$

A,B - Constants in eqn.(2-1)

ALPHA(I) - Used in computer programme to denote values of $\bar{f}''_{2I-1}(0)$ i.e., Y(7I-4) for body rotating in axial flow or $F'_{2I-1}(0)$ i.e., Y(7I-5) for body rotating in a quiescent fluid.

b - Semi-minor axis of an oblate spheroid

BETA(I) - Used in computer programme to denote values of $\bar{g}'_{2I-1}(0)$ i.e., Y(7I-2) for body rotating in axial flow or $G'_{2I-1}(0)$ i.e., Y(7I-3) for body rotating in a quiescent fluid.

c - Constant

D - Diameter of a sphere

e - Ratio of semi-minor to semi-major axis for oblate spheroid i.e., b/a.

$f_1, f_3$ - Coefficients in power series for the dimensionless stream function $\psi^*$.

$\bar{f}_{2n-1}$ - Product of $U_{2n-1}\ f_{2n-1}$

$F_1, F_3, \ldots$ - Coefficients in power series for $V_1^*$ for a body rotating in a quiescent fluid.

$g_1, g_3, \ldots$ - Coefficients in power series for $V_2^*$ for body rotating in axial flow.

$\bar{g}_{2n-1}$ - Product of $k_{2n-1}\ g_{2n-1}$

$G_1, G_3, \ldots$ - Coefficients in power series for $V_2^*$ for a body rotating in a quiescent fluid.

GAMMA(I)... - Used in computer programme to denote $\mathcal{H}'_{2(I-1)}(0)$ or $J'_{2(I-1)}(0)$ i.e., both Y(7I).

$h_c$ - local heat transfer or mass transfer coefficient.

$h_1, h_2, h_3$ - Scale factors in directions $X_1, X_2, X_3$.

$h_1^*, h_2^*, h_3^*$ - Dimensionless scale factors $h_1^*/L_c$, $h_2^*/L_c$, $h_3^*/L_c$.

$h_{\xi,0}, h_{\theta,0}, h_{\phi,0}$ - Scale factors on surface of oblate spheroid.

$h_{1,0}, h_{2,0}$ - Scale factors on body surface in directions $X_1, X_2$ respectively.

$H_0, H_2, \ldots$ - Coefficients in power series for $V_N^*$ body rotating in a quiescent fluid.

$J_0, J_2, \ldots$ - Coefficients in power series expansion for $X^*$, body rotating in a quiescent fluid.

J - Jacobi matrix defined in (4-12).

$K_T$ - Thermal Conductivity

$K_1, K_3$ - Coefficients in power series expansion for $h_{2,0}^*$

$\hat{K}_1, \hat{K}_3$ - Coefficients in power series expansion for $h_{2,0}$

K(e) - Function of e as defined in (3-191)

$l_0, l_2, \ldots$ - Coefficients in power series for $h_{1,0}^*$

$\hat{l}_0, \hat{l}_2, \ldots$ - Coefficients in power series for $h_{1,0}$

$L_c$ - Characteristic dimension - semi-major axis a for the oblate spheroid.

M - Mass or heat transfer number $\dfrac{\overline{Nu}}{\overline{R}_e \cdot \overline{Pr}^{1/3}}$

NM - Maximum number of equations to be solved.

NM2 - Number of pairs of $\bar{f}''_{2n-1}(0)$, $\bar{g}'_{2n-1}(0)$ supplied initially to computer programme.

NM7 - Number of $\mathcal{H}'_{2(n-1)}(0)$ supplied initially to computer programme.

N - Distance normal from body surface.

$N^*$ - Dimensionless distance normal from body surface, $N/L_c$.

Nu, $\overline{Nu}$ - Local Nusselt or Sherwood number $h_c L_c/\alpha_v$.

$Nu_o$ - Overall Nusselt number

P - Pressure

$P^*$ - Dimensionless pressure $P/\rho U_c^2$

Pr - Prandtl number $\nu/\alpha_v$

$\overline{Pr}$ Prandtl or Schmidt number $\nu/\alpha_v$ or $\nu/\mathcal{D}$

$q(x_1)$ - Heat flux or mass flux per unit area at $x_1$ on body surface.

R - Spin Reynolds number $\Omega d^2/\nu$

$R_s$ - Spin Reynolds number $L_c \cdot L_c \Omega / \nu$

$\overline{R_s}$ - Spin Reynolds number $2L_c \cdot L_c \Omega/\nu$

$R_e$ - Axial Reynolds number $U_c L_c/\nu$

$\overline{R_e}$ - Axial Reynolds number $2L_c \cdot U_c/\nu$

$r,\theta,\phi$ - Spherical polar co-ordinates

$r(x_1)$ - Normal distance from axis of symmetry to point at $X_1$ on body surface.

$r^*(x_1^*)$ - Given by $r(x_1)/L_c$

$r_1, r_3, \ldots$ - Coefficients in power series expansion for $r^*(x_1^*)$.

Sc - Schmidt number

Sh - Sherwood number $h_c L_c/\alpha_v$

t - time

T - Torque

$T_W$ - Absolute temperature at body surface.

$T_A$ - Absolute temperature in Main Stream.

U - Potential flow

$U_c$ - Characteristic velocity

$U^*$ - Dimensionless potential flow

$U_1, U_3, \ldots$ - Coefficients in power series for $U^*$.

$\overline{U}_1, \overline{U}_3, \ldots$ - Coefficients in power series for U.

u,v,w. - Components of velocity in directions $r,\theta,\phi$ respectively.

$\underline{v}$ - Velocity vector of fluid particle at $x_1, x_2, x_3$.

$V_1, V_2, V_3$ - Components of velocity in directions $X_1, X_2, X_3$.

$V_1^*, V_2^*, V_3^*$ - Dimensionless velocity components, $\frac{V_1}{U_c}, \frac{V_2}{U_c}, \frac{V_3}{U_c}$ for body in axial flow $\frac{V_1}{V_s}, \frac{V_2}{V_s}, \frac{V_3}{V_s}$

for body rotating in a quiescent fluid.

$V_s$ - Characteristic spin velocity.

$V_N$ - Component of velocity normal to body surface.

$V$ - Component of velocity in direction of co-ordinate

$V_\alpha$ - Component of velocity in direction of co-ordinate $\alpha$.

$V_3^{**}$ - Defined $V_3^* R_e^{\frac{1}{2}}$

$x$ - Distance along meridian from front stagnation point.

$X_1, X_2, X_3$ - General orthogonal curvilinear co-ordinate system.

$X_1^*, X_2^*, X_3^*$ - Dimensionless co-ordinates $\frac{x_1}{L_c}, \frac{x_2}{L_c}, \frac{x_3}{L_c}$.

$X_3^{**}$ - Defined $X_3^* R_e^{\frac{1}{2}}$.

$\overline{Y}$ - Column vector

$\underline{YG}$ - Differential of $\underline{Y}$ with respect to $\eta$ or $\alpha$ i.e. $\frac{d\underline{Y}}{d\alpha}$ or $\frac{d\underline{Y}}{d\eta}$.

$Z$ - Dimensionless distance from sphere surface.

$\underline{Z}$ - An n-dimensional vector, see (4-8).

Greek Symbols

$\alpha_v$ - Mass or heat diffusivity.

$\alpha_c, \beta_c, \gamma_c, \rho_c, \epsilon_c, \epsilon_c'$ - Constants of integration used in superposition principle, Chapter 4.

$\alpha$ - Dimensionless normal distance from body surface for body rotating in a quiescent fluid given by $N^* R_s^{\frac{1}{2}}$.

$\delta$ - Boundary layer thickness.

$\delta^*$ - Dimensionless boundary layer thickness.

$\eta$ - Dimensionless distance from body surface for body rotating in axial flow given by $N^* R_e^{\frac{1}{2}}$.

$\lambda$ - Spin parameter $(\Omega L_c/U_c)^2$

$\Omega$ - Angular velocity

$\mu$ - Viscosity of fluid

$\nu$ - Kinematic viscosity

$\xi, \theta, \phi$ - oblate spheroidal co-ordinates

$\rho$ - Density of fluid

$X^*$ - Dimensionless temperature or concentration distribution

$\kappa^*$ - Dimensionless stream functions

$\nabla$ - Vector operator del

Other Symbols

$\mathcal{D}$ - Mass or heat diffusivity

$\mathcal{H}_{2(n-1)}$ - Coefficients in power series expansion for $X^*$ for a body rotating in axial flow.

Subscripts

A - Axial flow

h - Homogeneous function

H - Heat transfer

i - An integer $\geqslant 1$

I - An integer $\geqslant 1$

IMP - Improved estimate

M - Mass transfer

n - An integer $\geqslant 1$

O - Overall value

P - Particular solution

Q - Quiescent fluid

S - Conditions at body surface

$\infty$ - Conditions in main stream or infinity

Superscripts

A - Body in axial flow

K+1 - K+1th iteration

O - Overall value

q - Body in quiescent fluid

* - Dimensionless variables

# BIBLIOGRAPHY


(1845) STOKES, G.G., Trans. Camb. Phil. Soc., 8, pp.287-319 or Mathematical and Physical papers (collected) 1, p.75.

(1904) PRANDTL, L., Proc. III Intern. Math. Congr. Heidelberg, Translation N.A.C.A. Tech. Mem., 452, (1928).

(1921) POHLHAUSEN, K., Z.A.M.M., 1, p.252.

(1921) KARMAN, T. VON, Z.A.M.M., 1, p.237.

(1922-23) JEFFERY, G.B., Proc. Roy. Soc., 102, p.161.

(1927) WEILSELBERGER, C., Phys. Z., 28, p.84.

(1932) MILLIKAN, C.B., Amer. Soc. Mech. Engrs. Trans., 54, p.29.

(1934) COCHRAN, W.G., Proc. Camb. Phil. Soc., 30, p.365.

(1935) LUTHANDER, S. and RYDBERG, A., Phys. Z., 36, p.552.

(1936) TOMOTIKA, S., Aero. Res. Council Rep. and Memo., 1678.

(1938) FROSSLING, N., Gerlands Beitr., Geophys., 52, p.170.

(1938) MILNE-THOMSON, 'Theoretical Hydrodynamics, MacMillan & Co.

(1946) KRAMERS, H., Physica Grav., 12, p.61.

(1948) WAGNER, C., J. Appl. Phys., 19, p.837.

(1949) SCHOLKEMEIR, F.W., Arch. D. Math., 1, p.270.

(1950) LINTON, W.H. and SHERWOOD, T.K., Chem. Eng. Progr., 46, p.258.

(1950) N.A.C.A. TECHMEMO. 1256.

(1951) HOWARTH, L., Phil. Mag., 42, pp.1308-1315.

(1952) HANNAH, D.M., A.R.C. Tech. Rept., R. and M. No.2772.

(1952) TIFFORD, A.N. and CHU, S.T., J. Aero. Sci., 19, pp.284-285.

(1952) SCHLICHTING, H. and TRUCKENHRODT, E., S.A.M.M., 32, pp.97-117.

(1952) MILLSAPS, K. and POHLHAUSEN, K., J. Aero. Sci., 19, p.120.

(1953) AKSEL'RUD, S.A., Zh. Fiz. Khim., 27, p.1445.

(1953) TIFFORD, A.N. and CHU, S.T., Proc. Third Midwestern Conf. on Fluid Mechanics, p.579.

(1953) ILLINGWORTH, C.R., Phil. Mag., Series 7, Vol.XLIV, pp.389-403.

(1954) NIGAM, S.D.N., Z.A.M.P., 5, pp.151-155.

(1954) FADNIS, B.S.F., Z.A.M.P., 5, pp.156-163.

(1955) HOSKIN, N.E., 50 Jahre Grenzschichtforschung (Freidr. Vieweg. V. Sohn. Braunschweig).

(1955) HU , S. and KITNER, R.C., A.I. Che. Journal, 1, p.42.

(1956) GEIS, T., J. Ratl. Mech. Anal., 5, p.678.

(1956) SCHLICHTING, H., N.A.C.A. Tech. Mem. 1415.

(1956) YAMAGA, J., Journal of Mech. Lab. No.1, 2, p.1.

(1956) COBB, E.C. and SAUNDERS, O.A., Proc. Roy. Soc., A236, p.343.

(1956) SUBRAMINUJAN, V., KRISHNA, M.S. and ADIVARAHAN, P., Indian Journ. Tech., 4, pp.353-358.

(1956) KNOPP, Prof. Konrad, 'Infinite Sequencies and Series', Dover Publications, N.Y.

(1957) STEWARTSON, K., Boundary Layer Research, I.U.A.T.M. Symposium Freiburg/BR., p.59.

(1957) KOBASHI, Y., J. Sci., Hiroshima Univ., A20, p.149.

(1958) OSTRACH, S. and THORNTON, P.R., N.A.C.A. Tech. Note No.4320.

(1958) FROSSLING, N., N.A.C.A. Tech. Mem. 1432.

(1958) GARNER, F.H. and SUCKLING, R.D., A.I.Ch.E. Journal, 4, p.114.

(1959) WU, C.S., Appl. Sci. Res., A8, p.140.

(1959) SPIEGEL, M.R., 'Vector Analysis', Shaum Publishing Co., N.Y.

(1959) NARSHAY, M., BOGUSZ, E., JOHNSON, M. and KITNER, R.C., Can. J. Chem. Eng., 37, p.29.

(1959) ROUSE, H., 'Advanced Mechanics of Fluids', John Wiley & Sons, N.Y.

(1959) KRISHNA, P.M., VENKATEOWARLU, D. and NARISIMHAMURTY, G.S.R., J. Chem. Eng. Data, 4, p.336.

(1960) TIEN, C.L., J. Heat Trans., 82, p.252.

(1960) LINTON, W.H. and SUTHERLAND, K.L., Chem. Eng. Sci., 12, p.213.

(1960) PASTERNAK, I.G. and GAURIN, W.H., Can. Journ. Chem. Engrs., 38, p.35.

(1960) SINGH, S.N., App. Sci. Res., A9, p.197-205.

(1960) GREGORY, N. and WALKER, W.S., J. Fluid Mech., 9, p.225.

(1960) ACRIVOS, A., Phys. Fluids, 3, p.657.

(1960) ROGERS, M.H., and LANCE, G.N., J. Fluid Mech., 7, p.617.

(1960) TIBOR and HARMATHY, A.I.Che. Journal 6, p.281.

(1961) CORNISH, A.R.U., Ph.D. thesis, Illinois Inst. Tech.

(1961-62) NORDLIE, R.L. and KREITH, F., Int. Dev. of Heat Transf., Proc. of 1961-62 Int. Ht. Trans. Conf., pp.461-467.

(1962) SIEKMANN, J., Z.A.M.P., 13, p.468.

(1962) GIBBONS, J.H., HOUGHTON, G. and COULL, J., A.I.Che. Journal, 8, p.274.

(1963) TIEN, C.L. and CAMPBELL, D.T., J. Fluid Mech., 17, pp.105-112.

(1963) GRAFTON, R.W., Chem. Eng. Sci., 18, p.457.

(1963) SKELLAND, A.H.P. and CORNISH, A.R.H., A.I.Che. Journ., 9, p.273.

(1963) ISHIZAWA, S., Jap. Soc. Mech. Eng. Bul., 6, No.23, pp.487-496.

(1963) KREITH, F., ROBERTS, L.G., SULLIVAN, J.A. and SINHA, S.N., Int. J. Heat and Mass Transf., 6, p.881-895.

(1963) BOWDEN, F.P. and LORD, R.G., Proc. Roy. Soc., A271, pp.143-152.

(1964) MARCHILDON, E.K., CLAMEN and GAUVIN, W.H., Can. J. Chem. Eng. 42.

(1964) JAYANEERA, K.O.L.F., MASON, B.I. and STACK, G.W., J.F. Mech., 20, p.121.

(1964-65) HAYDAY, A.A., Appl. Sci. Res., A14, 6, pp.405-419.

(1965) ROWE, P.N., CLAXTON, K.T. and LEWIS, J.B., Trans. Inst. Chem. Engrs., 43, p.14.

(1965) TIEN, C.L. and TSUJI, I.J., J. Heat Transf. A.S.M.E., Series C-J, 89, pp.139-145.

(1965) BENTON, E.R., J. Fluid Mech., 23, p.611.

(1965)[1] BANKS, W.H.H., Z.A.M.P., 16, p.780-788.

(1965)[2] BANKS, W.H.H., Quart. J. Appl. Math., 18, 4, pp.443-454.

(1965) DORFMAN, L.A. and SERAZETDINOV, A.Z., Int. Journ. Heat and Mass Transf., 8, pp.317-327.

(1965) ROSENHEAD, L., 'Laminar Boundary Layers', Oxford Press.

(1965) LEE, E.S. and FAU, L.T., Can. J. Chem. Eng., 46, pp.200-204.

(1965) VALENTINE, R.S., SATHER, N.F., and HEIDEGER, W.J., Chem. Eng. Sci., 20, p.719.

(1966) BEG, S.A., Ph.D. Thesis, Imperial College, London.

(1967) NOORDSIJ, P. and ROTTE, J.W., Chem. Eng. Sci., 22, p.1475.

(1967) ROJEY, A., M.Sc. Thesis, Imperial College, London.

(1967) KOH, J.C.Y. and PRICE, J.F., Trans. A.S.M.E., Series C-J, Journal Ht. Transf., 89, 1967.

(1967) MANOHAR, R., Z.A.M.P., 18, pp.320-330.

(1968) GREEN, M.B., Ph.D. Thesis, Imperial College, London.

(1968) LEE, E.S. and FAU, L.T., Can. Journ. Chem. Eng., 46, pp.200-204.

(1968) NOORDSIJ, P. and ROTTE, J.W., Chem. Eng. Sci., 23, p.657.

(1969) RITTMAN, VON K., Ing. Arch., 37, p.304.